The Pennsylvania State University
The Graduate School

SECURITY AND PRIVACY SUPPORT FOR MOBILE SENSING

A Dissertation in
Computer Science and Engineering
by
Qinghua Li

Submitted in Partial Fulfillment
of the Requirements
for the Degree of

Doctor of Philosophy

August 2013

The dissertation of Qinghua Li was reviewed and approved* by the following:

Guohong Cao
Professor of Computer Science and Engineering
Dissertation Advisor, Chair of Committee

Thomas F. La Porta
William E. Leonhard Professor
Director of Networking and Security Research Center

Sencun Zhu
Associate Professor of Computer Science and Engineering

Aylin Yener
Professor of Electrical Engineering

Lee Coraor
Associate Professor of Computer Science and Engineering
Graduate Officer

*Signatures are on file in the Graduate School.

Abstract

The proliferation and ever-increasing capabilities of mobile devices such as smart phones give rise to a variety of mobile sensing systems, which collect data from the embedded sensors of mobile devices to make sophisticated inferences about people and their surroundings. Mobile sensing can be applied to environmental monitoring, traffic monitoring, healthcare, etc. However, the large-scale deployment of mobile sensing applications is hindered by several challenges, including privacy leakage from sensing data, the lack of incentives for mobile device users to participate, and the lack of security mechanisms for data collection when communication infrastructure is unavailable.

The specific goal of this dissertation is to provide security and privacy support for mobile sensing. We achieve this goal by devising techniques to address the aforementioned challenges. First, to provide incentives for users to participate and at the same time preserve privacy, we propose two credit-based privacy-aware incentive schemes for mobile sensing. These schemes reward users with credits for their contributed data without exposing who contributes the data. They also ensure that dishonest users cannot abuse the system to earn unlimited credits. One scheme relies on a trusted third party to protect privacy. The other scheme removes the assumption of trusted third party, and provides unconditional privacy by combining blind signature, partially blind signature, and commitment techniques. Second, for a broad class of applications that need to periodically collect useful aggregate statistics of sensing data, we propose a privacy-preserving aggregation protocol for the Sum aggregate, which can provide differential privacy–a strong and provable privacy guarantee. To perform private and efficient aggregation, we design a novel HMAC-based encryption scheme which allows the aggregator to get the sum of all users' data but nothing else, and a novel ring-based overlapped grouping technique to efficiently deal with dynamic joins and leaves of users. We also extend the aggregation scheme for Sum to derive Max/Min and other aggregate s-

tatistics. Third, for mobile devices without communication infrastructure support, opportunistic mobile networking techniques are used to connect these devices. We address three security issues that may degrade the performance of sensing data collection in opportunistic mobile networks: social selfishness, flood attacks, and routing misbehavior. Specifically, we propose a Social Selfishness Aware Routing (SSAR) protocol which allows users to behave in the socially selfish way but improves routing performance by considering user selfishness into relay selection; we employ rate limiting to defend against flood attacks and design a distributed scheme which can probabilistically detect the violation of rate limit; to mitigate routing misbehavior, we devise a distributed scheme to detect packet dropping in opportunistic mobile networks and an algorithm to reduce the amount of packets forwarded to misbehaving users.

Table of Contents

List of Figures **x**

List of Tables **xiv**

Acknowledgments **xvi**

Chapter 1
Introduction **1**
1.1 Challenges 2
1.2 Focus of This Dissertation 3
1.2.1 Providing Privacy-Aware Incentives 4
1.2.2 Efficient and Privacy-Preserving Stream Aggregation 4
1.2.3 Secure Opportunistic Mobile Networking for Data Collection 5
1.3 Organization 8

Chapter 2
Providing Privacy-Aware Incentives **9**
2.1 Introduction 9
2.2 Preliminaries 10
2.2.1 System and Incentive Model 10
2.2.2 Adversary and Trust Model 13
2.2.3 Our Goals 14
2.2.4 Cryptographic Primitives 14
2.3 An Overview of our Approach 15
2.3.1 Basic Approach 15
2.3.2 Scheme Overview 16
2.4 A TTP-based Scheme 17

2.4.1 The Basic Scheme . . . 18
2.4.2 Dealing with Dynamic Joins and Leaves . . . 20
2.4.3 Addressing Timing Attacks . . . 21
2.4.4 Commitment Removal . . . 22
2.4.5 Security Analysis . . . 22
2.4.6 Cost Analysis . . . 23
2.5 A TTP-Free Scheme . . . 24
2.5.1 The Scheme . . . 24
2.5.2 Dealing with Dynamic Joins and Leaves . . . 27
2.5.3 Credential Removal . . . 28
2.5.4 Security Analysis . . . 28
2.5.5 Cost Analysis . . . 29
2.6 Evaluations . . . 29
2.7 Discussions . . . 31
2.8 Related Work . . . 32
2.9 Summary . . . 32

Chapter 3
Efficient and Privacy-Preserving Stream Aggregation 33
3.1 Introduction . . . 33
3.2 Related Work . . . 36
3.3 Preliminaries . . . 38
3.3.1 Problem Definition . . . 38
3.3.2 Threat and Trust Model . . . 39
3.3.3 Building Blocks . . . 40
3.3.3.1 Homomorphic Encryption . . . 40
3.3.3.2 Data Perturbation . . . 41
3.3.4 Overview of Solution . . . 42
3.4 Basic Encryption Scheme . . . 43
3.4.1 Scheme Overview . . . 43
3.4.2 A Straw-man Construction for Key Generation . . . 44
3.4.3 Our Construction for Key Generation . . . 47
3.5 Dealing with Dynamic Joins and Leaves . . . 52
3.5.1 Naive Grouping . . . 53
3.5.2 Overlapped Grouping . . . 53
3.5.2.1 Basic Idea . . . 53
3.5.2.2 Security Condition . . . 54
3.5.3 Ring-based Overlapped Grouping . . . 56
3.5.3.1 Ring-based Group Structure . . . 56
3.5.3.2 Properties . . . 57

3.5.3.3 Group Management . . . 59
3.5.3.4 Communication Cost Analysis . . . 67
3.6 Aggregation Protocol for Sum . . . 68
3.6.1 Encryption Method . . . 68
3.6.2 Data Perturbation . . . 68
3.6.3 Dealing with Dynamic Joins and Leaves . . . 69
3.6.4 Analysis . . . 70
3.6.4.1 Aggregation Error . . . 70
3.6.4.2 Communication Cost . . . 71
3.7 Evaluations . . . 71
3.7.1 Communication Cost . . . 72
3.7.2 Aggregation Error . . . 73
3.7.3 Computation Cost and Running Time . . . 74
3.8 Extensions and Discussions . . . 76
3.8.1 Aggregation Protocol for Min . . . 76
3.8.1.1 Basic Min Aggregation . . . 76
3.8.1.2 Low-cost Min Aggregation . . . 78
3.8.1.3 Practical Performances . . . 79
3.8.2 More Aggregate Statistics . . . 81
3.8.3 Honest-but-Curious Key Dealer . . . 81
3.8.4 Dealing with Node Failures . . . 82
3.9 Summary . . . 83

Chapter 4
Secure Opportunistic Mobile Networking for Data Collection 84
4.1 Social Selfishness Aware Routing . . . 85
4.1.1 Introduction . . . 85
4.1.2 SSAR Overview . . . 87
4.1.2.1 Design for User . . . 87
4.1.2.2 Network Model . . . 87
4.1.2.3 Willingness Table . . . 88
4.1.2.4 The Architecture . . . 89
4.1.2.5 The Protocol . . . 91
4.1.2.6 Forwarding Strategy . . . 92
4.1.3 Detailed Design . . . 92
4.1.3.1 Packet Priority . . . 92
4.1.3.2 Delivery Probability Estimation . . . 94
4.1.3.3 Forwarding Set Optimization . . . 97
4.1.4 Performance Evaluations . . . 99
4.1.4.1 Experiment Setup . . . 99

4.1.4.2 Routing Algorithms . . . 103
4.1.4.3 Metrics . . . 104
4.1.4.4 Results . . . 104
4.1.5 Related Work . . . 110
4.1.6 Summary . . . 112
4.2 Defending Against Flood Attacks . . . 113
4.2.1 Introduction . . . 113
4.2.2 Motivation . . . 115
4.2.3 Overview . . . 117
4.2.3.1 Problem Definition . . . 117
4.2.3.2 Models and Assumptions . . . 119
4.2.3.3 Basic Idea: Claim-Carry-and-Check . . . 120
4.2.4 Our Scheme . . . 122
4.2.4.1 Claim Construction . . . 122
4.2.4.2 Inconsistency Caused by Attack . . . 123
4.2.4.3 Protocol . . . 123
4.2.4.4 Local Data Structures . . . 125
4.2.4.5 Inconsistency Check . . . 126
4.2.4.6 Alarm . . . 127
4.2.4.7 Efficient T-claim Authentication . . . 128
4.2.4.8 Dealing with Different Rate Limits . . . 129
4.2.4.9 Replica Flood Attacks in Quota-based Protocols . . . 129
4.2.5 Meta Data Exchange . . . 130
4.2.5.1 Sampling . . . 131
4.2.5.2 Redirection . . . 132
4.2.5.3 The Exchange Process . . . 132
4.2.5.4 Meta Data Deletion . . . 133
4.2.6 Analysis . . . 133
4.2.6.1 Detection Probability . . . 133
4.2.6.2 Cost . . . 136
4.2.6.3 Parameter Selection . . . 137
4.2.6.4 Collusion . . . 138
4.2.7 Performance Evaluations . . . 138
4.2.7.1 Experiment Setup . . . 138
4.2.7.2 Routing Algorithms and Metrics . . . 139
4.2.7.3 Analysis Verification . . . 140
4.2.7.4 Detection Rate . . . 140
4.2.7.5 Detection delay . . . 143
4.2.7.6 Flooded Replicas under Collusion . . . 143
4.2.7.7 Cost . . . 143

4.2.8 Related Work . . . 146
4.2.9 Summary . . . 147
4.3 Mitigating Routing Misbehavior . . . 147
4.3.1 Introduction . . . 147
4.3.2 Preliminaries . . . 149
4.3.2.1 Network and Routing Model . . . 149
4.3.2.2 Security Model . . . 149
4.3.2.3 Overview of Our Approach . . . 150
4.3.2.4 Terms and Notations . . . 151
4.3.3 Packet Dropping Detection: A Basic Scheme . . . 151
4.3.3.1 Basic Idea . . . 151
4.3.3.2 Contact Record and Record Summary . . . 153
4.3.3.3 Packet Dropping Detection . . . 154
4.3.3.4 Misreporting Detection . . . 155
4.3.4 Dealing with Collusions . . . 156
4.3.4.1 Misreporting with Collusion . . . 157
4.3.4.2 Forge-Buffer . . . 158
4.3.4.3 Forge-Inactive . . . 159
4.3.4.4 Record and Summary Deletion . . . 160
4.3.4.5 Discussion . . . 161
4.3.5 Analysis of Misreporting Detection . . . 161
4.3.6 Routing Misbehavior Mitigation . . . 165
4.3.6.1 FP Maintenance . . . 167
4.3.6.2 Dealing with Packet Dropping . . . 168
4.3.7 Performance Evaluations . . . 169
4.3.7.1 Experiment Setup . . . 169
4.3.7.2 Routing Algorithms . . . 169
4.3.7.3 Metrics . . . 170
4.3.7.4 Experimental Results . . . 170
4.3.8 Related Work . . . 175
4.3.9 Summary . . . 176
4.4 Chapter Summary . . . 176

Chapter 5
Conclusions and Future Work **178**
5.1 Conclusions . . . 178
5.2 Future Directions . . . 180

Bibliography **182**

List of Figures

2.1 System model. 10

3.1 System model. 39
3.2 The intuition behind the straw-man construction. The aggregator computes the sum of a set of random numbers as the decryption key. These numbers are secretly allocated to the nodes, and each node computes the sum of its allocated numbers as the encryption key. The aggregator cannot know any node's encryption key since it does not know the mapping between the numbers and the nodes. 45
3.3 The intuition behind our construction in comparison with the straw-man construction. 48
3.4 The basic idea of overlapped grouping. In this example, groups $\mathcal{G}_1$ and $\mathcal{G}_2$ share node A. A is assigned secrets from both $\mathcal{G}_1$ and $\mathcal{G}_2$. A sets $k_A = h(f_{s_1}(t)) + h(f_{s_4}(t))$. B only receives secrets from group $\mathcal{G}_1$, and it sets $k_B = h(f_{s_2}(t)) - h(f_{s_1}(t))$. Other nodes set their keys similarly. The aggregator sets $k_0 = \sum_{i=\{2,3,5,6,8,9\}} h(f_{s_i}(t))$. The aggregator can only get the sum of *all nodes*. 54
3.5 Ring-based overlapped grouping. In this example, the nodes form eight groups, four disjoint groups in the outer ring ($\mathcal{G}_1$–$\mathcal{G}_4$) and four disjoint groups in the inner ring ($\mathcal{G}'_1$–$\mathcal{G}'_4$). Groups on different rings may overlap. Group $\mathcal{G}_1$ and $\mathcal{G}'_1$ overlap, and they share node 1 and 2. 56
3.6 Segment representation of groups. 57
3.7 The two patterns that two groups $\mathcal{G}$ and $\mathcal{A}$ may overlap where $|\mathcal{G}| \geq |\mathcal{A}|$. $\mathcal{G}$ and $\mathcal{A}$ are in different virtual rings. In (b) and (c), $\mathcal{G}$ overlaps with the left and right part of $\mathcal{A}$, respectively. 58
3.8 The regrouping (in Algorithm 2) when a node joins $\mathcal{G}$ and $\mathcal{A}$ which overlap in Pattern I. $\mathcal{G}$ is split into $\mathcal{G}_1$ and $\mathcal{G}_2$ if it has too many nodes. 60
3.9 The regrouping (in Alg. 3) when a node joins $\mathcal{G}$ and $\mathcal{A}$ which overlap in Pattern II. $\mathcal{B}$ is the neighbor of $\mathcal{A}$; it overlaps with $\mathcal{G}$ in Pattern I or II. 61

3.10 The regrouping in Alg. 4 and 5 when a node leaves $\mathcal{G}$ and $\mathcal{A}$ which overlap in Pattern I and II, respectively. 64
3.11 The communication cost of ring-based overlapped grouping. 73
3.12 Comparisons between our scheme and other schemes in the communication cost of dynamic joins and leaves (log-log scale). For dynamic leaves, the communication cost of Binary and JK is zero and thus not shown in the log-log plot. 73
3.13 An example of sum based on extended and concatenated derivative data. 77
3.14 An example of the process that obtains an approximate Min. 80

4.1 SSAR architecture and an example contact between node N and M. The dashed rectangles enclose the information exchanged in step 2 and step 3 (Sec. 4.1.2.5). 89
4.2 An example of willingness-aware forwarding. 91
4.3 Heuristics used to estimate buffer overflow dropping probability P_{over}. Triangles and squares are historical samples. 96
4.4 An example of social network graph generation in the 4 basic steps. 100
4.5 Comparison of algorithms in the forwarding mode. The Reality trace and contact-dependent graph are used. 104
4.6 Comparison of algorithms in the forwarding mode. The Reality trace and random graph are used. 105
4.7 Comparison of algorithms in the forwarding mode. The Infocom05 trace and contact-dependent graph are used. 105
4.8 Comparison of algorithms in the replication mode. The Reality trace and contact-dependent graph are used. 107
4.9 Comparison of algorithms on the Reality trace when nodes have different buffer sizes. The forwarding mode and contact-dependent graph are used. 108
4.10 Comparison of algorithms on the Reality trace when nodes have different average numbers of social ties. The replication mode and contact-dependent graph are used. 108
4.11 The effects of willingness awareness in SSAR. The forwarding mode and contact-dependent graph are used over the Reality trace. 109
4.12 The accuracy of our KNN-plus-Kcenter algorithm in estimating the buffer overflow dropping probability of the packets that fall into 10 priority intervals with the i^{th} interval being $[0.1 \cdot (i-1), 0.1 \cdot i]$. The forwarding mode and contact-dependent graph are used over the Reality trace. 109

4.13 Comparison of algorithms in selfishness satisfaction over the Reality trace. The forwarding mode is used. 111
4.14 Comparison of algorithms in selfishness satisfaction over the Infocom05 trace. The forwarding mode is used. 111
4.15 The effect of flood attacks on packet delivery ratio. In Absent Node, attackers are simply removed from the network. Attackers are selectively deployed to high-connectivity nodes. 116
4.16 The effect of flood attacks on wasted transmission. Attackers are randomly deployed. 117
4.17 The basic idea of flood attack detection. *cp* and *ct* are packet count and transmission count, respectively. The arrows mean the transmission of packet or meta data which happens when the two end nodes contact. 119
4.18 The conceptual structure of a packet and the changes made at each hop of the forwarding path. 123
4.19 The Merkle hash tree constructed upon eight T-claims TC_1,...,TC_8. In the tree, H_i is the hash of TC_i, and an inner node is the hash of its child nodes. The signature of TC_1 includes H_2, H_{34}, H_{58} and SIG. 129
4.20 The idea of redirection which is used to mitigate the stealthy attack. 131
4.21 (a) The basic attack considered for detection probability analysis. Attacker S floods packets to A and then to B. (b) The scenario when the lower bound detection probability can be obtained. (c) The scenario when the upper bound detection probability can be obtained. 133
4.22 Verification of analysis results on the synthetic trace. Spray-and-Wait is used as the routing protocol. Each attacker launches the basic attack once. 141
4.23 The detection rate under different conditions. In (d), Forward is used as the routing protocol. 141
4.24 The detection delay compared with the routing delay of Propagation. 143
4.25 The effect of undetected replicas on wasted transmissions when attackers collude to launch replica flood attacks. 144
4.26 The computation cost of our scheme. 145
4.27 The communication cost of our scheme. 145
4.28 The effects of routing misbehavior when SimBet and Delegation are used as the routing algorithms. 149
4.29 An overview of our approach. 150

4.30 Examples of packet dropping detection and misreporting detection. In (b), M reports the same contact record to N_2 and N_3 as its "previous" record, and then it has to assign the same sequence number to the contact with N_2 and N_3, which violates consistency rules. 152
4.31 Two colluding nodes M and M' try to hide the dropping of packet m by forging a contact (via the out-band channel) and reporting the forged contact record. The forged record may show that M has not received m, M has forwarded m to M', *etc.* 156
4.32 A decision-tree based exploration of misreporting 157
4.33 Examples of report window when $r = 2$. A node is required to report the records of the contacts in its current report window to the next contacted node. 159
4.34 Numerical results on misreporting detection where 20% of nodes are misbehaving (i.e., $q = 0.2$). (a) Detection probability when each misbehaving node misreports once. (b) The minimum w required to detect each misreporting node with probability not less than 0.95 when $n = 1000$. 164
4.35 Comparison results when misbehaving nodes are selectively deployed to high-connectivity nodes which drop all received packets. The Reality trace is used. 168
4.36 Comparison results when misbehaving nodes are randomly deployed and they only drop part of the received packets. The Reality trace is used, and the fraction of misbehaving nodes is fixed at 30%. . . . 172
4.37 Comparison of analysis and simulation results on the detection probability and detection delay of a single misreporting instance. The synthetic trace is used. 172
4.38 The detection rate of our scheme in the Reality trace. 173
4.39 The detection delay compared with the packet delivery delay. 173

List of Tables

2.1 Notations 18
2.2 The running time of our schemes when $M = 1000$ and $c_{max} = 5$ . . 30
2.3 The power consumption of our schemes on a smartphone 31

3.1 Comparison between existing schemes and our scheme. 34
3.2 Notations 43
3.3 Security levels of the straw-man construction when $\gamma = 0.1$. 46
3.4 The minimum values of c for 80-bit security in the straw-man construction. 47
3.5 The security level of our construction when $\gamma = 0.1$. 50
3.6 The values of c for 80-bit security in our construction. 50
3.7 The values of q for 80-bit security in our construction. 50
3.8 The security and cost of our construction and the straw-man construction. For computation cost, the value is the cost per time period. 52
3.9 The computation cost of our construction and the straw-man construction for 80-bit security when $\gamma = 0.1$. 52
3.10 The values of x and d for 80-bit security. 59
3.11 An example of Algorithm 6 69
3.12 The mean and standard deviation of aggregation error 74
3.13 The analytical computation cost of different schemes 75
3.14 The running time of different schemes 76
3.15 The relative error and cost of the basic Min aggregation scheme and the low-cost scheme. 79
3.16 The running time of our Min aggregation protocol and SCRCS-min when the relative error is smaller than 1%. 81
3.17 The running time of our Min aggregation protocol and SCRCS-min when the relative error is smaller than 0.1%. 81

4.1 The summary of the two traces used for evaluation 100
4.2 The default parameters used in the simulation 102

4.3 Variables used in the analysis 134
4.4 The storage (KB) used for claims and data packets 146
4.5 The average communication overhead per contact 174
4.6 The average storage overhead per node 174

Acknowledgments

I would like to thank all the people who have helped me during my Ph.D. study.

First of all, I would like to express my sincere gratitude to my advisor Professor Guohong Cao. Without his consistent supervision and support, this dissertation would not be possible. During my doctoral study, he has spent a lot of time and effort in training me to be a more matured researcher. He has kindly and unreservedly advised me in doing research, publishing papers, and performing professional services. It was because of his unreserved assistance and kind encouragement that I could go through many difficult times in my Ph.D study; it was because of his inspirational guidance and patient training that I could find my path in the research community. His spirit, attitude, and passion have profoundly influenced me, and will influence my future growth as a researcher and educator in computer science.

My gratitude also goes to other members of my dissertation committee, including Prof. Thomas La Porta, Prof. Sencun Zhu, and Prof. Aylin Yener. Their insightful comments for my dissertation have significantly helped me improve it. Besides, Prof. Thomas La Porta and Prof. Sencun Zhu influenced much of my early work on opportunistic mobile networks. Both of them have consistently provided me with valuable advice and support throughout my doctoral study. It is my great honor to have all these wonderful professors in my committee.

In addition to the committee members, I would like to thank my co-authors Wei Gao, Xuejun Zhuo, Eve M. Schooler, and Jianqing Zhang. I have been very lucky to collaborate with these great people on different research projects. The conversations and discussions with them have always been inspiring. Especially, thanks are given to Eve M. Schooler and Jianqing Zhang who served as my mentors during my summer internship at Intel Labs and provided insightful suggestions on

my research.

I also wish to thank the many unnamed fellow students in the MCN lab and at Penn State University for encouraging me on my research and providing friendship. They make my years of study at Penn State University a joyful journey.

Finally, I express my deepest gratitude to my family for their unconditional love. I am indebted to my parents who have always supported me in my life and encouraged me to do my best; I am also indebted to my wife for her persistent faith in me and sacrifices made during my candidature. Without their love, support, and encouragement, I would not be where I am.

Dedication

To my parents and my wife.

Chapter 1

Introduction

Today smartphones are proliferating, with more than one billion units installed worldwide by the third quarter of 2012 [1]. As these smartphones have matured as computing platforms, they are also acquiring richer functionality with the introduction of various sensors. For example, the Apple iPhone 5 includes eight different sensors: accelerometer, GPS, ambient light, dual microphones, proximity sensor, dual cameras, compass, and gyroscope. Besides smartphones, other mobile devices such as tablets, personal medical devices, and environmental monitoring devices are usually also equipped with various embedded sensors. For instance, BodyMedia FIT Armband [2] has sensors to measure galvanic skin response, skin temperature, heat flux, and acceleration, and RTI International's MicroPEM [3] has sensors to measure air pollution levels. These sensors are very useful in providing location-based services, as well as gathering data about people and their environments. For example, GPS enables new location-based applications including location search, navigation, and mobile social networks; cameras are used to take pictures or videos of the surroundings; microphones are used to record sounds of the surroundings. More recently, these embedded sensors have been used for mobile sensing research such as activity recognition, where people's activity such as walking, driving, sitting, talking, etc. can be identified, and have been applied to support more advanced applications in healthcare [4, 5], public safety, environmental monitoring [6], traffic monitoring [7], etc.

Mobile sensing applications can be divided into two categories: local sensing in which the sensing data collected on a mobile device are consumed by third

party applications on the same device, and participatory sensing in which the sensing data on multiple mobile devices are collected and consumed by remote data collectors. In this dissertation, we focus on participatory sensing, which is lately seeing many interesting applications [8, 9], e.g., assessing neighborhood safety, and developing citizen science and journalism [10, 11]. Other applications include tracking the spread of disease across a city [12], building a noise map [13], a pollution map [14, 15], identifying traffic congestions on city roads [7], etc.

1.1 Challenges

Although mobile sensing is very useful, several challenges impede the collection of sensing data, as summarized in the following.

The first challenge is privacy leakage. Data from sensors may be exploited to obtain private information about mobile device users. For example, to build a noise map for a city, a server may request each user to continuously upload his current location and the noise level at this location. However, from the location data, the server can learn where the user has been and possibly infer his activities, e.g., if he has gone to a hospital recently. There are also other well-known location tracking attacks [16, 17, 18]. For another example, to monitor the propagation of a new flu, a server will collect information on who have been infected by this flu. However, a patient may not want to provide such information if he is not sure whether the information will be abused by the server. Such possible privacy leakage may prevent users from contributing sensing data. Thus, it is critical to preserve privacy in mobile sensing applications.

The second challenge is the lack of incentives for users to participate. To participate, a user has to trigger his sensors to measure data (e.g., to obtain GPS locations), which may consume much power of his smartphone. For example, reading GPS consumes much power of a smartphone. Also, the user needs to upload data to a server which may consume much of his 3G data quota (e.g., when the data is photos or video clips). Moreover, the user may have to move to a specific location to sense the required data. Considering these efforts and resources required from the user, an incentive scheme is strongly desired for mobile sensing applications to proliferate.

The third challenge is the lack of pervasive and secure network connectivity. Collection of sensing data relies on some kind of network connectivity between mobile devices and remote data collectors. Although 3G and 4G are widely deployed today, such communication infrastructures do not cover every location, and are not always available (e.g., in disaster recovery scenarios). They are also not supported by all mobile devices. For instance, some tablets may not have 3G service, and some pollution sensing devices (e.g., MicroPEM by RTI International) do not support 3G communications at all. For mobile devices without infrastructure support and for circumstances of unavailable or cost-inefficient infrastructures, the lack of network connectivity is a key challenge to sensing data collection. Although opportunistic mobile networks (which employ the mobility of users and the short-range radios of their devices for communications) can be used to collect sensing data, data forwarding in such networks represents a challenge due to user selfishness and various security attacks.

To address these challenges, we also need to consider that mobile devices are resource-constrained. They usually have limited computing resources, which sets a stringent requirement on the computation cost of any solution to the above three challenges. Typically powered by batteries, mobile devices also have limited energy resources. Thus, energy consumption should always be a concern in the design of security and privacy solutions. In addition, communication and storage overhead should be kept low whenever possible.

1.2 Focus of This Dissertation

The goal of this dissertation is to provide security and privacy support for mobile sensing, and consequently facilitate the proliferation of mobile sensing applications. For this purpose, we devise techniques to address the challenges elaborated in Chapter 1.1. In particular, we focus on three important aspects, i.e., privacy-aware incentives, efficient and privacy-preserving stream aggregation, and secure opportunistic mobile networking techniques for sensing data collection. We briefly explain them in the following three subsections.

1.2.1 Providing Privacy-Aware Incentives

As discussed in Chapter 1.1, the large-scale deployment of mobile sensing applications is hindered by the lack of incentives for users to participate and the concerns on possible privacy leakage. Although incentive and privacy have been addressed separately in mobile sensing [19, 20, 21, 22], it is still an open problem to provide incentives while simultaneously protect privacy.

To address the problem of providing privacy-aware incentives for mobile sensing, we adopt a credit-based approach which allows each user to earn credits by contributing data without leaking what data it has contributed [23]. The approach also ensures that dishonest users cannot abuse the system to earn unlimited amount of credits. Following this approach, we propose two privacy-aware incentive schemes. The first scheme is designed for scenarios where a trusted third party (TTP) is available. It relies on the TTP to protect user privacy, and thus has very low computation and storage cost at each user. The second scheme considers scenarios where no TTP is available. It applies blind signature, partially blind signature and commitment techniques to protect privacy. To the best of our knowledge, they are the first privacy-preserving incentive schemes for mobile sensing. Implementation-based measurements on smartphones show that these schemes have short running time and low power consumption.

1.2.2 Efficient and Privacy-Preserving Stream Aggregation

In many monitoring applications, aggregate statistics need to be periodically computed from a stream of data contributed by a group of users [24], in order to identify interesting phenomena or track important patterns. For example, the average amount of daily exercises (which can be measured by motion sensors [5]) can be used to infer public health conditions. The average or maximum level of air pollution and pollen concentration is useful for people to plan their outdoor activities. Other statistics of interests include the lowest gasoline price in a city, the highest moving speed of road traffic during rush hour, etc. For these applications, it is important to allow an untrusted collector to obtain the desired aggregate statistics without knowing the content of each user's data. This problem is very challenging considering that the collector may have auxiliary information obtained elsewhere

(e.g., from the Internet), as recent studies [25, 26] have shown that such auxiliary information may help the collector to obtain private information about users from aggregate statistics. Existing approaches [27, 28, 29, 30] provide privacy guarantee by adding noise to each user's data and allowing the aggregator to get a noisy sum aggregate. However, these approaches either have high computation cost, high communication overhead when users join and leave, or accumulate a large noise in the sum aggregate which means high aggregation error.

To address these problems, we propose a scheme for privacy-preserving aggregation of time-series data in presence of untrusted aggregator [31, 32], which provides differential privacy [25, 26] for the sum aggregate. It provides provable guarantees that negligible information about individual users will be leaked from the aggregate statistic, even if the collector has arbitrary auxiliary information. Our scheme relies on a novel encryption technique to conceal the content of the user's data from the collector, but still allows the collector to get the sum of all users' data. This technique is purely built upon light-weight symmetric-key cryptography, and hence has very low computation overhead. Our scheme also leverages a novel ring-based overlapped grouping technique to efficiently deal with dynamic joins and leaves. When a user joins or leaves, only a small number of users need to update their cryptographic keys. Our scheme has very low aggregation error. The users only collectively add some necessary noise to the sum to ensure differential privacy, which is $O(1)$ with respect to the number of users. In addition, we extend the aggregation scheme for sum to derive Max/Min and other aggregate statistics.

Evaluations show that our scheme is orders of magnitude faster than existing solutions. Also, only a small number of users need to be communicated for each join or leave, irrespective of the total number of users that the system has. In addition, the aggregation error of our scheme is only 2-3 times of the minimum required for differential privacy.

1.2.3 Secure Opportunistic Mobile Networking for Data Collection

For mobile devices without infrastructure support and for circumstances of unavailable or cost-inefficient infrastructures, securely collecting data from mobile

nodes[1] is challenging. To broaden the scope of mobile sensing to these scenarios, we propose to use opportunistic mobile networks for data collection. Opportunistic mobile networks employ the mobility of users and the short-range radios (e.g., Bluetooth and WiFi) of their devices to provide communication support. Specifically, two users forward data to each other during an opportunistic contact (i.e., when they move into the wireless communication range of their devices). Through multiple-hop forwarding, sensing data can be delivered to remote collectors. Such mobility-assisted forwarding is especially helpful for delay-tolerant data collection. For example, pollution studies that collect pollution data for archival purposes may not be very sensitive to the delay of data collection. However, data forwarding in such networks is challenging due to unpredictable mobility, user selfishness, and attacks on security.

Effective data delivery relies on users to cooperatively forward data for each other. In practice, however, users are socially selfish. They are willing to forward data for those with whom they have social ties, but not others. Most existing routing protocols [33, 34, 35, 36, 37, 38] proposed for opportunistic mobile networks assume that each node is willing to relay packets for everyone else. They may not work well since some packets are forwarded to nodes unwilling to relay, and will be dropped. A couple of works [39, 40] have studied the selfishness problem, but they go to another extreme and assume that users do not forward packets for anyone else. Thus, they miss the opportunity of using social ties for data forwarding. Different from them, we propose a Social Selfishness Aware Routing (SSAR) algorithm to allow user selfishness and provide better routing performance in an efficient way [41, 42]. To select a forwarding node, SSAR considers both users' willingness to forward and their contact opportunity, resulting in a better forwarding strategy than purely contact-based approaches. Trace-driven simulations show that SSAR allows users to maintain selfishness and achieves better routing performance with low transmission cost. Our work is the first to incorporate both social and selfish aspects of users' natures into forwarding decisions, and study correlations between users' social selfishness and performance of data forwarding in opportunistic mobile networks.

Due to the limitation in network resources such as contact opportunity and

[1]In this dissertation, we use node and user interchangeably when the context is clear.

buffer space, opportunistic mobile networks are vulnerable to flood attacks in which attackers send as much sensing data as possible to the network, in order to deplete or overuse the limited network resources. Unfortunately, little work has been done to address flood attacks. In this dissertation, we employ rate limiting [43] to defend against flood attacks [44], such that each node has a limit over the number of packets that it can generate in each time interval and a limit over the number of replicas that it can generate for each packet. We propose a distributed scheme to detect if a node has violated its rate limits. To address the challenge that it is difficult to count all the packets or replicas sent by a node due to lack of communication infrastructure, our detection adopts *claim-carry-and-check*: Each node itself counts the number of packets or replicas that it has sent and claims the count to other nodes; the receiving nodes carry the claims when they move, and cross-check if their carried claims are inconsistent when they contact. The claim structure uses the pigeonhole principle to guarantee that an attacker will make inconsistent claims which may lead to detection. We provide rigorous analysis on the probability of detection, and evaluate the effectiveness and efficiency of our scheme with extensive trace-driven simulations.

Besides launching flood attacks, malicious nodes may also drop received data packets. Such routing misbehavior prevents sensing data from being delivered and wastes system resources such as power and bandwidth. Although techniques have been proposed to mitigate routing misbehavior in mobile ad hoc networks [45, 46, 47, 48, 49], they cannot be directly applied to opportunistic mobile networks because of the intermittent connectivity between nodes. To address the problem, we propose a distributed scheme to detect packet dropping in opportunistic mobile networks [50]. In our scheme, a node is required to keep a few signed contact records of its previous contacts, based on which the next contacted node can detect if the node has dropped any packet. Since misbehaving nodes may misreport their contact records to avoid being detected, a small part of each contact record is disseminated to a certain number of witness nodes, which can collect appropriate contact records and detect the misbehaving nodes. We also propose a scheme to mitigate routing misbehavior by limiting the number of packets forwarded to the misbehaving nodes [50]. Trace-driven simulations show that our solutions are efficient and can effectively mitigate routing misbehavior.

1.3 Organization

The remainder of the dissertation is organized as follows. Chapter 2 presents our privacy-aware incentives schemes. Chapter 3 focuses on our schemes for differentially private aggregation of stream data. Chapter 4 introduces secure mobile networking techniques for sensing data collection, and describes our approaches for addressing user selfishness, flood attacks, and routing misbehavior. Chapter 5 concludes this dissertation and discusses future work.

Chapter 2

Providing Privacy-Aware Incentives

2.1 Introduction

Although the data contributed by mobile users is very useful, currently most mobile sensing applications rely on a small number of volunteers to contribute data, and hence the amount of collected data is limited. There are two factors that hinder the large-scale deployment of mobile sensing applications. First, there is a lack of incentives for users to participate in mobile sensing. To participate, a user has to trigger his sensors to measure data (e.g., to obtain GPS locations), which may consume much power of his smart phone. Also, the user needs to upload data to a server which may consume much of his 3G data quota (e.g., when the data is photos). Moreover, the user may have to move to a specific location to sense the required data. Considering these efforts and resources required from the user, an incentive scheme is strongly desired for mobile sensing applications to proliferate. Second, in many cases the data from individual user is privacy-sensitive. For instance, to monitor the propagation of a new flu, a server will collect information on who have been infected by this flu. However, a patient may not want to provide such information if he is not sure whether the information will be abused by the server.

Several schemes [19, 20, 21] have been proposed to protect user privacy in mobile sensing, but they do not provide incentives for users to participate. A recent work [22] designs incentives based on gaming and auction theories, but it does not consider privacy. Thus, it is still an open problem to provide incentives

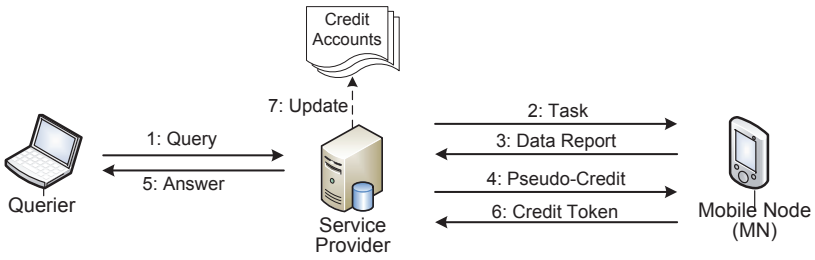

Figure 2.1. System model.

for mobile sensing without privacy leakage.

In this chapter, we address the problem of providing privacy-aware incentives for mobile sensing. We adopt a credit-based approach which allows each user to earn credits by contributing his data without leaking which data he has contributed. At the same time, the approach ensures that dishonest users cannot abuse the system to earn unlimited amount of credits. Following this approach, we propose two privacy-aware incentive schemes. The first scheme is designed for scenarios where a trusted third party (TTP) is available. It relies on the TTP to protect user privacy, and thus has very low computation and storage cost at each user. The second scheme considers scenarios where no TTP is available. It applies blind signature, partially blind signature and commitment techniques to protect privacy.

2.2 Preliminaries

2.2.1 System and Incentive Model

Figure 2.1 shows our system model. The system mainly consists of a dynamic set of mobile nodes (MNs), a mobile sensing Service Provider (SP), and a set of queriers. MNs are mobile devices with sensing, computation and communication capabilities, e.g., smart phones. MNs are carried by people or mounted to vehicles and other objects. They have (possibly intermittent) Internet access via 3G, WiFi or other available networks. Queriers use the mobile sensing service. They send queries to the SP to request the desired statistics and context information, e.g., "*What is the pollen level in Central Park?*" The SP collects sensor readings from MNs and answers the queries based on the collected data.

The SP pays credits to the carrier of a MN for the sensing data that it con-

tributes[1]. The credits earned by a MN can be used to buy mobile sensing service from the SP, exchanged for discount of the MN's 3G service, or converted to other real-world rewards. Thus, MNs are incentivized to participate.

The basic workflow is as follows. A querier sends a query to the SP. To answer the query, the SP transforms the query into one or more tasks and adds them into a *task queue*. A task specifies what sensor readings to report, and when and where to sense. The task also specifies an expiration time, after which it should be deleted. When a MN has network access, it (using a random pseudonym generated by itself) polls the SP to retrieve tasks. After retrieving a task, the MN decides whether to accept the task based on certain criteria (e.g., if it has the required sensing capability). If the MN accepts the task, it will collect its sensor data at the time and location specified by the task, and generate one report. Then it submits the report to the SP using a new pseudonym in a new communication session. In the same communication session, the SP pays a certain number of credits to the reporting MN. Since it does not know the real identity of the MN, it issues pseudo-credits to the MN which will be used to generate real credit tokens. After the SP collects enough reports for a task, it deletes the task from the task queue. It aggregates the reported data to obtain the answer for the appropriate query, and sends the answer back to the querier. When the MN receives the pseudo-credits, it transforms them into credit tokens. After a random time (to avoid timing attacks), it deposits each credit token to the SP with its real identity. The SP updates the MN's credit account accordingly. Cashing a pseudo-credit for a credit token relies on a secret which is only known by the MN, such that the SP cannot link the credit token to the pseudo-credit and hence does not know the report from which the credit was earned.

When a MN retrieves tasks, the SP sends a random subset of tasks (e.g., 100 tasks) in the queue to the MN[2]. Since there may be many tasks, delivering a subset of them can reduce the communication cost. In this approach, a MN may repeatedly retrieve the same tasks. Here performance is sacrificed for privacy. If

[1]The carrier of a MN is the person that carries the MN, or the owner of the vehicle where the MN is mounted. In this chapter, we use MN and carrier interchangeably.

[2]In future work, we will consider other methods to determine which subset of tasks the SP should send. For example, it may send recently created tasks. Also, a MN may specify certain attributes that retrieved tasks should satisfy, on condition that the revealed attributes do not cause much privacy leakage.

the MN reveals the tasks that it retrieved before, it is easier for the SP to link the tasks accepted by the MN. Although the MN may retrieve a task multiple times, it accepts the task at most once. To mitigate timing attacks, the MN waits a random time between successive task retrievals.

Among the tasks that a MN retrieves in the same communication session with the SP, at most one task will be accepted by the MN. Here we sacrifice performance for privacy. If the MN accepts multiple tasks retrieved in the same session and the SP does not send these tasks to other MNs, the SP knows that the collected reports must be submitted by the same MN. Such knowledge can help the SP to infer the real identity of the MN.

The amount of credits paid for different reports may be different. It depends on the type of sensor reading to report and the amount of effort needed to submit the report. For example, suppose it requires the carrier to take a high-definition photograph to generate a report. Since the generation process needs user intervention and the submission of the report causes much network traffic, more credits should be paid for the report. In contrast, if a report just needs an accelerator reading which can be obtained without human intervention and does not induce much communication cost, less credits can be paid for it. Let c denote the number of credits paid for a report. The value of c is set by the SP. A MN may not accept a task if the amount of credits paid for the task is less than its expectation. Thus, the SP should set an appropriate c for each task (e.g., higher values for more challenging tasks). We assume that c has integer values ranging from 1 to a certain maximum c_{max}. We expect that c_{max} is not large in practice, e.g., $c_{max} = 5$.

The SP may charge queriers fees for using its service. The fee charged for a query is more than the amount of credits that the SP pays for the reports collected to answer the query, such that the SP can make a profit. To control the cost of answering queries, the SP needs to control the number of reports that each MN can submit for each task. In this chapter, we assume that each task allows one report from each MN.

In practice, many queries can be answered by a single report containing the required sensor reading, e.g., *What is the temperature in Central Park?* Other queries that need a series of reports can be answered by creating multiple tasks each of which only needs one report. For a query that requires periodical sensor

readings (e.g., *What is the hourly pollen level in Central Park?*), the SP can create one single-report task in every period. For a query that requires event-driven reports (e.g., *What is your location when you drive over a pothole?*), the SP can ensure that there is always a single-report task for this query in the task queue, such that MNs can always retrieve it. We will explore more efficient techniques to support such queries in future work.

2.2.2 Adversary and Trust Model

Threats to Incentive MNs may want to earn as many credits as possible. To achieve this goal, a MN may submit a lot of reports for each task (using a different pseudonym to submit each report), and try to obtain more than c credit tokens for the task. A number of MNs may collude. A malicious MN may compromise some other MNs, and steal their credentials to earn more credits. For example, it steals their credit tokens and deposits these tokens to its own credit account.

With respect to incentive, we assume that the SP behaves honestly. It will not repudiate valid credit tokens deposited by MNs, since this will discourage the MNs from contributing sensing data in the future. As discussed in Chapter 2.2.1, the SP may make profits from providing mobile sensing service, and thus it is not of interest for the SP to discourage MNs from participation. Also, the SP will not manipulate any MN's credit account (e.g., reducing the credits without its approval).

Malicious MNs may submit false sensor readings to prevent the SP from obtaining correct answers. Such data pollution attacks are outside the scope of this chapter. However, the effect of false readings can be mitigated by using an anonymous reputation scheme (e.g., IncogniSense [21]) to filter the reports submitted by the MNs with low reputations.

Threats to Privacy The SP is curious about which tasks a MN has accepted, and what reports the MN has submitted.

The SP may craft a task which targets a narrow set of MNs and thus makes it easier to identify the MNs accepting this task. For example, the crafted task only allows the faculty members of a university to report their data. For such a task, even a single report may leak the reporter's affiliation. This problem is not unique

to our scenario, and it can be addressed as follows [19]: A registration authority is used to verify that no task targets a narrow set of MNs, and only verified tasks with the authority's signature can be published by the SP. In this chapter, we do not consider tasks that target a narrow set of MNs, but the aforementioned solution to this problem can be easily applied to our approach.

Trust Model We assume that the SP and each MN have a pair of public and private keys, which can be used to authenticate each other. These keys are issued by a (possibly offline) certificate authority. An adversary may compromise a MN and know its keys, but the adversary cannot bind the compromised MN to a new pair of authentication keys. Similar to [19], we assume that the communications between MNs and the SP are anonymized (e.g., with IP and MAC address recycling techniques and Mix Networks).

2.2.3 Our Goals

With respect to incentive, we ensure that no MN can earn more credits than allowed by the SP. More formally, suppose the SP is willing to pay c credits for one report of a task. Then each MN can earn at most c credits by submitting reports for this task. We have two goals in preserving privacy. First, given a report, the SP cannot tell which MN has submitted this report. Second, given multiple reports submitted by the same MN, the SP cannot tell if these reports are submitted by the same MN.

2.2.4 Cryptographic Primitives

Blind Signature A blind signature scheme [51] enables a user to obtain a signature from a signer on a message, such that the signer learns nothing about the message being signed. More formally, to obtain a signature on message m, the user first blinds the content of m with a random blinding factor, and then sends the blinded message m' to the signer. The signer signs on m' using a standard signing algorithm (e.g., RSA), and passes the signature σ' back to the user. The user removes the blinding factor from σ', and obtains a signature σ on m which can be verified using the signer's public key. This process satisfies two properties. The first property is blindness, which ensures that the signer cannot link $\langle m, \sigma \rangle$

to m' or σ'. The second property is unforgeability, which ensures that from σ' the user cannot obtain a valid signature for any other message $m'' \neq m$.

We use the blind RSA signature scheme [52] due to its simplicity. However, our approach can be easily adapted to other schemes as well. The blind RSA signature scheme works as follows. Let Q denote the public modulus of RSA, e denote the signer's public key and d denote the signer's private key. To obtain a blind signature on message m, the user selects a random value z which is relatively prime to Q, and computes $m' = mz^e \mod Q$. The signer computes the signature $\sigma' = (m')^d \mod Q$. From σ', the user obtains the signature for m by computing $\sigma = (\sigma' \cdot z^{-1}) \mod Q$.

Partially Blind Signature A partially blind signature scheme (e.g., [53]) is quite similar to a blind signature scheme in that it also allows a user to obtain a signature from a signer on a message, without revealing the content of the message to the signer. The only difference is that it allows the signer to explicitly include some common information (e.g., date of issue), which is under agreement with the user, in the signature. If the common information is attached to many signatures, the signer cannot link a signature to the secret message. Our approach does not assume any specific partially blind signature scheme. We simply use $PBS_K(p, m)$ to denote a partially blind signature, where K is the signing key, m is the secret message and p is the common information attached to the signature. Note that the signer cannot link the signature to the communication session in which the signature is generated.

2.3 An Overview of our Approach

2.3.1 Basic Approach

To achieve the incentive goal that each MN can earn at most c credits from each task, our approach satisfies three conditions: (i) each MN can accept a task at most once, (ii) the MN can submit at most one report for each accepted task, and (iii) the MN can earn c credits from a report. To satisfy the first condition, the basic idea is to issue one *request token* for each task to each MN. The MN consumes the token when it accepts the task. Since it does not have more tokens for the

task, it cannot accept the task again. Similarly, to satisfy the second condition, each MN will be given one *report token* for each task. It consumes the token when it submits a report for the task and thus cannot submit more reports. To satisfy the last condition, when the SP receives a report, it issues pseudo-credits to the reporting MN which can be transformed to *c credit tokens*. The MN will deposit these tokens to its credit account.

To achieve the privacy goals, all tokens are constructed in a privacy-preserving way, such that a request (report) token cannot be linked to a MN and a credit token cannot be linked to the task and report from which the token is earned.

Thus, our approach precomputes privacy-preserving tokens for MNs which are used to process future tasks. To ensure that MNs will use the tokens appropriately (i.e., they will not abuse the tokens), commitments to the tokens are also precomputed such that each request (report) token is committed to a specific task and each credit token is committed to a specific MN.

2.3.2 Scheme Overview

Following the aforementioned approach, we propose two schemes. The first scheme assumes a trusted third party (TTP), and uses the TTP to generate tokens for each MN and their commitments. This scheme relies on the TTP to protect each MN's privacy, and thus has very low computation and storage cost at each MN. The second scheme does not assume any TTP. Each MN generates its tokens and commitments in cooperation with the SP using blind signature and partially blind signature techniques. The use of blind and partially blind signatures protects the MN's privacy against attacks by any third party. Certainly, such unconditional privacy is not free: each MN has higher computation and storage overhead.

Both schemes work in five phases as follows.

Setup In this phase, the tokens and their commitments that each MN and the SP will use to process the next M (which is a system parameter) tasks are precomputed, and distributed to each MN and the SP. The distribution process ensures that each MN cannot get the report token for a task unless it is approved by the SP to accept the task, and it cannot get the credit tokens for a task unless it submits a report for the task.

Task assignment Suppose a MN has retrieved a task i from the SP via an anonymous communication session. If the MN decides to accept this task, it sends a request to the SP. The request includes the MN's request token. The SP verifies that the token has been committed for task i in the setup phase. If the SP allows the MN to accept this task, it returns an approval message to the MN. From the approval message, the MN can compute a report token for task i. However, the MN cannot derive a valid report token without the approval message.

Report submission After the MN generates a report for task i, it submits the report via another anonymous communication session. The MN's report token for task i is also submitted. The SP verifies that the report token has been committed for task i, and then sends pseudo-credits to the MN. From the pseudo-credits, the MN computes c credit tokens, where c is the number of credits paid for each report of task i. It cannot obtain any credit token without the pseudo-credits.

Credit deposit After the MN gets a credit token, it deposits the token to the SP after a random period of time to mitigate timing attacks. The SP verifies that the token has been committed for the MN, and then increases the MN's credit account by one.

Token and commitment renewal When the previous M tasks have been processed, the tokens and their commitments for the next M tasks should be precomputed and distributed similar to the setup phase.

Note that in the setup, credit deposit and token renewal phases, each MN communicates with the SP using its real identity. However, in the task assignment and report submission phases, each MN uses a random pseudonym generated by itself to communicate with the SP. The pseudonym cannot be linked to the real identity of the MN.

The notations used in this chapter are summarized in Table 2.1.

2.4 A TTP-based Scheme

This scheme assumes the existence of a TTP which always has Internet access.

Table 2.1. Notations

M	The num. of tasks for which credentials are precomputed
N, V	The num. of real MNs and virtual MNs in the system
$c_i \in [1, c_{max}]$	The number of credits paid for each report of task i
τ, δ, ϵ	Request token, report token, credit token
r, r_1, r_2, r_3	The secrets assigned to a MN
$K_0, ..., K_3$	The private keys of the SP to generate signatures
e, d	The SP's public and private key for blind RSA signature
sk	The secret key assigned to the SP
NID, PID	The real identity and pseudonym of a MN
H	A cryptographic hash function

2.4.1 The Basic Scheme

Setup In this phase, the TTP precomputes and distributes the tokens and commitments that will be used to process the next M tasks. Without loss of generality, suppose the IDs of these tasks are $1, 2, ..., M$.

The TTP assigns and delivers a secret r to each MN and a secret key sk to the SP. The secrets for different MNs are different. The TTP also generates a nonce ρ to identify this set of secrets, and sends it to each MN and the SP. If a new set of secrets are assigned to the SP and MNs later, a new nonce will be generated. The TTP computes other credentials using the set of secrets and the nonce.

We first describe how to generate the tokens and commitments for a single MN. Let r denote the secret of this MN. From r and the nonce ρ, the TTP derives three other secrets $r_1 = H(r|\rho|1)$, $r_2 = H(r|\rho|2)$ and $r_3 = H(r|\rho|3)$. Then it generates the tokens and commitments in three steps.

Step 1. The TTP computes M request tokens for the MN. Each token will be used for one task. The token for task i ($i \in [1, M]$) is $\tau_i = H(0|H^i(r_1))$. Here, the one-wayness of hash chain is exploited to calculate τ_i (see explanations in Chapter 2.4.2). The commitment to τ_i is $\langle H(\tau_i), i\rangle$.

Step 2. The TTP computes M report tokens for the MN, with each token used for one task. The token for task i is $\delta_i = \text{HMAC}_{r_2}(i|\text{HMAC}_{sk}(\rho|\tau_i))$. Its commitment is $\langle H(\delta_i), i\rangle$.

Step 3. The TTP computes $M \cdot c_{max}$ credit tokens. Since at this time the TTP does not know the number of credits that the SP will pay for each task, it generates the maximum possible number of credit tokens for each task. The tokens for task i are computed as $\epsilon_{ij} = \text{HMAC}_{r_3}(j|i|(s' \oplus H^j(s'')))$ for $j = 0, ..., c_{max} - 1$,

where $s' = \text{HMAC}_{sk}(0|\rho|\delta_i)$ and $s'' = \text{HMAC}_{sk}(1|\rho|\delta_i)$. The commitment of ϵ_{ij} is $\langle H(\epsilon_{ij}), NID\rangle$, where NID is the MN's real identity.

Following these steps, the TTP can also generate the tokens and commitments for other MNs. The TTP randomly shuffles each category of commitments and sends them to the SP.

At the end of this phase, each MN gets one secret and one nonce. The SP gets one secret key, one nonce, $N \cdot M$ commitments for request (report) tokens and $N \cdot M \cdot c_{max}$ commitments for credit tokens. The TTP stores the secret key of the SP, the secret of each MN and the nonce.

Task Assignment Suppose a MN has retrieved a task i. If it decides to accept this task, it sends a request to the SP using a pseudonym PID_1. The request contains its request token for this task, which is $\tau_i = H(0|H^i(r_1))$ where $r_1 = H(r|\rho|1)$.

$$\text{MN} \rightarrow \text{SP}: \quad PID_1, i, \tau_i \tag{2.1}$$

The SP verifies that $\langle H(\tau_i), i\rangle$ is a valid commitment and deletes this commitment to avoid token reuse. Then it sends an approval message to the MN:

$$\text{SP} \rightarrow \text{MN}: \quad \text{HMAC}_{sk}(\rho|\tau_i) \tag{2.2}$$

From this message, the MN computes its report token for task i, i.e.,
$\delta_i = \text{HMAC}_{r_2}(i|\text{HMAC}_{sk}(\rho|\tau_i))$ where $r_2 = H(r|\rho|2)$.

Report Submission When the MN, using a pseudonym PID_2, submits a report for task i, it also submits its report token δ_i for this task:

$$\text{MN} \rightarrow \text{SP}: \quad PID_2, i, \delta_i, report \tag{2.3}$$

The SP verifies that $\langle H(\delta_i), i\rangle$ is a valid commitment and deletes this commitment to avoid token reuse. Then it computes $s' = \text{HMAC}_{sk}(0|\rho|\delta_i)$, $s'' = \text{HMAC}_{sk}(1|\rho|\delta_i)$ and $s''' = H^{c_{max}-c_i}(s'')$ and sends the following back to the MN.

$$\text{SP} \rightarrow \text{MN}: \quad s', s''' \tag{2.4}$$

Using s' and s''', the MN computes c_i credit tokens

$\epsilon_j = \text{HMAC}_{r_3}(j|i|(s' \oplus H^j(s''))) = \text{HMAC}_{r_3}(j|i|(s' \oplus H^{c_{max}-c_i+j}(s')))$ for $j = 0, ..., c_i - 1$. Due to the one-way property of H, the MN cannot obtain other credit tokens.

Credit Deposit After the MN gets a credit token ϵ, it waits a length of time randomly selected from $(0, T]$ to mitigate timing attacks (see Chapter 2.4.3) and then deposits the token using its real identity NID:

$$\text{MN} \rightarrow \text{SP}: \quad NID, \epsilon \tag{2.5}$$

The SP verifies that $\langle H(\epsilon), NID \rangle$ is a valid commitment and deletes this commitment to avoid token reuse. Then it increases the MN's credit account by one.

Commitment Renewal When the first M tasks have been processed, the SP should communicate with the TTP again to obtain another set of commitments for the next M tasks. The commitments for the previous M tasks will be deleted later as discussed in Chapter 2.4.4. The SP's secret key, each MN's secret and the nonce are not changed.

2.4.2 Dealing with Dynamic Joins and Leaves

Join In the setup phase, the TTP assumes the existence of V (a system parameter) virtual MNs besides the N real MNs. It generates the tokens and commitments for both real and virtual MNs. Also, it sends the commitments to the request and report tokens of the virtual MNs, mixed with the commitments for the real MNs, to the SP.

When a new MN joins, the TTP maps it to an unused virtual MN and sends the virtual MN's secret r to it. Also, the TTP generates the credit tokens for the new MN (i.e., the mapped virtual MN) and sends their commitments to the SP. Afterward, it tags the mapped virtual MN as used.

If there is no available unused virtual MN when the new MN joins, the TTP reruns the setup phase again in which a new set of secrets are issued to the SP and all the current MNs as well as a new set of virtual MNs. Some MNs may not have network access during the setup phase and hence cannot receive the new nonce and their new secrets. To address this problem, whenever a MN retrieves tasks from the SP, it checks if it has the same nonce ρ with the SP. Note that the SP

always has the latest version of nonce. If the MN's nonce is out of date, it means that the MN has missed the previous setup phase and its secret is also out of date. In this case, the MN connects to the TTP to update its secret and nonce.

In practice, the value of parameter V can be adjusted according to churn rate. If the churn rate is high (i.e., new MNs join frequently), a larger V can be used to reduce the number of reruns of the expensive setup phase, at the cost of higher storage at the SP. If the churn rate is low, a smaller V can be used to reduce the storage overhead at the SP.

Leave When a MN leaves, its request tokens for future tasks should be invalidated at the SP. Note that if the request token for a future task is invalidated, the report token and credit tokens for the same task are also invalidated automatically, since the the leaving MN will not be able to compute them. Let r denote the leaving MN's secret, ρ denote the current nonce and $r_1 = H(r|\rho|1)$. The TTP releases $\lambda = H^i(r_1)$ to the SP, where i is the next task to be published. From λ, the SP can compute the request tokens of the leaving MN for future tasks. For example, the token for a future task $i + j$ is $H(0|H^j(\lambda))$. The SP will invalidate these tokens. However, due to the one-way property of H, the SP cannot derive the tokens that the leaving MN used in previous tasks. No changes are made to other MNs.

2.4.3 Addressing Timing Attacks

If a MN deposits a credit token earned from a report immediately after it submits the report, since it uses its real identity to deposit the token, the SP may be able to link the report to it via timing analysis. Thus, the MN should wait some time before it deposits the credit token. Specially, after a MN gets a credit token, it waits a length of time randomly selected from $(0, T]$ and then deposits the token.

The parameter T is large enough (e.g., one month) such that, in each time interval T, many tasks can be created and most MNs have chances to connect to the SP. The SP will store the commitments to the credit tokens for a time period of at least $2T$ (see Chapter 2.4.4), such that most MNs can deposit their credit tokens before the commitments are deleted. If a MN (e.g., with very infrequent network access) wants to deposit some credit tokens after their commitments are deleted, the SP can check the validity of these tokens with the TTP, and update

the MN's credit account accordingly.

2.4.4 Commitment Removal

The SP removes the commitments to the previous M tasks as follows. Note that part of commitments are removed to avoid token reuse immediately after the corresponding tokens are verified. Since not all MNs accept all tasks, some commitments may remain after the previous M tasks have been processed. Let t_{exp} denote the maximum time at which each of the previous M tasks will expire. Note that all reports for the M tasks are submitted before t_{exp} and all credit tokens paid for these reports are sent to MNs before t_{exp}. Thus, the SP can remove the remaining commitments to request and report tokens after time t_{exp}. To allow MNs to deposit their earned credit tokens, the SP stores the remaining commitments to credit tokens for another time period of $2T$ (as discussed in Chapter 2.4.3), and removes them after time $t_{exp} + 2T$.

2.4.5 Security Analysis

Attacks on Incentive Without loss of generality, let us consider a task i which is paid at a rate of c credits per report.

Our scheme ensures that each MN can earn at most c credits from the task by satisfying three conditions. First, the MN can only obtain one request token for the task and hence can only be approved by the SP once to report for the task. Second, from the approval message sent by the SP, the MN can only get one report token and thus can submit at most one report for the task. Third, after submitting a report, the MN can only obtain c credit tokens.

Also, if a MN is not approved by the SP to accept the task, it cannot obtain the report token and thus cannot submit a report for the task. Without submitting a report, it cannot obtain the credit tokens and thus cannot earn credits from the task.

A dishonest MN may forge tokens, but the forged tokens cannot pass the commitment check. The MN may use the request token of task j (i.e., τ_j) to request for task i, but this will fail since the commitment to τ_j (i.e., $\langle H(\tau_j), j\rangle$) has bound τ_j to j. Similarly, the MN cannot use the report token of one task to another task.

A dishonest MN may have compromised a number of other MNs and obtained their secrets. It may use the request token of a compromised MN to request for task i, use the report token of the compromised MN to submit a report and obtain some credit tokens. However, the obtained credit tokens have been bound to the compromised MN by their commitments, and thus cannot be deposited to the dishonest MN's credit account. If the dishonest MN is not approved to report for task i but those compromised MNs are, it may submit its own tokens from one compromised MN and earn c credits. However, it still cannot increase its credits using the tokens of the compromised MNs. Thus, the dishonest MN cannot earn more than c credits from task i no matter how many MNs it compromises.

Attacks on Privacy Since each MN uses pseudonyms to retrieve tasks, request tasks and submits reports, the SP cannot know the MN that has submitted a specific report from whom it is communicating with. Also, the SP cannot know the information from the request and report tokens, since the tokens have been randomized (i.e., anonymized) by each MN's secrets that the SP does not know. For similar reasons, the SP cannot link multiple reports submitted by the same MN.

The SP can link a credit token to a MN, since the MN uses its real identity to deposit the credit token. However, the SP cannot link the credit token to the report and task (or the report token and request token) from which the credit is earned, since the connection between them has been anonymized using the MN's secret r_3. Thus, linking a credit token to a MN does not help the SP to break the MN's privacy.

2.4.6 Cost Analysis

Each MN only stores one secret and one nonce. The TTP stores the secret key of the SP, the secret of each MN and the nonce. It can be seen that the storage at each MN and the TTP is low. The SP mainly stores $M(N+V)(2c_{max}+1)$ commitments for the next M tasks, where N (V) is the number of real (virtual) MNs. It also stores $(N+V)c_{max}$ credit token commitments for each task created in the past time window $2T$. Let us consider a simple case. Suppose $N = 10000$, $V = 1000$, $M = 1000$, $c_{max} = 5$, $T = 30$ days and 1000 tasks are generated per

day. Also, suppose SHA-256 is used as the hash function H, and each task ID or node ID has 8 bytes. Then the storage at the SP is about 137GB. We expect that such storage cost is not an issue for modern servers.

For each task (throughout the setup, task assignment, report submission and credit deposit phases), each MN computes at most $c_{max} + 2$ hashes and $c_{max} + 1$ HMACs, the SP computes at most $2N(c_{max} + 1)$ hashes and $3N$ HMACs, and the TTP computes $(N + V)(3c_{max} + 4)$ hashes and $(N + V)(c_{max} + 4)$ HMACs. Since hash and HMAC are extremely efficient, the computation cost is low.

Since each message that a MN sends and receives mainly contains one or two hash values, the communication cost is about two hundred bytes per task for each MN, which is low.

2.5 A TTP-Free Scheme

To provide privacy-aware incentives for the scenarios where no TTP is available, we design a TTP-free scheme. It uses blind signature and partially blind signature to generate tokens and commitments for MNs in a privacy-preserving way.

2.5.1 The Scheme

The SP has three private keys K_1, K_2 and K_3 which are used to generate partially blind signatures, and another private key K_0 which is used to generate traditional digital signatures. The SP also has a private key d and public key e which are used to generate blind RSA signatures. These keys are assigned by a (possibly offline) certificate authority. Besides, the SP has a secret key sk generated by itself, and each MN has three secrets r_1, r_2 and r_3 generated by itself.

Setup Each MN communicates with the SP with its real identity to obtain the tokens and commitments for the first M tasks. Suppose these tasks' identifier are $1, 2, ..., M$.

For each task i $(i = 1, 2, ..., M)$, the MN computes c_{max} random values $m_{ij} = H(i|j|H^i(r_1))$ where $j = 1, 2, ..., c_{max}$. Each value and the SP's RSA signature over the value constitute one credit token, which is $\epsilon_{ij} = \langle m_{ij}, SIG_d(m_{ij})\rangle$. However, the MN cannot obtain the RSA signature until it submits a report for this task.

To commit to credit token ϵ_{ij}, the MN sends $H(m_{ij})$ and its real identity NID to the SP. The SP signs on $\langle H(m_{ij}), NID\rangle$ with key K_0 and returns the signature $SIG_{K_0}(H(m_{ij})|NID)$. Then the MN obtains the commitment to ϵ_{ij}, which is $\langle H(m_{ij}), NID, SIG_{K_0}(H(m_{ij})|NID)\rangle$. To reduce the computation cost, the SP can build a Merkle hash tree [54] over all $\langle H(\epsilon_{ij}), NID\rangle$ of the same MN, and generates just one digital signature for all of them. The SP ensures that no two $H(m_{ij})$ (of the same MN or different MNs) are identical. Since each m_{ij} is a result of the hash function H, the probability of generating two identical m_{ij} (and $H(m_{ij})$) is negligible.

For each m_{ij}, the MN generates a random blinding factor $z_{ij} = H(i|j|H^i(r_2)|x)$, where x is the smallest positive integer such that z_{ij} is relatively prime to the pubic modulus Q of the RSA signature. From each pair of m_{ij} and z_{ij}, the MN computes $\mu_{ij} = m_{ij} \cdot z_{ij}^e \mod Q$. Then it computes c_{max} report token components for task i which are $b_{ij} = H(\mu_{i1}|\mu_{i2}|...|\mu_{ij}|i|j)$ where $j = 1, 2, ..., c_{max}$. Each b_{ij} and the SP's partially blind signature $PBS_{K_2}(i, b_{ij})$ over it constitute one possible report token for task i, which is $\delta_{ij} = \langle b_{ij}, PBS_{K_2}(i, b_{ij})\rangle$. However, the MN cannot obtain the signature until it is approved by the SP to accept this task. Only one report token for task i will be obtained by each MN.

To commit to report token δ_{ij}, the MN obtains a partially blind signature $PBS_{K_3}(i, b_{ij})$ from the SP. However, the SP does not send this signature to the MN in plaintext. It encrypts the signature with key $k_{ij} = H(sk|i|j)$, and sends the ciphertext $E_{k_{ij}}(PBS_{K_3}(i, b_{ij}))$ to the MN. Given i and j, the SP uses the same encryption key k_{ij} for all MNs.

For each task i, the MN generates a request token $\tau_i = H(0|H^i(r_3))$. Similar to the TTP-based scheme, hash chain is used to calculate τ_i. To commit to token τ_i, it obtains a partially blind signature $PBS_{K_1}(i, \tau_i)$ from the SP.

In the end, each MN obtains M commitments to request tokens, $M \cdot c_{max}$ encrypted commitments to report tokens, and $M \cdot c_{max}$ commitments to credit tokens. The tokens τ_i, δ_{ij}, and ϵ_{ij} can be stored for later use or generated on the fly.

Since b_{ij} is committed, $\mu_{i1}, \mu_{i2}, ..., \mu_{ij}$ are also committed due to the one-way property of H. Considering that m_{ij} is committed, the random blinding factor z_{ij} is fixed. Thus, each MN cannot change its credentials after the setup phase.

Task Assignment When the SP publishes task i, it also publishes c_i, which is the number of credits paid for each report of task i. In the following, we omit the subscript and refer to the number as c for simplicity. The SP also publishes a key $k' = k_{ic} = H(sk|i|c)$. Note that in the setup phase, each MN generated c_{max} report token components for task i and obtained an encrypted commitment for each of them. From c, each MN knows that the report token component it should use for task i is $b_{ic} = H(\mu_{i1}|\mu_{i2}|...|\mu_{ic}|i|c)$. Using key k', it can decrypt the commitment to b_{ic}, which is $PBS_{K_3}(i, b_{ic})$.

Suppose a MN has retrieved a task i. If it decides to accept task i, it sends a request to the SP using a pseudonym PID_1. The request includes the MN's request token τ_i and its commitment $PBS_{K_1}(i, \tau_i)$.

$$\text{MN} \rightarrow \text{SP}: \;\; PID_1, i, \tau_i, PBS_{K_1}(i, \tau_i) \tag{2.6}$$

The SP verifies the signature $PBS_{K_1}(i, \tau_i)$, and knows that token τ_i has been committed for task i. Then the MN obtains a partially blind signature $PBS_{K_2}(i, b_{ic})$ on b_{ic} from the SP via a standard partially blind signature scheme. Conceptually, the SP delivers the signature in an approval message:

$$\text{SP} \rightarrow \text{MN}: \;\; PBS_{K_2}(i, b_{ic}) \tag{2.7}$$

Now the MN obtains a report token for task i, which is $\delta_{ic} = \langle b_{ic}, PBS_{K_2}(i, b_{ic})\rangle$.

Report Submission When the MN, using a pseudonym PID_2, submits a report for task i, it also submits its report token for this task and the commitment:

$$\text{MN} \rightarrow \text{SP}: PID_2, i, b_{ic}, PBS_{K_2}(i, b_{ic}), PBS_{K_3}(i, b_{ic}), \mu_{i1}, \mu_{i2}, ..., \mu_{ic}, report \tag{2.8}$$

Signature $PBS_{K_2}(i, b_{ic})$ ensures that the MN has been approved by the SP to report for task i, and signature $PBS_{K_3}(i, b_{ic})$ ensures that b_{ic} has been committed for task i. If the two signatures are valid, the SP can issue c pseudo-credits to the MN. Specifically, the SP first verifies that $b_{ic} \equiv H(\mu_{i1}|\mu_{i2}|...|\mu_{ic}|i|c)$. Due to the one-way property of H, the SP knows that each μ_{ij} $(j = 1, 2, ..., c)$ has also been committed for task i. Then it signs each μ_{ij} with the private key d and sends the

signatures to the MN.

$$\text{SP} \rightarrow \text{MN:}\ \ SIG_d(\mu_{i1}), SIG_d(\mu_{i2}), ..., SIG_d(\mu_{ic}) \tag{2.9}$$

From each signature $SIG_d(\mu_{ij})$, the MN removes the blinding factor $z_{ij}^e \mod Q$ and gets a blind RSA signature for m_{ij} which is $SIG_d(m_{ij})$. Then it obtains c credit tokens $\epsilon_{ij} = \langle m_{ij}, SIG_d(m_{ij}) \rangle$ $(j = 1, 2, ..., c)$.

Credit Deposit After the MN gets a credit token $\epsilon = \langle m, SIG_d(m) \rangle$, it waits a length of time randomly selected from $(0, T]$ to mitigate timing attacks (see Chapter 2.4.3) and then deposits the token using its real identity NID:

$$\text{MN} \rightarrow \text{SP:}\ NID, m, SIG_d(m), SIG_{K_0}(H(m)|NID) \tag{2.10}$$

The second signature means that the credit token has been committed to this MN. The SP verifies the two signature and then increases the MN's credit account by one.

Token and Commitment Renewal When the first M tasks have finished or expired, each MN should communicate with the SP to obtain a new set of commitments (as done in the setup phase) for the next M tasks whose identifiers are $M + 1, M + 2, ..., 2M$. The keys used by each MN and the SP do not change. Similarly, renewal is needed for every task group $[k \cdot M + 1, (k + 1)M]$ $(k \geq 0)$.

The SP may launch isolation attacks, in which it only issues the commitments for the next M tasks to one MN. When the MN submits reports for these tasks, the SP can link the reports to it. To address this attack, each MN generates a signature over the task ID range (i.e., the smallest and largest ID) of the next M tasks. Before submitting a report for a task, each MN makes sure that the SP has collected signatures from a large-enough number of MNs (e.g., half of the MNs).

2.5.2 Dealing with Dynamic Joins and Leaves

Let i denote identifier of the most recently created task. Suppose $k \cdot M \leq i < (k + 1)M$. When a new MN joins, it obtains the commitments for the tasks in range $[i + 1, (k + 1)M]$ from the SP, as done in the setup phase. When a node leaves, its credentials for the tasks in range $[i + 1, (k + 1)M]$ should be revoked.

Let r_1, r_2 and r_3 denote its secrets. The MN releases $H^{i+1}(0|r_1)$, $H^{i+1}(0|r_2)$ and $H^{i+1}(0|r_3)$ to the SP. From them, the SP can compute the leaving MN's tokens and commitments for those tasks, and invalidate them. Due to the one-way property of hash function H, the SP cannot derive the credentials that the leaving MN used for previous tasks.

2.5.3 Credential Removal

A MN removes the credentials for a task if it decides not to accept the task. For the tasks that it accepted, the tokens and commitments can be removed after they are submitted or deposited to the SP.

2.5.4 Security Analysis

Attacks on Incentive Similar to the analysis in Chapter 2.4.5, the TTP-free scheme also ensures that each MN can earn at most c credits from a task.

A dishonest MN may forge tokens but these tokens will fail the commitment check. Since the commitment to each request (report) token binds the token to a task identifier, the MN cannot use the request (report) token of one task to process another task.

A dishonest MN may compromise a number of other MNs but it still cannot earn more than c credits from a task. Since the commitment of each credit token binds the token to a specific MN, the dishonest MN cannot deposit the credit tokens of the compromised MNs to its own account. It may use the report tokens of a compromised MN to submit reports, but the obtained credit tokens have been committed to the compromised MN. This is because, given b_{ij}, the μ_{i1}, ..., μ_{ij} used to generate b_{ij} are determined due to the one-wayness of hash function H. Due to the unforgeability of blind signature, the m_{i1}, ..., m_{ij} are also determined. In the next token renewal phase, the dishonest MN may want to bind the credit tokens of the compromised MNs (in addition to its own credit tokens) to its own identity, but the binding of more than one set of credit tokens to the same MN will be detected by the SP.

Attacks on Privacy Since each request and report token (as well as its commitment) is constructed using a partially blind signature, the SP cannot know the MN

that has submitted a specific report, and cannot link multiple reports submitted by the same MN. Although the SP can link a credit token to a MN, since the connection between the credit token and its corresponding report token is anonymized using a blind RSA signature (i.e., the connection between m_{ij} and μ_{ij} is blinded with the random factor z_{ij}), the SP cannot link the credit token to the report from which the credit is earned. Thus, linking a credit token to a MN does not lead to any privacy leakage.

2.5.5 Cost Analysis

Each MN mainly stores $M(2c_{max}+1)$ commitments for the next M tasks. It also stores the credit tokens earned during the past time interval T. Let us consider a simple case. Suppose the parameters are the same as in Chapter 2.4.6, and a MN accepts 100 tasks per day. Also, suppose RSA (1024-bit) is used as the digital signature scheme and partially blind RSA [55] is used as the partially blind signature scheme. Then the storage at each MN is about 2.7MB. The cost is not an issue for modern smart phones with many gigabytes of storage.

For the whole life cycle of each task, each MN mainly performs one modular exponentiation and participates in the generation of $c_{max}+2$ partially blind signatures. In the setup phase, the SP generates $N \cdot M \cdot c_{max}$ digital signatures and $NM(c_{max}+1)$ partially blind signatures. Later on, when the SP receives a request, report or credit token, it generates at most c_{max} signatures and verifies at most two signatures.

Each message mainly contains at most c_{max} signatures or hashes. Since expectedly c_{max} is not large in practice, the communication cost is low. Under the aforementioned parameter settings, it is about 4.5KB per task. Considering that setup and credit deposit can run when the MN has WiFi access, the remaining cost is about 1.4KB per task.

2.6 Evaluations

To study the feasibility of our solution, we have built a prototype and implemented our schemes in Java. The prototype has three components: a MN, a SP and a

Table 2.2. The running time of our schemes when $M = 1000$ and $c_{max} = 5$

		Setup	Task Assignment	Report Submission	Credit Deposit
TTP-based	TTP	45ms*	-	-	-
	SP	-	4μs	8μs	4μs
	MN	-	0.56ms	2.4ms	-
TTP-free	SP	32s*	4.1ms	8.2ms	0.2ms
	MN	37s	6.3ms	0.5ms	-

* The time is needed to generate credentials for each MN.

TTP. The MN is implemented on Android Nexus S Phone, which is equipped with 1GHz CPU, 512MB RAM, running Android 4.0.4 OS. The SP and TTP are implemented on a Windows laptop with 2.6GHz CPU and 4GB RAM. For simplicity, our prototype uses RSA as the digital signature scheme and partially blind RSA [55] as the partially blind signature scheme. SHA-256 is used as the hash function.

Table 2.2 shows the running time of our schemes when $M = 1000$ and $c_{max} = 5$. In the TTP-based scheme, every phase can be finished within tens of milliseconds, which means the computation cost is very low. In the TTP-free scheme, the task assignment, report submission and credit deposit phases only take several milliseconds. The running time of the setup phase is long (around half a minute) for both the MN and the SP, which means high computation cost. However, such cost is amortized among 1000 tasks. Also, the running time can be significantly reduced if other more efficient signature schemes are used instead of RSA. Using other native libs (e.g., OpenSSL) in combination with Java can also reduce the running time. Moreover, the SP can be implemented on more powerful high-end servers to further shorten the running time. Lastly, since the setup phase for certain tasks is run before these tasks are created, the running time is not a big issue even for tasks with real-time requirements.

We also measure the power consumption of the smartphone. In the experiment, the smartphone iteratively runs the whole life cycle of one task (setup, task retrieval & assignment, report submission, and credit deposit) for 2500 (500) tasks in the TTP-based (TTP-free) scheme. The smartphone communicates with the laptop using TCP connections via WiFi, and it initiates a new TCP connection for each phase. In this process, we use Agilent E3631A Power Supply to power the smartphone at a constant voltage and program it to capture the current of the

Table 2.3. The power consumption of our schemes on a smartphone

Scheme	TTP-based	TTP-free
Power (W)	0.363	0.349
Energy cost per task (J)	0.05	0.22
Num. of Tasks per Battery (3.7V, 1500mAh)	399600	90818

smartphone. From the voltage and current, the power consumption can be easily calculated. Table 2.3 shows the results. The TTP-based scheme only consumes 0.05 joules to process each task. The TTP-free scheme consumes a little more energy, which is 0.22 joules, due to the use of computation expensive cryptography. However, the power consumption of both schemes is low. For example, a fully-charged standard battery for a Nexus S phone (3.7V, 1500 mAh) can support 400 (90) thousand tasks when the TTP-based (TTP-free) scheme is used.

2.7 Discussions

The SP may infer if a MN has accepted a task from the number of credits that the MN has earned, and then cause privacy leakage. For instance, suppose the SP has published 100 tasks, each of which is paid at a rate of one credit per report. If a participant Bob has earned 100 credits, the SP can infer that Bob has submitted a report for every task. If one of the tasks is "Report the temperature at 10:00 AM in Central Park," the SP knows that Bob is in Central Park at 10:00 AM. To launch this attack, the SP may create multiple tasks that require the MN to appear at close-by times (e.g., 10:01 AM) and locations. In the above example, suppose 51 tasks require a temperature reading near Central Park around 10:00AM. If Bob has earned 50 credits, at least one credit is earned from those 51 tasks. Thus the SP knows that Bob is near Central Park around 10:00 AM.

To address this attack, each MN should carefully select the tasks that it will accept and limit the number of accepted tasks. One possible approach is as follows. Among the tasks that it is able to report for, the MN identifies the "similar" tasks which may reveal the same privacy information about it (e.g., its location around a certain time). For each group of similar tasks, it accepts one of them with a certain probability (e.g., 0.5). This ensures that the number of its accepted tasks does not exceed the number of similar-task groups. From the number of credits earned

by a MN, the SP does not know which tasks the MN has reported for, and thus cannot infer any private information about the MN. Since each MN intentionally omits some tasks, this approach sacrifices some chances of earning credits for better privacy. We plan to explore this topic in future work.

2.8 Related Work

Many schemes [19, 20, 21, 56, 57, 58, 59, 60, 61, 31] have been proposed to protect user privacy in mobile sensing. AnonySense [19] and PEPSI [20] enable anonymous data collection from mobile users. DeCristofaro et al [62] considered scenarios where external entities query specific users' sensing data and proposed a scheme to hide which user matches a query. Gilbert et al [63] proposed to use TPM to secure user data. Privacy-aware data aggregation in mobile sensing has also been studied by several works [64, 65, 32]. However, these schemes cannot provide incentives for users to participate. Christin et al [21] proposed a privacy-aware reputation scheme for mobile sensing which uses reputation to filter incorrect sensor readings, but their solution does not address incentive either. Recently, Yang et al [22] proposed incentive schemes for mobile sensing based on gaming and auction theories, but their work does not consider the protection of user privacy. Privacy-aware incentives designed for other applications (e.g., publish-subscribe systems) [66] cannot be directly applied here since they do not consider the requirements of mobile sensing.

2.9 Summary

To facilitate large-scale deployment of mobile sensing applications, we proposed two credit-based privacy-aware incentive schemes to promote user participation, corresponding to scenarios with and without a TTP respectively. Based on hash and HMAC functions, the TTP-based scheme has very low computation and storage cost at each MN. Based on blind and partially blind signatures, the TTP-free scheme has higher overhead at each MN but it ensures that no third party can break the MN's privacy. Both schemes can efficiently support dynamic joins and leaves.

Chapter 3

Efficient and Privacy-Preserving Stream Aggregation

3.1 Introduction

In many scenarios, stream data from the mobile users over time can be collected, aggregated, and mined for obtaining or identifying useful patterns or statistics over a population [24]. In applications such as CarTel [67] and N-SMARTS [68], participants generate time-series data such as their location, speed, the pollution density and noise level in their surroundings, etc. These data can be aggregated to obtain the traffic pattern and pollution map. For another example, the average amount of exercise (which can be measured by motion sensors on smartphones [5]) that people do in every day can be used to infer public health conditions.

Although aggregation statistics computed from time-series data is very useful, in many scenarios, the data from individual user may be privacy-sensitive, and users do not trust any single third-party aggregator to see their data in cleartext. For instance, to monitor the propagation of a new flu, the aggregator will count the number of users infected by this flu. However, a user may not want to directly provide his true status ("1" if being infected and "0" otherwise) if he is not sure whether the information will be abused by the aggregator. Accordingly, systems that collect users' true data values and compute aggregate statistics over them may not meet users' privacy requirement [24]. Thus, an important challenge is how to

Table 3.1. Comparison between existing schemes and our scheme.

Scheme	Comm. per interval	Comm. model	Aggregation error	Dynamic join & leave	Comm. per join & leave	Cryptography
[27]	$O(n)$	N $\leftrightarrow$ A	$O(1)$	No	-	Public-key
[28]	$O(n)$	N $\rightarrow$ A	$O(1)$	No	$O(n)$	Public-key
[29]	$O(n \log n)$	N $\rightarrow$ A	$\tilde{O}((\log n)^{\frac{3}{2}})$	Yes	$O(1)$	Public-key
[30]	$O(n)$	N $\rightarrow$ A	$O(1)$	Yes	$O(1)$	Public-key
Our scheme	$O(n)$	N $\rightarrow$ A	$O(1)$	Yes	$O(d)$	Symmetric-key

$N \rightarrow A$: node-to-aggregator uni-directional.
$N \leftrightarrow A$: interactive between node and aggregator.
n: number of nodes. d: a parameter of our scheme (smaller than 100 in most settings).

protect the users' privacy in mobile sensing, especially when the aggregator is untrusted.

Recently, the problem of privacy-preserving aggregation of time-series data in presence of untrusted aggregator has been studied by Rastogi et al. [27] and Shi et al. [28]. They combine differential privacy [25, 26] and cryptography techniques to provide distributed differential privacy, such that only negligible information about the node can be leaked even if the aggregator has arbitrary auxiliary information. In these schemes, each node independently adds appropriate noise to his data before aggregation, and the aggregator gets a noisy sum instead of the accurate sum. A large enough noise is accumulated in the aggregate to achieve differential privacy. These schemes also rely on a special encryption technique where each node encrypts its noisy data with a key, sends the encrypted data to the aggregator which can decrypt the sum of the nodes' noisy data without learning anything else.

However, these schemes cannot efficiently support dynamic joins and leaves. For example, in [28], when a node joins or leaves, the encryption keys of all nodes are updated, which means high communication overhead in a large system. Thus, they are not suitable for mobile sensing applications with many nodes and high churn rate. Also, they have high computation overhead due to the use of asymmetric-key cryptography. For example, for an application in which the plaintext space of sensing data can reach 10^{41} and the system scale reach one million nodes, the construction in [28] requires 30 seconds to decrypt the sum on a modern

[1]For instance, carbon dioxide levels can range from 350 ppm outdoors to over 10000 ppm in industrial workplaces [69]. In applications that monitor the carbon dioxide levels that people are exposed to [70, 71], the plaintext space can reach 10^4.

64-bit desktop PC. Hence, they are inefficient for an aggregator to run realtime monitoring applications with short aggregation intervals and to collect multiple aggregate statistics simultaneously. Chan *et al.* [29] propose a binary interval tree technique which can reduce the communication cost for joins and leaves, but their scheme has high aggregation error (i.e., the difference between the noisy sum and the accurate sum), which means poor utility of the aggregate. A recent scheme [30] can efficiently support dynamic joins and leaves, but it still has high computation overhead due to the use of public-key cryptography. Moreover, none of these existing schemes considers the Min aggregate (i.e., the minimum value) of time-series data, which is also important in many mobile sensing applications.

In this chapter, we propose a new differentially private protocol for mobile sensing to obtain the sum aggregate of time-series data in the presence of an untrusted aggregator. Different from previous works which use computationally expensive asymmetric-key cryptography (see Table 3.1), our protocol is purely built upon computationally efficient symmetric-key cryptography (i.e., HMAC). Hence, it has very low computation cost. The second nice property of our protocol is that it can efficiently deal with dynamic joins and leaves. Specifically, when a node joins or leaves, only a small number of nodes need to update their encryption keys, which is in the order of tens in most practical settings irrespective of the total number of nodes. Another nice property is that our protocol has low aggregation error. All nodes only *collectively* add $O(1)$ noise (required for differential privacy) to the sum aggregate. These salient properties make our protocol more appropriate for application scenarios with resource-constrained mobile devices, high aggregation loads, and high node dynamics.

Our aggregation protocol for Sum relies on two novel techniques. The first technique is an efficient HMAC-based encryption scheme (see Chapter 3.4), which allows the aggregator to obtain the sum of all nodes' data but nothing else (e.g., any individual node's data or intermediate result). In this scheme, each node (the aggregator) only needs to compute a very small number of HMACs to encrypt his data (decrypt the sum), which is very efficient in computation. Also, this scheme only needs to add a small amount of noise to the sum aggregate, leading to low aggregation error. The second technique is overlapped grouping (see Chapter 3.5), which is devised to efficiently deal with dynamic joins and leaves. Specifically, we

design a novel ring-based overlapped grouping construction, which divides nodes into groups of smaller size such that at most three (four) groups of nodes need to be updated for each join (leave).

Based on the sum aggregation protocol, we also propose a protocol to obtain the Min aggregate. To our best knowledge, this is the first privacy-preserving solution to obtain the Min of time-series data in mobile sensing with just one round of node-to-aggregator communication. Our protocols for Sum and Min can be easily adapted to derive many other aggregate statistics such as Count, Average and Max.

3.2 Related Work

Many works have addressed various security and privacy issues in mobile sensing networks and systems (e.g., [23, 58, 20, 44]), but they do not consider data aggregation. There are a lot of existing works (e.g., [72, 73, 74, 75]) on security and privacy-preserving data aggregation, but most of them assume a trusted aggregator and cannot protect user privacy against untrusted aggregators. For example, in [74], the aggregator knows the encryption key used by each participant and thus can know the data of any individual user. Yang et al. [76] proposed an encryption scheme that allows an untrusted aggregator to obtain the sum of multiple nodes's data without knowing any specific node's data. However, their scheme requires expensive re-keying operations to support multiple time steps, and thus may not work for time-series data. Secure multiparty computation techniques [77] can be used for sum aggregation, but they require interactions among nodes and the computational overhead will be significantly increased as the number of nodes increases.

Shi et al. [65] proposed a privacy-preserving data aggregation scheme based on data slicing and mixing techniques. However, their scheme relies on peer-to-peer communications among nodes, which is nontrivial in mobile sensing scenarios due to the high mobility of nodes. Also, their scheme does not work well for time-series data, since each node may need to select a new set of peers in each aggregation interval due to mobility. Besides, their scheme for non-additive aggregates (e.g., Max/Min) requires multiple rounds of bi-directional communications between the

aggregator and mobile nodes which means long delays. In contrast, our scheme obtains those aggregates with just one round of uni-directional communication from nodes to the aggregator.

To achieve privacy-preserving sum aggregation of time-series data, Rastogi and Nath [27] designed an encryption scheme based on threshold Paillier cryptosystem [78], where the decryption key is divided into portions and distributed to the nodes. The aggregator collects the ciphertexts of nodes, multiplies them together and sends the aggregate ciphertext to all nodes. Each node decrypts a share of the sum aggregate. The aggregator collects all the shares and gets the final sum. However, their scheme requires an extra round of interaction between the aggregator and nodes in every aggregation period, which means high communication cost. Moreover, it requires all nodes to be online until decryption is completed, which may not be practical in many mobile sensing scenarios due to node mobility and the heterogeneity of node connectivity.

Based on an efficient additive homomorphic encryption scheme, Rieffel et al. [79] proposed a construction that does not require an extra round of interaction between the aggregator and the nodes. In their scheme, the computation and storage cost is roughly equal to the number of colluding nodes that the system can tolerate. Thus, their scheme has high overhead to achieve good resistance to collusion, especially when the system is large and a large number of nodes collude. In contrast, our scheme tolerates a high fraction of colluding nodes (e.g., 30%) with very small cost even when the system is large. Acs and Castelluccia [80] also proposed a scheme based on additive homomorphic encryption, but in their scheme each node shares a pairwise key with any other node.

Shi et al. [28] proposed a construction for sum aggregation based on the assumption that the Decisional Diffie-Hellman problem is hard over finite cyclic groups. In their construction, each node sends his ciphertext to the aggregator and no communication is needed from the aggregator to the nodes. To decrypt the sum, however, their construction needs to traverse the possible plaintext space of sum, and thus it is not efficient for a large system with large plaintext spaces. Also, their scheme redistributes encryption keys to all nodes when a node joins or leaves, which means high communication overhead. Two other schemes [80, 81] proposed for smart metering and cognitive radio networks also cannot efficiently

support dynamic joins and leaves.

To efficiently deal with dynamic joins and leaves, Chan et al. [29] extend the construction in [28] with a binary interval tree technique which reduces expensive rekeying operations. However, in their scheme, since each node's data is aggregated into multiple sums, a large noise is added to each node's data to provide differential privacy, which leads to high aggregation error. Recent designs [82, 83] employ an honest-but-curious proxy server to tolerate the churn of a small fraction of nodes, but it is unknown how they work when many nodes leave.

Jawurek and Kerschbaum [30] proposed a fault-tolerant scheme which provides differential privacy for sum, but it employs Paillier cryptosystem which is very expensive in computation.

Grouping has been recently used for differentially-private publication of graph topologies [84, 85]. These solutions divide a dataset into *disjoint* groups, which is different from our *overlapped* grouping technique.

3.3 Preliminaries

3.3.1 Problem Definition

Our system model is shown in Figure 3.1. An aggregator wants to get the sum aggregate of n mobile nodes periodically. Let $x_i^{(t)}$ ($x_i^{(t)} \in \{0, 1, ..., \Delta\}$) denote the data of node i in aggregation period t ($t = 1, 2, 3, ...$). Then the sum aggregate for time period t is $\sum_{i=1}^{n} x_i^{(t)}$. Since the accurate sum may leak node privacy in presence of side information [25, 26], the aggregator is only allowed to obtain a noisy sum (i.e., the accurate sum plus some noise). In each time period t, each node i adds noise $r_i^{(t)}$ to his data $x_i^{(t)}$, encrypts the noisy data $\hat{x}_i^{(t)} = x_i^{(t)} + r_i^{(t)}$ with his key $k_i^{(t)}$ and sends the ciphertext to the aggregator. The aggregator uses the capability $k_0^{(t)}$ to decrypt the noisy sum $\sum_{i=1}^{n}(x_i^{(t)} + r_i^{(t)})$. Here, $k_i^{(t)}$ and $k_0^{(t)}$ change in every time period. In the following, when we describe our solution, we usually focus on the aggregation scheme in one time period. For simplicity, we omit the superscript t and write x_i, r_i, k_i and k_0 instead.

Each mobile node communicates with the aggregator via 3G, WiFi, or other available access networks. Peer-to-peer communication among the nodes is not

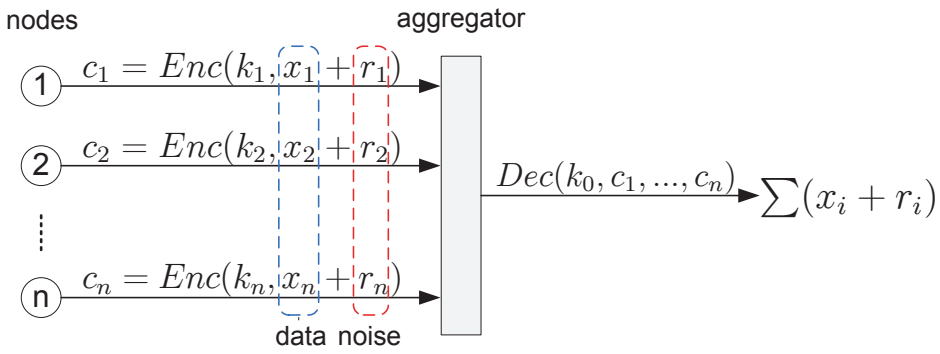

Figure 3.1. System model.

required, because nodes may not know each other for privacy reasons and such communication is nontrivial due to the mobility of nodes in mobile sensing. We assume that time is synchronized among nodes. In mobile sensing, mobile devices (e.g., smartphones) usually have embedded GPS receivers, which can easily synchronize time without communications among them.

There are three requirements regarding privacy. First, the aggregator only learns the noisy sum but nothing else (e.g., intermediate results). Second, a party without the aggregator capability learns nothing. This is *aggregator obliviousness* [28]. The third requirement is *differential privacy*. Intuitively, the sum obtained by the aggregator is roughly the same no matter if a specific node is in the system or not.

3.3.2 Threat and Trust Model

The aggregator is untrusted. A number of nodes may collude with the aggregator and reveal their data and noise values. We refer to these nodes as *compromised nodes* and refer to others as *good nodes*. We assume that the fraction of compromised nodes that collude is at most γ ($0 \leq \gamma < 1$), and nodes are equally likely to collude. Similar to [28], we assume that the system has an a priori estimate over the upper bound of γ, and uses it in our protocol. The aggregator may eavesdrop all messages sent to/from every node. Also, all entities are computationally bounded.

We also assume a key dealer which issues keys to the nodes and the aggregator via a secure channel. For now, we assume that the key dealer is trusted, and

we relax this assumption in Chapter 3.8.3. Malicious nodes may also perform data pollution attacks in which they provide false data values in order to sway the final aggregate statistics. Data pollution attacks are outside the scope of this chapter, and their influence can be bounded if each node uses a non-interactive zero-knowledge proof to prove that his data lies in a valid range.

3.3.3 Building Blocks

3.3.3.1 Homomorphic Encryption

One building block of our solution is the additive homomorphic encryption scheme proposed by Castelluccia et al. [86, 74]. This scheme works as follows.
Encryption:

1. Represent message m as an integer within range $[0, M-1]$ where M is a large integer.

2. Let k be a randomly generated key, $k \in \{0,1\}^{\lambda}$, where λ is a security parameter.

3. Output ciphertext $c = (m + h(f_k(r))) \mod M$, where f_k is a pseudorandom function (PRF) that uses k as a parameter, h is a length-matching hash function (see details below) and r is a nonce for this message.

Decryption:

1. Output plaintext $m = (c - h(f_k(r))) \mod M$.

f_k is a function of the PRF family $\mathbb{F}_\lambda = \{f_k : \{0,1\}^{\lambda} \rightarrow \{0,1\}^{\lambda}\}_{k \in \{0,1\}^{\lambda}}$ indexed by k. Since provably secure PRFs are usually computationally expensive, Castelluccia et al. [74] advocate using keyed hash functions (e.g., HMAC) as PRFs. HMAC is a PRF if the underlying compression function of the hash function in use is a PRF [87]. When HMAC is used, $f_k(r)$ is the HMAC of r with k as the key.

The purpose of h is to shorten a long bit string. It maps the output of f_k to a shorter bit string of length α, where α is the modulus size of M (i.e., $\alpha = |M|$). h is not required to be collision-consistent, but its output should be uniformly

distributed over $\{0,1\}^{\alpha}$. An example construction for h is to truncate the output of f_k into shorter bit strings of length α, take exclusive-OR on all these strings and use it as the output of h. This scheme is proved to be semantically secure [74].

This scheme allows additive homomorphic encryption. Given two ciphertexts $c_1 = (m_1 + h(f_k(r))) \mod M$ and $c_2 = (m_2 + h(f_{k'}(r))) \mod M$, an individual that knows k and k' can compute the sum of m_1 and m_2 directly from the aggregate ciphertext $c = c_1 + c_2$:

$$m = m_1 + m_2 = (c - h(f_k(r)) - h(f_{k'}(r))) \mod M.$$

To correctly compute the sum of n messages m_1, m_2, ..., m_n, M must be larger than $\sum_{i=1}^{n} m_i$. In practice, M should be selected as $M = 2^{\lceil \log_2 (max(m_i) \cdot n) \rceil}$.

3.3.3.2 Data Perturbation

Another building block of our solution is the data perturbation method proposed in [28]. To achieve differential privacy for the Sum aggregate of time-series data, that method adds a noise that follows diluted geometric distribution to each node's data.

Definition 1. *Geometric Distribution. Let $\alpha > 1$. Geom(α) denotes the symmetric geometric distribution with parameter α. Its probability mass function at k ($k = 0, \pm 1, \pm 2, ...$) is $\frac{\alpha-1}{\alpha+1} \cdot \alpha^{-|k|}$.*

Definition 2. *Diluted Geometric Distribution. Let $\alpha > 1$ and $0 < \beta \leq 1$. A random variable follows β-diluted Geometric distribution Geom$^{\beta}(\alpha)$ if it is sampled from Geom(α) with probability β, and is set to 0 with probability $1 - \beta$.*

Specifically, in time period t, node i generates a noise r_i from Geom$^{\beta}(\alpha)$ and computes $\hat{x}_i = x_i + r_i$. Parameters α and β are set as $\alpha = e^{\frac{\epsilon}{\Delta}}$ and $\beta = \min(\frac{1}{(1-\gamma)n} \ln \frac{1}{\delta}, 1)$, where ϵ and δ are privacy parameters. Given that the encryption method is aggregator oblivious (i.e., the aggregator only learns the noisy sum but nothing else), the data perturbation procedure achieves (ϵ,δ)-differential privacy [28]:

Theorem 1. *Let $0 < \delta < 1$, $\epsilon > 0$, $\alpha = e^{\frac{\epsilon}{\Delta}}$ and $\beta = min(\frac{1}{(1-\gamma)n} \ln \frac{1}{\delta}, 1)$, where γ is the maximum fraction of nodes compromised. If each node adds diluted Geo-*

metric noise Geom$^{\beta}(\alpha)$, the above perturbation procedure achieves (ϵ,δ)-distributed differential privacy[2]*.*

With this data perturbation method, roughly one copy of geometric noise Geom(α) is added to the sum, which is required to ensure ϵ-differential privacy [88].

3.3.4 Overview of Solution

Our solution to Sum aggregation has two components. The first component is an encryption method, which allows the aggregator to obtain the sum of all nodes' noisy data but nothing else. The second component is a data perturbation method, which adds an appropriate amount of noise to each node's data to achieve differential privacy. For data perturbation, our solution uses the method described in Chapter 3.3.3.2 due to its simplicity. Then we focus on devising an encryption method that is efficient in computation and can efficiently support dynamic joins and leaves.

To derive such an encryption method, we first propose a basic encryption scheme which has very low computation overhead (see Chapter 3.4). Since this scheme has high communication cost when a node joins or leaves, we then propose an overlapped grouping scheme which can effectively reduce the communication cost of dealing with dynamic joins and leaves (see Chapter 3.5).

By combining these two schemes and the data perturbation method, we obtain our aggregation protocol for Sum (see Chapter 3.6). Strictly speaking, our protocol achieves differential privacy against polynomial-time adversaries, since the encryption method is secure against polynomial-time adversaries.

We note that our overlapped grouping technique can also be applied upon other aggregator oblivious encryption schemes (e.g., [79, 28]) with different tradeoffs.

Table 3.2 summarizes the notations used in this chapter.

[2]If each node is compromised independently with probability γ, the data perturbation procedure is proved to achieve (ϵ,δ)-computational differential privacy [29].

Table 3.2. Notations

n	The number of nodes
γ	The maximum fraction of compromised nodes
x_i	The data of node i
r_i	The noise that node i adds to his data
$\hat{x}_i$	The noisy data of node i with $\hat{x}_i = x_i + r_i$
Δ	Each node's data is from $\{0, 1, ..., \Delta\}$
c	Number of secrets assigned to each node in the aggregation scheme for Sum
q	Number of secrets assigned to the aggregator in the aggregation scheme for Sum
M	$M = 2^{\lceil \log_2 (n\Delta) \rceil}$
$\mathbb{F}_\lambda$	$\mathbb{F}_\lambda = \{f_s : \{0,1\}^\lambda \to \{0,1\}^\lambda\}_{s \in \{0,1\}^\lambda}$ is a family of pesudorandom functions indexed by key s
h	A length-matching hash function, $h : \{0,1\}^\lambda \to \{0,1\}^\alpha$, where $\alpha = \lceil \log_2 (n\Delta) \rceil$
ϵ, δ	Parameters of differential privacy
α, β	Parameters used to generate noise
d, x	Parameters of our proposed scheme
g	The number of groups in Naive Grouping and our scheme
k_0	The capability used by the aggregator to decrypt noisy sum
k_i	The encryption key used by node i
l	The required security level is l-bit, e.g., $l = 80$

3.4 Basic Encryption Scheme

In this section, we propose a basic encryption scheme which allows the aggregator to get the sum of all nodes' data but nothing else.

3.4.1 Scheme Overview

Setup: The trusted authority assigns a set of secret values (*secrets* for short) to each node and the aggregator.

Enc: In each time period, node i ($i \in [1, n]$) generates encryption key k_i using the secrets that it is assigned. It encrypts its noisy data $\hat{x}_i$ by computing

$$c_i = (k_i + \hat{x}_i) \mod M \tag{3.1}$$

where $M = 2^{\lceil \log_2 (n\Delta) \rceil}$. Then it sends the ciphertext c_i to the aggregator.

AggrDec: In each time period, the aggregator generates decryption key k_0 using the secrets that it is assigned, and decrypts the sum aggregate $\hat{S} = \sum_{i=1}^{n} \hat{x}_i$ by computing

$$\hat{S} = (\sum_{i=1}^{n} c_i - k_0) \mod M. \tag{3.2}$$

The keys are generated using a PRF family and a length-matching hash function (see later). According to [86], the aggregator can get the correct sum so long as the following equation holds:

$$k_0 = (\sum_{i=1}^{n} k_i) \mod M. \tag{3.3}$$

In our protocol, the setup phase only runs once. After the setup phase, the trusted authority does not need to distribute secrets to the nodes and the aggregator again. In addition, the nodes and the aggregator do not have to synchronize their key generations with communications in every time period. These restrictions make it challenging for the nodes and the aggregator to generate their keys such that Equation 3.3 holds *in every time period* and the encryption (decryption) key used by each node (the aggregator) cannot be learned by any other party besides the trusted authority.

We propose a construction for key generations which preserves the privacy of each node and the Sum aggregate efficiently. Before presenting our construction, we first discuss a straw-man construction which is very efficient for the nodes but not efficient for the aggregator. Then we extend this straw-man scheme to derive our construction.

Both constructions include three processes, which are *secret setup*, *encryption key generation* and *decryption key generation*. They proceed in the Setup phase, Enc phase and AggrDec phase of the aggregation protocol, respectively.

3.4.2 A Straw-man Construction for Key Generation

Intuition Figure 4.17 shows the intuition of the straw-man construction. Suppose there are nc random numbers. The aggregator has access to all the numbers, and it computes the sum of these numbers as the decryption key k_0. These numbers are divided into n random disjoint subsets, each of size c. These n subsets are assigned to the n nodes, where each node has access to one subset of numbers. node i computes the sum of the numbers assigned to it as the encryption key k_i.

Clearly, Equation 3.3 holds. The aggregator cannot know any node's encryption key since it does not know the mapping between the random numbers and

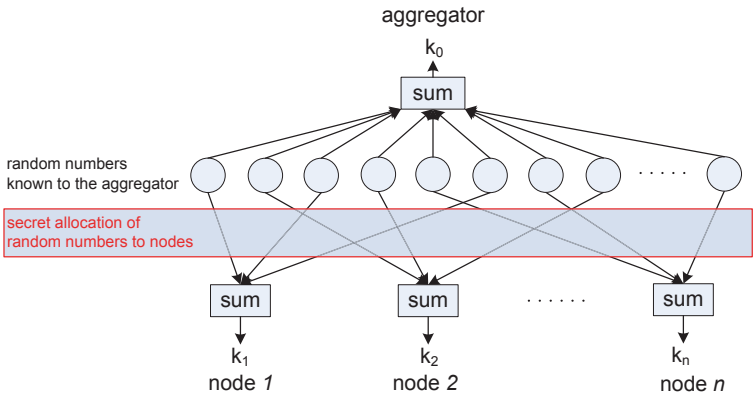

Figure 3.2. The intuition behind the straw-man construction. The aggregator computes the sum of a set of random numbers as the decryption key. These numbers are secretly allocated to the nodes, and each node computes the sum of its allocated numbers as the encryption key. The aggregator cannot know any node's encryption key since it does not know the mapping between the numbers and the nodes.

the nodes. When c is large enough, it is infeasible for the aggregator to guess the numbers assigned to a particular node with a brute-force method. The aggregator's decryption key cannot be revealed by any node since no node knows all the numbers.

Construction The construction is as follows:

Secret Setup: The trusted authority generates nc random and different secrets s_1, ..., s_{nc}. It divides these secrets into n random disjoint subsets, with c secrets in each subset. Let $\mathcal{S}$ denote the set of all secrets, and let $\mathcal{S}_i$ denote the i^{th} subset. Clearly, $\mathcal{S} = \bigcup_{i=1}^{n} \mathcal{S}_i$ and $\forall i \neq j, \mathcal{S}_i \bigcap \mathcal{S}_j = \phi$. The trusted authority sends the secrets in subset $\mathcal{S}_i$ to node i and sends all the secrets in $\mathcal{S}$ to the aggregator.

Encryption Key Generation: In time period $t \in \mathbb{N}$, node i generates its encryption key as follows:

$$k_i = (\sum_{s' \in \mathcal{S}_i} h(f_{s'}(t))) \mod M. \tag{3.4}$$

Decryption Key Generation: In time period $t \in \mathbb{N}$, the aggregator generates the decryption key as follows:

$$k_0 = (\sum_{s' \in \mathcal{S}} h(f_{s'}(t))) \mod M. \tag{3.5}$$

Table 3.3. Security levels of the straw-man construction when $\gamma = 0.1$.

$n = 10^2$	c	10	11	12	13	14
	p_b	$2^{-76.3}$	$2^{-84.1}$	$2^{-92.0}$	$2^{-99.9}$	$2^{-107.7}$
$n = 10^3$	c	6	7	8	9	10
	p_b	$2^{-64.9}$	$2^{-76.0}$	$2^{-87.2}$	$2^{-98.4}$	$2^{-109.6}$
$n = 10^4$	c	4	5	6	7	8
	p_b	$2^{-56.0}$	$2^{-70.4}$	$2^{-84.8}$	$2^{-99.3}$	$2^{-113.8}$
$n = 10^5$	c	3	4	5	6	7
	p_b	$2^{-51.5}$	$2^{-69.2}$	$2^{-87.0}$	$2^{-104.8}$	$2^{-122.6}$
$n = 10^6$	c	2	3	4	5	6
	p_b	$2^{-40.6}$	$2^{-61.5}$	$2^{-82.5}$	$2^{-103.6}$	$2^{-124.7}$

In Equation 3.4, since each $h(f_{s'}(t))$ is uniformly distributed over $\{0,1\}^\alpha$, k_i is also uniformly distributed over $\{0,1\}^\alpha$. Thus, the encryption keys satisfy the security requirement of the underlying cryptosystem. Equation 3.3 also holds since

$$\begin{aligned}\sum_{i=1}^{n} k_i &= (\sum_{i=1}^{n} \sum_{s' \in \mathcal{S}_i} h(f_{s'}(t))) \mod M \\ &= (\sum_{s' \in \mathcal{S}} h(f_{s'}(t))) \mod M \\ &= k_0 \mod M.\end{aligned}$$

Security level If the aggregator knows the c secrets used by a node, it can obtain the encryption key of the node. We can derive the probability that the aggregator finds the c secrets used by a node. Let p_b denote the probability that in a single trial the aggregator can successfully guess the secrets assigned to the node. Recall that γ is the maximal fraction of nodes that collude with the aggregator. In the worst case, the aggregator knows the γnc secrets assigned to the colluding nodes, but it does not know how the remaining $(1-\gamma)nc$ secrets are assigned to other nodes. There are $\binom{(1-\gamma)nc}{c}$ possible secret assignments for each node. Hence we have:

$$p_b = \frac{1}{\binom{(1-\gamma)nc}{c}}. \tag{3.6}$$

With a smaller p_b, better security can be achieved. Table 3.3 shows the values of p_b for varying parameters n and c. As c increases, the security level increases quickly.

Given the number of nodes n and an estimate of γ, we can derive the minimum value of c to achieve a certain required security level. (c is minimized to minimize

Table 3.4. The minimum values of c for 80-bit security in the straw-man construction.

n	10^2	10^3	10^4	10^5	10^6
$\gamma = 0, 0.1, 0.2, 0.3$	11	8	6	5	4

the cost.) For l-bit security (e.g., $l = 80$), c should be selected as the minimum value that satisfies $p_b \leq 2^{-l}$. Table 3.4 shows the values of c for 80-bit security.

A fraction of nodes may collude against the aggregator to reveal the aggregate. To achieve this goal, they need to obtain all the secrets that the aggregator has. However, each participant only knows a subset of the secrets. So long as not all nodes collude, they cannot obtain all the secrets.

Cost In each time period, each node computes c PRFs and the aggregator computes nc PRFs. Since c is small as shown in Table 3.4, the computation cost at each node is very low. However, when the number of nodes n is very large, the computation cost at the aggregator is high.

3.4.3 Our Construction for Key Generation

Our construction extends the straw-man construction to reduce the computation overhead at the aggregator.

Intuition Consider an equation:

$$a_1 + a_2 + \cdots + a_{nc} = a_1 + a_2 + \cdots + a_{nc}. \tag{3.7}$$

If we remove $nc - q$ summands from the right side and subtract them from the left side, the derived equation

$$a_1 + \cdots + a_{nc} + (-a_1) + \cdots + (-a_{nc-q}) = a_{nc-q+1} + \cdots + a_{nc} \tag{3.8}$$

is equivalent to the original equation.

To meet the requirement of Equation 3.3, the straw-man construction essentially mimics Equation 3.7, i.e., the nodes collectively generate the summands on the left side and add them to the aggregate, while the aggregator alone generates the summands on the right side and subtracts them from the perturbed aggregate (see Figure 3.3(a)). Each summand is generated from a secret. Since Equation 3.7 and 3.8 are equivalent, we can remove some summands from the aggregator

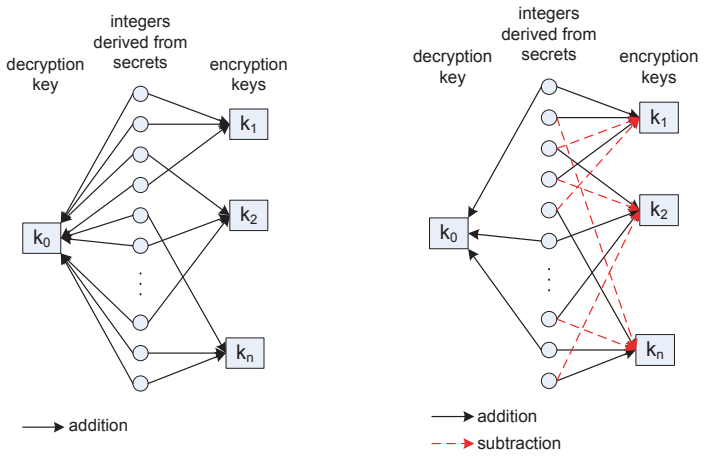

(a) Straw-man construction (b) Our construction

Figure 3.3. The intuition behind our construction in comparison with the straw-man construction.

side and subtract them from the node side without violating Equation 3.3. Now the aggregator has less computation overhead since it needs to generate less summands. The reduced computation does not come for free, as it is amortized among the nodes such that each node generates more summands (see Figure 3.3(b)). A nice property is that it is now more difficult to guess the summands generated by each node and thus each node has better security.

Construction The construction is as follows:

Secret Distribution: The trusted authority generates nc random and different secrets s_1, ..., s_{nc}. Let $\mathcal{S}$ denote the set composed of all the secrets. The trusted authority divides these secrets into n random disjoint subsets, with c secrets in each subset. For convenience, we call these subsets *additive subsets*. Let $\mathcal{S}_i$ denote the i^{th} additive subset. Clearly, $\mathcal{S} = \bigcup_{i=1}^{n} \mathcal{S}_i$.

Out of the nc secrets, the trusted authority randomly selects q secrets and assigns them to the aggregator. Let $\hat{\mathcal{S}}$ denote the set of secrets assigned to the aggregator. The trusted authority divides the remaining $nc-q$ secrets evenly into n random disjoint subsets. Among them, $(nc-q)-n\lfloor\frac{nc-q}{n}\rfloor$ subsets have $\lfloor\frac{nc-q}{n}\rfloor+1$ secrets each, and the other $n(1+\lfloor\frac{nc-q}{n}\rfloor)-nc+q$ subsets have $\lfloor\frac{nc-q}{n}\rfloor$ secrets each. For convenience, we call these subsets *subtractive subsets*. Let $\bar{\mathcal{S}}_i$ denote the i^{th} subtractive subset. Clearly, $\mathcal{S} = (\bigcup_{i=1}^{n} \bar{\mathcal{S}}_i) \bigcup \hat{\mathcal{S}}$. The trusted authority assigns the secrets in the additive subset $\mathcal{S}_i$ and subtractive subset $\bar{\mathcal{S}}_i$ to node i.

Encryption Key Generation: In time period $t \in \mathbb{N}$, node i generates its encryption key by computing

$$k_i = (\sum_{s' \in \mathcal{S}_i} h(f_{s'}(t)) - \sum_{s' \in \bar{\mathcal{S}}_i} h(f_{s'}(t))) \mod M. \tag{3.9}$$

Decryption Key Generation: In time period $t \in \mathbb{N}$, the aggregator generates the decryption key by computing

$$k_0 = (\sum_{s' \in \hat{\mathcal{S}}} h(f_{s'}(t))) \mod M. \tag{3.10}$$

The requirement in Equation 3.3 is satisfied since

$$\begin{aligned}
\sum_{i=1}^{n} k_i &= (\sum_{i=1}^{n} (\sum_{s' \in \mathcal{S}_i} h(f_{s'}(t)) - \sum_{s' \in \bar{\mathcal{S}}_i} h(f_{s'}(t)))) \mod M \\
&= (\sum_{s' \in \mathcal{S}} h(f_{s'}(t)) - \sum_{s' \in \bigcup_{i=1}^{n} \bar{\mathcal{S}}_i} h(f_{s'}(t))) \mod M \\
&= (\sum_{s' \in \hat{\mathcal{S}}} h(f_{s'}(t))) \mod M \\
&= k_0.
\end{aligned}$$

Security level The aggregator cannot learn any node's encryption key since it does not know the additive secrets (i.e., secrets in the additive subset) and the subtractive secrets (i.e., secrets in the subtractive subset) assigned to this node. Each node has c additive secrets and at least $\lfloor \frac{nc-q}{n} \rfloor$ subtractive secrets. The aggregator may know the secrets assigned to itself and those to its γn colluders, but there are still $(1-\gamma)nc$ additive secrets and at least $(1-\gamma)n\lfloor \frac{nc-q}{n} \rfloor$ subtractive secrets that the aggregator does not know how they are assigned to the good nodes. There are at least $\binom{(1-\gamma)nc}{c} \cdot \binom{(1-\gamma)n\lfloor \frac{nc-q}{n} \rfloor}{\lfloor \frac{nc-q}{n} \rfloor}$ possible secret assignments for each good node. Thus,

$$p_b \leq \frac{1}{\binom{(1-\gamma)nc}{c} \cdot \binom{(1-\gamma)n\lfloor \frac{nc-q}{n} \rfloor}{\lfloor \frac{nc-q}{n} \rfloor}}. \tag{3.11}$$

p_b decreases (i.e., the security for the nodes is better) when n and c increase, but p_b increases when γ increases.

Table 3.5. The security level of our construction when $\gamma = 0.1$.

$n = 10^2$	c	4	5	6	7	8
	p_b	$2^{-51.0}$	$2^{-66.5}$	$2^{-82.1}$	$2^{-97.7}$	$2^{-113.3}$
$n = 10^3$	c	3	4	5	6	7
	p_b	$2^{-52.2}$	$2^{-74.3}$	$2^{-96.4}$	$2^{-118.7}$	$2^{-140.9}$
$n = 10^4$	c	2	3	4	5	6
	p_b	$2^{-40.4}$	$2^{-68.8}$	$2^{-97.5}$	$2^{-126.3}$	$2^{-155.2}$
$n = 10^5$	c	1	2	3	4	5
	p_b	$2^{-16.5}$	$2^{-50.4}$	$2^{-85.5}$	$2^{-120.8}$	$2^{-156.2}$
$n = 10^6$	c	1	2	3	4	5
	p_b	$2^{-19.8}$	$2^{-60.3}$	$2^{-102.1}$	$2^{-144.0}$	$2^{-186.1}$

Table 3.6. The values of c for 80-bit security in our construction.

n	10^2	10^3	10^4	10^5	10^6
$\gamma = 0, 0.1, 0.2$	6	5	4	3	3
$\gamma = 0.3$	7	5	4	3	3

Under the same total computation cost, the smaller q is, the more subtractive secrets the nodes are assigned and the better security the nodes have. However, if q is too small, the secrets (and hence the decryption key) used by the aggregator may be learned by a number of colluding nodes in the brute-force way. We can derive the minimum value of q to make it infeasible for γ fraction of nodes to collusively obtain the decryption key. These colluders know at most γnc subtractive secrets, but they do not know which q of the remaining $(1-\gamma)nc$ secrets the aggregator has. There are $\binom{(1-\gamma)nc}{q}$ possible secret assignments for the aggregator. Let p_c denote the probability that the q secrets assigned to the aggregator can be guessed in a single trial. We have

$$p_c \leq \frac{1}{\binom{(1-\gamma)nc}{q}}. \tag{3.12}$$

When q increases, p_c decreases which means better security for the aggregator.

Practical considerations To achieve l-bit security for each node and the aggregator, it is required that $p_b \leq 2^{-l}$ and $p_c \leq 2^{-l}$ respectively. Given parameters n

Table 3.7. The values of q for 80-bit security in our construction.

n	10^2	10^3	10^4	10^5	10^6
$\gamma = 0$	12	8	6	5	4
$\gamma = 0.1$	13	8	6	5	4
$\gamma = 0.2$	13	8	6	5	4
$\gamma = 0.3$	13	9	7	5	5

and γ, large-enough values should be set for c and q to meet these requirements.

Since the values of c and q depend on each other, which can be seen from Equation 3.11 and 3.12, they can be set as follows. First, we assume $q \in (0, n]$. Under this assumption, Equation 3.11 can be rewritten as:

$$p_b \leq \frac{1}{\binom{(1-\gamma)nc}{c} \cdot \binom{(1-\gamma)n(c-1)}{c-1}}. \tag{3.13}$$

We can derive the minimum value of c that makes the right-hand side of Equation 3.13 smaller than 2^{-l}. Then we apply the derived value of c to Equation 3.12, and obtain the minimum value of q that makes the right-hand side of Equation 3.12 smaller than 2^{-l}. If the obtained value of q falls into the assumed range $(0, n]$, the values of c and q are accepted. Otherwise, we can increase the value of c, until the minimum value of q that makes the right-hand side of Equation 3.12 smaller than 2^{-l} is not larger than n.

This method of setting c and q ensures that $q \leq n$, and thus p_b is given in Equation 3.13. Table 3.5 shows the values of p_b when n and c change. Table 3.6 and Table 3.7 show the values of c and q respectively for 80-bit security. It can be seen that both c and q are very small.

Cost Since the setup phase is run only once, we analyze the cost of our construction in each aggregation period. The computation cost is measured by the number of PRFs computed, since the length-matching hash function (which mainly consists of exclusive-OR operations) and arithmetic addition are much less expensive in computation.

In each time period, each node computes $2c - \frac{q}{n}$ PRFs on average, while the aggregator computes q PRFs. As for the storage cost, the trusted authority stores nc secrets as well as $2nc$ mappings between the secrets and the nodes/aggregator. Each node stores $2c - \frac{q}{n}$ secrets on average, while the aggregator stores q secrets. Besides sending the encrypted data to the aggregator, each node does not make any extra communications.

Comparisons with the Straw-man Construction Table 3.8 compares our construction to the straw-man construction in security and cost. When the total computation cost (for nodes and the aggregator) is the same, our construction achieves better security. Also, it has smaller computation cost at the aggregator.

Table 3.8. The security and cost of our construction and the straw-man construction. For computation cost, the value is the cost per time period.

	Straw-man	Ours
p_b	$\frac{1}{\binom{(1-\gamma)nc}{c}}$	$\frac{1}{\binom{(1-\gamma)nc}{c} \cdot \binom{(1-\gamma)n(c-1)}{c-1}}$
Comp. (total)	$2nc$	$2nc$
Comp. (node)	c	$2c - \frac{q}{n}$
Comp. (aggregator)	nc	$q(q < n)$
Storage (node)	c	$2c - q$
Storage (aggregator)	nc	q

Table 3.9. The computation cost of our construction and the straw-man construction for 80-bit security when $\gamma = 0.1$.

	n	10^2	10^3	10^4	10^5	10^6
node	Straw-man	11	8	6	5	4
	Ours	12	10	8	6	6
Aggregator	Straw-man	1100	8000	$6 \cdot 10^4$	$5 \cdot 10^5$	$4 \cdot 10^6$
	Ours	13	8	6	5	4

Upon initial inspection, our construction may seem to double the computation cost at each node (i.e., from c to roughly $2c$). In practice, however, it can use a smaller c to achieve the same security level. Table 3.9 shows the computation cost of the two constructions at the same security level. For a wide range of n ($10^2 - 10^6$), the computation cost at each node is slightly higher (i.e., one or two PRFs) in our construction, but the computation cost at the aggregator is orders of magnitude smaller.

3.5 Dealing with Dynamic Joins and Leaves

In the basic encryption scheme (see Chapter 3.4), when a node joins or leaves, the key dealer must issue a new set of secrets to every node and the aggregator to ensure security. This induces high communication overhead and makes it impractical for large-scale mobile sensing applications with high churn rate. Thus, efficient techniques should be proposed to deal with dynamic joins and leaves.

3.5.1 Naive Grouping

Intuitively, we can apply grouping on top of the basic encryption scheme to reduce the communication cost of dynamic joins and leaves.

Naive Grouping. The n nodes are divided into g *disjoint groups* of equal size, and the basic encryption scheme is applied to each group independently. The aggregator has the capability to decrypt the sum of each group. To provide differential privacy, one copy of geometric noise is added to the sum of each group, using the data perturbation method described in Chapter 3.3.3.2. As some positive and negative noises cancel out, the accumulated noise in the final aggregate is $O(\sqrt{g})$ with high probability. When a node joins or leaves a group, only the $\frac{n}{g}$ nodes in this group are redistributed secrets.

The problem with Naive Grouping is that it cannot achieve both low communication cost for dynamic joins and leaves and low aggregation error, since these two goals require the parameter g to be tuned in reverse directions. Thus, it is nontrivial to use grouping to achieve both churn resilience and low aggregation error.

3.5.2 Overlapped Grouping

Although grouping can be used to reduce the communication overhead of dynamic joins and leaves, the naive grouping scheme has high aggregation error since it adds one independent copy of geometric noise to each group. To address this problem, we propose to use a new technique called *overlapped grouping*. This technique allows the aggregator to obtain the sum of *all* nodes' data but nothing else, and thus all nodes only need to *collectively* add one copy of geometric noise to the sum, resulting in low aggregation error.

3.5.2.1 Basic Idea

The basic idea is to divide the nodes into *overlapped groups*, where each group shares some nodes with other groups. In the setup phase, an independent set of secrets are assigned to each group of nodes and the aggregator similarly as that in the basic encryption scheme. For each group, the aggregator does not know the secrets assigned to each member of the group. A node that belongs to

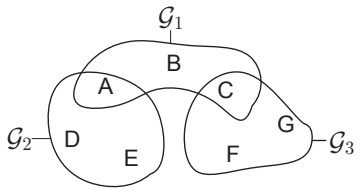

$\mathcal{G}_1 : \mathcal{S}_A\{s_1\}, \bar{\mathcal{S}}_A\{\}, \mathcal{S}_B\{s_2\}, \mathcal{S}_B\{s_1\}, \mathcal{S}_C\{s_3\}, \bar{\mathcal{S}}_C\{\}$ $\hat{\mathcal{S}}_{Agg} = \{s_2, s_3\}$
$\mathcal{G}_2 : \mathcal{S}_A\{s_4\}, \bar{\mathcal{S}}_A\{\}, \mathcal{S}_D\{s_5\}, \mathcal{S}_D\{s_4\}, \mathcal{S}_E\{s_6\}, \bar{\mathcal{S}}_E\{\}$ $\hat{\mathcal{S}}_{Agg} = \{s_5, s_6\}$
$\mathcal{G}_3 : \mathcal{S}_C\{s_7\}, \bar{\mathcal{S}}_C\{\}, \mathcal{S}_F\{s_8\}, \bar{\mathcal{S}}_F\{s_7\}, \mathcal{S}_G\{s_9\}, \bar{\mathcal{S}}_G\{\}$ $\hat{\mathcal{S}}_{Agg} = \{s_8, s_9\}$

Figure 3.4. The basic idea of overlapped grouping. In this example, groups $\mathcal{G}_1$ and $\mathcal{G}_2$ share node A. A is assigned secrets from both $\mathcal{G}_1$ and $\mathcal{G}_2$. A sets $k_A = h(f_{s_1}(t))+h(f_{s_4}(t))$. B only receives secrets from group $\mathcal{G}_1$, and it sets $k_B = h(f_{s_2}(t)) - h(f_{s_1}(t))$. Other nodes set their keys similarly. The aggregator sets $k_0 = \sum_{i=\{2,3,5,6,8,9\}} h(f_{s_i}(t))$. The aggregator can only get the sum of *all nodes*.

multiple groups will receive secrets from each group it belongs to. Each node (the aggregator) uses the union of the secrets that it receives to derive its encryption key (decryption capability). The encryption (decryption) process is the same as the basic encryption scheme. Clearly the aggregator can decrypt the sum.

Overlapped grouping guarantees that *the aggregator cannot learn the sum of any individual group or the sum of any subset of (not all) nodes* (see the example below), and thus the nodes can collectively add just one copy of geometric noise to the aggregate, minimizing the aggregation error. When a node joins or leaves a group, the key dealer runs the setup phase again for this group only. Thus the communication cost is low.

We use the example in Figure 3.4 to show how overlapped grouping provides that guarantee. Seven nodes are divided into three overlapped groups, where group $\mathcal{G}_1$ shares node A with $\mathcal{G}_2$ and shares C with $\mathcal{G}_3$. The secrets assigned to each node and the aggregator are shown in the figure. Suppose the aggregator tries to get the sum of group $\mathcal{G}_2$, i.e., $\hat{x}_A + \hat{x}_D + \hat{x}_E$. From A's, D's and E's ciphertexts $\hat{x}_A + h(f_{s_1}(t)) + h(f_{s_4}(t))$, $\hat{x}_D + h(f_{s_5}(t)) - h(f_{s_4}(t))$ and $\hat{x}_E + h(f_{s_6}(t))$, it sums them and gets $(\hat{x}_A+\hat{x}_D+\hat{x}_E)+h(f_{s_1}(t))+h(f_{s_5}(t))+h(f_{s_6}(t))$. Although it knows $\hat{\mathcal{S}}_{Agg} = \{s_5, s_6\}$ and can get $h(f_{s_5}(t)) + h(f_{s_6}(t))$, it does not know s_1 (i.e., the secrets assigned to A in group $\mathcal{G}_1$) and hence cannot get the sum of $\mathcal{G}_2$. Similarly, it cannot get the sum of $\mathcal{G}_1$, $\mathcal{G}_3$ or any other strict and non-empty subset of nodes.

3.5.2.2 Security Condition

When nodes may be compromised, overlapped grouping should satisfy the following security condition.

Condition 1: *Let* $\mathbb{S}$ *denote an arbitrary strict and non-empty subset of groups. There exists a good node* N*, group* $\mathcal{G} \in \mathbb{S}$ *and group* $\mathcal{G}' \notin \mathbb{S}$*, such that* $N \in \mathcal{G}$ *and* $N \in \mathcal{G}'$*.*

The following theorem explains why Condition 1 is needed.

Theorem 2. *In overlapped grouping, the aggregator cannot obtain the sum of any strict and nonempty subset of good nodes if and only if Condition 1 is satisfied.*

Proof. The necessity of Condition 1 can be seen from a counterexample in Fig. 3.4. Suppose $\mathbb{S} = \{\mathcal{G}_2\}$ is the subset of groups in consideration, which only shares node A with the outside world. If A is compromised (which violates Condition 1) and A reveals s_1, the aggregator will be able to get the sum of $\mathcal{G}_2$.

Proof of sufficiency. Since the aggregator knows the secret of each compromised node, without loss generality, we shrink each group by removing the compromised nodes. Suppose the aggregator aims to obtain the sum of a strict and nonempty subset (denoted by $\mathcal{S}$) of good nodes. There are four cases. *Case 1:* $\mathcal{S}$ is a strict subset of a group $\mathcal{G}$ (e.g., $\mathcal{S} = \{D\}$ in Fig. 3.4). Since the encryption basic scheme is applied to $\mathcal{G}$, the aggregator does not know the secrets assigned to any good node in $\mathcal{G}$ (or $\mathcal{S}$), and thus it cannot get the sum aggregate of $\mathcal{S}$. *Case 2:* $\mathcal{S}$ contains the same nodes as a group $\mathcal{G}$ (e.g., $\mathcal{S} = \{A, D, E\}$ in Fig. 3.4). The aggregator knows how to offset the effect of the secrets assigned to group $\mathcal{G}$. However, due to Condition 1, $\mathcal{S}$ shares at least one good node with another group $\mathcal{G}'$. This node uses not only the secrets received from group $\mathcal{G}$ but also the secrets received from $\mathcal{G}'$ to encrypt its data. Since the aggregator does not the secrets that the node receives from $\mathcal{G}'$, it cannot get the sum of $\mathcal{S}$. *Case 3:* $\mathcal{S}$ is the union of a number of overlapped groups (e.g., $\mathcal{S} = \{A, B, C, D, E\}$ in Fig. 3.4). The proof is quite similar to Case 2. *Case 4:* $\mathcal{S}$ is an arbitrary combination of the above three cases (e.g., $\mathcal{S} = \{A, B, C, D, F\}$ in Fig. 3.4). The proofs for the above three cases can be easily generalized to this case. □

According to Theorem 2, any specific overlapped grouping scheme needs to and only needs to satisfy Condition 1. Thus, Condition 1 can be used to guide the construction of overlapped grouping schemes. In the next section, we present such a scheme based on a ring structure.

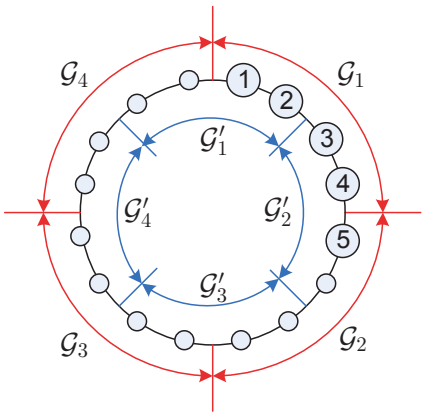

Figure 3.5. Ring-based overlapped grouping. In this example, the nodes form eight groups, four disjoint groups in the outer ring ($\mathcal{G}_1$–$\mathcal{G}_4$) and four disjoint groups in the inner ring ($\mathcal{G}'_1$–$\mathcal{G}'_4$). Groups on different rings may overlap. Group $\mathcal{G}_1$ and $\mathcal{G}'_1$ overlap, and they share node 1 and 2.

3.5.3 Ring-based Overlapped Grouping

For overlapped grouping, it is nontrivial to satisfy Condition 1. With a total of g groups, there are about 2^g possible subsets of groups. Unless g is very small, it is infeasible to adjust each possible subset to satisfy the condition. In this section, we present a novel overlapped grouping construction which addresses this challenge with a ring structure.

3.5.3.1 Ring-based Group Structure

As shown in Figure 3.5, the nodes are arranged into a *node ring*, which is mirrored to two virtual rings, the *outer ring* and *inner ring*. Each virtual ring is partitioned into segments, and the nodes in a segment form a group. Each node belongs to two groups, one in each virtual ring. Groups in the same virtual ring are disjoint, but groups in different virtual rings may overlap (i.e., they share at least one node). A group in the inner (outer) ring will overlap with one or more groups in the outer (inner) ring.

The Basic Structure Since the node ring and the two virtual rings are identical, we use "the ring" to refer to the structure when the context is clear. Suppose there are n ($n \geq 2d$) nodes in the ring indexed from 0 to $n-1$ in the clockwise order. For convenience, we use a directed segment to represent a group, say $\mathcal{G}$ (see Fig.

(a) Group with nodes l', ..., r (b) Two neighbor groups

Figure 3.6. Segment representation of groups.

3.6(a)). The direction from left to right corresponds to the clockwise order in the ring. Let l' and r denote the indexes of the leftmost and rightmost node in $\mathcal{G}$. Then the left and right boundary of $\mathcal{G}$ are defined as $\mathcal{G}.left = l' - 0.5$ and $\mathcal{G}.right = r + 0.5$, respectively. Let $|\mathcal{G}|$ denote the number of nodes in $\mathcal{G}$. We have $|\mathcal{G}| = (\mathcal{G}.right - \mathcal{G}.left) \mod n$.

Suppose $\mathcal{L}$ and $\mathcal{R}$ are two neighbor groups in the same virtual ring, and $\mathcal{L}.right = \mathcal{R}.left$ (see Fig. 3.6(b)). $\mathcal{L}.right$ (or $\mathcal{R}.left$) is the border between $\mathcal{L}$ and $\mathcal{R}$. Term "move $\mathcal{L}.right$ to the right by y" means that $\mathcal{L}.right$ and $\mathcal{R}.left$ are increased by $y \mod n$, i.e., the leftmost y nodes of $\mathcal{R}$ are moved to $\mathcal{L}$. Term "move $\mathcal{R}.left$ to the left by y" is interpreted similarly.

Overlap patterns Two groups in different virtual rings can overlap in two patterns (see Figure 3.7). In *Pattern I*, one group is a strict subset of the other group. In *Pattern II*, the two groups have nodes in common, but each group also has some nodes that the other group does not have.

3.5.3.2 Properties

To satisfy Condition 1 and reduce the communication cost of dealing with dynamic joins and leaves, the ring-based group structure has the following properties:

Overlap Property: Any two groups that overlap share at least x nodes. x is large enough to make it infeasible (i.e., with probability smaller than 2^{-l}) that none of the shared nodes is good (see later).

Interleave Property: If two neighboring nodes in the ring belong to two neighboring groups in one virtual ring, they belong to the same group in the other virtual ring.

Group Size Property: Each group has d ($d > 2x$) to $2d - 1$ nodes.

An example of the interleave property is shown in Figure 3.5. Two neighboring nodes 4 and 5 belong to neighboring groups $\mathcal{G}_1$ and $\mathcal{G}_2$ in the outer ring, and they are in the same group $\mathcal{G}'_2$ in the inner ring. The group size property is required by

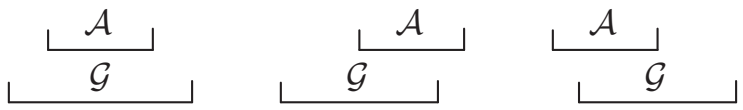

(a) Pattern I (b) Pattern II (c) Pattern II

Figure 3.7. The two patterns that two groups $\mathcal{G}$ and $\mathcal{A}$ may overlap where $|\mathcal{G}| \geq |\mathcal{A}|$. $\mathcal{G}$ and $\mathcal{A}$ are in different virtual rings. In (b) and (c), $\mathcal{G}$ overlaps with the left and right part of $\mathcal{A}$, respectively.

our group adjustment algorithms.

Theorem 3. *In ring-based overlapped grouping, the overlap and interleave property ensure that Condition 1 is satisfied.*

Proof. Let us consider the set that consists of all groups. Let $\mathbb{S}$ denote an arbitrary strict and non-empty subset of groups, and $\bar{\mathbb{S}}$ denote its complement. It is sufficient to prove that $\mathbb{S}$ shares at least x nodes with $\bar{\mathbb{S}}$. Since $\mathbb{S}$ is a strict subset, there must be at least one node i in $\mathbb{S}$ who has one neighbor node j that belongs to $\bar{\mathbb{S}}$. We can find two groups $\mathcal{G}_1$ and $\mathcal{G}_2$, which satisfy that (i) $i \in \mathcal{G}_1$, (ii) $j \in \mathcal{G}_2$, and (iii) $\mathcal{G}_1$ and $\mathcal{G}_2$ are neighbors in one virtual ring and they belong to $\mathbb{S}$ and $\bar{\mathbb{S}}$ respectively. Due to the interleave property, i and j belong to one group (denoted by $\mathcal{G}_3$) in the other virtual ring. $\mathcal{G}_3$ overlaps with both $\mathcal{G}_1$ and $\mathcal{G}_2$, and it shares at least x nodes with them according to the overlap property. Since $\mathcal{G}_1$ and $\mathcal{G}_2$ belong to $\mathbb{S}$ and $\bar{\mathbb{S}}$ respectively, no matter which subset $\mathcal{G}_3$ belongs to, the number of shared nodes between $\mathbb{S}$ and $\bar{\mathbb{S}}$ is at least x, and there is at least one shared good node. Thus, Condition 1 is satisfied. □

Comments: Due to Theorem 2 and 3, *the ring-based construction guarantees that the aggregator cannot obtain the sum of any strict and nonempty subset of good nodes.* For convenience, we say the ring-based grouping is *secure* if the overlap, interleave and group size property hold.

Practical Considerations In practice, the value of x should be sufficiently large such that for any two groups that overlap, with a high probability (denoted by p_s) at least one of their shared nodes is good. Since each node can be compromised with the same probability, with standard combinatorial techniques, we can derive that $p_s = 1 - \binom{\gamma n}{x} / \binom{n}{x}$. When n is large, $p_s \gtrsim 1 - \gamma^x$. Parameter x can be set as the minimum value that satisfies $p_s > 1 - 2^{-l}$:

Table 3.10. The values of x and d for 80-bit security.

γ	0	0.01	0.05	0.1	0.15	0.2
x	1	13	19	25	30	35
d	3	27	39	51	61	71

$$x = \lceil -l \log_\gamma 2 \rceil. \tag{3.14}$$

To minimize the communication cost of dynamic joins and leaves (see later), parameter d can be set as the minimum value that satisfies $d > 2x$, i.e., $d = 2x + 1$. Table 3.10 shows the values of x and d for 80-bit security.

Algorithm 1 initGroup(): Group initialization.

Require: Nodes 0,...,$n-1$. Without loss of generality, n is divisible by d.
Ensure: $\frac{2n}{d}$ groups $\mathcal{G}_1$, ..., $\mathcal{G}_{\frac{n}{d}}$, $\mathcal{G}'_1$, ..., $\mathcal{G}'_{\frac{n}{d}}$, each of size d.
1: **for** i from 1 **to** $\frac{n}{d}$ **do**
2: Add nodes $(i-1)\frac{n}{d}$, $(i-1)\frac{n}{d}+1$, ..., $(i-1)\frac{n}{d}+d-1$ to group $\mathcal{G}_i$
3: Add nodes $(i-1)\frac{n}{d}+\frac{d}{2} \mod n$, $(i-1)\frac{n}{d}+\frac{d}{2}+1 \mod n$, ..., $(i-1)\frac{n}{d}+\frac{d}{2}+d-1 \mod n$ to group $\mathcal{G}'_i$
4: **end for**

3.5.3.3 Group Management

Suppose initially there are n nodes. Algorithm 1 initializes them into $\frac{2n}{d}$ groups. Figure 3.5 shows an instance of initialized groups for $n = 16$ and $d = 4$. Clearly, each group overlaps with two other groups and shares $\frac{d}{2}$ nodes with each overlapping group. It is easy to verify that the grouping is secure.

When a new node joins, it is inserted to a random location in the ring, and added to the two groups that cover the location of insertion. The two changed groups may violate the group size property (i.e., having more than $2d-1$ nodes). Similarly, when a node leaves, it is removed from the ring and from the two groups it belonged to, which may violate the group size property and overlap property. In these cases, the nodes should be regrouped so that the three properties still hold.

Algorithm 2-5 show the group adjustment algorithms. Suppose the grouping is secure before the node joins or leaves. Lemma 1-4 show that these algorithms make the grouping secure. Their proofs can be found in Appendix.

Lemma 1. *Suppose a node joins two groups which overlap in Pattern I. After Algorithm 2 is run, the grouping is secure.*

Algorithm 2 adjust(JOIN, I): Re-grouping after a node joins two groups which overlap in pattern I (see Fig. 3.8).

Require: $\mathcal{G}$, $\mathcal{A}$: The two groups that the node joins, $|\mathcal{G}| > |\mathcal{A}|$.
1: **if** $|\mathcal{G}| < 2d$ **then**
2: **return**;
3: **else**
4: Split $\mathcal{G}$ in the middle into two groups, each of size d;
5: **end if**

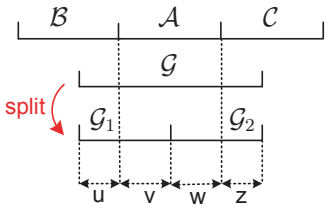

Figure 3.8. The regrouping (in Algorithm 2) when a node joins $\mathcal{G}$ and $\mathcal{A}$ which overlap in Pattern I. $\mathcal{G}$ is split into $\mathcal{G}_1$ and $\mathcal{G}_2$ if it has too many nodes.

Proof. Algorithm 2 only affects groups $\mathcal{G}$, $\mathcal{A}$, and the two neighbors of $\mathcal{A}$ (see Figure 3.8). Thus it is sufficient to prove that for these groups the group size property, overlap property and interleave property still hold. According to the ways that Algorithm 2 will be executed, the proof proceeds in two cases.

Case I: $|\mathcal{G}| < 2d$ (line 1-2). After the participant joins, $|\mathcal{G}|$ and $|\mathcal{A}|$ increases by 1. Since $|\mathcal{G}| < 2d$ and $|\mathcal{A}| < |\mathcal{G}|$, the group size property is satisfied. The overlap between $\mathcal{G}$ and $\mathcal{A}$ increases, the overlap between $\mathcal{G}$ and $\mathcal{B}$ ($\mathcal{C}$) does not change. Hence the overlap property holds.

Case II: $|\mathcal{G}| = 2d$ (line 3-4): After $\mathcal{G}$ is split, clearly the group size property is satisfied. The overlap between $\mathcal{G}_1$ and $\mathcal{B}$ after the split is the same as the overlap between $\mathcal{G}$ and $\mathcal{B}$ before the split. Thus, $u = |\mathcal{G}_1 \bigcap \mathcal{B}| \geq x$. Similarly, $z = |\mathcal{G}_2 \bigcap \mathcal{C}| \geq x$. Let $v = |\mathcal{G}_1 \bigcap \mathcal{A}|$ and $w = |\mathcal{G}_2 \bigcap \mathcal{A}|$. $w = |\mathcal{A}| - v = |\mathcal{A}| - (|\mathcal{G}_1| - u) = |\mathcal{A}| + u - |\mathcal{G}_1| \geq d + x - d = x$. Similarly, $v \geq x$. Thus, the overlap property holds.

Clearly, in both cases the interleave property holds. □

Lemma 2. *Suppose a node joins two groups which overlap in Pattern II. After Algorithm 3 is run, the grouping is secure.*

Proof. Algorithm 3 only affects groups $\mathcal{G}$, $\mathcal{A}$, $\mathcal{B}$ and possibly the right neighbor of $\mathcal{B}$ (see Figure 3.9). It is sufficient to prove that these groups satisfy the group size

Algorithm 3 adjust(JOIN, II): Re-grouping after a node joins two groups which overlap in pattern II (see Fig. 3.9(a)).

Require: $\mathcal{G}$, $\mathcal{A}$: the two groups that the node joins, $|\mathcal{G}| \geq |\mathcal{A}|$.
Require: $\mathcal{B}$: $\mathcal{A}$'s neighbor group which also overlaps with $\mathcal{G}$.
Require: Without loss of generality, $\mathcal{G}$ overlaps with the right part of $\mathcal{A}$, i.e., $\mathcal{G}.left > \mathcal{A}.left$ and $\mathcal{G}.right > \mathcal{A}.right$. In this case, $\mathcal{B}$ is the right neighbor of $\mathcal{A}$. See Figure 3.9(a).

```
if |G| < 2d then
    return;
else
    Split G in the middle into two groups, each of size d;
    Move A.right to the position P = max{G.left + x, A.left + d};
    if |B| < 2d then
        return;
    else
        Create a group C, with C.left = A.right and C.right = C.left + d;
        B.left ← C.right;
    end if
end if
```

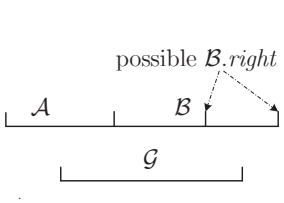

(a) Groups before join

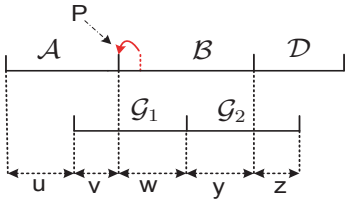

(b) Before join, $\mathcal{B}.right < \mathcal{G}.right$: Split $\mathcal{G}$ to $\mathcal{G}_1$, $\mathcal{G}_2$; move $\mathcal{A}.right$.

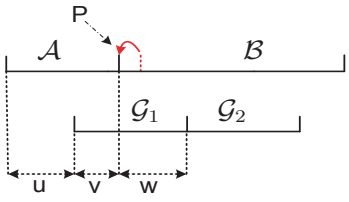

(c) Before join, $\mathcal{B}.right > \mathcal{G}.right$. After splitting $\mathcal{G}$ and moving $\mathcal{A}.right$, $|\mathcal{B}| < 2d$.

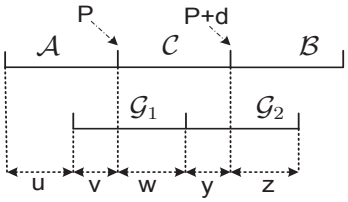

(d) Before join, $\mathcal{B}.right > \mathcal{G}.right$. After splitting $\mathcal{G}$ and moving $\mathcal{A}.right$, $|\mathcal{B}| = 2d$. Thus, $\mathcal{C}$ is created.

Figure 3.9. The regrouping (in Alg. 3) when a node joins $\mathcal{G}$ and $\mathcal{A}$ which overlap in Pattern II. $\mathcal{B}$ is the neighbor of $\mathcal{A}$; it overlaps with $\mathcal{G}$ in Pattern I or II.

property, overlap property and interleave property. According to the ways that Algorithm 3 will be executed, the proof proceeds in three cases.

Case I: Line 1-2 are run. The proof is similar to the proof of Lemma 1.

Case II: Line 3-7 are run. Suppose $\mathcal{G}$ is split into $\mathcal{G}_1$ and $\mathcal{G}_2$, each of size d (see Figure 3.9(b)). First, we prove that the group size property holds. Clearly, $\mathcal{G}_1$, $\mathcal{G}_2$ and $\mathcal{B}$ satisfy the condition. Since $|\mathcal{A}| = \mathcal{A}.right - \mathcal{A}.left = max\{\mathcal{G}.left + x, \mathcal{A}.left + d\} - \mathcal{A}.left \geq (\mathcal{A}.left + d) - \mathcal{A}.left = d$, $\mathcal{A}$ also satisfies the group size property.

Then we prove that the overlap property holds. $v = |\mathcal{A} \bigcap \mathcal{G}_1| = \mathcal{A}.right - \mathcal{G}_1.left = max\{\mathcal{G}.left + x, \mathcal{A}.left + d\} - \mathcal{G}_1.left \geq (\mathcal{G}_1.left + x) - \mathcal{G}_1.left = x$. Since the overlap property holds before the join, $u \geq x$. $v = max\{\mathcal{G}_1.left + x, \mathcal{A}.left + d\} - \mathcal{G}_1.left \leq max\{\mathcal{G}_1.left + x, \mathcal{G}_1.left - u + d\} - \mathcal{G}_1.left = max\{x, d - u\} \leq max\{x, d - x\} = d - x$. Then we have $w = |\mathcal{B} \bigcap \mathcal{G}_1| = |\mathcal{G}_1| - v = d - v \geq d - (d - x) = x$. For the overlap between $\mathcal{B}$ and $\mathcal{G}_2$, there are two cases:

- If $\mathcal{B}$ overlaps with $\mathcal{G}$ in Pattern I before $\mathcal{G}$ splits, i.e., $\mathcal{B}.right < \mathcal{G}_2.right$ (see Figure 3.9(b)), $y = |\mathcal{B} \bigcap \mathcal{G}_2| = |\mathcal{B}| + v - |\mathcal{G}_1| \geq d + x - d = x$; also, the overlap between $\mathcal{G}_2$ and the right neighbor of $\mathcal{B}$ is identical to the overlap between $\mathcal{G}$ and the right neighbor of $\mathcal{B}$ before the join, which means $z \geq x$.

- If $\mathcal{B}$ overlaps with $\mathcal{G}$ in Pattern II before $\mathcal{G}$ splits, i.e., $\mathcal{B}.right > \mathcal{G}_2.right$ (see Figure 3.9(c)), $|\mathcal{B} \bigcap \mathcal{G}_2| = |\mathcal{G}_2| = d > x$.

Thus the overlap property holds.

Case III: Line 3-5, 8-10 are run. Suppose $\mathcal{G}$ is split into $\mathcal{G}_1$ and $\mathcal{G}_2$ (see Figure 3.9(d)). In this case, $\mathcal{B}.right > \mathcal{G}_2.right$. First we prove that the group size property holds. Similar as in Case II, $\mathcal{G}_1$, $\mathcal{G}_2$, $\mathcal{A}$ and $\mathcal{C}$ satisfy the group size property. The distance between $\mathcal{B}.right$ and $\mathcal{A}.left$ is equal to the size of $\mathcal{B}$ plus the size of $\mathcal{B}$ before group $\mathcal{C}$ is created. Hence we have $\mathcal{B}.right - \mathcal{A}.left \leq ((2d-1)+1)+(2d-1) = 4d-1$. $|\mathcal{B}| = \mathcal{B}.right - \mathcal{A}.left - |\mathcal{A}| - \mathcal{C} \leq 4d - 1 - d - d = 2d - 1$.

Then we prove that the overlap property holds. Similar as in Case II, $x \leq v \leq d-x$. Since $w = |\mathcal{G}_1| - v = d - v$, $x \leq w \leq d-x$. Similarly, since $y = |\mathcal{C}| - w = d - w$ and $z = |\mathcal{G}_2| - y = d - y$, we get $x \leq y \leq d - x$ and $x \leq z \leq d - x$.

Clearly in these cases the interleave property holds. □

Algorithm 4 adjust(LEAVE, I): Re-grouping after a node leaves two groups which overlap in pattern I (see Fig. 3.10(a)).

Require: $\mathcal{G}$, $\mathcal{A}$: the two groups that the node leaves, with $|\mathcal{G}| < |\mathcal{A}|$.
Require: $\mathcal{C}$, $\mathcal{E}$: the right neighbor of $\mathcal{G}$ and $\mathcal{A}$, respectively. See Figure 3.10(a).
1: **if** $|\mathcal{G}| \geq d$ **then**
2: **return**;
3: **else if** $|\mathcal{C}| = d$ **then**
4: Merge $\mathcal{G}$ and $\mathcal{C}$;
5: **else**
6: $u \leftarrow |\mathcal{C} \bigcap \mathcal{A}|$;
7: **if** $u \geq x + 1$ **then**
8: Move $\mathcal{G}.right$ to the right by 1;
9: **else if** $u = x$ **and** $|\mathcal{C}| \geq d + 2x$ **then**
10: Move $\mathcal{G}.right$ to the right by $2x$;
11: **else if** $u = x$ **and** $|\mathcal{C}| < d + 2x$ **then**
12: Move both $\mathcal{G}.right$ and $\mathcal{A}.right$ to the right by 1;
13: **end if**
14: **end if**

Lemma 3. *Suppose a node leaves two groups which overlap in Pattern I. After Algorithm 4 is run, the grouping is secure.*

Proof. Algorithm 4 only affects groups $\mathcal{G}$, $\mathcal{A}$ and their right neighbors (see Figure 3.10(a)). Thus we prove that these groups satisfy the group size property, overlap property and interleave property. According to the ways that Algorithm 4 will be executed, the proof proceeds in four cases:
Case I: $|\mathcal{G}| \geq d$ (line 1-2). Since $|\mathcal{A}| > |\mathcal{G}|$, $|\mathcal{A}| > d$. The group size property holds. Since $|\mathcal{G} \bigcap \mathcal{A}| = |\mathcal{G}| \geq d > x$, the overlap property is also satisfied.
Case II: $|\mathcal{G}| = d - 1$, $|\mathcal{C}| = d$ (line 3-4). Since $|\mathcal{A}| > |\mathcal{G}|$, $|\mathcal{A}| \geq d$. Let $\mathcal{G}'$ denote the group derived from the merge of $\mathcal{G}$ and $\mathcal{C}$; i.e., $\mathcal{G}'.left = \mathcal{G}.left$ and $\mathcal{G}'.right = \mathcal{C}.right$. Clearly, $|\mathcal{G}'| = 2d - 1$. Thus the group size property holds. $|\mathcal{G}' \bigcap \mathcal{A}| \geq |\mathcal{G}| = d - 1 > x$. Because the overlap property holds before the leave, $|\mathcal{C} \bigcap \mathcal{E}| \geq x$. Then $|\mathcal{G}' \bigcap \mathcal{E}| = |\mathcal{C} \bigcap \mathcal{E}| \geq x$. Hence the overlap property holds.
Case III: $|\mathcal{G}| = d - 1$, $|\mathcal{C}| \geq d + 1$ (line 5-12). Let $u = |\mathcal{C} \bigcap \mathcal{A}|$.

- Subcase 1: $u \geq x + 1$ (line 7-8). Similar as in case II, $|\mathcal{A}| \geq d$. Clearly, $|\mathcal{G}| = (d - 1) + 1 = d$ and $|\mathcal{C}| \geq (d + 1) - 1 = d$. The group size property holds. After the move of $\mathcal{G}.right$, $|\mathcal{G} \bigcap \mathcal{A}| = d > x$ and $|\mathcal{A} \bigcap \mathcal{C}| = u - 1 \geq x$. Hence, the overlap property holds.

- Subcase 2: $u = x$ and $|\mathcal{C}| \geq d + 2x$ (line 9-10). Similar as in Subcase 1,

(a) Regrouping in Alg. 4 (b) Regrouping in Alg. 5

Figure 3.10. The regrouping in Alg. 4 and 5 when a node leaves $\mathcal{G}$ and $\mathcal{A}$ which overlap in Pattern I and II, respectively.

$|\mathcal{A}| \geq d$. $|\mathcal{G}| = (d-1) + 2x$. Since $x < \frac{d}{2}$, $d < |\mathcal{G}| < 2d - 1$. $|\mathcal{C}| \geq (d+2x) - 2x = d$. The group size property holds. After the move of $\mathcal{G}.right$, $|\mathcal{G} \bigcap \mathcal{A}| = d - 1 + x > x$, $|\mathcal{G} \bigcap \mathcal{E}| = x$, and $|\mathcal{C} \bigcap \mathcal{E}| \geq d - x > x$. Hence, the overlap property holds.

- Subcase 3: $u = x$ and $|\mathcal{C}| < d + 2x$ (line 11-12). The participant's leave decreases the size of $\mathcal{A}$ and $\mathcal{G}$ by one, but the move (see line 11) increases their size by one. As a result, their size is the same as before the join. Clearly, $|\mathcal{C}| \geq d$. Before the participant joins, $|\mathcal{E}| \geq d + 1$. This is because if $|\mathcal{E}| = d$ (which means $\mathcal{E}.right < \mathcal{C}.right$), the overlap between $\mathcal{C}$ and the right neighbor of $\mathcal{E}$ satisfies that $|\mathcal{C}| - |\mathcal{E}| - u < (d + 2x) - d - x = x$, which violates the assumption that the overlap property holds before the participant joins. Then after the move $|\mathcal{E}| \geq (d+1) - 1 = d$. Therefore, the group size property holds. It is easy to see that $|\mathcal{A} \bigcap \mathcal{G}| = d$, $|\mathcal{A} \bigcap \mathcal{C}| = x$, and $|\mathcal{E} \bigcap \mathcal{C}| = |\mathcal{C}| - u \geq d - x > x$. Hence, the overlap property holds.

Clearly in these cases the interleave property holds. □

Lemma 4. *Suppose a node leaves two groups which overlap in Pattern II. After Algorithm 5 is run, the grouping is secure.*

Proof. Algorithm 5 only affects groups $\mathcal{G}$, $\mathcal{A}$ and their neighbors (see Figure 3.10(b)). Thus we prove that these groups satisfy the group size property, overlap property and interleave property. According to the ways that Algorithm 5 will be executed, the proof proceeds in eight cases. Let $u = |\mathcal{G} \bigcap \mathcal{A}|$.
Case I: $u \geq x$, $|\mathcal{G}| \geq d$, $|\mathcal{A}| \geq d$ (line 2-4). Clearly, the group size property and the overlap property are satisfied.
Case II: $u \geq x$, $|\mathcal{G}| = d - 1$, $|\mathcal{A}| \geq d$ (line 5-11).

Algorithm 5 adjust(LEAVE, II): Re-grouping after a node leaves two groups which overlap in pattern II (see Fig. 3.10(b)).

Require: $\mathcal{G}$, $\mathcal{A}$: the two groups that the node leaves.
Require: $\mathcal{D}$, $\mathcal{E}$: $\mathcal{G}$'s neighbors. $\mathcal{D}$ overlaps with $\mathcal{A}$; $\mathcal{E}$ does not.
Require: $\mathcal{B}$, $\mathcal{F}$: $\mathcal{A}$'s neighbors. $\mathcal{B}$ overlaps with $\mathcal{G}$; $\mathcal{F}$ does not.
Require: Without loss of generality, suppose $\mathcal{G}.left > \mathcal{A}.left$ and $\mathcal{G}.right > \mathcal{A}.right$ (see Fig. 3.10(b)).

if $|\mathcal{G} \bigcap \mathcal{A}| \geq x$ **then**
  if $|\mathcal{G}| \geq d$ **and** $|\mathcal{A}| \geq d$ **then**
    return;
  end if
  if $|\mathcal{G}| = d - 1$ **then**
    if $|\mathcal{E}| = d$ **then**
      Merge $\mathcal{G}$ and $\mathcal{E}$;
    else
      Move $\mathcal{G}.right$ to the right by 1;
    end if
  end if
  if $|\mathcal{A}| = d - 1$ **then**
    if $|\mathcal{F}| = d$ **then**
      Merge $\mathcal{A}$ and $\mathcal{F}$;
    else
      Move $\mathcal{A}.left$ to the left by 1;
    end if
  end if
else
  if $|\mathcal{G}| \geq d$ **and** $|\mathcal{A}| \geq d$ **then**
    if $|\mathcal{B}| \geq d + 1$ **then**
      Move $\mathcal{A}.right$ to the right by 1;
    else if $|\mathcal{D}| \geq d + 1$ **then**
      Move $\mathcal{G}.left$ to the left by 1;
    else
      Move $\mathcal{D}.right$ to the right by $2x - 1$;
    end if
  end if
  if $|\mathcal{G}| = d - 1$ **then**
    if $|\mathcal{D}| = d$ **then**
      Merge $\mathcal{G}$ and $\mathcal{D}$;
    else
      Move $\mathcal{G}.left$ to the left by 1;
    end if
  end if
  if $|\mathcal{A}| = d - 1$ **then**
    if $|\mathcal{B}| = d$ **then**
      Merge $\mathcal{A}$ and $\mathcal{B}$;
    else
      Move $\mathcal{A}.right$ to the right by 1;
    end if
  end if
end if

- Subcase 1: $|\mathcal{E}| = d$ (line 6-7). The proof is similar to Case II in the proof of Lemma 3.

- Subcase 2: $|\mathcal{E}| \geq d+1$ (line 8-9). After the move, $|\mathcal{G}| = d$ and $|\mathcal{E}| \geq d$. The group size property holds. The overlap between $\mathcal{G}$ and $\mathcal{B}$ increases, and thus they still satisfy the overlap property. The overlap between $\mathcal{B}$ and $\mathcal{E}$ decreases. If $\mathcal{B}.right > \mathcal{E}.right$, $|\mathcal{B} \bigcap \mathcal{E}| = |\mathcal{E}| \geq d > x$; if $\mathcal{B}.right < \mathcal{E}.right$ as shown in Figure 3.10(b), $w = |\mathcal{B} \bigcap \mathcal{E}| = |\mathcal{B}| + u - |\mathcal{G}| \geq d + x - d = x$. Thus, the overlap property holds.

Case III: $u \geq x$, $|\mathcal{G}| \geq d$, $|\mathcal{A}| = d-1$ (line 12-18). The proof is similar to Case II.
Case IV: $u \geq x$, $|\mathcal{G}| = d-1$, $|\mathcal{A}| = d-1$ (line 5-18). The proof simply combines the proofs of Case II and Case III together.
Case V: $u = x-1$, $|\mathcal{G}| \geq d$, $|\mathcal{A}| \geq d$ (line 20-28).

- Subcase 1: $|\mathcal{B}| \geq d+1$ (line 21-22): The participant's leave decreases the size of $\mathcal{A}$ by one, but the move increases it by one. Thus, $\mathcal{A}$'s size is the same as before the participant joins. After the move, the size of $\mathcal{B}$ decreases by one, but $|\mathcal{B}| \geq (d+1) - 1 = d$. The group size property holds. It is easy to see that $|\mathcal{A} \bigcap \mathcal{G}| = (x-1) + 1 = x$, and $|\mathcal{B} \bigcap \mathcal{G}| \geq d - |\mathcal{A} \bigcap \mathcal{G}| = d - x \geq x$. Thus, the overlap property holds.

- Subcase 2: $|\mathcal{B}| = d$, $|\mathcal{D}| \geq d+1$ (line 23-24): The proof is similar to Subcase 1.

- Subcase 3: $|\mathcal{B}| = d$ and $|\mathcal{D}| = d$ (line 25-26): It can be proved that $|\mathcal{G}| \geq d + 2x - 1$ before the move. We first prove that $\mathcal{G}.right > \mathcal{B}.right$ by contradiction. Assume $\mathcal{G}.right < \mathcal{B}.right$. Let $w = |\mathcal{B} \bigcap \mathcal{E}|$. The participant's leave does not affect w. $w = |\mathcal{B}| + u - |\mathcal{G}| \leq d + (x-1) - d = x - 1$, which violates the assumption that the overlap property holds before the leave. Thus, $\mathcal{G}.right > \mathcal{B}.right$. Then we can see that $|\mathcal{G}| \geq u + |\mathcal{B}| + x \geq d + 2x - 1$.

  The move increases (decreases) the size of $\mathcal{D}$ ($\mathcal{G}$) by $2x-1$. After the move, $|\mathcal{D}| = d + 2x - 1 < 2d - 1$, and $|\mathcal{G}| \geq (d + 2x - 1) - (2x - 1) = d$. The group size property holds. Since $|\mathcal{D} \bigcap \mathcal{A}| = |\mathcal{A}| \geq d > x$, $|\mathcal{D} \bigcap \mathcal{B}| = x$, and $|\mathcal{G} \bigcap \mathcal{B}| = |\mathcal{B}| - x = d - x > x$, the overlap property holds.

Case VI: $u = x - 1$, $|\mathcal{G}| = d - 1$, $|\mathcal{A}| \geq d$ (line 29-35). The proof is similar to Case II.

Case VII: $u = x - 1$, $|\mathcal{G}| \geq d$, $|\mathcal{A}| = d - 1$ (line 36-42). The proof is similar to Case III.

Case VIII: $u = x - 1$, $|\mathcal{G}| = d - 1$, $|\mathcal{A}| = d - 1$ (line 29-42). The proof is similar to Case IV.

Clearly, in these cases the interleave property holds. □

3.5.3.4 Communication Cost Analysis

We measure the communication cost of dynamic joins and leaves by the number of nodes that the key dealer should reissue secrets to (*number of updated nodes* for short). The communication cost of ring-based overlapped grouping is given in the following theorem.

Theorem 4. *In ring-based overlapped grouping, when a node joins (leaves), at most three (four) existing groups are updated and the number of updated nodes has an upper bound* $4d$ *(*$6d$*).*

Proof. When a node joins, if Alg. 2 is run, at most two groups ($\mathcal{G}$ and $\mathcal{A}$ in Fig. 3.8) are updated, and the number of updated nodes is bounded by $2d$, including the joining node. If Alg. 3 is run, at most three existing groups are updated ($\mathcal{G}$, $\mathcal{A}$ and $\mathcal{B}$ in Fig. 3.9(a)). The number of updated nodes is $max\{\mathcal{G}.right - \mathcal{A}.left, \mathcal{B}.right - \mathcal{A}.left\} < 4d$.

When a node leaves, if Alg. 4 is run (see Fig. 3.10(a)), at most four groups are updated, and the number of updated nodes is $max\{\mathcal{E}.right - \mathcal{A}.left, \mathcal{C}.right - \mathcal{A}.left\} < 4d$. If Alg. 5 is run, at most four groups are updated. They are $\mathcal{G}$, $\mathcal{E}$, $\mathcal{A}$ and $\mathcal{F}$ (line 5-18 in Alg. 5) or $\mathcal{G}$, $\mathcal{D}$, $\mathcal{A}$ and $\mathcal{B}$ (line 22-31). The first case happens when $|\mathcal{G}| = |\mathcal{A}| = d$, and the number of updated nodes is $|\mathcal{E}| + |\mathcal{F}| + (\mathcal{G}.right - \mathcal{A}.left) < 2d + 2d + 2d = 6d$. The second case also happens when $|\mathcal{G}| = |\mathcal{A}| = d$, and the number of updated nodes is smaller than $|\mathcal{B}| + |\mathcal{A}| + |\mathcal{D}| < 2d + d + 2d = 5d$. Hence, the number of updated nodes is bounded by $6d$. □

This theorem indicates that the communication cost of ring-based overlapped grouping depends on parameter d, which in turn depends on parameter γ (see

Table 3.10), the maximum fraction of compromised nodes. According to Table 3.10, the value of d is not large when γ is not too high. Thus, the communication cost is low. Note that the cost does not change with the number of nodes in the system.

3.6 Aggregation Protocol for Sum

In this section, we combine the basic encryption scheme in Chapter 3.4 and the ring-based overlapped grouping scheme in Chapter 3.5 to derive our privacy-preserving aggregation protocol for Sum.

3.6.1 Encryption Method

Setup: The key dealer divides the nodes into groups using Alg. 1, and independently assigns secrets for each group as done in the basic encryption scheme. Each node i gets secrets from the two groups that it is in. Let $\mathcal{S}_{i1}$ and $\bar{\mathcal{S}}_{i1}$ denote the sets of secrets received from one group, and $\mathcal{S}_{i2}$ and $\bar{\mathcal{S}}_{i2}$ denote the sets of secrets received from the other group. The node merges the secrets as follows: $\mathcal{S}_i = \mathcal{S}_{i1} \bigcup \mathcal{S}_{i2}$ and $\bar{\mathcal{S}}_i = \bar{\mathcal{S}}_{i1} \bigcup \bar{\mathcal{S}}_{i2}$. Let g denote the number of groups generated by Alg. 1. The aggregator obtains $\hat{\mathcal{S}}_1$, ..., $\hat{\mathcal{S}}_g$, where each $\hat{\mathcal{S}}_j$ is the decryption capability of one group. It sets the overall decryption capability as $\hat{\mathcal{S}} = \bigcup_{i=j}^{g} \hat{\mathcal{S}}_j$.
Encryption: The same as in the basic encryption scheme.
Decryption: The same as in the basic encryption scheme.

Due to the guarantee provided by ring-based overlapped grouping, the aggregator can only decrypt the noisy sum but nothing else.

3.6.2 Data Perturbation

The perturbation algorithm is the same as in Chapter 3.3.3.2, except that parameter β is set differently (see below).

Table 3.11. An example of Algorithm 6

step	operation	u_1	u_2	u_3	u_4	u_5	u_6	n
0	initialize	3	3	4	4	-	-	4
1	Node 5 joins	3	5	4	4	5	-	5
2	Node 6 joins	6	5	4	4	5	6	6
3	Node 2 leaves	5	-	4	4	5	3	5
4	Node 1 leaves	-	-	4	4	3	3	4

3.6.3 Dealing with Dynamic Joins and Leaves

When a node joins or leaves, the key dealer runs Algorithm 2-5 to adjust grouping. For each adjusted group, it reruns the setup phase to distribute a new set of secrets to the nodes of the group and to the aggregator. In this process, it only communicates with the nodes in the adjusted groups, which constitute only a small portion of all nodes.

In the data perturbation algorithm presented in Chapter 3.3.3.2, each node uses the number of nodes n to set parameter β (i.e., $\beta = \min(\frac{1}{(1-\gamma)n} \ln \frac{1}{\delta}, 1)$), such that all nodes collectively add just one copy of geometric noise to the aggregate. However, it requires communications with all nodes upon every join and leave to send the exact value of n to them. Obviously, it nullifies the benefits of grouping in reducing the communication cost. To address this issue, we relax the accuracy requirement on the value of n such that n does not have to be updated to every node upon every join and leave. As a tradeoff, a little more noise is added.

Specifically, each node records the value of n according to its knowledge. Let u denote the value recorded by the node. u may not always reflect n, which is the real number of nodes. Each node uses u to set parameter β for data perturbation, i.e., $\beta = \min(\frac{1}{(1-\gamma)u} \ln \frac{1}{\delta}, 1)$. The smaller u is, the more noise is added. u should not be larger than n to ensure that at least one copy of geometric noise is added to provide differential privacy, but u cannot be too small to avoid too much aggregation error. Thus, the values of u at the nodes should be updated appropriately upon dynamic joins or leaves. The challenge is how to update u without incurring too much communication cost.

We propose Alg. 6 to address this challenge. Table 3.11 shows a running example of it.

3.6.4 Analysis

3.6.4.1 Aggregation Error

Theorem 5. *Algorithm 6 guarantees that* $\forall i,\ u_i \in (\frac{n}{2}, n]$.

Proof. By induction, we prove that the sorted values of u always follow one of the following two patterns:
n is even: $\lfloor\frac{n}{2}\rfloor+1,\ \lfloor\frac{n}{2}\rfloor+1,\ \lfloor\frac{n}{2}\rfloor+2,\ \lfloor\frac{n}{2}\rfloor+2,\ ...,\ n,\ n$
n is odd: $\lfloor\frac{n}{2}\rfloor+1,\ \lfloor\frac{n}{2}\rfloor+2,\ \lfloor\frac{n}{2}\rfloor+2,\ ...,\ n,\ n$.

Clearly, the statement is true for the initial values of u. In the induction step, we prove that the statement is still true after a participant joins or leaves. The induction step proceeds in four cases.
First, the initial pattern is $\lfloor\frac{n}{2}\rfloor+1,\ \lfloor\frac{n}{2}\rfloor+1,\ \lfloor\frac{n}{2}\rfloor+2,\ \lfloor\frac{n}{2}\rfloor+2,\ ...,\ n,\ n$, and a participant joins. After the join, the pattern becomes $\lfloor\frac{n}{2}\rfloor+1,\ \lfloor\frac{n}{2}\rfloor+2,\ \lfloor\frac{n}{2}\rfloor+2,\ ...,\ n+1,\ n+1$, and the number of participants becomes $n+1$. Since n is even, $\lfloor\frac{n}{2}\rfloor+1=\lfloor\frac{n+1}{2}\rfloor+1$. Thus, the statement is still true.
Second, the initial pattern is $\lfloor\frac{n}{2}\rfloor+1,\ \lfloor\frac{n}{2}\rfloor+1,\ \lfloor\frac{n}{2}\rfloor+2,\ \lfloor\frac{n}{2}\rfloor+2,\ ...,\ n,\ n$, and a participant leaves. No matter which participant leaves, the pattern becomes $\lfloor\frac{n-1}{2}\rfloor+1,\ \lfloor\frac{n}{2}\rfloor+1,\ \lfloor\frac{n}{2}\rfloor+1,\ ...,\ n-1,\ n-1$ and the number of participants becomes $n-1$. The statement is still true.
Third, the initial pattern is $\lfloor\frac{n}{2}\rfloor+1,\ \lfloor\frac{n}{2}\rfloor+2,\ \lfloor\frac{n}{2}\rfloor+2,\ ...,\ n,\ n$, and a participant joins. After the join, $\lfloor\frac{n}{2}\rfloor+1$ changes to $n+1$, and the pattern becomes $\lfloor\frac{n}{2}\rfloor+2,\ \lfloor\frac{n}{2}\rfloor+2,\ ...,\ n+1,\ n+1$. Note that the number of participants becomes $n+1$. The statement is still true.
Fourth, the initial pattern is $\lfloor\frac{n}{2}\rfloor+1,\ \lfloor\frac{n}{2}\rfloor+2,\ \lfloor\frac{n}{2}\rfloor+2,\ ...,\ n,\ n$, and a participant leaves. After the leave, the pattern becomes $\lfloor\frac{n-1}{2}\rfloor+1,\ \lfloor\frac{n}{2}\rfloor+1,\ \lfloor\frac{n}{2}\rfloor+2,\ \lfloor\frac{n}{2}\rfloor+2,\ ...,\ n-1,\ n-1$. Since n is odd, the pattern is equivalent to $\lfloor\frac{n-1}{2}\rfloor+1,\ \lfloor\frac{n-1}{2}\rfloor+1,\ \lfloor\frac{n-1}{2}\rfloor+2,\ \lfloor\frac{n-1}{2}\rfloor+2,\ ...,\ n-1,\ n-1$. Note that the number of participants becomes $n+1$. The statement is still true. □

Comments: Since $u \le n$, at least one copy of geometric noise is added to the sum aggregate to provide differential privacy; since $u > \frac{n}{2}$, at most one more copy of geometric noise is added. Thus, *the average aggregation error is roughly within twice of the geometric noise required for differential privacy.*

3.6.4.2 Communication Cost

Alg. 6 only incurs very small communication cost. When a node joins, the joining node and another node with the minimum u are updated; when a node leaves, (at most) two remaining nodes with the maximum u are updated. Thus, the u of at most two nodes are updated for each join or leave. Considering this property and Theorem 4, the overall communication cost is as follows.

Corollary 1. *When a node joins (leaves), our scheme communicates with at most $4d + 2$ ($6d + 2$) nodes to update their secret keys and their values of u.*

Algorithm 6 Procedures run by the key dealer to manage the values of u for nodes.

Require: n: the real number of nodes
Require: u_i: the number of nodes that node i uses to set parameter β
Initialization:
if n is even **then**
    $u_1, u_2, ..., u_n \leftarrow \lfloor \frac{n}{2} \rfloor + 1, \lfloor \frac{n}{2} \rfloor + 1, \lfloor \frac{n}{2} \rfloor + 2, \lfloor \frac{n}{2} \rfloor + 2, ..., n, n$;
else
    $u_1, u_2, ..., u_n \leftarrow \lfloor \frac{n}{2} \rfloor + 1, \lfloor \frac{n}{2} \rfloor + 2, \lfloor \frac{n}{2} \rfloor + 2, ..., n, n$;
end if

Join:
if Node i joins **then**
    $n \leftarrow n + 1$;
    $u_i \leftarrow n$;
    Find a node j with $u_j = \min\{u_1, u_2, ..., u_n\}$;
    $u_j \leftarrow n$;
end if

Leave:
if Node i leaves **then**
    $n \leftarrow n - 1$;
    Find a node j with $u_j = \max\{u_1, u_2, ..., u_n\}$;
    if There exists another node m with $u_m = u_j$ **then**
        $u_m \leftarrow u_i$;
    end if
    $u_j \leftarrow \lfloor \frac{n}{2} \rfloor + 1$;
end if

3.7 Evaluations

This section evaluates the communication cost (measured by the number of updated nodes per join or leave) and the aggregation error of our solution through

simulations, and evaluates the computation cost via implementation-based measurements. We compare our solution against four other schemes: the scheme proposed in [28] (denoted by *SCRCS*), the *Binary* scheme [29], the scheme proposed in [30] (denoted by *JK*), and the *Naive Grouping* scheme presented in Chapter 3.5.1.

3.7.1 Communication Cost

We first evaluate the communication cost of ring-based overlapped grouping, and study how it is affected by parameter γ (i.e., the maximum fraction of nodes compromised). We set x and d according to Table 3.10. To measure the communication cost of join (leave), we first generate a random initial grouping structure that includes 2000 (102,000) nodes, and then simulate 10^5 joins (leaves) over it, resulting in 102,000 (2000) nodes in the end. We compute the mean and standard deviation over the 10^5 measurements.

Figure 3.11 shows the simulation results as well as the analytical upper bound (see Theorem 4). As γ increases, the communication cost increases. This is because x is larger (see Eq. 3.14) and the group size is larger. However, only 170 nodes are updated even when 20% of nodes are compromised. Also, we found that the communication cost of our scheme is roughly half of the analytical upper bound.

We also simulated the communication cost under a mix of joins and leaves. The results do not deviate much from the cost of pure joins and leaves.

We then compare our solution against the other four schemes in communication cost. In Naive Grouping, parameter g is set such that our scheme and Naive Grouping have the same average aggregation error. In our scheme, $\gamma = 0.05$. We vary the number of nodes n. For each value of n, we compute the mean and standard deviation over 10000 runs.

Figure 3.12 shows the results. Clearly, the communication cost of our scheme is much smaller than SCRCS and Naive Grouping, and is close to Binary and JK. This is because the ring-based overlapped grouping can effectively reduce the number of nodes that should be updated for dynamic joins and leaves. Also, the communication cost of our scheme does not change with parameter n, and hence it can scale to large systems. Interestingly, our scheme has much smaller communication cost than Naive Grouping with the same aggregation error, which demonstrates

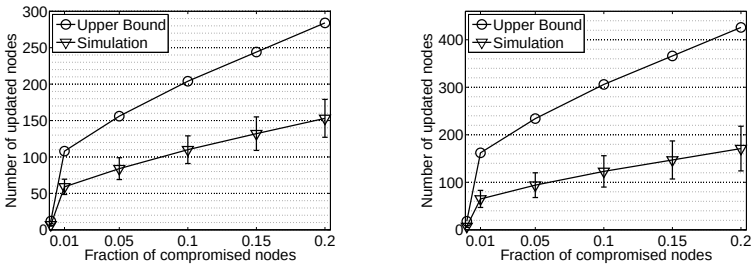

(a) Join (b) Leave

Figure 3.11. The communication cost of ring-based overlapped grouping.

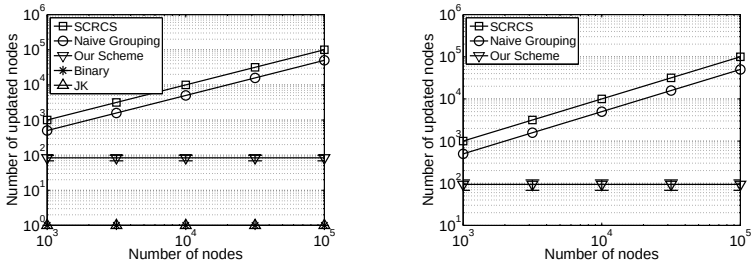

(a) Join (b) Leave

Figure 3.12. Comparisons between our scheme and other schemes in the communication cost of dynamic joins and leaves (log-log scale). For dynamic leaves, the communication cost of Binary and JK is zero and thus not shown in the log-log plot.

that overlapped grouping achieves a better balance between communication cost and aggregation error.

3.7.2 Aggregation Error

We compare our scheme with the other four schemes on aggregation error. In Naive Grouping, the parameter g is set such that Naive Grouping and our scheme have the same average communication cost for leave. In the simulation, we assume each node's data is either 0 or 1 (i.e., $\Delta = 1$). We vary parameters n, ϵ and δ. For each parameter, we measure the mean and standard deviation of aggregation error over 10000 runs.

Table 3.12 shows the mean and standard deviation of aggregation error. As the number of node increases, the aggregation error of Binary and Naive Grouping also increases quickly. However, the aggregation error of Our scheme, SCRCS and JK does not change too much, because on average they add a constant number

Table 3.12. The mean and standard deviation of aggregation error

	$n = 10^3$	3162	10^4	31623	10^5
Binary	247/211	300/260	360/308	386/333	439/381
Naive Grp.	63/48	112/85	199/152	358/269	631/479
Our Sch.	26/23	27/22	26/23	26/22	26/22
SCRCS	18/17	18/17	18/17	18/17	18/17
JK	9.9/9.8	10.2/10.1	10/9.9	10.1/10	10/9.9
	$\epsilon = 0.05$	0.1	0.2	0.3	0.4
Binary	704/609	363/307	178/153	121/103	88/75
Naive Grp.	398/301	199/152	100/75	66/51	50/38
Our Sch.	52/44	26/22	13/11	9/7	6/5
SCRCS	36/34	18/17	8.7/8.5	5.8/5.6	4.6/4.3
JK	19.9/19.8	10/9.9	5.1/5	3.3/3.2	2.5/2.4
	$\delta = 0.01$	0.05	0.1	0.15	
Binary	409/341	363/307	328/285	315/281	
Naive Grp.	248/189	199/152	174/132	159/120	
Our Sch.	33/27	26/22	23/20	20/19	
SCRCS	23/20	18/17	16/15	15/13	
JK	10.2/10.1	10/9.9	10/9.8	9.9/9.9	

The number on the left (right) of "/" is mean (standard deviation).
By default, $n = 10000$, $\gamma = 0.05$, $\epsilon = 0.1$ and $\delta = 0.05$.

of copies of geometric noise to the aggregate. As privacy parameter ϵ (δ, resp.) decreases, which means a stricter requirement for differential privacy, all schemes have a higher aggregation error, since each node needs to add more noise to meet the stronger privacy requirement. In nearly all cases, the aggregation error in our scheme is one order of magnitude smaller than Binary and Naive Grouping, and it is within 1.5 (2.5) times of the aggregation error SCRCS (JK). Thus, our scheme has low aggregation error.

3.7.3 Computation Cost and Running Time

We implemented a prototype system in Java. The prototype has two components which are used as the mobile node and the aggregator respectively. The mobile node component is implemented on a Android Nexus S Phone, which has 1GHz CPU and 512MB RAM, and runs Android 4.0.4 OS. The aggregator component is implemented on a Windows Laptop with 2.6GHz CPU, 4GB RAM and 64-bit Windows 7 OS. By running experiments over the prototype, we measured the time needed for the phone to encrypt a data value and the time needed for the laptop to decrypt the sum aggregate. For comparison, we also implemented SCRCS, JK and

Table 3.13. The analytical computation cost of different schemes

	Mobile Node	Aggregator
Our Scheme	$4c$ PRFs	$\frac{2nq}{d}$ PRFs
JK	2 Paillier encryptions & 1 signature generation	2 Paillier decryptions & $2n$ mod. multiplications & n sig. verifications
SCRCS	2 mod. exp.	$\sqrt{n\Delta}$ mod. exp.
Binary	$2(\lfloor \log_2 n \rfloor + 1)$ mod. exp.	$\sqrt{n\Delta}$ mod. exp.

Binary and measured their running time. As to the JK scheme, the data consumer and the key manager (see [30]) are implemented together as the aggregator.

Table 3.13 shows the computation overhead of these schemes (see [32, 28, 29, 30] for details). In the implementation, HMAC-SHA256 is used as the PRF of our scheme. For JK, the Paillier cryptosystem uses a 1024-bit modulus, and RSA (1024-bit) is used as the digital signature algorithm. For SCRCS and Binary, the high-speed elliptic curve "curve25519" is used for modular exponentiation.

Table 3.14 shows the running time of these schemes. Compared with JK, our scheme is two orders of magnitude faster in both encryption and decryption. This is because JK uses the Paillier cryptosystem which is very expensive in computation, but our scheme is based on HMAC which is very efficient. Compared with SCRCS (Binary), our scheme is one (two) order(s) of magnitude faster in encryption, and two or three orders of magnitude faster in decryption when the plaintext space is 1000 or larger. SCRCS and Binary are very slow in decryption because they need to traverse the possible plaintext space to decrypt sum, computing one modular exponentiation for each possible value. Thus, our scheme is the most efficient in computation.

Comments. Our scheme's high efficiency in computation makes it a better choice for large-scale mobile sensing applications with large plaintext spaces, high aggregation loads (e.g., many parallel aggregation tasks per node or per aggregator, short aggregation period), resource-constraint mobile devices (e.g., personal healthcare devices besides smartphones) and rich statistics.

Table 3.14. The running time of different schemes

	Enc.	Decryption			
	-	$n = 10^3$	10^4	10^5	10^6
Our Scheme	3.4ms	1.2ms	12ms	0.12s	1.2s
JK	236ms	175ms	1.5s	15s	150s
SCRCS ($\Delta = 10^3$)	45ms	5.6s	18s	56s	177s
SCRCS ($\Delta = 10^4$)	45ms	18s	56s	177s	560s
SCRCS ($\Delta = 10^5$)	45ms	56s	177s	560s	1770s
Binary ($\Delta = 10^3$)	0.5∼0.9s	5.6s	18s	56s	177s
Binary ($\Delta = 10^4$)	0.5∼0.9s	18s	56s	177s	560s
Binary ($\Delta = 10^5$)	0.5∼0.9s	56s	177s	560s	1770s

The encryption time of Binary depends on n, and range [0.5, 0.9] is obtained for $n \in [10^3, 10^6]$. In our scheme, $\gamma = 0.2$.

3.8 Extensions and Discussions

3.8.1 Aggregation Protocol for Min

The Min aggregate is defined as the minimum value of the nodes' data. This section presents a protocol which employs the Sum aggregate to get Min.

3.8.1.1 Basic Min Aggregation

This scheme gets the Min aggregate of each time period using $\Delta + 1$ parallel Sum aggregates in the same time period. The sums used to obtain Min are based on a number of 1-bit *derivative data* (denoted by d) derived from the nodes' raw data x. Without loss of generality, we assume that Δ is a power of two.

The scheme works as follows. In each time period, each node generates $\Delta + 1$ derivative data $d[0]$, $d[1]$, ..., $d[\Delta]$, where each derivative data corresponds to one possible data value in the plaintext space. For each $j \in [0, \Delta]$, the node assigns 1 to $d[j]$ if its raw data value is equal to j and assigns 0 otherwise. For each $j \in [0, \Delta]$, the aggregator can obtain the Sum aggregate of $d[j]$ using the sum aggregation protocol presented in Chapter 3.4. Then Min is the smallest j that returns a positive sum.

In each time period, each node involves in $\Delta + 1$ sum aggregates over $\Delta + 1$ derivative data. Note that in the sum aggregation protocol each node computes $2c$ PRFs to encrypt his data. It is inefficient to compute $2c$ PRFs for each derivative data. Since these data are independent, we use a more efficient technique that concatenates multiple data together and encrypts them as a whole.

User	Derivative data			
	d[1]	d[2]	d[3]	d[4]
1	1	0	0	0
2	0	0	1	0
3	0	0	1	0
Sum	1	0	2	0

(a) Original derivative data

User	Derivative data							
	d[1]		d[2]		d[3]		d[4]	
1	0	1	0	0	0	0	0	0
2	0	0	0	0	0	1	0	0
3	0	0	0	0	0	1	0	0
Sum	0	1	0	0	1	0	0	0

(b) Extended and concatenated data

Figure 3.13. An example of sum based on extended and concatenated derivative data.

This technique extends each derivative data from one bit to $\lceil \log (n+1) \rceil$ bits by adding $\lceil \log (n+1) \rceil - 1$ 0's on the left, and then concatenates all extended derivative data into a single bit string. The sum of the concatenated string (interpreted as an integer) is obtained using the sum aggregation protocol. The obtained sum is considered as a bit string, and split into substrings of $\lceil \log (n+1) \rceil$ bits each. Each substring, when interpreted as an integer, represents the sum of one derivative data. Note that these substrings do not affect each other (i.e., no carries among them), since the sum of each derivative data does not exceed n. Figure 3.13 shows an example of this process.

Clearly, the concatenated data has $(\Delta+1)\lceil \log (n+1) \rceil$ bits. The ciphertext generated by each node has $\alpha = (\Delta+1)\lceil \log (n+1) \rceil$ bits. If α is larger than H, which is the size of the output generated by the PRF (i.e., an HMAC), we can divide the derivative data into $\frac{(\Delta+1)\lceil \log (n+1) \rceil}{H}$ groups and apply the above technique to each group. Thus, $\frac{(\Delta+1)\lceil \log (n+1) \rceil}{H}$ instances of the sum aggregation protocol are needed in each time period. For example, when $n = 1000$, $\Delta = 10000$ and SHA-512 is used as the hash function of HMAC, 196 instances of the sum aggregation protocol are needed.

Each node uses just one set of secrets for all instances of the sum aggregation protocol. For instance j, it uses $h(f_{s'}(j|t))$ to generate the encryption key instead of using $h(f_{s'}(t))$ in the original protocol (see Equation 3.9). Similarly, the aggregator also uses just one set of secrets.

Since the sum aggregation protocol does not leak the derivative data of any node, the aggregator cannot know the data value of any specific node.

3.8.1.2 Low-cost Min Aggregation

When the plaintext space is large, the cost of the basic Min aggregation scheme is high. In some application scenarios, it may not be necessary to get the exact Min, but an approximate answer is good enough. For such scenarios, the basic Min aggregation scheme can be extended to get an approximate Min with much smaller cost.

Specifically, we wish to obtain an approximate Min where the relative error (defined as $\frac{|\text{Exact Min}-\text{Approximate Min}|}{max\{\text{Exact Min},1\}}$) is required to be lower than $\frac{1}{2^\epsilon}$ ($\epsilon \geq 0$). To meet this requirement, the exact value of Min should be obtained if Min is smaller than or equal to 2^ϵ, and the ϵ-bit segment of Min (when Min is interpreted as a bit string) that starts from the first '1' bit should be obtained if Min is larger than 2^ϵ. For example, suppose Min is 42 (00101010) out of 8-bit data. To make the relative error smaller than $\frac{1}{2^3}$, it is sufficient to know that Min has the bit pattern $00101xxx$. Then we can set the bit that follows the known bits as 1 and set other bits as 0. The obtained approximate Min is 00101100, which is 44. The relative error is $\frac{1}{21}$, which is smaller than the required $\frac{1}{2^3}$.

To obtain the approximate Min, each node appends $\epsilon + 1$ padding bits to its raw data. If the data value is zero, the first padding bit is 1 and the others are 0; otherwise, all the padding bits are 0. The padded data has $\log \Delta + \epsilon + 2$ bits and at least one bit is 1. The first '1' bit of Min may appear in any of the first $\log \Delta + 2$ bits of the padded data. In the case it appears at the first padding bit, Min is zero.

Suppose in the binary representation of data value, the weight of bit decreases from the left to the right. Let δ ($\delta \in [1, \log \Delta + 2]$) denote the location (indexed from the left) of the first '1' bit of Min. Smaller δ means larger Min. Let σ denote the value of the $(\epsilon - 1)$-bit segment of Min that follows δ. When δ is the same, a larger σ means larger Min. Clearly, there are $2^{\epsilon-1}(\log \Delta + 2)$ possible combinations of $\langle \delta, \sigma \rangle$. We map these combinations to an *auxiliary* plaintext space 0, 1, ..., $2^{\epsilon-1}(\log \Delta + 2) - 1$, such that if one combination means smaller Min than another combination, it is mapped to a smaller value in the auxiliary plaintext space than that combination. Let $v[\delta, \sigma]$ denote the value that combination $\langle \delta, \sigma \rangle$ maps to.

In each time period, each node converts its padded raw data to a value x' in

Table 3.15. The relative error and cost of the basic Min aggregation scheme and the low-cost scheme.

	Basic	Low-cost
Relative error	0	$\leq \frac{1}{2^\epsilon}$
Encryption (PRFs)	$\frac{2c(\Delta+1)\lceil\log(n+1)\rceil}{H}$	$\frac{2^\epsilon c(\log\Delta+2)}{H}$
Decryption (PRFs)	$\frac{q(\Delta+1)\lceil\log(n+1)\rceil}{H}$	$\frac{2^{\epsilon-1}q(\log\Delta+2)}{H}$
Ciphertext size (bit)	$(\Delta+1)\lceil\log(n+1)\rceil$	$2^{\epsilon-1}(\log\Delta+2)$

H is the size of the output generated by the PRF.

the auxiliary plaintext space as follows: if in its padded raw data the first '1' bit appears at δ' and the value of the $(\epsilon-1)$-bit segment that follows the first '1' bit is σ', it sets $x' = v[\delta', \sigma']$. The aggregator can get the Min of x' using the basic Min aggregation scheme, and reversely map the Min of x' to a pair of $\langle\delta, \sigma\rangle$. It knows that the first '1' bit of the Min aggregate over padded raw data appears at location δ, and the $(\epsilon-1)$-bit segment that follows the first '1' bit is σ. Then it sets the bit that follows the $(\epsilon-1)$-bit segment as 1, and sets the remaining bits as 0. This derives the Min aggregate over padded raw data, which has the form $\{0\}^{\delta-1}\{1\}^1\{0,1\}^{\epsilon-1}\{1\}^1\{0\}^{\log\Delta+2-\delta}$. From this bit string, the last $\epsilon+1$ padding bits are removed and then the approximate Min of nodes' raw data is obtained.

Figure 3.14 shows a running example of this process. In this example, $\Delta = 4$ and $\epsilon = 3$. The four nodes' auxiliary data values are $x'_1 = 12$, $x'_2 = 12$, $x'_3 = 10$ and $x'_4 = 4$. The Min of the auxiliary data is 4, and it is reversely mapped to $\langle\delta, \sigma\rangle = \langle 3, 00\rangle$. Thus, the approximate Min of padded raw data is 0010010. After the last four padding bits are removed, the output is 001.

In total, this scheme uses $2^{\epsilon-1}(\log\Delta+2)$ Sum aggregates of 1-bit derivative data. Thus, $\frac{2^{\epsilon-1}(\log\Delta+2)}{H}$ instances of the sum aggregation protocol are needed in each time period. For example, when $\Delta = 10^4$, SHA-512 is used as the hash function of HMAC and it is required to limit the relative error to 1% (i.e., $\epsilon = 7$), only 2 instances are needed.

Table 3.15 summarizes the relative error and cost of the basic Min aggregation scheme and the low-cost scheme.

3.8.1.3 Practical Performances

Our low-cost Min aggregation scheme derives Min from $2^{\epsilon-1}(\log\Delta+2)$ parallel Sum aggregates of 1-bit data, where each sum is obtained using our Sum aggregation

	x[1]	x[2]	x[3]	x[4]	x[5]	x[6]	x[7]
x_1=4	1	0	0	0	0	0	0
x_2=4	1	0	0	0	0	0	0
x_3=3	0	1	1	0	0	0	0
x_4=1	0	0	1	0	0	0	0
	Raw data			Padding bits			

(a) Padded raw data

δ	1				2				3				4			
σ	11	10	01	00	11	10	01	00	11	10	01	00	11	10	01	00
$v[\delta,\sigma]$	15	14	13	12	11	10	9	8	7	6	5	4	3	2	1	0
x_1=4	0	0	0	1	0	0	0	0	0	0	0	0	0	0	0	0
x_2=4	0	0	0	1	0	0	0	0	0	0	0	0	0	0	0	0
x_3=3	0	0	0	0	0	1	0	0	0	0	0	0	0	0	0	0
x_4=1	0	0	0	0	0	0	0	0	0	0	0	1	0	0	0	0
Sum	0	0	0	2	0	1	0	0	0	0	0	1	0	0	0	0

(b) Derivative data

Figure 3.14. An example of the process that obtains an approximate Min.

protocol. Here, each sum can also be obtained using SCRCS, and we refer to the Min aggregation scheme that uses SCRCS as a building block as *SCRCS-Min*. In SCRCS-Min, each node computes $2^{\epsilon}(\log\Delta+2)$ modular exponentiations to encrypt his data, and the aggregator computes $2^{\epsilon-1}\sqrt{n}(\log\Delta+2)$ modular exponentiations to decrypt the Min.

According to the bench-marking data reported by eBACS [89], it takes roughly 0.3 *ms* to compute a modular exponentiation using high-speed elliptic curves such as "curve25519" on a 64-bit desktop PC, and it takes roughly 0.26 μs[3] to compute an HMAC when SHA-512 is used as the hash function.

Based on these numbers, Table 3.16 and 3.17 show the running time of our Min aggregation protocol and SCRCS-min at different levels of relative error. Here, the plaintext space is set as $\Delta = 10^4$. The parameters of our protocol are set according to Table 3.6 and Table 3.7 when $\gamma = 0.2$. In all the shown cases, our protocol is at least five (six) orders of magnitude faster than SCRCS-min in encryption (decryption). Especially, as the system scale increases, the running time of decryption in SCRCS-min increases quickly which shows the poor scalability of SCRCS-min, but the running time of our protocol decreases and is always very

[3]According to eBACS, it takes 0.13 μs to compute one SHA-512. Since one HMAC mainly computes two hashes, we simply double this time to get the running time of HMAC.

Table 3.16. The running time of our Min aggregation protocol and SCRCS-min when the relative error is smaller than 1%.

	Encryption				Decryption			
	$n = 10^3$	10^4	10^5	10^6	10^3	10^4	10^5	10^6
SCRCS-min	587ms	587ms	587ms	587ms	9.3s	29s	93s	294s
Ours	5μs	4μs	3μs	3μs	4μs	3μs	2.5μs	2μs

Table 3.17. The running time of our Min aggregation protocol and SCRCS-min when the relative error is smaller than 0.1%.

	Encryption				Decryption			
	$n = 10^3$	10^4	10^5	10^6	10^3	10^4	10^5	10^6
SCRCS-min	4.7s	4.7s	4.7s	4.7s	74s	235s	743s	2348s
Ours	40μs	32μs	24μs	24μs	32μs	24μs	20μs	16μs

low, which shows that our protocol is scalable.

3.8.2 More Aggregate Statistics

From Sum and Min, many other aggregate statistics can be easily derived, such as Count (i.e., the number of nodes that satisfy certain predicate), Average (which is derivable from Sum and Count), and Max (which can be obtained from the Min of $\Delta - x$).

Also, in the basic aggregation scheme for Min presented in Chapter 3.8.1.1, the aggregator can actually get the number of times that each possible data value appears, and derive the accurate distribution of the nodes' data in the plaintext space $[0, \Delta]$. From the distribution, other aggregate statistics such as Median, Percentile and Histogram can be obtained. In this process, the aggregator knows nothing about each individual node's data.

3.8.3 Honest-but-Curious Key Dealer

The assumption of trusted key dealer can be relaxed. Instead, we can assume an honest-but-curious key dealer that does not collude with the aggregator. It follows our protocol as specified, but may attempt to infer the data value of nodes from the the protocol transcript and from eavesdropping all communications. Under this semi-honest model, the only adaptation that should be made to our protocol is adding one more encryption/decryption to the data that each node submits to the aggregator. Specifically, each node first encrypts its noisy data as previously

specified with the secrets received from the key dealer, deriving an intermediate result c, and then encrypts c using a pre-shared key shared with the aggregator. It sends the final ciphertext to the aggregator. The aggregator first decrypts each node's intermediate result c using the pre-shared key, and then decrypts the noisy sum as previously specified. So long as the key dealer does not collude with the aggregator, it cannot get any node's intermediate result c, and thus cannot get the node's data value. In future work, we will explore how to completely remove the key dealer.

3.8.4 Dealing with Node Failures

Fault tolerance is not the major focus of this chapter, but our solution can be adapted in the following way such that, when some nodes fail, the aggregator can still obtain the aggregate over the remaining nodes.

Since the key dealer knows the secrets assigned to every node, if some nodes fail to submit data, the aggregator asks the dealer to submit data on behalf of those failed nodes. The dealer sets the data value as zero, adds a large-enough (see below) noise r to it, encrypts the noisy data with the secrets of all those failed nodes, and submits the obtained ciphertext to the aggregator. The aggregator can decrypt the sum over the functioning nodes' data. This method incurs a round trip communication between the key dealer and the aggregator. The overall communication cost is still $O(n)$.

Even if all nodes are functioning, the aggregator may dishonestly claim the failure of a subset $\tilde{\mathbb{S}}$ of nodes. (It can only claim one subset per aggregation period.) Then it can obtain two independent noisy sums, $S = \sum_i (x_i + r_i)$ and $S' = \sum_{i \notin \tilde{\mathbb{S}}} (x_i + r_i) + r$. It is easy to see that each node is included in at most two sums. Roughly speaking, to provide differential privacy, it suffices to add two copies of geometric noise to each sum. Thus, all nodes collectively add two copies of geometric noise to S and the key dealer itself adds two copies of geometric noise to S'. Considering that Alg. 6 may at most double the noise added to S, the final aggregation error is less than six copies of geometric noise when there is node failure, and less than four copies without node failure. Obviously, this method maintains $O(1)$ aggregation error.

If a node has failed for a long time, it can be removed from the system as a "leave". The recovery of a failed node can be processed as a "join".

In this method, the key dealer needs to be online, but it only makes online communications when there is node failure. In future work, we will study other solutions for fault tolerance, e.g., by exploring the direction pointed out in [29].

3.9 Summary

To facilitate the collection of useful aggregate statistics in mobile sensing without infringing mobile users' privacy, we proposed a new differentially private protocol to obtain the Sum aggregate of time-series data. The protocol utilizes a novel HMAC-based encryption scheme to perform computationally efficient aggregation, and a novel ring-based overlapped grouping technique to efficiently deal with dynamic joins and leaves of users. Implementation-based measurements show that operations at user and aggregator in our protocol are orders of magnitude faster than existing work. Also, our solution achieves O(1) aggregation error irrespective of the number of nodes in the system. More importantly, it has very low communication overhead for dynamic joins and leaves. Simulation results show that only a small number of nodes need to be updated for each join or leave when on average 20% of nodes are compromised, irrespective of the system scale. Thus, our protocol can be applied to a wide range of mobile sensing systems with various scales, plaintext spaces, aggregation loads and resource constraints.

Based on the Sum aggregation protocol, we also proposed two schemes to derive the Min aggregate of time-series data. One scheme can obtain the accurate Min while the other one can obtain an approximate Min with provable error guarantee at much lower cost.

Chapter 4

Secure Opportunistic Mobile Networking for Data Collection

For mobile devices without infrastructure support (e.g., a tablet without 3G service) and for circumstances of unavailable or cost-inefficient infrastructures (e.g., in disaster recovery scenarios), the lack of network connectivity is a key challenge to sensing data collection. To address this challenge, we observe that the mobility of users and the short-range radios of their devices can be used to form an Opportunistic Mobile Network, and sensing data can be delivered to remote collectors in this network.

Opportunistic mobile networks consist of mobile nodes carried by human beings [90, 91], vehicles [34, 92], etc. In these networks, due to lack of consistent connectivity, two nodes can only exchange data when they move into the transmission range of each other (which is called a *contact* between them). These contact opportunities can be employed for data forwarding with "store-carry-and-forward"; i.e., when a node receives some data packets, it stores these packets in its buffer, carries them around until it contacts another node, and then forwards them. Such a node with data is called a *relay*. Opportunistic mobile networks are also known as Delay/Disruption Tolerant Networks [93] or Pocket Switched Networks [90].

Opportunistic mobile networks can deliver sensing data in the following way. Due to mobility, nodes of mobile sensing systems only have opportunistic and intermittent network connectivity to access points and to each other. If a node

has connectivity to an access point, it can directly upload sensing data, assuming that data collectors are accessible via the Internet. If a node does not have such connectivity, it delivers sensing data using store-carry-and-forward. Specifically, it forwards its sensing data to another node (i.e., a relay). The relay may forward the data to another relay when they contact. The data is eventually delivered when some relay moves into the physical vicinity of an access point.

The effectiveness of opportunistic mobile networks relies on nodes to cooperatively forward packets for each other, and make best use of the limited network resources (e.g., contact opportunities) for data forwarding. However, several security issues make it challenging to deliver sensing data using such networks. Users are selfish, and they may not forward packets for everyone else. Misbehaving nodes may drop all received packets, causing sensing data undelivered. Malicious nodes may also flood their sensing data to the network in order to increase their chance of being delivered or deplete network resources. If these issues are not well dealt with, performances of data delivery will degrade. In the following, we address these problems, i.e., user selfishness, flood attacks, and misbehavior that drop received packets.

4.1 Social Selfishness Aware Routing

4.1.1 Introduction

Since routing in opportunistic mobile networks relies on mobile nodes to forward packets for each other, the routing performance (e.g., the number of packets delivered to their destinations) depends on if nodes are willing to forward for others.

In the real world, most people are *socially selfish*. As being social, they are willing to forward packets for others with whom they have social ties[1] such as family members and friends even at the cost of their own resources. Also, they give different preferences to those with social ties, i.e., they will provide better service to those with stronger ties than to those with weaker ties, especially when there are resource constraints. As being selfish, they are unwilling to forward

[1]In this section, a social tie means an interpersonal tie that falls into the *strong* or *weak* category defined by Granovetter [94].

packets for those with whom they have no social ties in order to save their own storage and power resources. For convenience, the above social and selfish behavior will be referred to as *social selfishness*.

As far as we know, social selfishness has not been addressed before. Although many routing algorithms [33, 34, 35, 36, 37, 38] have been proposed for opportunistic mobile networks, most of them do not consider users' willingness and implicitly assume that a node is willing to forward packets for all others. They may not work well since some packets are forwarded to nodes unwilling to relay, and will be dropped. A few recent studies [39, 40] have considered the selfish side of users, where selfish nodes are stimulated to forward packets for all other nodes to maintain high performance. However, these schemes go to another extreme; i.e., they assume that a node is not willing to forward packets for anyone else. For convenience, such selfishness is called *individual selfishness*.

In this section, we aim to answer the following question: *How to design a routing protocol for opportunistic mobile networks composed of socially selfish users?* From the network's point of view, the protocol should force every node to forward packets for all others, since this can achieve the highest network performance. However, this solution does not consider the users' willingness and users cannot behave as they are willing to. Different from it, our philosophy is "design for user", i.e., we take social selfishness as a user demand and allow nodes to be socially selfish. Following this philosophy, we propose a Social Selfishness Aware Routing (SSAR) protocol, in which a node only forwards packets for those with social ties, and it gives priority to packets received from those with stronger social ties when there are not enough resources.

Since each node only forwards packets for part of the nodes, it is important to know how this will affect the routing performance. To achieve high performance, SSAR considers both user willingness and contact opportunity when selecting relays. It combines the two factors through mathematical modeling and machine learning techniques, and obtains a new metric to measure the forwarding capability of a relay. With SSAR, a packet will most likely be forwarded to the relay that has strong willingness to forward as well as high direct or indirect/transitive contact opportunity with the destination. To further improve performance, SSAR formulates the forwarding process as a Multiple Knapsack Problem with Assign-

ment Restrictions (MKPAR). It provides a heuristic-based solution that forwards the most effective packets for social selfishness and routing performance. Extensive trace-driven simulations show that SSAR can achieve good routing performance with low transmission cost.

4.1.2 SSAR Overview

In this section, we first introduce our design philosophy and then discuss our models and assumptions. Finally, we give an overview of SSAR and explain how it works.

4.1.2.1 Design for User

Existing work in mobile ad hoc networks and opportunistic mobile networks has focused on addressing individual selfishness using reputation-based [95], credit-based [96], or game-theory based [39] approaches to stimulate users to cooperate and forward packets for others. If the nodes cooperate with others, they will be able to get help from others; if not, they will be punished, e.g., being deprived of access to the network.

These incentive-based schemes may not be directly applied to deal with social selfishness, since they do not consider social selfishness. In these schemes, every node has to provide service to others no matter there is a social tie or not. Thus, social selfishness is not allowed. In essence, these approaches follow the philosophy of "design for network" because they sacrifice the user's requirement for selfishness (i.e., resource saving) to achieve high performance.

We address this problem from a different point of view. We allow social selfishness but also try to maintain good routing performance under social selfish behavior. Our underlying philosophy is that social selfishness is a kind of user demand that should be satisfied. It should be treated as a new design dimension that measures the user satisfaction, similar to other traditional dimensions such as performance. Such design philosophy is referred to as "design for user".

4.1.2.2 Network Model

In opportunistic mobile networks, nodes have limited bandwidth and computational capability. As in other studies [34], we assume each node has unlimited

buffer space for its own packets, but limited buffer space for packets received from other nodes. We also assume each packet has a certain lifetime denoted by T-TL. A packet becomes useless and should be dropped after it expires. We further assume bidirectional links, which can be provided by some MAC layer protocols, e.g., IEEE 802.11.

4.1.2.3 Willingness Table

Each node maintains a table that contains its willingness values for other nodes in the network. In this table, each item has the format $\langle nodeID, value \rangle$. The value of willingness is a real number within $[0, 1]$, where 0 means unwilling to forward and 1 means the most willing to forward. A node's willingness value for another node depends on the social tie between them. The stronger the social tie is, the larger the willingness is.

Each user manages his willingness table in an off-line style through some user interface provided by the mobile device (e.g., the keypad of a smart phone). Note that a user does not need to know all other users in the network. He only needs to set his willingness value via the user interface for each other user with whom he has a social tie, and set a default willingness value (e.g., 0) for all other (possibly unknown) users without any social tie. Thus, most likely, the willingness table has one item for each node with a social tie and an additional item for all other nodes. A user only needs to manually configure his willingness table when he joins the network or migrates to a new mobile device, and update the table when he has new social ties or his old social ties have changed.

Sociological studies have found that the number of social ties a human being may have is only a few hundred (150 and 290 according to Dunbar [97] and McCarty et al. [98], resp.) and social ties are usually stable over time [99]. This means that the update of willingness table is quite infrequent. Thus, only a low manual intervention from the user is required, and the usability will not be affected much. Actually, the maintenance of willingness table is comparable to the maintenance of address book in a cell phone, which can be well handled by users.

Here, one concern is whether users can quantify the strength of their social ties into the range of $[0, 1]$. This has been shown to be feasible by a recent study which requires users to quantitatively rate their friendships [100]. To be more user-

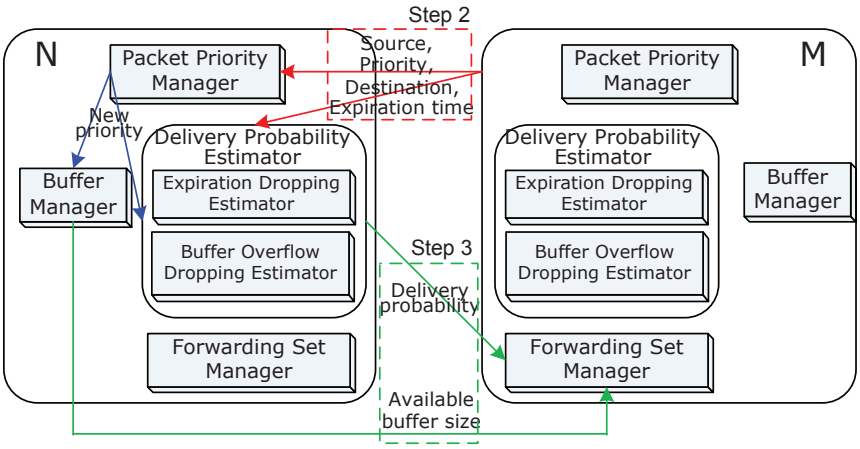

Figure 4.1. SSAR architecture and an example contact between node N and M. The dashed rectangles enclose the information exchanged in step 2 and step 3 (Sec. 4.1.2.5).

friendly, the user interface can even provide several preset willingness levels for the user to choose from, and convert each chosen willingness level into numerical values in the background. For example, with six preset willingness levels "very strong", "strong", "average", "weak", "very weak" and "none", they can be converted into 1.0, 0.8, 0.6, 0.4, 0.2 and 0, respectively.

4.1.2.4 The Architecture

Figure 4.1 shows the architecture of SSAR. In the following we introduce the components and their functions.

Packet priority manager: A node assigns a priority between 0 and 1 to each buffered packet based on its willingness for the source node and the previous hop. The priority of a packet measures the social importance of this packet for this node. More details on priority calculation will be given in Sec. 4.1.3.1.

Buffer manager: A node manages buffers based on packet priority: (i) Packets with priority 0 will not be buffered; (ii) When buffer overflows, packets of low priority are dropped first. The second rule indicates that a new incoming packet can preempt the buffer occupied by a lower-priority packet. The buffer policy together with the priority assignment method allows nodes to be socially selfish (see Sec. 4.1.3.1).

Delivery probability estimator: It estimates a node's *delivery probability* for a

packet, which is used to measure the node's forwarding capability for that packet. When two nodes are in contact, each packet is forwarded from the node with a lower delivery probability to the node with a higher delivery probability.

Traditionally, the quality of a relay is measured solely based on contact opportunity, which can be the relay's direct contact opportunity to the destination node or the transitive contact opportunity provided by the relay's contacted nodes or both. SSAR measures the delivery probability of a node based on both of its contact opportunity to the destination and its willingness to forward. It is straightforward that a node with a low contact opportunity should not be a relay. Interestingly, a node with a high contact opportunity but low willingness should not be a relay either. This is illustrated in Figure 4.2. Suppose S has a packet $m1$ to send to D, and its contact opportunity with D within the packet lifetime is low (0.3). Suppose S successively meets A, C, and B. If only contact opportunity is considered, it will forward $m1$ to A whose contact opportunity is 0.9. Unfortunately, A will drop $m1$ since it is unwilling to forward for S (the willingness is 0). SSAR will avoid such forwarding. Although C has a higher contact opportunity and it is willing to forward $m1$ for S, its willingness is so low that $m1$ may suffer a high risk of being dropped, so SSAR will also avoid such forwarding. As a result, B is the optimal forwarder for $m1$ in this scenario, since it has high willingness to forward and a high contact opportunity.

Our approach to deriving delivery probability includes the mathematical modeling of the probability that a packet will be dropped due to expiration with Markov's Inequality and the estimation of the probability that the packet will be dropped due to buffer overflow with a machine learning technique that combines two known classification algorithms from the literature. More details will be provided in Chapter 4.1.3.2.

Forwarding set manager: After a node determines a set of packets that should be forwarded to a better relay, existing protocols (e.g., [36]) greedily transmit them no matter the receiver has enough buffer to hold these packets or not. Obviously, bandwidth will be wasted if the transmitted packets are dropped due to buffer overflow. To address this issue, the forwarding set manager decides which packet to transmit by solving an MKPAR (Multiple Knapsack Problem with Assignment Restrictions). It considers the buffer constraint and transmits the packets that are

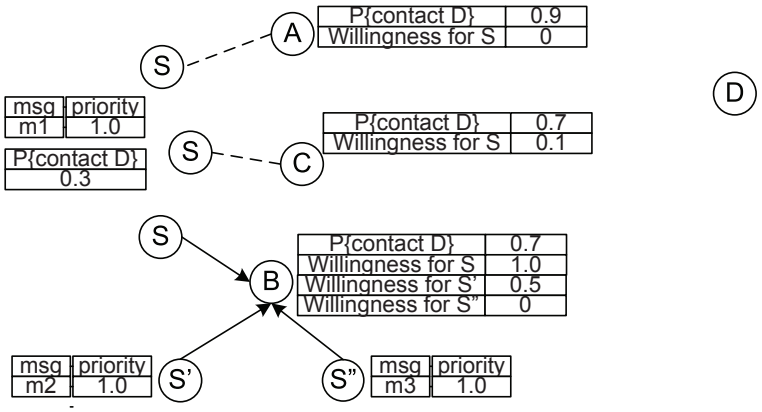

Figure 4.2. An example of willingness-aware forwarding.

the most effective for social selfishness and routing performance.

4.1.2.5 The Protocol

We use an example (Fig. 4.1) to illustrate how SSAR works in the following five steps:

1. After neighbor discovery, node N and M deliver packets destined to each other in the decreasing order of priority.

2. Suppose M still buffers some other packets. Then M sends N a summary list of ⟨source ID, destination ID, expiration time, priority⟩ for these packets.

3. From the source ID and priority information, N calculates the new priority value for each packet in the list (Sec. 4.1.3.1). Based on the new priority, the destination ID and expiration time, N calculates its delivery probability (Sec. 4.1.3.2) and available buffer size (Sec. 4.1.3.3) for each packet, and returns them to M.

4. M determines a candidate set of packets for which N has higher delivery probabilities.

5. Considering the available buffer size information, M further decides which candidates to transmit by solving the MKPAR (Sec. 4.1.3.3) formulation.

In Step 3, if the new priority of a packet is zero, N's delivery probability and available buffer size for it are also zero. In this case, N does not need to go

through the procedures in Sec. 4.1.3.2 and 4.1.3.3. Without loss of generality, in the last four steps we only describe how node M determines which packets to transfer to N. Node N does so in similar ways.

Sometimes a node may be in contact with multiple neighbors at the same time. Then it would be very difficult to extend the MKPAR formulation to the whole neighborhood. As a simple solution, the node interacts with its neighbors one by one.

4.1.2.6 Forwarding Strategy

SSAR can work in two modes, *forwarding mode* and *replication mode*. In the forwarding mode, a node deletes its own copy after it transmits a packet to its neighbor (which has a higher delivery probability). Thus, any packet can simultaneously have at most one copy in the network. In the replication mode, however, the node keeps its own copy after transmitting the packet. Therefore, the packet may have many replicas in the network. The number of replicas depends on the mobility pattern and is non-deterministic. Generally speaking, the replication mode can deliver more packets than the forwarding mode but it also requires more resources such as buffer and bandwidth. Which mode to use should be application-specific.

4.1.3 Detailed Design

This section describes the detailed design of the packet priority calculation, the delivery probability estimation, and the forwarding set optimization.

4.1.3.1 Packet Priority

When a node receives a packet from a previous hop, it assigns a priority to the packet. The priority determines if this node will relay the packet (i.e., the priority is positive) or not (i.e., the priority is zero). To be socially selfish, the node only forwards the packet if it is from a node with a social tie. There are two cases. First, the source of the packet has a social tie with this node, and hence forwarding the packet means helping the source. Second, the previous hop has a social tie with this node, no matter the source has a social tie or not. In this case, the previous hop has taken over the responsibility (probably from its own social tie) to deliver

the packet. Thus, even if the source does not have a social tie with this node, this node should still relay the packet to help the previous hop. Actually, this is motivated by the real-world phenomenon that people usually would like to help a friend's friend. The priority should also measure the social importance of the packet to this node. For example, when other conditions are the same, packets from the node with a stronger social tie should have a higher priority.

Let p_{curr} denote the new priority of a packet in the current hop, and p_{prev} denote the old priority of the packet in its previous hop. Let ω_{src} and ω_{prev} denote the current hop's willingness for the packet source and the previous hop, respectively. Then the current hop calculates the new priority in the following ways (Note that the initial priority of a packet is set as 1 by the source node.): (1) If neither the source nor the previous hop has a social tie with the current hop, then $p_{curr} = 0$. (2) If the source has a social tie but the previous hop does not, then $p_{curr} = \omega_{src}$. (3) If the previous hop has a social tie but the source does not, then $p_{curr} = p_{prev} \cdot \omega_{prev}$. This calculation method borrows the idea of transitive trust [101] from the reputation system literature. (4) If both the source and the previous hop have a social tie with the current hop, $p_{curr} = max\{\omega_{src}, p_{prev} \cdot \omega_{prev}\}$. The calculation method can be summarized as:

$$p_{curr} = \begin{cases} 0 & \omega_{src} = 0, \omega_{prev} = 0 \\ \omega_{src} & \omega_{src} > 0, \omega_{prev} = 0 \\ p_{prev} \cdot \omega_{prev} & \omega_{src} = 0, \omega_{prev} > 0 \\ max\{\omega_{src}, p_{prev} \cdot \omega_{prev}\} & \omega_{src} > 0, \omega_{prev} > 0 \end{cases} \tag{4.1}$$

The priority assignment method and the buffer management policy can enforce social selfishness. Packets that traverse different social links will receive different forwarding service. As shown in Figure 4.2, although $m1$, $m2$, and $m3$ have the same priority in the source, they will receive different service at relay B after being transmitted to B. That is, $m3$ will not receive any forwarding service, and $m1$ will receive better service than $m2$.

The priority of a packet does not consider the destination of the packet due to the following reason. If a node forwards all the packets destined to its social ties no matter where these packets are from, a malicious source can exploit this vulnerability to send unsolicited packets (e.g., advertisement) via this node to its

social ties, although the source has no social tie with this node or its social ties. We note that the malicious source can launch attacks (e.g., source address forgery) to achieve similar goals, but these security issues are out of the scope of this section.

4.1.3.2 Delivery Probability Estimation

Suppose each packet has some expiration time, the question is: at a given time t, how to estimate node N's probability of delivering packet m to its destination D before its expiration time t_{exp}?

Overall Delivery Probability We assume N can deliver m when it contacts D if it still buffers m at the time of contact. Then m will either be dropped before N contacts D or delivered when N contacts D. There are two cases of dropping. First, m expires before N contacts D and is then dropped. This dropping is due to N's insufficient contact opportunity with D. Second, N drops m in order to allocate the buffer space originally occupied by m to other newly received packets which have a higher priority. This dropping happens because m's priority is too low and N does not have sufficient buffers for it.

Suppose the next contact between N and D happens at time t_c, and N has to drop m due to buffer overflow at time t_{over}. Further denote the overall delivery probability by $P_{delivery}$. Then the probabilities of the first and second type of dropping are given by $P\{t_{exp} \leq t_c\}$ and $P\{t_{over} \leq t_c\}$, respectively. Note that the temporal order of t_c and t_{exp} is determined by system parameters and the mobility pattern of N and D, while the time of buffer overflow depends on N's traffic load. Thus we assume that the two dropping events are independent. We integrate them to get the delivery probability:

$$P_{delivery} = (1 - P\{t_{exp} \leq t_c\})(1 - P\{t_{over} \leq t_c\}) \tag{4.2}$$

In opportunistic mobile networks with unpredictable connectivity, when N makes such estimation it is impossible to know the exact t_c, and thus it is impossible to compute the r.h.s of Eq. 4.2. Thus, we have to make some approximations. When $t_{exp} > t_c$, $P\{t_{over} \leq t_c\} \leq P\{t_{over} \leq t_{exp}\}$ because the probability density function of t_{over} is nonnegative. After inserting this inequation into Eq. 4.2, we get a conservative estimation:

$$P_{delivery} \geq (1 - P\{t_{exp} \leq t_c\})(1 - P\{t_{over} \leq t_{exp}\}) \tag{4.3}$$

The above estimation of $P_{delivery}$ can be seen as determined by two independent droppings, $\{t_{exp} \leq t_c\}$ and $\{t_{over} \leq t_{exp}\}$. The first one means that the packet expires before N's next contact with D, so we call it *expiration dropping*. The second one means that the packet overflows before expiration, so we call it *buffer overflow dropping*. Let P_{exp} and P_{over} denote the expiration dropping probability and buffer overflow dropping probability, respectively. Next, we describe how to estimate them.

Expiration Dropping Probability To estimate P_{exp}, we adopt an approach similar to that in [39]. Let random variable X denote the inter-contact time between N and the destination D. Assume that each inter-contact time is independent, then by Markov's Inequality:

$$P_{exp} = P\{X > t_{exp} - \hat{t}\} \leq E(X)/(t_{exp} - \hat{t}) \tag{4.4}$$

where $E(X)$ is the mean of X and $\hat{t}$ is the most recent contact time between N and D before the estimation time t. $E(X)$ can be approximated by the average of historical inter-contact times. The value of P_{exp} should be bounded by 1. Eq. 4.4 intuitively means that nodes with a lower average inter-contact time (i.e., a higher contact frequency) with the destination have a lower expiration dropping probability.

Buffer Overflow Dropping Probability The most important factor that affects P_{over} is m's priority value p due to the buffer policy. Two other minor factors are the current empty buffer size L_0 and the residual time $t_r = t_{exp} - t$ before expiration. L_0 is positively related to how long m can stay before being removed. But t_r is negatively related: the longer t_r is, the more likely it will be dropped due to buffer overflow.

Without clear knowledge of how these factors interact, it is extremely hard to theoretically model P_{over}. Therefore we turn to machine learning techniques and model it as a supervised learning problem. Whenever N drops or forwards a packet, it generates a record $< p, L_0, t_r, \beta >$. With machine learning terminology, each record is called a *sample*, p, L_0, and t_r are called *feature dimensions* and β is

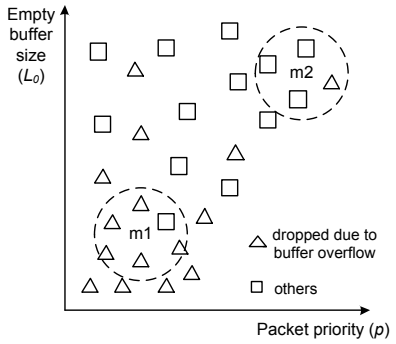

Figure 4.3. Heuristics used to estimate buffer overflow dropping probability P_{over}. Triangles and squares are historical samples.

called *class label*. $\beta = 1$ if N drops the packet due to buffer overflow and $\beta = 0$ if N does not drop it or drops it due to expiration.

Our basic heuristic is that the probability that m will be dropped is similar to some historical packets which have similar feature values when they enter N's buffer. Suppose we match m to a set $\mathcal{S}$ of similar packets, and within $\mathcal{S}$ the subset of packets being dropped due to buffer overflow is $\mathcal{S}_{drop}$. Then P_{over} is estimated as:

$$P_{over} = |\mathcal{S}_{drop}|/|\mathcal{S}| \tag{4.5}$$

Figure 4.3 illustrates the idea in a two-dimensional space $< p, L_0 >$, where the historical packets in the dashed circle are the matched ones. In this example, the estimated P_{over} of $m1$ and $m2$ are $5/6 = 0.83$ and $1/4 = 0.25$, respectively.

To match m to similar packets, we choose the K-Nearest-Neighbor (KNN)[102] algorithm from the machine learning literature, which identifies the K packets that have the shortest distance to m in the feature space. However, KNN traverses all samples during matching, which induces high online computation cost, and leaves less contact duration time for data transmission. Although some techniques [103] have been proposed to improve its online matching time, they are too complex to be applied to mobile nodes. To address this problem, we combine KNN with the Kcenter algorithm [104] to propose a two-phase solution:

- In the offline phase (when not in contact with others), nodes use the Kcenter algorithm to cluster samples into $\hat{K}$ clusters around $\hat{K}$ points in the feature

space[2].

- In the online phase, nodes scan the $\hat{K}$ points in the increasing order of their distance with m's feature vector until K samples are included in the scanned clusters.

Based on previous work in this area [105], we set $K = \sqrt{n}$, where n is the number of samples. We also set $\hat{K} = \sqrt{n}$. Simulations show that they perform well. The time and space complexity of offline clustering is $O(n\sqrt{n})$ and $O(n)$. The time complexity of online matching is $O(\sqrt{n}\log n)$, which is much smaller than that of naive KNN (i.e., $O(n\sqrt{n})$). To reduce the computation cost, the offline phase does not have to be run whenever a packet is dropped or forwarded; it can be run when a certain number of packets have been dropped or forwarded since the last run.

Both the online and offline phase need to compute the distance between two feature vectors. When doing so, L_0 is normalized to $[0, 1]$ based on the total buffer size of N, and t_r is normalized to $[0, 1]$ based on the packet TTL. Moreover, since Euclidean distance performs poorly when samples are sparse in the feature space, we propose a distance metric by assigning different weights to different feature dimensions. We observe that if dropped samples spread narrowly in one feature dimension, this dimension is sensitive and should be highly weighted and vice versa. Suppose m_1 and m_2 are two feature vectors. Then their distance is $D(m_1, m_2) = \sqrt{\sum_{i=1}^{3} \frac{\hat{\sigma_i}^2}{\sigma_i^2}(m_1^i - m_2^i)^2}$, where σ_i^2 and $\hat{\sigma_i}^2$ denote the variance of feature i in dropped samples and all samples, respectively.

4.1.3.3 Forwarding Set Optimization

In this subsection, we solve the following problem: suppose a node M contacts N, and M has determined a candidate packet set $\mathcal{C}$ for which N has higher delivery probabilities. Since N's buffer may be inadequate to accept all packets in $\mathcal{C}$, we need to find out how to determine a subset of $\mathcal{C}$ to transmit.

We follow two principles. First, M will not forward a packet to N if N does not have sufficient buffers for that packet. According to the buffer management rule, N's available buffer size L_m for m is:

[2]We refer to the original paper for details.

Algorithm 7 : Greedy algorithm for forwarding set selection, pseudo-code for M

```
1: Compute the selfish gain g for each packet in C
2: Sort C in the decreasing order of g/l (Let i denote the i^th packet in C)
3: for Packet i from 1 to |C| do
4:    if N is not in contact with M anymore then
5:       break
6:    end if
7:    if L_i ≥ l_i then
8:       Forward i to N
9:       for Packet j from i + 1 to |C| do
10:         L_j − = l_i
11:      end for
12:   else
13:      continue
14:   end if
15: end for
```

$$L_m = L_0 + \sum_{\{k|p_k<p\}} l_k \tag{4.6}$$

where L_0 denotes N's empty buffer size, $\{k|p_k < p\}$ denotes the packets in N's buffer whose priority is smaller than that of m (i.e., p), and l_k denotes the size of packet k. Second, M tries to maximize its selfish gain through this contact, which is defined as follows.

Definition 1 (Selfish Gain) The selfish gain g that M achieves by forwarding m to N is the product of m's priority p in M and the increment of delivery probability, i.e., $g = p \cdot \Delta P_{delivery}$.

Both factors in the definition are related to selfishness. p means how socially important the packet is. The larger p is, the more selfishness is gained. $\Delta P_{delivery}$ means how much this forwarding can increase the packet's probability to be delivered. The larger $\Delta P_{delivery}$ is, the more help is provided. So their product is a natural representation of the gained selfishness.

Suppose all the packets in $\mathcal{C}$ are sorted by priority in the increasing order. Then we can simply use i to denote the i^{th} packet. Let X_i denote if packet i is selected to be transmitted ($X_i = 1$) or not ($X_i = 0$). According to the above two principles, the problem can be formulated as:

$$max \quad \sum_{i\in\mathcal{C}} g_i X_i \quad s.t. \quad \forall i \quad \sum_{j\le i} X_j l_j \le L_i \tag{4.7}$$

In a special case that all candidate packets have the same priority, Eq. 4.7 becomes a standard Knapsack problem. Thus, Eq. 4.7 is a variant of the Knapsack problem. Next we show that it can be converted into an MKPAR [106], where each item can only be assigned to a subset of the knapsacks. Suppose the original buffer is divided into $|\mathcal{C}|+1$ knapsacks such that the first knapsack has size $\mathbb{S}_1 = L_1$, the j^{th} ($j \in \{2, ..., |\mathcal{C}|\}$) one has size $\mathbb{S}_j = L_j - L_{j-1}$, and the $(|\mathcal{C}|+1)^{th}$ one consists of buffers that cannot be preempted by any packet in $\mathcal{C}$. Then packet i can only be packed into knapsacks indexed smaller than or equal to i. Let X_{ij} denote if packet i is packed into knapsack j ($X_{ij} = 1$) or not ($X_{ij} = 0$). Then $X_{ij} = 0$ when $i < j$. Eq. 4.7 can be rewritten as:

$$max \quad \sum_{i=1}^{|\mathcal{C}|} \sum_{j=1}^{|\mathcal{C}|} g_i X_{ij} \quad s.t. \quad \forall i \ \sum_{j} X_{ij} \leq 1, \quad \forall j \ \sum_{i} X_{ij} l_i \leq \mathbb{S}_j \tag{4.8}$$

Since the problem is NP-hard, we give a greedy algorithm, which ranks the packets in the decreasing order of selfish gain weighted by packet size, and packs them one by one until no more packets can be packed. The details are shown in Algorithm 7. The time complexity of this algorithm is $O(|\mathcal{C}|^2)$, which is acceptable because most handsets have such computing capability.

4.1.4 Performance Evaluations

In this section, we evaluate the performance of SSAR and compare it to other routing algorithms.

4.1.4.1 Experiment Setup

We evaluate SSAR over two traces collected from real-world opportunistic mobile networks: Haggle Infocom05 [107] and MIT Reality [108]. Both are available from the CRAWDAD project in Dartmouth [109]. These traces record contacts among users carrying Bluetooth devices, which periodically discover peer devices and record contacts between them. The chosen traces cover a diversity of environments, from college campuses (Reality) to conference sites (Infocom05), and with experimental periods from several days (Infocom05) to several months (Reality). Table 4.1 summarizes their main characteristics.

Table 4.1. The summary of the two traces used for evaluation

Trace	Infocom05	Reality
Network type	Bluetooth	Bluetooth
Number of devices	41	97
Number of contacts	22 thousand	110 thousand
Duration	3 days	9 months
Granularity	120 seconds	300 seconds

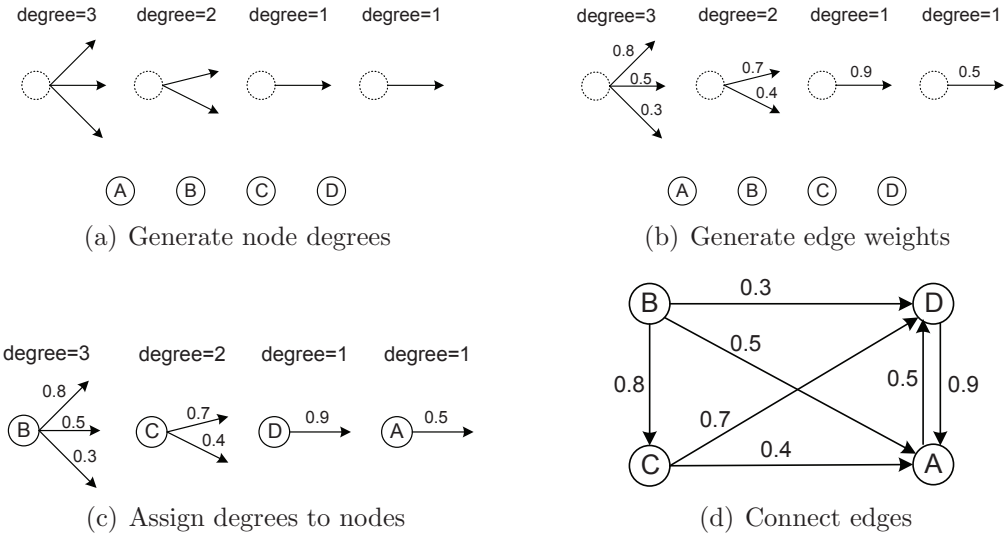

(a) Generate node degrees (b) Generate edge weights

(c) Assign degrees to nodes (d) Connect edges

Figure 4.4. An example of social network graph generation in the 4 basic steps.

Since the traces do not have the accurate social relationship information among participants (i.e., nodes), we need to construct a weighted directed social network graph upon them. In the graph, a vertex denotes a node in the trace, and an edge denotes a social tie between nodes. Edge weight means the strength of the social tie, and it also means the willingness to forward. For instance, the weight of edge $\overrightarrow{NM}$ is node N's willingness to forward packets for M. The weight of edge $\overrightarrow{NM}$ and that of $\overrightarrow{MN}$ may be different.

Several measurement studies (e.g., [110]) have empirically found that in real-world social networks node degrees follow power-law distributions. Also, in one recent study [100] participants rate the strength of their friendships nearly uniformly between 0 and 1, which is the best empirical data we can find about the distribution of social tie strength. Thus, we try to ensure that the constructed social network graph have these two basic properties.

Our construction process involves four steps as illustrated in Fig. 4.4. *Step 1*:

Generate power-law distributed node degrees. Since the degree of a node means the number of edges emitted from this node, we denote a degree d with d arrows in Fig. 4.4. *Step 2*: Generate weights for these arrows (which will become edges in the finished graph) that follow the uniform distribution between 0 and 1. *Step 3*: Assign those degrees to nodes. When this step is complete, each node has a number of edges emitting from it. *Step 4*: Connect each of these edges to another node.

To better evaluate SSAR, we generate two types of social network graphs which differ in the last two steps. The first type is *contact-dependent graph*, where the contact frequency between nodes probabilistically determines how degrees are assigned to nodes and how edges are connected. It is based on the following heuristic which has been verified by sociology studies [94]. The stronger tie two individuals have, the more likely they contact frequently. Individuals with more social ties are more likely to meet other people. Let f_* denote the overall contact frequency of the whole trace, f_N denote node N's overall contact frequency, and f_{NM} denote the contact frequency between N and M. Then the last two steps for contact-dependent graph are as follows:

- *Step 3*: Repeatedly assign node degrees to nodes, i.e., assign the largest degree to a node in such a way that node N's probability to be selected is f_N/f_*, and repeat this for the remaining degrees and nodes.

- *Step 4*: For each node N, connect its edges to other nodes. First connect the edge with the highest weight to another node in a way that node M's probability to be connected is f_{NM}/f_N, and repeat this for the other edges and nodes that have not been connected to N. In the end, for any ordered node pair NM that has not been connected yet, the willingness of N for M is set 0.

The second type of graph is *random graph*. To construct it, in the third and fourth step we simply assign degrees to random nodes and connect each edge of a node to another random node. Though we believe random graph is less realistic than contact-dependent graph, we still use it in order to evaluate SSAR under diversified social graphs.

Table 4.2. The default parameters used in the simulation

Parameter	Value
Bandwidth	2 Mbps
Buffer Size	5 MB
Packet Size	Random between [50,100] KB
Packet TTL	100 days (Reality), 48 hours (Infocom05)
Packet Generation Rate	1 pkt/node/day (Reality) 6 pkt/node/hour (Infocom05)
Avg. Number of Social Ties per Node	25 (Reality), 8 (Infocom05)

The power-law coefficient used to generate node degrees is fixed at 1.76, which is based on the result of an empirical study [110]. To generate discrete node degrees, we use the Zeta distribution with exponent $s = 1.32$ which is the discrete equivalent of the power-law distribution with coefficient 1.76. Since each trace has a certain number of nodes, it is meaningless to generate node degrees equal to or larger than the number of nodes in the trace. In our simulations, we only generate node degrees which fall into range $[1, 96]$ and $[1, 40]$ for the Reality trace and Infocom05 trace, respectively. Let l and u denote the lower and upper boundary (inclusive) of the range, respectively. Then each degree $l \leq d \leq u$ will be generated with probability $\frac{1/d^s}{\sum_{a=l}^{u}(1/a^s)}$. In this manner, the generated node degree has finite mean and variance. One important feature of social network is the average number of social ties that each node has. In some networks, each node only has a few social ties; while in others, each node has many social ties. We tune parameter l to generate social network graphs with different average numbers of social ties per node.

In the simulation, each node generates packets to random destinations. Each packet has a certain TTL and will be removed after it expires. All packets have initial priority 1. In each run, the first 1/3 (1/10, resp.) of the Reality (Infocom05, resp.) trace is used for warm-up, and the results are collected from the remaining part. To avoid end-effects, no packet is generated in the last 1/3 (1/10, resp.) of the Reality (Infocom05, resp.) trace. The default parameters used in the simulation are given in Table 4.2.

4.1.4.2 Routing Algorithms

We compare SSAR with two other benchmark algorithms, PROPHET [33] and SimBet [35]. PROPHET is a standard non-oblivious benchmark that has been used to compare against several previous works [37]. It calculates a metric, delivery predictability, based on contact histories, and relays a packet to a node with higher delivery predictability. We use the same parameters as in [33]. SimBet has also been used as a benchmark in several works [38]. It calculates a simbet metric using two social measures (similarity and betweenness). A packet is forwarded to a node if that node has a higher simbet metric than the current one. We use the same parameters as in [35].

Since the original algorithms do not define the order of packets to be transmitted during a contact, we adopt the transmission order used in RAPID [36]. Because this order has been shown to be the most effective, we believe such refinement does not favor SSAR in comparison. Since the original algorithm either assumes infinite buffer (SimBet) or assumes finite buffer but does not specify the packet dropping policy (PROPHET), we apply three policies (drop-tail, random drop, and minimum-utility-drop-first) in simulation, and only present the results of the best policy here, i.e., minimum-utility-drop-first. Since it is impossible to traverse all dropping policies and choose the optimal one, we tried our best to impose the minimum influence on the original algorithms.

PROPHET and SimBet are designed without considering social selfishness. For fair comparison, we modified them so that they have some basic selfishness awareness. That is, nodes do not forward packets to others who are not willing to forward for them, and avoid immediate droppings caused by selfishness. However, when nodes forward packets to others who are willing to forward for them, they still follow the aforementioned transmission order and buffer policy. To show the effect of such selfishness-awareness, we also include the basic PROPHET in our simulations. For convenience, we label the selfishness-aware PROPHET *PROPHET-2*, and label the basic one *PROPHET-1*.

We evaluate SSAR and these algorithms under the forwarding mode and replication mode introduced in Sec. 4.1.2.6.

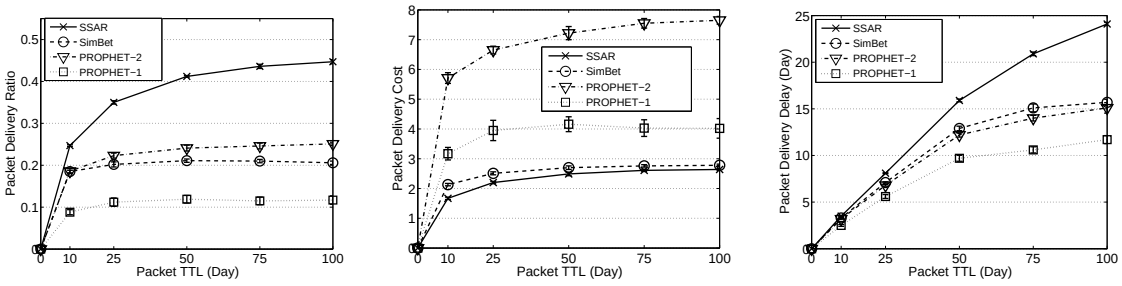

(a) Performance (b) Cost (c) Delay

Figure 4.5. Comparison of algorithms in the forwarding mode. The Reality trace and contact-dependent graph are used.

4.1.4.3 Metrics

We use the following metrics to evaluate these algorithms: 1) **Packet delivery ratio:** The proportion of packets that are delivered to their destinations out of the total unique packets generated. 2) **Packet delivery cost:** The total number transmissions divided by the number of unique packets generated. 3) **Packet delivery delay:** From the time a packet is generated to the time the packet is delivered. In the results, we plot the average delay of all delivered packets. 4) **Selfishness satisfaction (SS):** A node's SS is defined as the ratio of the average priority of the packets it forwards or delivers over the average priority of the packets it drops. SS reflects how much the user is satisfied with the network, because a larger SS indicates more important messages are served. In the results, we plot the average SS of all nodes.

4.1.4.4 Results

The Effects of TTL We first evaluate the algorithms when the forwarding mode (see Sec. 4.1.2.6) is used, i.e., each packet has only one copy in the network, so that the effect of packet replication can be separated. Figure 4.5 shows the results over the Reality trace when the contact-dependent graph is used.

Figure 4.5(a) compares the algorithms in packet delivery ratio. When the T-TL increases all algorithms deliver more packets to the destinations. However, as the TTL becomes large the increment in packet delivery ratio becomes marginal, because at that time the forwarding capacity of the network becomes the performance bottleneck. Among all algorithms, SSAR has the highest packet delivery

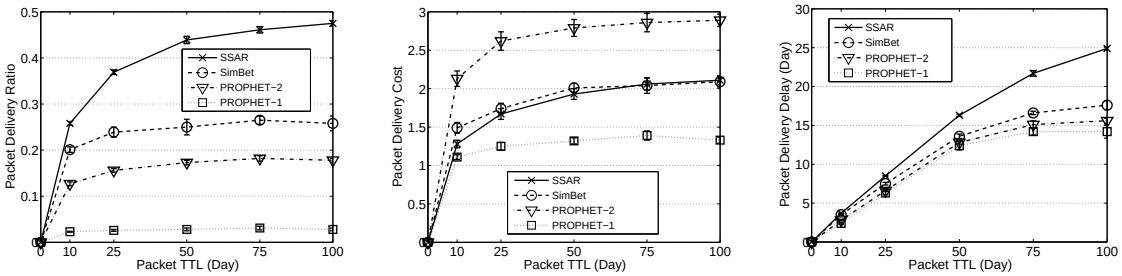

(a) Performance (b) Cost (c) Delay

Figure 4.6. Comparison of algorithms in the forwarding mode. The Reality trace and random graph are used.

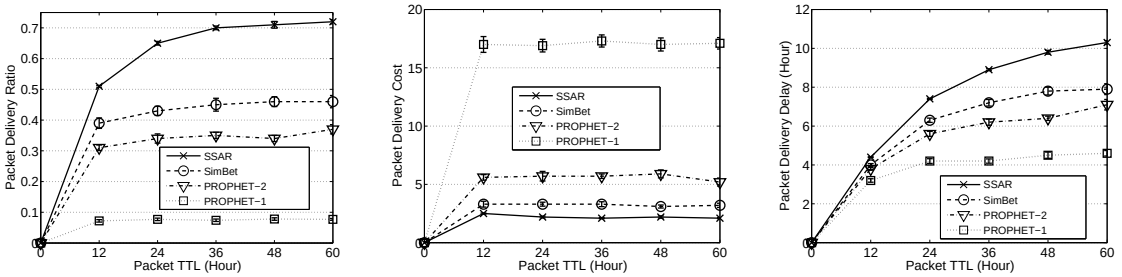

(a) Performance (b) Cost (c) Delay

Figure 4.7. Comparison of algorithms in the forwarding mode. The Infocom05 trace and contact-dependent graph are used.

ratio. For example, when the TTL is 100 days it outperforms PROPHET-2, SimBet and PROPHET-1 by 80%, 120% and 300%, respectively. This is because SSAR incorporates user willingness, buffer constraint, and contact opportunity into relay selection. It avoids low-willingness nodes or overloaded hot spots when selecting relays, and has much less packet dropping caused by these nodes. In contrast, PROPHET and SimBet cannot avoid those nodes since they only consider contact opportunity when selecting relays. Another reason is that the MKPAR formulation of SSAR does not forward a packet to the next hop whose buffer is insufficient to hold this packet, but PROPHET and SimBet may make such transmissions and result in packet dropping. PROPHET-1 performs much worse than PROPHET-2 because PROPHET-1 is not selfishness-aware. It forwards many packets to those who are unwilling to forward, and those packets are dropped.

Figure 4.5(b) compares the algorithms in packet delivery cost. As the TTL increases, all algorithms have more transmissions, because packets stay longer in the

network and have more opportunities to be transmitted. Among the algorithms SSAR has the smallest cost, since it makes very cautious forwarding decisions, i.e., it forwards a packet only when the next hop has both a good contact opportunity and high willingness. PROPHET-1 has much lower cost than PROPHET-2, because most packets are dropped early.

SSAR's gain in packet delivery ratio and cost does not come for free. As shown in Figure 4.5(c), its packet delivery delay is longer than that of the other three algorithms, because it does not forward packets to the relays that have a good contact opportunity (which usually means a shorter delivery delay) but low willingness. However, the packets forwarded to these relays also have a high risk of being dropped due to the low willingness. Thus, there is a tradeoff between packet delivery ratio and delay.

Similar results are also found in the Infocom05 trace as shown in Fig. 4.7.

Figure 4.6 shows the results on the Reality trace when the random graph is used. Similar as under the contact-dependent graph and for similar reasons, SSAR delivers more packets than the other algorithms (see Fig. 4.6(a)) but also has longer packet delivery delays (see Fig. 4.6(c)). The cost of SSAR is lower than that of PROPHET-2 and SimBet but higher than that of PROPHET-1 (see Fig. 4.6(b)). Here, PROPHET-1 has the lowest cost since most packets are dropped quite early, which can be seen from its extremely low packet delivery ratio.

Comparing the results under the two types of social network graph in the Reality trace (see Fig. 4.5 and 4.6), we found that SimBet delivers around 30% more packets under the random graph than it does under the contact-dependent graph. This is because in the contact-dependent graph a socially popular node is very likely to be a hot spot node in contact, while in the random graph such probability is much lower. Since SimBet tends to forward packets to socially popular nodes, it overloads more hot spot nodes under the contact-dependent graph. PROPHET-1 also delivers much less packets under the random graph. The reason is that PROPHET-1 forwards packets out no matter the contacted nodes are socially tied or not, and in the random graph the contacted nodes are more likely to be the ones without social ties, resulting in more packet dropping. PROPHET-2 delivers 25%-35% less packets in the random graph, since less contacts that happen between social ties can be used for packet forwarding. SSAR delivers similar amounts of

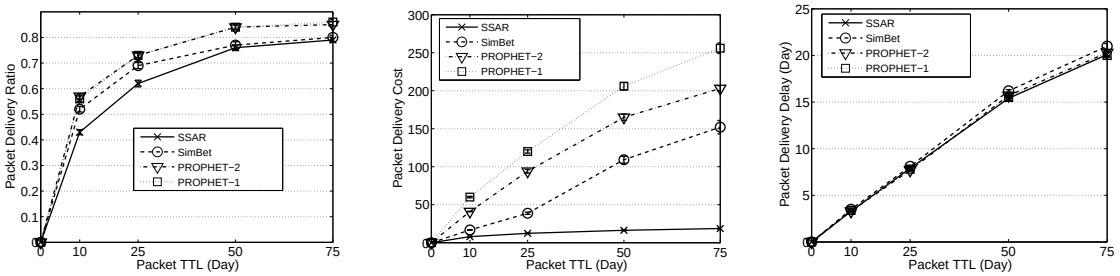

(a) Performance (b) Cost (c) Delay

Figure 4.8. Comparison of algorithms in the replication mode. The Reality trace and contact-dependent graph are used.

packets under the two types of social network graph. The cost of all algorithms is lower in the random graph since fewer contacts happen between socially tied nodes. Packet delivery delay does not change much in the two graphs.

Next we evaluate the algorithms when the replication mode (see Sec. 4.1.2.6) is used over the Reality trace. The packet generation rate is 0.1 packets per node per day. As shown in Fig. 4.8(a), all algorithms have a similar packet delivery ratio; however, SSAR achieves such performance at much lower cost (see Fig. 4.8(b)). For example, when TTL is 75 days, the cost in SSAR is only 8%-13% of that in the other three algorithms. Again, this is because SSAR makes very cautious but effective transmissions. If a packet has a high probability to be dropped by the next hop, most likely SSAR will not replicate the packet. In contrast, the other three algorithms are more greedy in replication. Many replicas only play a marginal role in packet delivery, and very likely such transmissions are wasted. In addition, the MKPAR formulation of SSAR also avoids many useless transmissions. As shown in Fig. 4.8(c), all algorithms have similar packet delivery delays.

The Effects of Buffer Size To evaluate how SSAR performs when nodes have different storage resources, we change the buffer size of each node from 1MB to 10MB over the Reality trace and show the results in Fig. 4.9. When the buffer size increases, all the three metrics (packet delivery ratio, cost and delay) also increase. SSAR delivers much more packets than the other three algorithms at lower cost but it also has a longer packet delivery delay for aforementioned reasons.

The Effects of the Average Number of Social Ties per Node Fig. 4.10 shows the results on the Reality trace when each node generates 0.1 packets per

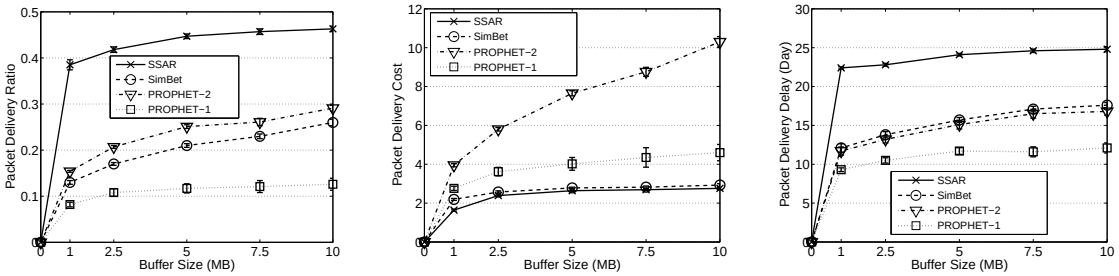

(a) Performance (b) Cost (c) Delay

Figure 4.9. Comparison of algorithms on the Reality trace when nodes have different buffer sizes. The forwarding mode and contact-dependent graph are used.

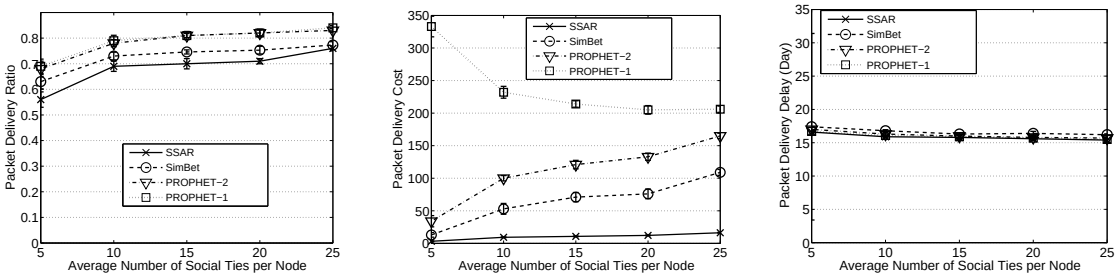

(a) Performance (b) Cost (c) Delay

Figure 4.10. Comparison of algorithms on the Reality trace when nodes have different average numbers of social ties. The replication mode and contact-dependent graph are used.

day and the TTL is 50 days. When nodes have more social ties the packet delivery ratio of all algorithms increases. The packet delivery cost of SSAR, SimBet and PROPHET-2 also increases. Obviously, the increment in packet delivery ratio and cost is because more nodes can be used for relays and packets have more chances to be transmitted. SSAR achieves similar performance with other algorithms at much lower cost, and these algorithms have very similar delays that do not change much with the average number of social ties.

The Effects of Willingness-aware Forwarding Fig. 4.11 compares SSAR with its variant where willingness is not considered in relay selection (i.e., only contact opportunity is considered). The Reality trace is used and the buffer size is 1MB. As shown in Fig. 4.11(a) and 4.11(b), SSAR achieves a higher packet delivery ratio at lower cost than its variant that does not consider willingness, and their difference is more significant when the workload is higher. This is because willingness significantly affects the probability that a packet will be dropped by a

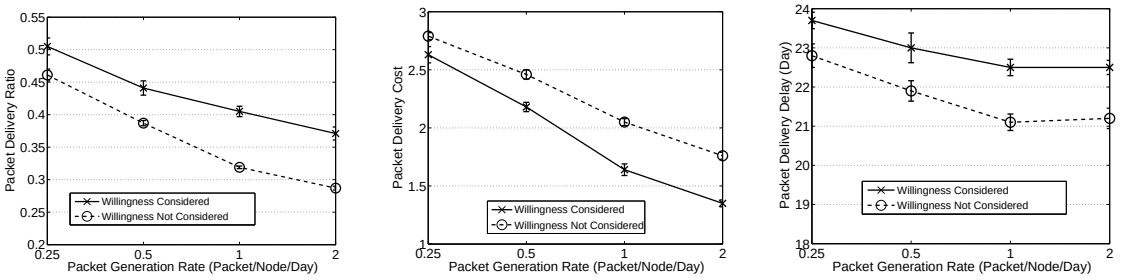

(a) Performance (b) Cost (c) Delay

Figure 4.11. The effects of willingness awareness in SSAR. The forwarding mode and contact-dependent graph are used over the Reality trace.

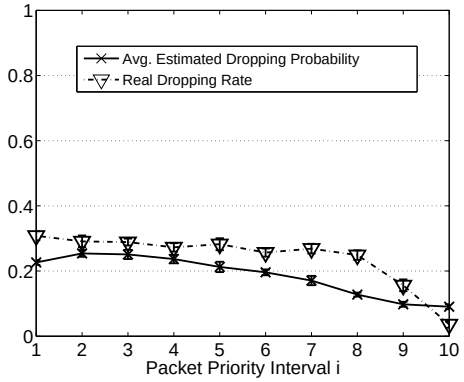

Figure 4.12. The accuracy of our KNN-plus-Kcenter algorithm in estimating the buffer overflow dropping probability of the packets that fall into 10 priority intervals with the i^{th} interval being $[0.1 \cdot (i-1), 0.1 \cdot i]$. The forwarding mode and contact-dependent graph are used over the Reality trace.

node, especially when the workload is high. For instance, when each node generates only 0.25 packets per day, SSAR outperforms its variant by 10% in packet delivery ratio with 7% lower cost. However, when each node generates 2 packets per day, SSAR outperforms its variant by 31% in packet delivery ratio at 23% lower cost. When delay is considered (see Fig. 4.11(c)), SSAR and its variant has a small difference which is only 4%-7%. Thus, willingness-aware forwarding is effective.

Estimation Accuracy Now we evaluate the accuracy of our KNN-plus-Kcenter algorithm in estimating the probability that a packet will be dropped due to buffer overflow. Since packet priority is the major factor that affects this probability, we divide the packets into 10 groups whose priority falls into 10 intervals evenly spanned in $[0, 1]$, i.e., the i^{th} priority interval is $[0.1 \cdot (i-1), 0.1 \cdot i]$ $(1 \leq i \leq 10)$. We compare the average estimated dropping probability of each

group of packets with the real dropping rate of the same group in Fig. 4.12, where SSAR works in the forwarding mode over the Reality trace and the buffer size is 1MB. As shown in Fig. 4.12, the estimation result of our algorithm is close to the real dropping rate, and our algorithm can correctly predict that low-priority packets are more likely to be dropped than high-priority packets. Thus, it helps direct packets to those relays with high willingness to forward.

Allowed Selfishness To compare SSAR with other algorithms on how much selfishness is allowed, we plot the SS metric in Fig. 4.13 and 4.14. The buffer size is 1MB and 5MB in the Reality and Infocom05 trace, respectively. The two figures show that SSAR allows better selfishness than the other three algorithms. This is because SSAR's buffer management policy satisfies social selfishness. Also, due to the selfish gain metric and the MKPAR formulation, high-priority packets are more likely to be forwarded than low-priority ones. In contrast, the other three algorithms manage buffers without selfishness information and forward packets purely based on contact opportunity, so they perform much worse. We noted that the SS in SSAR drops as the packet generation rate increases. This is because when the workload is higher more packets are dropped. Thus, the average priority of dropped packets increases and SS decreases. In the extreme, if the workload is so high that nearly all packets are dropped, the SS will be close to 1.

4.1.5 Related Work

Many algorithms have been proposed for routing and data dissemination in opportunistic mobile networks, and they vary in what information is used to evaluate a node's forwarding capability and make forwarding decisions. Earlier works [33, 34] evaluate the forwarding capability of a node by the historic contact information, while more recent studies [35, 37, 111, 112] employ the social property (e.g., betweenness and centrality) of nodes or transient contact patterns [113] for relay selection. Gao and Cao [114] also propose a social centrality metric that considers the social contact patterns and interests of mobile users simultaneously and achieves effective relay selection. However, these approaches do not consider the social willingness of users to forward packets for others, and implicitly assume nodes are fully willing to forward packets for each other, which may not be al-

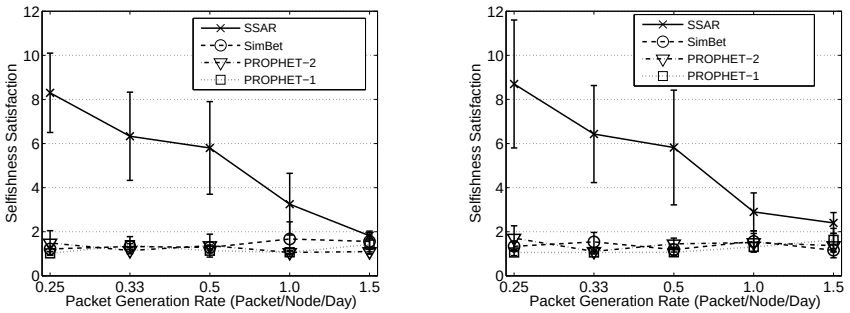

(a) Contact-dependent Graph (b) Random Graph

Figure 4.13. Comparison of algorithms in selfishness satisfaction over the Reality trace. The forwarding mode is used.

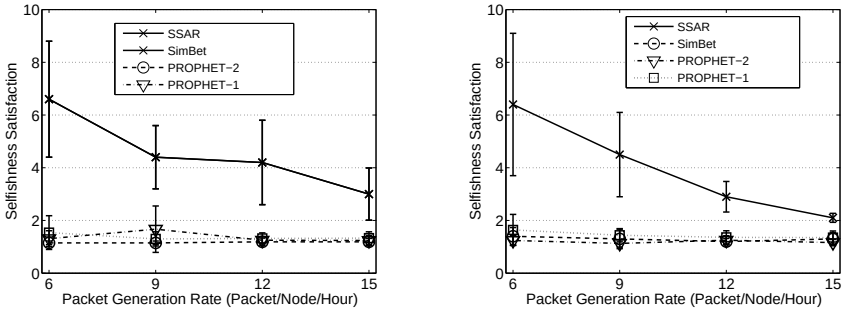

(a) Contact-dependent Graph (b) Random Graph

Figure 4.14. Comparison of algorithms in selfishness satisfaction over the Infocom05 trace. The forwarding mode is used.

ways true in reality. Algorithms [115, 116] have also been proposed for finding the right relays for data forwarding in vehicular ad hoc networks, but they consider a different scenario from this work.

Hui et al. [117] study the impact of altruistic behavior on the communication throughput of mobile social networks. The "altruism" concept in their work is similar to the willingness concept in this work in that altruism also describes if a node will forward packets for other nodes. However, there is important difference between the two. Altruism is used in an absolute sense and it denotes the probability that a node will forward a received packet. On the contrast, willingness is used in a relative sense, and it takes effect only when multiple packets contend for shared limited resource (e.g., buffer and bandwidth). More importantly, their focus is the impact of altruism on opportunistic communication but our focus is to design an effective and efficient routing protocol that considers user willingness.

Thus, this work and their work are complementary to each other.

Most existing routing algorithms explicitly or implicitly assume unlimited buffer (e.g., delegation forwarding [38]) which is unrealistic. Though some algorithms [36, 34] consider the buffer constraint in design, their attention is limited to which packets to drop when buffer overflows. However, SSAR integrates the buffer constraint into relay selection and takes it as a factor of delivery probability. Some work (e.g., RAPID [36]) has addressed in which order candidate packets should be transmitted to a better relay during a contact, but existing approaches ignore that the forwarded packets may be immediately dropped by the relay due to the buffer constraint. SSAR uses MKPAR to determine both which subset of candidate packets to forward and in what order to forward them. The formulation is different from the Knapsack formulation in [112] and [111]. Recently, Thompson *et al* [118] propose a congestion control scheme for opportunistic mobile networks which uses the local dropping information to control packet replications. Their scheme is different from SSAR since it controls a node's overall amount of replications but does not determine which node is a better relay.

Individual selfishness has been widely studied in mobile ad hoc networks [96, 95] and even in opportunistic mobile networks [40, 39]. The solutions proposed so far fall into three categories, credit-based approaches (e.g., [96, 40]), reputation-based approaches (e.g., [95]) and gaming-based approaches (e.g., [39]). The principle idea is to stimulate users to forward packets for others. As discussed in Chapter 4.1.2.1, they cannot be directly applied to the social selfishness problem.

4.1.6 Summary

In this section, we investigated the social selfishness problem in opportunistic mobile networks, and proposed a routing protocol SSAR for sensing data delivery which allows users to behave in the socially selfish way. Different from existing routing protocols that only consider contact opportunity when selecting relays, SSAR considers both user willingness and contact opportunity to measure the quality of relay, which is a better strategy for socially selfish networks. We designed novel machine learning techniques to incorporate user willingness into relay selection. To make better use of the limited contact opportunities, we modeled

the data forwarding process as an MKPAR, and gave a heuristic solution. Extensive simulations on the MIT Reality trace and Infocom05 trace show that SSAR can maintain social selfishness and achieve very good routing performance in an efficient way.

4.2 Defending Against Flood Attacks

4.2.1 Introduction

In opportunistic mobile networks, since the contacts between nodes are opportunistic and the duration of a contact may be short because of mobility, the usable bandwidth which is only available during the opportunistic contacts is a limited resource. Also, mobile nodes may have limited buffer space.

Due to the limitation in bandwidth and buffer space, opportunistic mobile networks are vulnerable to flood attacks. In flood attacks, maliciously or selfishly motivated attackers inject as many packets as possible into the network, or instead of injecting different packets the attackers forward replicas of the same packet to as many nodes as possible. For convenience, we call the two types of attack *packet flood attack* and *replica flood attack*, respectively. Flooded packets and replicas can waste the precious bandwidth and buffer resources, prevent benign packets from being forwarded and thus degrade the network service provided to good nodes. Moreover, mobile nodes spend much energy on transmitting/receiving flooded packets and replicas which may shorten their battery life. Therefore, it is urgent to secure opportunistic mobile networks against flood attacks.

Although many schemes have been proposed to defend against flood attacks on the Internet [119] and in wireless sensor networks [120], they assume persistent connectivity and cannot be directly applied to opportunistic mobile networks that have intermittent connectivity. In opportunistic mobile networks, little work has been done on flood attacks, despite the many works on routing [35, 34, 41], data dissemination [112, 121], blackhole attack [122], wormhole attack [123] and selfish dropping behavior [39, 124]. We noted that the packets flooded by outsider attackers (i.e., the attackers without valid cryptographic credentials) can be easily filtered with authentication techniques (e.g., [125]). However, authentication alone

does not work when insider attackers (i.e., the attackers with valid cryptographic credentials) flood packets and replicas with valid signatures. Thus, it is still an open problem is to address flood attacks in opportunistic mobile networks.

In this section, we employ rate limiting [43] to defend against flood attacks in opportunistic mobile networks. In our approach, each node has a limit over the number of packets that it, as a source node, can send to the network in each time interval. Each node also has a limit over the number of replicas that it can generate for each packet (i.e., the number of nodes that it can forward each packet to). The two limits are used to mitigate packet flood and replica flood attacks respectively. If a node violates its rate limits, it will be detected and its data traffic will be filtered. In this way, the amount of flooded traffic can be controlled.

Our main contribution is a technique to detect if a node has violated its rate limits. Although it is easy to detect the violation of rate limit on the Internet and in telecommunication networks where the egress router and base station can account each user's traffic, it is challenging in opportunistic mobile networks due to lack of communication infrastructure and consistent connectivity. Since a node moves around and may send data to any contacted node, it is very difficult to count the number of packets or replicas sent out by this node. Our basic idea of detection is *claim-carry-and-check*. Each node *itself* counts the number of packets or replicas that it has sent out, and claims the count to other nodes; the receiving nodes carry the claims around when they move, exchange some claims when they contact, and cross-check if these claims are inconsistent. If an attacker floods more packets or replicas than its limit, it has to use the same count in more than one claim according to the pigeonhole principle[3], and this inconsistency may lead to detection. Based on this idea, we use different cryptographic constructions to detect packet flood and replica flood attacks.

Because the contacts in opportunistic mobile networks are opportunistic in nature, our approach provides probabilistic detection. The more traffic an attacker floods, the more likely it will be detected. The detection probability can be flexibly adjusted by system parameters that control the amount of claims exchanged in a contact. We provide a lower and upper bound of detection probability and

[3]The pigeonhole principle states that if α items are put into β pigeonholes with $\alpha > \beta$, then at least one pigeonhole must contain more than one item.

investigate the problem of parameter selection to maximize detection probability under a certain amount of exchanged claims. The effectiveness and efficiency of our scheme are evaluated with extensive trace-driven simulations.

4.2.2 Motivation

The Potential Prevalence of Flood Attacks Many nodes may launch flood attacks for malicious or selfish purposes. Malicious nodes, which can be the nodes deliberately deployed by the adversary or subverted by the adversary via mobile phone worms [126], launch attacks to congest the network and waste the resources of other nodes.

Selfish nodes may also exploit flood attacks to increase their communication throughput. In opportunistic mobile networks, a single packet usually can only be delivered to the destination with a probability smaller than 1 due to the opportunistic connectivity. If a selfish node floods many replicas of its own packet, it can increase the likelihood of its packet being delivered, since the delivery of any replica means successful delivery of the packet. With packet flood attacks, selfish nodes can also increase their throughput, albeit in a subtler manner. For example, suppose Alice wants to send a packet to Bob. Alice can construct 100 variants of the original packet which only differ in one unimportant padding byte, and send the 100 variants to Bob independently. When Bob receives any one of the 100 variants, he throws away the padding byte and gets the original packet.

The Effect of Flood Attacks To study the effect of flood attacks on routing and motivate our work, we run simulations on the MIT Reality trace [108] (see more details about this trace in Chapter 4.2.7).

We consider three general routing strategies. 1) *Single-copy routing* (e.g., [42, 35]): After forwarding a packet out, a node deletes its own copy of the packet. Thus, each packet only has one copy in the network. 2) *Multi-copy routing* (e.g., [127]): The source node of a packet sprays a certain number of copies of the packet to other nodes and each copy is individually routed using the single-copy strategy. The maximum number of copies that each packet can have is fixed. 3) *Propagation routing* (e.g., [108, 33, 128]): When a node finds it appropriate (according to the routing algorithm) to forward a packet to another encountered node, it replicates

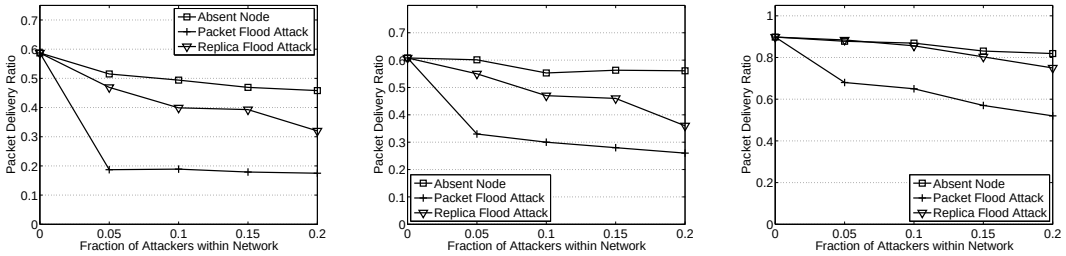

(a) Single-copy Routing (b) Multi-copy Routing (c) Propagation Routing

Figure 4.15. The effect of flood attacks on packet delivery ratio. In Absent Node, attackers are simply removed from the network. Attackers are selectively deployed to high-connectivity nodes.

that packet to the encountered node and keeps its own copy. There is no preset limit over the number of copies a packet can have. In our simulations, SimBet [35], Spray-and-Focus [127] (3 copies allowed for each packet) and Propagation are used as representatives of the three routing strategies respectively. In Propagation, a node replicates a packet to another encountered node if the latter has more frequent contacts with the destination of the packet.

Two metrics are used, The first metric is packet delivery ratio, which is defined as the fraction of packets delivered to their destinations out of all the unique packets generated. The second metric is the fraction of wasted transmissions (i.e., the transmissions made by good nodes for flooded packets). The higher fraction of wasted transmissions, the more network resources are wasted. We noticed that the effect of packet flood attacks on packet delivery ratio has been studied by Burgess et al [129] using a different trace [34]. Their simulations show that packet flood attacks significantly reduce the packet delivery ratio of single-copy routing but do not affect propagation routing much. However, they do not study replica flood attacks and the effect of packet flood attacks on wasted transmissions.

In our simulations, a packet flood attacker floods packets destined to random good nodes in each contact until the contact ends or the contacted node's buffer is full. A replica flood attacker replicates the packets it has generated to every encountered node that does not have a copy. Each good node generates thirty packets on the 121^{st} day of the Reality trace, and each attacker does the same in replica flood attacks. Each packet expires in 60 days. The buffer size of each node is 5MB, bandwidth is 2Mbps and packet size is 10KB.

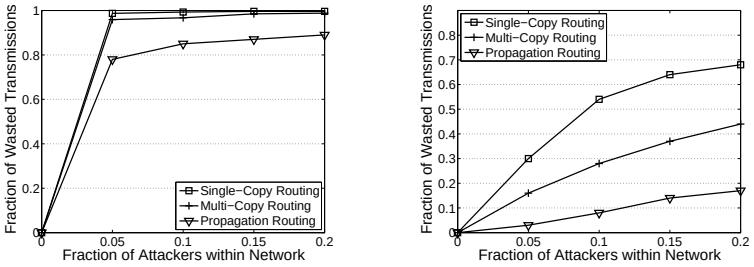

(a) Packet Flood Attack (b) Replica Flood Attack

Figure 4.16. The effect of flood attacks on wasted transmission. Attackers are randomly deployed.

Figure 4.15 shows the effect of flood attacks on packet delivery ratio. Packet flood attack can dramatically reduce the packet delivery ratio of all three types of routing. When the fraction of attackers is high, replica flood attack can significantly decrease the packet delivery ratio of single-copy and multi-copy routing, but it does not have much effect on propagation routing.

Figure 4.16 shows the effect of flood attacks on wasted transmission. Packet flood attack can waste more than 80% of the transmissions made by good nodes in all routing strategies when the fraction of attackers is higher than 5%. When 20% of nodes are attackers, replica flood attack can waste 68% and 44% of transmissions in single-copy and multi-copy routing respectively. However, replica flood attack only wastes 17% of transmissions in propagation routing. This is because each good packet is also replicated many times.

Remarks. The results show that all the three types of routing are vulnerable to packet flood attack. Single-copy and multi-copy routing are also vulnerable to replica flood attack, but propagation routing is much more resistant to replica flood. *Motivated by these results, this section addresses packet flood attack without assuming any specific routing strategy, and addresses replica flood attack for single-copy and multi-copy routing only.*

4.2.3 Overview

4.2.3.1 Problem Definition

Defense against Packet Flood Attacks We consider a scenario where each node has a rate limit L on the number of unique packets that it as a source can

generate and send into the network within each time interval T. The time intervals start from time 0, T, $2T$, etc. The packets generated within the rate limit are deemed legitimate, but the packets generated beyond the limit are deemed flooded by this node. To defend against packet flood attacks, our goal is to detect if a node as a source has generated and sent more unique packets into the network than its rate limit L per time interval.

A node's rate limit L does not depend on any specific routing protocol, but it can be determined by a service contract between the node and the network operator as discussed later. Different nodes can have different rate limits and their rate limits can be dynamically adjusted.

The length of time interval should be set appropriately. If the interval is too long, rate limiting may not be very effective against packet flood attacks. If the interval is too short, the number of contacts that each node has during one interval may be too nondeterministic and thus it is difficult to set an appropriate rate limit. Generally speaking, the interval should be short under the condition that most nodes can have a significant number of contacts with other nodes within one interval, but the appropriate length depends on the contact patterns between nodes in the specific deployment scenario.

Defense against Replica Flood Attacks As motivated in Chapter 4.2.2, the defense against replica flood considers single-copy and multi-copy routing protocols. These protocols require that, for each packet that a node buffers no matter if this packet has been generated by the node or forwarded to it, there is a limit l on the number of times that the node can forward this packet to other nodes. The values of l may be different for different buffered packets. Our goal is to detect if a node has violated the routing protocol and forwarded a packet more times than its limit l for the packet.

A node's limit l for a buffered packet is determined by the routing protocol. In multi-copy routing, $l = L'$ (where L' is a parameter of routing) if the node is the source of the packet, and $l = 1$ if the node is an intermediate hop (i.e., it received the packet from another node). In single-copy routing, $l = 1$ no matter if the node is the source or an intermediate hop. Note that the two limits L and l do not depend on each other.

We discuss how to defend against replica flood attacks for quota-based routing

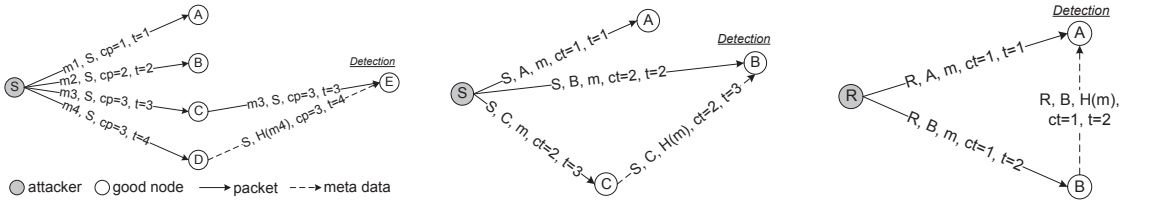

(a) Packet flood ($L = 3$)

(b) Replica flood by the source ($l = 2$)

(c) Replica flood by a relay ($l = 1$)

Figure 4.17. The basic idea of flood attack detection. *cp* and *ct* are packet count and transmission count, respectively. The arrows mean the transmission of packet or meta data which happens when the two end nodes contact.

[130, 127, 131] in Chapter 4.2.4.9.

Setting the Rate Limit L One possible method is to set L in a request-approve style. When a user joins the network, he requests for a rate limit from a trusted authority which acts as the network operator. In the request, this user specifies an appropriate value of L based on prediction of his traffic demand. If the trusted authority approves this request, it issues a *rate limit certificate* to this user, which can be used by the user to prove to other nodes the legitimacy of his rate limit. To prevent users from requesting unreasonably large rate limits, a user pays an appropriate amount of money or virtual currency (e.g., the credits that he earns by forwarding data for other users [40]) for his rate limit. When a user predicts an increase (decrease) of his demand, he can request for a higher (lower) rate limit. The request and approval of rate limit may be done offline. The flexibility of rate limit leaves legitimate users' usage of the network unhindered. This process can be similar to signing a contract between a smartphone user and a 3G service provider: the user selects a data plan (e.g., 200MB/month) and pays for it; he can upgrade or downgrade the plan when needed.

4.2.3.2 Models and Assumptions

Network Model In opportunistic mobile networks, since contact durations may be short, a large data item is usually split into smaller packets (or fragments) to facilitate data transfer. For simplicity, we assume that all packets have the same predefined size. Although in opportunistic mobile networks the allowed delay of packet delivery is usually long, it is still impractical to allow unlimited delays.

Thus, we assume that each packet has a lifetime. The packet becomes meaningless after its lifetime ends and will be discarded.

We assume that every packet generated by nodes is unique. This can be implemented by including the source node ID and a locally unique sequence number, which is assigned by the source for this packet, in the packet header.

We also assume that time is loosely synchronized, such that any two nodes are in the same time slot at any time. Since the inter-contact time in opportunistic mobile networks is usually at the scale of minutes or hours, the time slot can be at the scale of one minute. Such loose time synchronization is not hard to achieve.

Adversary Model There are a number of attackers in the network. An attacker can flood packets and/or replicas. When flooding packets, the attacker acts as a source node. It creates and injects more packets into the network than its rate limit L. When flooding replicas, the attacker forwards its buffered packets (which can be generated by itself or received from other nodes) more times than its limit l for them. The attackers may be insiders with valid cryptographic keys. Some attackers may collude and communicate via out-band channels.

Trust Model We assume that a public-key cryptography system is available. For example, Identity-Based Cryptography (IBC) [132] has been shown to be practical for opportunistic mobile networks [133]. In IBC, only an offline Key Generation Center (KGC) is needed. KGC generates a private key for each node based on the node's id, and publishes a small set of public security parameters to the node. Except the KGC, no party can generate the private key for a node id. With such a system, an attacker cannot forge a node id and private key pair. Also, attackers do not know the private key of a good node (not attacker).

Each node has a *rate limit certificate* obtained from a trusted authority. The certificate includes the node's ID, its approved rate limit L, the validation time of this certificate and the trusted authority's signature. The rate limit certificate can be merged into the public key certificate or stand alone.

4.2.3.3 Basic Idea: Claim-Carry-and-Check

Packet Flood Detection To detect the attackers that violate their rate limit L, we must count the number of unique packets that each node as a source has generated and sent to the network in the current interval. However, since the node

may send its packets to any node it contacts at any time and place, no other node can monitor all of its sending activities. To address this challenge, our idea is to let the node itself count the number of unique packets that it, as a source, has sent out, and *claim* the up-to-date packet count (together with a little auxiliary information such as its ID and a timestamp) in each packet sent out. The node's rate limit certificate is also attached to the packet, such that other nodes receiving the packet can learn its authorized rate limit L. If an attacker is flooding more packets than its rate limit, it has to dishonestly claim a count smaller than the real value in the flooded packet, since the real value is larger than its rate limit and thus a clear indicator of attack. The claimed count must have been used before by the attacker in another claim, which is guaranteed by the pigeonhole principle, and these two claims are inconsistent. The nodes which have received packets from the attacker *carry* the claims included in those packets when they move around. When two of them contact, they *check* if there is any inconsistency between their collected claims. The attacker is detected when an inconsistency is found.

Let us look at an example in Fig. 4.17(a). S is an attacker that successively sends out four packets to A, B, C and D, respectively. Since $L = 3$, if S claims the true count 4 in the fourth packet $m4$, this packet will be discarded by D. Thus, S dishonestly claims the count to be 3, which has already been claimed in the third packet $m3$. $m3$ (including the claim) is further forwarded to node E. When D and E contact, they exchange the count claims included in $m3$ and $m4$, and check that S has used the same count value in two different packets. Thus, they detect that S as an attacker.

Replica Flood Detection Claim-carry-and-check can also be used to detect the attacker that forwards a buffered packet more times than its limit l. Specifically, when the source node of a packet or an intermediate hop transmits the packet to its next hop, it claims a transmission count which means the number of times it has transmitted this packet (including the current transmission). Based on if the node is the source or an intermediate node and which routing protocol is used, the next hop can know the node's limit l for the packet, and ensure that the claimed count is within the correct range $[1, l]$. Thus, if an attacker wants to transmit the packet more than l times, it must claim a false count which has been used before. Similarly as in packet flood attacks, the attacker can be detected. Examples are

given in Fig. 4.17(b) and 4.17(c).

4.2.4 Our Scheme

Our scheme uses two different cryptographic constructions to detect packet flood and replica flood attacks independently. When our scheme is deployed to propagation routing protocols, the detection of replica flood attacks is deactivated.

The detection of packet flood attacks works independently for each time interval. Without loss of generality, we only consider one time interval when describing our scheme. For convenience, we first describe our scheme assuming that all nodes have the same rate limit L, and relax this assumption in Chapter 4.2.4.8. In the following, we use $SIG_i(*)$ to denote node i's signature over the content in the brackets.

4.2.4.1 Claim Construction

Two pieces of meta data are added to each packet (see Fig. 4.18), Packet Count Claim (P-claim) and Transmission Count Claim (T-claim). P-claim and T-claim are used to detect packet flood and replica flood attacks, respectively.

P-claim is added by the source and transmitted to later hops along with the packet. T-claim is generated and processed hop-by-hop. Specifically, the source generates a T-claim and appends it to the packet. When the first hop receives this packet, it peels off the T-claim; when it forwards the packet out, it appends a new T-claim to the packet. This process continues in later hops. Each hop keeps the P-claim of the source and the T-claim of its previous hop to detect attacks.

P-claim When a source node S sends a new packet m (which has been generated by S and not sent out before) to a contacted node, it generates a P-claim as follows:

$$\text{P-claim: } S, c_p, t, H(m), SIG_S(H(H(m)|S|c_p|t)) \tag{4.9}$$

Here, t is the current time. c_p ($c_p \in [1, L]$) is the packet count of S, which means that this is the c_p^{th} new packet S has created and sent to the network in the current time interval. S increases c_p by one after sending m out.

The P-claim is attached to packet m as a header field, and will always be forwarded along with the packet to later hops. When the contacted node receives

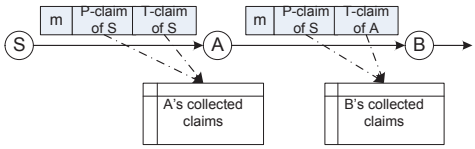

Figure 4.18. The conceptual structure of a packet and the changes made at each hop of the forwarding path.

this packet, it verifies the signature in the P-claim, and checks the value of c_p. If c_p is larger than L, it discards this packet; otherwise, it stores this packet and the P-claim.

T-claim When node A transmits a packet m to node B, it appends a T-claim to m. The T-claim includes A's current transmission count c_t for m (i.e., the number of times it has transmitted m out) and the current time t. The T-claim is:

$$\text{T-claim:} \quad A, B, H(m), c_t, t, SIG_A(H(A|B|H(m)|c_t|t)) \tag{4.10}$$

B checks if c_t is in the correct range based on if A is the source of m. If c_t has a valid value, B stores this T-claim.

In single-copy and multi-copy routing, after forwarding m for enough times, A deletes its own copy of m and will not forward m again.

4.2.4.2 Inconsistency Caused by Attack

In a dishonest P-claim, an attacker uses a smaller packet count than the real value. (We do not consider the case where the attacker uses a larger packet count than the real value, since it makes no sense for the attacker.) However, this packet count must have been used in another P-claim generated earlier. This causes an inconsistency called *count reuse*, which means the use of the same count in two different P-claims generated by the same node. For example in Fig. 4.17(a) the count value 3 is reused in the P-claims of packet $m3$ and $m4$. Similarly, count reuse is also caused by dishonest T-claims.

4.2.4.3 Protocol

Suppose two nodes contact and they have a number of packets to forward to each other. Then our protocol is sketched in Algorithm 8.

When a node forwards a packet, it attaches a T-claim to the packet. Since many packets may be forwarded in a contact and it is expensive to sign each T-claim separately, an efficient signature construction is proposed in Chapter 4.2.4.7. The node also attaches a P-claim to the packets that are generated by itself and have not been sent to other nodes before (called *new packet* in line 3, Algorithm 8).

When a node receives a packet, it gets the P-claim and T-claim included in the packet. It checks them against the claims that it has already collected to detect if there is any inconsistency (see Sec. 4.2.4.5). Only the P-claims generated in the same time interval (which can be determined by the time tag) are cross-checked. If no inconsistency is detected, this node stores the P-claim and T-claim locally (see Sec. 4.2.4.4).

To better detect flood attacks, the two nodes also exchange a small number of the recently collected P-claims and T-claims and check them for inconsistency. This meta data exchange process is separately presented in Sec. 4.2.5.

When a node detects an attacker, it adds the attacker into a blacklist and will not accept packets originated from or forwarded by the attacker. The node also disseminates an alarm against the attacker to other nodes (see Sec. 4.2.4.6).

Algorithm 8 : The protocol run by each node in a contact

```
 1: Meta data (P-claim and T-claim) exchange and attack detection
 2: if Have packets to send then
 3:     For each new packet, generate a P-claim;
 4:     For all packets, generate their T-claims and sign them with a hash tree;
 5:     Send every packet with the P-claim and T-claim attached;
 6: end if
 7: if Receive a packet then
 8:     if Signature verification fails or the count value in its P-claim or T-claim is invalid then
 9:         Discard this packet;
10:     end if
11:     Check the P-claim against those locally collected and generated in the same time interval
        to detect inconsistency;
12:     Check the T-claim against those locally collected for inconsistency;
13:     if Inconsistency is detected then
14:         Tag the signer of the P-claim (T-claim, resp.) as an attacker and add it into a blacklist;
15:         Disseminate an alarm against the attacker to the network;
16:     else
17:         Store the new P-claim (T-claim, resp.);
18:     end if
19: end if
```

4.2.4.4 Local Data Structures

Each node collects P-claims and T-claims from the packets that it has received and stores them locally to detect flood attacks. Let us look at a received packet m and the P-claim and T-claim included in this packet. Initially, this pair of P-claim and T-claim are stored in full with all the components shown in Formula 4.9 and 4.10. When this node removes m from its buffer (e.g., after m is delivered to the destination or dropped due to expiration), it compacts this pair of claims to reduce the storage cost. If this pair of claims have been sampled for meta data exchange, they will be stored in full until the exchange process ends and be compacted afterward.

Compact P-claim Storage Suppose node W stores a P-claim $\mathbb{C}_P = \{S, c_p, t, H(m), SIG_S\}$. It compacts the P-claim as follows. Using the timestamp t, W gets the index i of the time interval that t belongs to. The signature is discarded since it has been verified. The compacted P-claim is:

$$S, i, c_p, \widetilde{H}_8 \tag{4.11}$$

where $\widetilde{H}_8$ is a 8-bit string called *hash remainder*. It is obtained by concatenating 8 random bits of the packet hash $H(m)$. The indices of these 8 bits in the hash are determined by 8 locators. The locators are randomly and independently generated by W for S at the beginning of the i^{th} interval, and are shared by all the P-claims issued by S in the i^{th} interval. Each locator only has $\log_2 h$ bits where h denotes the size of a hash (e.g., 256 for SHA-256). W keeps these locators secret.

Suppose node W has collected n P-claims generated by S in interval i. For all these claims, only one source node ID and interval index is stored. Also, instead of directly storing the packet count values c_p included in these P-claims, the compact structure uses a L-bit long bit vector to store them. If value c appears in these P-claims, the c^{th} bit of the vector is set. Let $\mathcal{C}_S^i$ denote the compact structure of these P-claims. Then:

$$\mathcal{C}_S^i = S, i, \textit{bit-vector}, \textit{locators}, [\widetilde{H}_{8_1}, \widetilde{H}_{8_2}, ..., \widetilde{H}_{8_n}] \tag{4.12}$$

Compact T-claim Storage Suppose node W stores a T-claim

$\mathbb{C}_T = \{R, W, H(m), c_t, t, SIG_R\}$ issued by node R. The signature is discarded since it has been verified. W does not need to store its own ID and t is not useful for inconsistency check. Then the compacted T-claim is:

$$R, c_t, \widetilde{H}_{32} \tag{4.13}$$

where $\widetilde{H}_{32}$ is a 32-bit hash remainder defined similarly as $\widetilde{H}_8$. Suppose W has collected n T-claims generated by R. Then the compact structure of these T-claims is:

$$\mathcal{C}_R = R, \mathit{locators}, [\widetilde{H}_{32_1}, c_{t_1}], ..., [\widetilde{H}_{32_n}, c_{t_n}] \tag{4.14}$$

The locators are randomly and independently generated by W for R, and are shared by all the T-claims issued by R.

4.2.4.5 Inconsistency Check

Suppose node W wants to check a pair of P-claim and T-claim against its local collections to detect if there is any inconsistency. The inconsistency check against full claims is trivial: W simply compares the pair of claims with those collected. In the following, we describe the inconsistency check against compactly stored claims.

Inconsistency Check with P-claim From the P-claim node W gets: the source node ID S, packet count c_p, timestamp t and packet hash H. To check inconsistency, W first uses S and t to map the P-claim to the structure $\mathcal{C}_S^i$ (see Eq. 4.12). Then it reconstructs the hash remainder of H using the locators in $\mathcal{C}_S^i$. If the bit indexed by the packet count c_p is set in the bit-vector but the hash remainder is not included in $\mathcal{C}_S^i$, count reuse is detected and S is an attacker.

The inconsistency check based on compact P-claims does not cause false positive, since a good node never reuses any count value in different packets generated in the same interval. The inconsistency check may cause false negative if the two inconsistent P-claims have the same hash remainder. However, since the attacker does not know which bits constitute the hash remainder, the probability of false negative is only 2^{-8}. Thus, it has minimal effect on the overall detection probability.

Inconsistency Check with T-claim From the T-claim node W gets: the sender ID R, receiver ID Q and transmission count c_t. If Q is W itself (which is possible if the T-claim has been sent out by W but returned by an attacker), W takes no action. Otherwise, it uses R to map the T-claim to the structure $\mathcal{C}_R$ (see Eq. 4.14). If there is a 2-tuple $[\widetilde{H}'_{32}, c'_t]$ in $\mathcal{C}_R$ that satisfies 1) $\widetilde{H}'_{32}$ is the same as the remainder of H, and 2) $c'_t = c_t$, then the issuer of the T-claim (i.e., R) is an attacker.

The inconsistency check based on compact T-claims does not cause extra false negative. False positive is possible but it can be kept low as follows. Node W may falsely detect a good node R as an attacker if it has received two T-claims generated by R that satisfy two conditions: (i) they are generated for two different packets, and (ii) they have the same hash remainder. For 32-bit hash remainder, the probability that each pair of T-claims lead to false detection is 2^{-32}. In most cases, we expect that the number of T-claims generated by R and received by W is not large due to the opportunistic contacts, and thus the probability of false detection is low. As W receives more T-claims generated by R, it can use a longer (e.g., 64-bit) hash remainder for R to keep the probability of false detection low. Moreover, such false detection is limited to W only, since W cannot convince other nodes to accept the detection with compact T-claim.

4.2.4.6 Alarm

Suppose in a contact a node receives a claim $\mathbb{C}_r$ from a forwarded data packet or from the meta data exchange process (see Sec. 4.2.5.3) and it detects inconsistency between $\mathbb{C}_r$ and a local claim $\mathbb{C}_l$ that the node has collected. $\mathbb{C}_r$ is a full claim as shown in Formula 4.9 (or 4.10), but $\mathbb{C}_l$ may be stored as a full claim or just a compact structure shown in Formula 4.11 (or 4.13).

If $\mathbb{C}_l$ is a full claim, the node can broadcast (via Epidemic routing [134]) a *global alarm* to all the other nodes to speed up the attacker detection process. The alarm includes the two full claims $\mathbb{C}_l$ and $\mathbb{C}_r$. When a node receives an alarm, it verifies the inconsistency between the two included claims and their signatures. If the verification succeeds, it adds the attacker into its blacklist and broadcasts the alarm further; otherwise, it discards the alarm. The node also discards the alarm if it has broadcast another alarm against the same attacker.

If the detecting node stores $\mathbb{C}_l$ as a compact structure, it cannot convince other

nodes to trust the detection since the compact structure does not have the attacker's signature. Thus it cannot broadcast a global alarm. However, since the attacker may have reused the count value of $\mathbb{C}_r$ to other claims besides $\mathbb{C}_l$, the detecting node can disseminate a *local alarm* that only contains $\mathbb{C}_r$ to its contacted nodes who have received those claims. These contacted nodes can verify the inconsistency between $\mathbb{C}_r$ and their collected claims, and also detect the attacker. If any of these nodes still stores a full claim inconsistent with $\mathbb{C}_r$, it can broadcast a global alarm as done in the previous case; otherwise, it disseminates a local alarm. As this iterative process proceeds, the attacker can be quickly detected by many nodes. Each node only disseminates one local alarm for each detected attacker.

A local alarm and a global alarm against the same attacker may be disseminated in parallel. If a node receives the global alarm first and then receives the local alarm, it discards the local alarm. If it receives the local alarm first, when it receives the global alarm later, it discards the local alarm and keeps the global alarm.

An attacker may falsify an alarm against a good node. However, since it does not have the node's private key (as our assumption), it cannot forge the node's signatures for the claims included in the alarm. Thus, the alarm will be discarded by other nodes and this attack fails.

4.2.4.7 Efficient T-claim Authentication

The T-claims of all the packets transmitted in a contact should be signed by the transmitting node. Since the contact may end at any unpredictable time, each received T-claim must be individually authenticated. A *naive* approach is to protect each T-claim with a separate public-key signature, but it has high computation cost in signature operations.

Our scheme uses Merkle hash tree [54] to amortize the computation cost of public-key based signature on all the T-claims that the node sends out in a contact. Specifically, after a node generates the T-claims (without signature) for all the packets it want to send, it constructs a hash tree upon these partial T-claims, and signs the root of the tree with a public-key based signature. Then the signature of a T-claim includes this root signature and a few elements of the tree. Fig. 4.19 shows the hash tree constructed upon eight T-claims and the tree elements included in

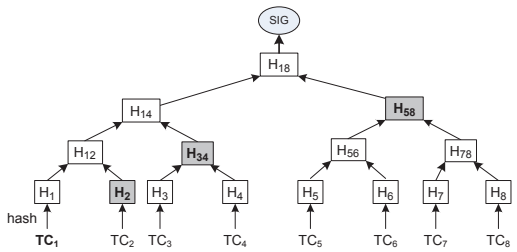

Figure 4.19. The Merkle hash tree constructed upon eight T-claims TC_1,...,TC_8. In the tree, H_i is the hash of TC_i, and an inner node is the hash of its child nodes. The signature of TC_1 includes H_2, H_{34}, H_{58} and SIG.

the signature of the first T-claim. We refer to the original paper [54] for details. In this way, for all the T-claims sent by the sender in a contact, only one public-key based signature is generated by the sender and verified by the receiver.

4.2.4.8 Dealing with Different Rate Limits

Previously we have assumed that all nodes have the same rate limit L. When nodes have different rate limits, for our detection scheme to work properly, each intermediate node that receives a packet needs to know the rate limit L of the source of the packet, such that it can check if the packet count is in the correct range 1, 2, ..., L. To do so, when a source node sends out a packet, it attaches its rate limit certificate to the packet. The intermediate nodes receiving this packet can learn the node's authorized rate limit from the attached certificate.

4.2.4.9 Replica Flood Attacks in Quota-based Protocols

Our scheme to detect replica flood attacks can also be adapted to quota-based routing protocols [130, 127, 131].

Quota-based routing works as follows. Each node has a quota for each packet that it buffers, and the quota specifies the number of replicas into which the current packet is allowed to be split. When a source node creates a packet, its quota for the packet is L' replicas, where L' is a system parameter. When the source contacts a relay node, it can split multiple replicas to the relay according to the quality of the relay. After the split, the relay's quota for the packet is the number of replicas split to it, and the source node's quota is reduced by the same amount. This procedure continues recursively, and each node carrying the packet can split out a number of

replicas less than its current quota for the packet. It can be seen that each packet can simultaneously have at most L' replicas in the network.

In quota-based routing, replica flood attacks (where an attacker sends out more replicas of a packet than its quota) can be detected by our approach as follows.

First, we observe that quota-based routing (with the total quota determined at the source) can be emulated by single-copy routing if different replicas of the same packet appear different to intermediate nodes and each replica is forwarded in a similar way as single-copy routing. A node can split multiple replicas of a packet to another node, but it can only send each replica out once. For instance, if a node has forwarded Replica 1 to one relay, it must remove Replica 1 from its local buffer, and it cannot forward this replica again to another relay.

To differentiate replicas, the source assigns a unique index to each replica as a header field, and signs the replica to prevent intermediate nodes from modifying the index. The index value should be in range $[1, L']$, and replicas with invalid index will be discarded. In this way, a node's local quota for a packet is represented by the number of replicas (with different indices) that it buffers. Note that an intermediate node cannot increase its quota by forging replicas since it does not have the source node's key to generate a valid signature.

To prevent a node from abusing its quota, we need to ensure that the node only forwards each replica once. T-claim can be used to achieve this goal. Particularly, when a node splits multiple replicas of a packet to another node, it generates a T-claim for each replica. The inconsistency check (see Chapter IV.E) can be applied here to detect the attackers that transmit the same replica more than once.

4.2.5 Meta Data Exchange

When two nodes contact they exchange their collected P-claims and T-claims to detect flood attacks. If all claims are exchanged, the communication cost will be too high. Thus, our scheme uses sampling techniques to keep the communication cost low. To increase the probability of attack detection, one node also stores a small portion of claims exchanged from its contacted node, and exchanges them to its own future contacts. This is called redirection.

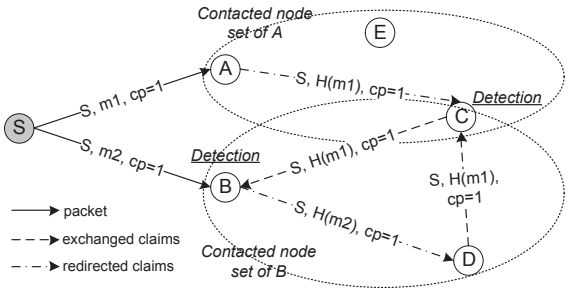

Figure 4.20. The idea of redirection which is used to mitigate the stealthy attack.

4.2.5.1 Sampling

Since P-claims and T-claims are sampled together (i.e., when a P-claim is sampled the T-claim of the same packet is also sampled), in the following we only consider P-claims.

A node may receive a number of packets (each with a P-claim) in a contact. It randomly samples Z (a system parameter) of the received P-claims, and exchanges the sampled P-claims to the next K (a system parameter) different nodes it will contact, excluding the sources of the P-claims and the previous hop from which these P-claims are received.

However, a vulnerability to tailgating attack should be addressed. In tailgating attack, one or more attackers tailgate a good node to create a large number (say, d) of frequent contacts with this node, and send Z packets (not necessarily generated by the attackers) to it in each contact. If this good node sends the Zd P-claims of these contacts to the next K good nodes it contacts, much effective bandwidth between these good nodes will be wasted, especially in a large network where K is not small.

To address this attack, the node uses an inter-contact sampling technique to determine which P-claims sampled in historical contacts should be exchanged in the current contact. Let $\mathcal{S}_K$ denote a set of contacts. This set includes the minimum number of most recent contacts between this node and at least K other different nodes. Within this set, all the contacts with the same node are taken as one single contact and a total of Z P-claims are sampled out of these contacts. This technique is not vulnerable to the tailgating attack since the number of claims exchanged in each contact is bounded by a constant.

4.2.5.2 Redirection

There is a stealthy attack to flood attack detection. For replica flood attacks, the condition of detection is that at least two nodes carrying inconsistent T-claims can contact. However, suppose the attacker knows that two nodes A and B never contact. Then, it can send some packets to A, and invalidly replicate these packets to B. In this scenario, this attacker cannot be detected since A and B never contact. Similarly, the stealthy attack is also harmful for some routing protocols like Spray-and-Wait [127] in which each packet is forwarded from the source to a relay and then directly delivered from the relay to the destination.

To address the stealthy attack, our idea is to add one level of indirection. A node redirects the Z P-claims and T-claims sampled in the current contact to one of the next K nodes it will contact, and this contacted node will exchange (but not redirect again) these redirected claims in its own subsequent contacts. Look at the example in Fig. 4.20. Suppose attacker S sends mutually inconsistent packets to two nodes A and B which will never contact. Suppose A and B redirect their sampled P-claims to node C and D, respectively. Then so long as C and B or D and A or C and D can contact, the attack has a chance to be detected. Thus, the successful chance of stealthy attack is significantly reduced.

4.2.5.3 The Exchange Process

Each node maintains two separate sets of P-claims (T-claims, resp. in the following) for meta data exchange, a *sampled set* which includes the P-claims sampled from the most recent contacts with K different nodes (i.e., $\mathcal{S}_K$ in Chapter 4.2.5.1), and a *redirected set* which includes the P-claims redirected from those contacts. Both sets include Z P-claims obtained in each of those contacts.

When two nodes A and B contact, they first select KZ P-claims from each set with the inter-contact sampling technique (see Sec. 4.2.5.1), and then send these P-claims to each other. When A receives a P-claim, it checks if this P-claim is inconsistent with any of its collected P-claims using the method described in Sec 4.2.4.5. If the received P-claim is inconsistent with a locally collected one and the signature of the received P-claim is valid, A detects that the issuer (or signer) of the received P-claim is an attacker.

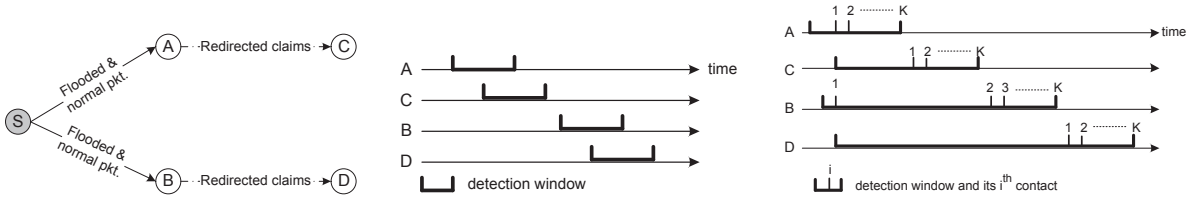

(a) Considered basic attack (b) Lower bound scenario (c) Upper bound scenario.

Figure 4.21. (a) The basic attack considered for detection probability analysis. Attacker S floods packets to A and then to B. (b) The scenario when the lower bound detection probability can be obtained. (c) The scenario when the upper bound detection probability can be obtained.

Out of all the P-claims received from B, A randomly selects Z of the P-claims from the sampled set of B, and stores them to A's redirected set. All other P-claims received from B are discarded after inconsistency check.

4.2.5.4 Meta Data Deletion

A node stores the P-claims and T-claims collected from received data packets for a certain time denoted by τ and deletes them afterward. It deletes the claims redirected from other nodes immediately after it has exchanged them to K different nodes.

4.2.6 Analysis

This section presents rigorous analysis over the security and cost of our scheme, and discusses the optimal parameter to maximize the effectiveness of flood attack detection under a certain amount of exchanged meta data per contact.

4.2.6.1 Detection Probability

The following analysis assumes uniform and independent contacts between nodes, i.e., at any time each node's next contacted node can be any other node with the same probability. This assumption holds for mobility models such as Random Waypoint where the contacts between all node pairs can be modeled as i.i.d. Poisson processes [135]. When analyzing the detection probability, we assume that each attacker acts alone. The case of collusion is analyzed separately in Chapter 4.2.6.4.

Table 4.3. Variables used in the analysis

$\mathcal{S}_i$	The K nodes that node i ($i \in \{A, B, C, D\}$) exchanges its sampled or redirected claims to.
e_i	A boolean event which means if node i ($i \in \{A, B\}$) has sampled at least one flooded packet ($e_i = TRUE$) or not ($e_i = FALSE$)
$\hat{e}_{AB}$	A boolean event which means if node A and B have sampled at least one pair of inconsistent packets ($\hat{e}_{AB} = TRUE$) or not
P_s	The probability that event $e_A = TRUE$ (or $e_B = TRUE$, resp.)
P_{ovp}	The conditional probability that if $e_A = e_B = TRUE$ then $\hat{e}_{AB} = TRUE$.
P_d	The probability that S is detected.
P_d^l	The lower-bound of P_d.
P_d^u	The upper-bound of P_d.
N	The number of nodes in the network.
M	The number of attackers in the network.
r	The proportion of good nodes, i.e., $r = \frac{N-M}{N}$.
K	The number of nodes that a claim is exchanged to. $K \ll N$.
a	The number of flooded packets sent to A and B.
n	The total number of packets sent to A and B.
y	The proportion of flooded packets sent to A and B, i.e., $y = \frac{a}{n}$.

The Basic Attack First we consider a basic attack (see Fig. 4.21(a)) in which an attacker S floods two sets of mutually inconsistent packets to two good nodes A and B, respectively. Each flooded packet received by A is inconsistent with one of the flooded packets received by B. In the contacts with A and B, S also forwards some normal, not flooded, packets to A and B to make the attack harder to detect. Let y denote the proportion of flooded packets among those sent by S. For simplicity, we assume y is the same in both contacts. Suppose A and B redirect the claims sampled in the contact with S to C and D, respectively.

To consider the worst-case performance, suppose the flooded packets are not forwarded from A and B to other nodes (which is the case in Spray-and-Wait [127]), i.e., only A and B have the inconsistent claims. Note that the analysis also applies to the detection of replica flood attacks.

For convenience, we define node A's (or B's) *detection window* as from the time it receives the flooded packets to the time it exchanges the sampled claims to K nodes, and node C's (or D's) detection window as from the time it receives the redirected claims to the time it exchanges them to K nodes. The attacker has a chance to be detected if node pairs $\langle A, B\rangle$, $\langle A, D\rangle$, $\langle C, B\rangle$ and $\langle C, D\rangle$ can contact within their detection windows. Table 4.3 shows the variables used in the analysis.

Lower Bound The lower bound of detection probability is obtained in the

following scenario (see Fig. 4.21(b)): When B receives the packets from S, both A and C have finished their detection window. Due to the effect of sampling, the attacker can be detected 1) by A if $A \in \mathcal{S}_B$ and $e_B = TRUE$; or 2) by A if D is a good node, $A \in \mathcal{S}_D$ and $e_B = TRUE$; or 3) by C if C is a good node, $C \in \mathcal{S}_B$ and $\hat{e}_{AB} = TRUE$; or 4) by C if both C and D are good nodes, $C \in \mathcal{S}_D$ and $\hat{e}_{AB} = TRUE$.

Since each of A and B exchanges the sampled claims to K nodes other than itself, and C (D) exchanges the redirected claims to K nodes other than A (B), according to the uniform contact assumption, we have:

$$\begin{aligned} P_d =& P_s[1 - (1 - \frac{K}{N-1}) \cdot (1 - r\frac{K}{N-2}) \cdot \\ & (1 - r\frac{K}{N-1}P_sP_{ovp}) \cdot (1 - r^2\frac{K}{N-2}P_sP_{ovp})] \end{aligned} \tag{4.15}$$

The expected number of flooded packets that A or B can sample is yZ. Since Z is typically small while a is not that small (which we believe realistic), P_{ovp} is negligible. Considering that $K \ll N$, P_d is approximated as follows:

$$P_d \approx P_s[1 - (1 - \frac{K}{N-1})(1 - r\frac{K}{N-2})] \approx P_s\frac{1+r}{N}K$$

Since random sampling is used, it is trivial to get:

$$\begin{aligned} P_s =& 1 - \frac{n-a}{n}\frac{n-a-1}{n-1} \cdots \frac{n-a-Z+1}{n-Z+1} \\ & \geq 1 - (1 - a/n)^Z = 1 - (1-y)^Z \end{aligned}$$

Thus, we have $P_d \geq K\frac{1+r}{N}(1 - (1-y)^Z)$, and a lower bound of the detection probability is:

$$P_d^l = K\frac{1+r}{N}(1 - (1-y)^Z) \tag{4.16}$$

Upper Bound The upper bound of detection probability is obtained in the following scenario (see Fig. 4.21(c)): D receives the redirected claims from B not later than the time C receives the redirected claims from A, and they are the first node that A and B encounter after the contact with S. Besides the four cases that we discussed when deriving the lower bound, the attacker can also be detected 1)

by B if $B \in \mathcal{S}_A$ and $e_A = TRUE$; or 2) by B if C is a good node, $B \in \mathcal{S}_C$ and $e_A = TRUE$; or 3) by D if D is a good node, $D \in \mathcal{S}_A$ and $\hat{e}_{AB} = TRUE$; or 4) by D if both C and D are good nodes, $D \in \mathcal{S}_C$ and $\hat{e}_{AB} = TRUE$.

Similarly as in the lower bound case, we can obtain that the detection probability is $P_d \approx 2K\frac{1+r}{N}P_s$. Since $P_s \leq 1$, an upper bound of the detection probability is:

$$P_d^u = \frac{2K(1+r)}{N} \tag{4.17}$$

Stronger Attacks We use the number of times that a count value is reused to represent the strength of an attack. Intuitively, if each count value is used many times, the attacker floods a lot of packets or replicas. Let X denote the number of times a count value is reused. We want to derive the relation between X and the probability that the attacker will be detected.

The stronger attacks we consider extends the basic attack as follows. Suppose the attacker has sent a set of packets to a good node G_0, and then it successively sends the same number of packets (reusing the count values of the packets sent to G_0) to X good nodes G_1, ..., G_X. All other parameters in the basic analysis apply here. From a global point of view, a total of $\frac{X(X+1)}{2}$ node pairs have inconsistent packets, and each pair can detect the attacker independently as in the basic attack. Then the attacker will be detected by at least one node pair with a probability:

$$P_d^X = 1 - (1 - P_d)^{\frac{X(X+1)}{2}} \tag{4.18}$$

We can see that the stronger the attack is, the more likely the attacker will be detected.

4.2.6.2 Cost

Communication The communication cost mainly has two parts. One part is the P-claim and T-claim transmitted with each packet, and the other part is the partial claims transmitted during meta data exchange. As to the latter, at most $4ZK$ P-claims and $4ZK$ T-claims are exchanged in each contact, with one half for sampled and the other half for redirected claims.

Computation As to signature generation, a node generates one signature for each newly generated packet. It also generates one signature for all its T-claims as

a whole sent in a contact. As to signature verification, a node verifies the signature of each received packet. It also verifies one signature for all the T-claims as a whole received in one contact.

Storage Most P-claims and T-claims are compacted when the packets are forwarded. The Z sampled P-claims and T-claims are stored in full until the packets are forwarded or have been exchanged to K nodes, whichever is later, and then compacted. For each received packet, less than 20 bytes of compact claims are stored for time duration τ.

4.2.6.3 Parameter Selection

We study the following question: If we fix the communication cost of meta data exchange (note that little can be done with the transmission of claims within packets), then how should we set parameter K and Z to maximize the detection probability? Note that the communication cost of meta data exchange is proportional to ZK. As to detection probability, we consider the lower-bound detection probability for the basic attack which can be written as $P_d = cK(1-(1-y)^Z)$.

Lemma 5. *If the communication cost of meta data exchange is fixed at $ZK = C$, then P_d is maximized at $K = C$ and $Z = 1$.*

Proof. P_d can be rewritten as $P_d = cC\frac{1-(1-y)^Z}{Z}$. The derivative of P_d over Z is:

$$P_d'(Z) = \frac{cC}{Z^2}[(1-y)^Z(1-\ln(1-y)^Z)-1] \tag{4.19}$$

Let $u = (1-y)^Z$ $(0 < u \leq 1)$, then $P_d'(Z) = \frac{cC}{Z^2}(u - u\ln u - 1)$. Let $g(u) = u - u\ln u - 1$. Then $g'(u) = -\ln u \geq 0$, which means $g(u)$ monotonically increases. Since $g(1) = 0$, $g(u) \leq 0$ when $0 < u \leq 1$. Therefore, $P_d'(Z) \leq 0$, which means P_d monotonically decreases with Z. Thus, to maximize P_d, Z should be set the minimum value 1. □

Remarks In this parameter setting, the lower-bound detection probability can be written as $P_d = yK\frac{1+r}{N}$. Suppose the attacker launches attacks independently. Then it can be detected after $\frac{N}{yK(1+r)}$ attacks. If the attacker wants to stay undetected for a longer time, it should maintain a smaller y, which means the attack effect is weaker; if it wants to make a big attack impact, it should maintain a high

y, but this means it will be detected in a shorter time. From another point of view, since the attacker only uses y proportion its capacity for flood attack, it is equivalent that the attacker can attack at full capacity for only $\frac{N}{K(1+r)}$ contacts. Thus, the attacks can be effectively mitigated.

4.2.6.4 Collusion

Packet Flood Attack One attacker may send a packet with a dishonest packet count to its colluder, which will forward the packet to the network. Certainly, the colluder will not exchange the dishonest P-claim with its contacted nodes. However, so long as the colluder forwards this packet to a good node, this good node has a chance to detect the dishonest claim as well as the attacker. Thus, the detection probability is not affected by this type of collusion.

Replica Flood Attack When attackers collude, they can inject invalid replicas of a packet without being detected, but the number of flooded replicas is effectively limited in our scheme. More specifically, in our scheme for a unique packet all the M colluders as a whole can flood a total of $M-1$ invalid replicas without being detected. To the contrast, when there is no defense, a total of $N-M$ invalid replicas can be injected by the colluders for each unique packet. Since the number of colluders is not very large, our scheme can still effectively mitigate the replica flood attack. This will be further evaluated in Sec. 4.2.7.

4.2.7 Performance Evaluations

4.2.7.1 Experiment Setup

To evaluate the performance and cost of our scheme, we run simulations on a synthetic trace generated by the Random Waypoint (RWP) [135] mobility model and on the MIT Reality trace [108] collected from the real world.

In our synthetic trace, 97 nodes move in a 500×500 square area with the RWP model. The moving speed is randomly selected from $[1, 1.6]$ to simulate the speed of walking, and the transmission range of each node is 10 to simulate that of Bluetooth. Each simulation lasts 5×10^5 time units.

The Reality trace has been shown [136, 37] to have social community structures. 97 smartphones are carried by students and staff at MIT over 10 months.

These phones run Bluetooth device discovery every five minutes and log about 110 thousand contacts. Each contact includes the two contact parties, the start time and duration of the contact.

In the simulations, 20% of nodes are deployed as attackers. They are randomly deployed or selectively deployed to high-connectivity nodes. The buffer size of each node is 5MB, the Drop Tail policy is used when buffer overflows. The bandwidth is 2Mbps. Each node generates packets of 10KB with random destinations at a uniform rate. Parameter $Z = 1$.

4.2.7.2 Routing Algorithms and Metrics

We use the following routing protocols in evaluations:

- **Forward** A single-copy routing protocol where a packet is forwarded to a relay if the relay has more frequent contacts with the destination.
- **SimBet** [35] A single-copy routing protocol where a packet is forwarded to a relay if the relay has a higher simbet metric, which is calculated from two social measures (similarity and betweenness).
- **Spray-and-Wait** [127] A multi-copy protocol, where the source replicates a packet to $L' = 3$ relays and each relay directly delivers its copy to the destination when they contact.
- **Spray-and-Focus** [127] It is similar to Spray-and-Wait, but each packet copy is individually routed to the destination with Forward.
- **Propagation** A packet is replicated to a relay if the relay has more frequent contacts with the destination.

We use the following performance evaluation metrics:

- **Detection rate** The proportion of attackers that are detected out of all the attackers.
- **Detection delay** From the time the first invalid packet is sent to the time the attacker is detected.

- **Computation cost** The average number of signature generations and verifications per contact.
- **Communication cost** The number of P-claim/T-claim pairs transmitted into the air, normalized by the number of packets transmitted.
- **Storage cost** The time-averaged kilobytes stored for P-claims and T-claims per node.

4.2.7.3 Analysis Verification

We use the synthetic trace to verify our analysis results given in Chapter 4.2.6, since in this trace the contacts between node pairs are i.i.d. [135] which conforms to our assumption for the analysis. We divide the trace into 10 segments, each with 5×10^4 time units, and run simulations on each of the $3^{rd} - 7^{th}$ segments 3 times with different random seeds. Each data point is averaged over the individual runs. Spray-and-Wait is used as the routing protocol to consider the worst case of packet flood detection (see Sec. 4.2.6.1). Here we only verify the detection probability for the basic attack, since the detection probability for the strong attack can be derived from it in a straightforward way. In this group of simulations, each attacker launches the basic attack once. It sends out two sets of packets to two good nodes with 10 packets in each set (i.e., $n = 10$), and these two sets contain mutually inconsistent packets. We first fix parameter $y = 1.0$ (see Table 4.3) but change parameter K from 0 to 10, and then we fix parameter $K = 10$ but change y from 0 to 1.0. The results are shown in Fig. 4.22(a) and 4.22(b), respectively. It can be seen that the simulation results are between the analytical lower bound and upper bound, which verifies the correctness of our analysis.

4.2.7.4 Detection Rate

The Reality trace is used. We divide the trace into segments of one month, and run simulations on each of the $3^{rd} - 7^{th}$ segments 3 times with different random seeds. Each data point is averaged over the individual runs. By default, each attacker launches the basic attack once, and it floods one packet out (i.e., $n = 1$, $y = 1.0$). By default, attackers are selectively deployed to high-connectivity nodes.

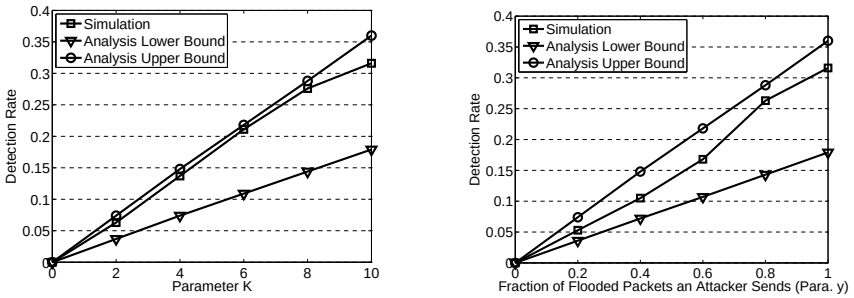

(a) Effect of Parameter K (b) Strength of Attack (Para. y)

Figure 4.22. Verification of analysis results on the synthetic trace. Spray-and-Wait is used as the routing protocol. Each attacker launches the basic attack once.

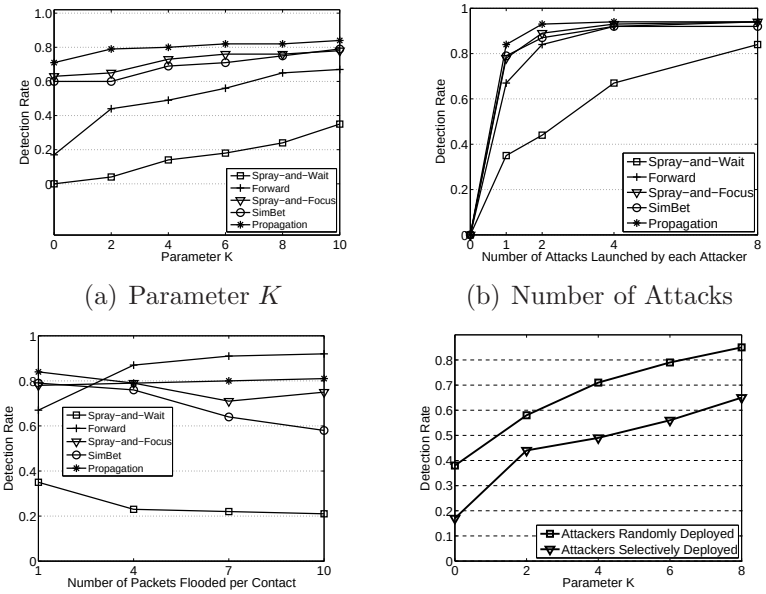

(a) Parameter K (b) Number of Attacks

(c) Packets Flooded per Contact (d) Attacker Deployment

Figure 4.23. The detection rate under different conditions. In (d), Forward is used as the routing protocol.

Fig. 4.23(a) shows the effect of parameter K in different routing protocols. Generally speaking, when K increases, the detection rate also increases because the inconsistent packets are exchanged to more nodes and have more chances to be detected. When $K = 0$, no attacker is detected in Spray-and-Wait, since no meta data is exchanged for detection. However, attackers can still be detected in the other three algorithms, because the inconsistent packets are forwarded to multiple nodes and the node that receives two inconsistent packets can detect the

attacker. Among these protocols, Propagation achieves the highest detection rate since it replicates inconsistent packets the most number of times. Between the two single-copy routing protocols, SimBet has a higher detection rate than Forward. This is because SimBet tends to forward packets to the more socially connected nodes and thus these nodes are more likely to collect inconsistent packets.

Fig. 4.23(b) shows the results when each attacker launches the basic attack independently for a varying number of times. As the attackers launch more attacks, the detection rate quickly increases for obvious reasons.

Fig. 4.23(c) shows the effect of the number of packets that an attacker floods in each contact (i.e., parameter n). As an attacker floods more packets in each contact, the detection rate decreases in Spray-and-Wait and SimBet, increases in Forward and does not change much in Spray-and-focus and Propagation. The opposite trends are due to two factors that affect the detection rate reversely. On the one hand, sampling decreases detection rate. To explain this more clearly, let us look at the basic attack scenario in Fig. 4.21(a) for Spray-and-Wait. Since $Z = 1$, A (B, resp.) only samples one packet out of all the packets received from the attacker and redirects it to C (D, resp.). When $n = 1$, C and D will receive mutually inconsistent claims, which means in Equation 4.15 $P_{ovp} = 1.0$. However, when n is larger than 1, C and D may not receive a pair of inconsistent claims due to the independent sampling by A and B. As n increases, P_{ovp} decreases and thus the detection rate also decreases. On the other hand, for the routing protocols where each packet is forwarded in multiple hops, when an attacker sends more attack packets in each contact, it is more likely that one pair of inconsistent packets are forwarded to the same intermediate node and lead to detection.

Fig. 4.23(d) shows the effect of attacker deployment. The detection rate is lower when attackers are selectively deployed to high-connectivity nodes. This is because when attackers are selectively deployed they have more contacts with good nodes. The probability that a good node exchanges its sampled claims to attackers rather than to other good nodes is higher, but attackers do not run detection against each other.

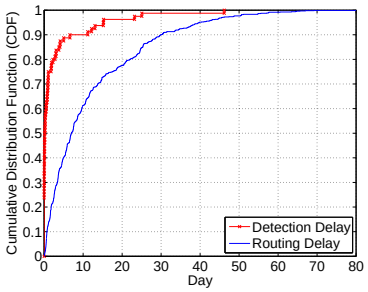

Figure 4.24. The detection delay compared with the routing delay of Propagation.

4.2.7.5 Detection delay

Fig. 4.24 shows the CDF of detection delay when Propagation is used as the routing protocol on the Reality trace. For comparison, the CDF of routing delay (i.e., from the time a packet is generated to the time it is delivered) is also plotted. Here, no lifetime is set for packets. It can be seen that 90% of the attacks can be detected by our scheme within 10 days. On the contrary, within 10 days only 60% of data packets can be delivered by the routing protocol. Hence, the detection delay of our scheme is much lower than the routing delay.

4.2.7.6 Flooded Replicas under Collusion

As mentioned in Sec. 4.2.6.4, colluders can flood a small number of replicas without being detected. To evaluate their effect, we run simulations on the Reality trace when all attackers collude. The simulation settings are the same as in Chapter 4.2.2. We compare our scheme with the case of no defense. As shown in Fig. 4.25, even when 20% of nodes are attackers and collude, our scheme can still limit the percentage of wasted transmissions to 14% in single-copy routing (SimBet) and 6% in multi-copy routing (Spray-and-Focus), which is only 1/7-1/5 of the wasted transmissions when there is no defense.

4.2.7.7 Cost

To evaluate the cost of our scheme in a steady state (i.e., all attackers have been detected), no attackers are deployed in this group of simulations. The Reality trace is used. Packets are generated between the 61^{st} and 120^{th} day of the trace, and statistics are collected from the 91^{th} day. By default, each node generates 2

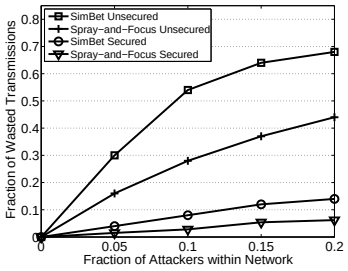

Figure 4.25. The effect of undetected replicas on wasted transmissions when attackers collude to launch replica flood attacks.

packets per day, parameter τ (i.e., the time a claim is stored) is 30 days and K is 10. In a contact, a node may receive some packets but then immediately drop them due to buffer overflow. In such cases, the transmission of the claims attached to these packets is counted into the communication overhead, and the signature generations for these claims are counted into the computation overhead. Since the receiver does not buffer these packets, it does not store these claims or verify their signatures.

We first evaluate the computation cost of our scheme, and Fig. 4.26 shows the results. When Forward is used as the routing protocol (see Fig. 4.26(a)), as the packet generation rate increases, the computation cost also increases since more packets need to be signed and verified. But the cost is still low, less than 20 signature generations and verifications, when each node generates 10 packets per day. Also, it can be seen that there are less signature generations than verifications. This is because in each contact our scheme only signs P-claims for the newly generated packets (which constitute a very small portion of the packets transmitted), and it generates only one signature in total for the T-claims of all forwarded packets due to the use of authentication tree. When Propagation is used as the routing protocol (see Fig. 4.26(b)), similar trends hold. When the packet generation rates crosses 1, the signature verification cost turns to decrease. This is because when the traffic load is high many received packets are dropped due to buffer overflow.

Then we evaluate the communication cost. The communication overhead mainly comes from two sources, the transmission of claims attached to data packets, and the transmission of claims in meta data exchange. The total communication cost and the two components are shown in Fig. 4.27. When K increases from 2

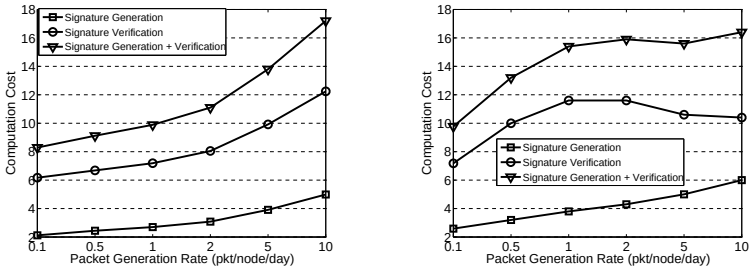

(a) Forward (b) Propagation

Figure 4.26. The computation cost of our scheme.

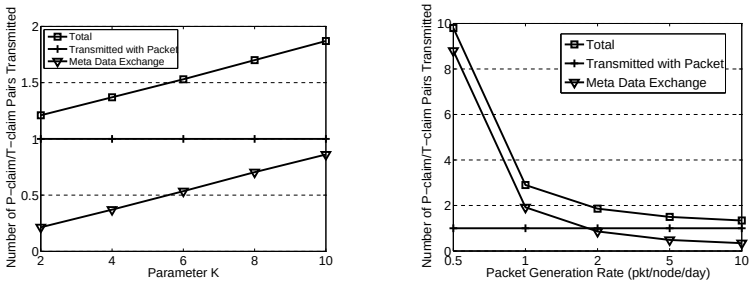

(a) (b)

Figure 4.27. The communication cost of our scheme.

to 10 (see Fig. 4.27(a)), the cost caused by meta data exchange increases linearly since each sampled claim is transmitted more times. The cost caused by the transmission of claims attached to packets is always 1 due to the normalization. In total, less than 2 pairs of P-claim/T-claim are transmitted per transmission of data packet. When the packet generation rate increases (see Fig. 4.27(b)), the total normalized communication cost decreases, because more data packets are transmitted in each contact but the number of claims transmitted for meta data exchange in each contact does not change with the traffic load. When the packet generation rate is larger than 1, the communication cost is smaller than 3. When the packet generation rate is 0.5, the communication cost is higher (i.e., 10). However, at this point the number of packet transmissions is very small, and hence the communication overhead is not an issue. Moreover, since the claims are small in size, they can be attached to and transmitted with data packets and will not incur extra transmissions. Thus, the communication overhead is low.

Finally, we evaluate the storage cost of our scheme against two factors, the time a claim is stored (parameter τ) and the packet generation rate. The results are

Table 4.4. The storage (KB) used for claims and data packets

τ (days)	10	20	30	40	50	-
Claims	67	101	125	139	145	-
Packets	3330	3301	3321	3336	3316	-
Pkt. Generation Rate (pkt/node/day)	0.1	0.5	1	2	5	10
Claims	65	93	113	125	124	114
Packets	334	1572	2596	3321	3716	3808

shown in Table 4.4. We can see that the storage space used for claims is low, only less than 150 kilobytes per node. This is due to the compact structures we use to store P-claims and T-claims. We noticed that the storage cost does not increase after the packet generation rate reaches 2 packets per node per day, because when the traffic load is high many received packets are dropped due to buffer overflow.

4.2.8 Related Work

Our scheme bears some similarity with previous approaches (e.g., [137]) that detect node clone attacks in sensor networks. Both rely on the identification of some kind of inconsistency to detect the attacker. However, their approaches assumes consistent connectivity between nodes which is unavailable in opportunistic mobile networks. Also, they do not handle the long delays of detection.

A few recent works [122, 40, 39, 123, 124] also address security issues in opportunistic mobile networks. Li *et al.* [122] studied the blackhole attack in which malicious nodes forge routing metrics to attract packets and drop all received packets. Their approach uses a primitive called encounter ticket to prove the existence of contacts and prevent the forgery of routing metrics, but encounter ticket cannot be used to address flood attacks. Li and Cao [124] also proposed a distributed scheme to mitigate packet drop attacks, which works no matter if the attackers forge routing metrics or not. Ren *et al.* [123] studied wormhole attacks in opportunistic mobile networks. Chen and Choon [40] proposed a credit-based approach and Shevade *et al.* proposed a gaming-based approach [39] to provide incentives for packet forwarding. Privacy issues have also be addressed [58, 32]. However, these work do not address flood attacks. Other works (e.g., Sprite [96]) deter abuse by correlating the amount of network resources that a node can use with the node's contributions to the network in terms of forwarding. This approach has been pro-

posed for mobile ad hoc networks, but it is still not clear how the approach can be applied to opportunistic mobile networks, where nodes are disconnected most of the time. Zhu *et al.* [125] proposed a batch authentication protocol which verifies multiple packet signatures in an aggregated way. Their work is complementary to ours, and their protocol can be used in our scheme to further reduce the cost of authentication.

Parallel to our work, Natarajan et al. [138] also proposed a scheme to detect resource misuse in opportunistic mobile networks. In their scheme, the gateway of an opportunistic mobile network monitors the activities of nodes and detects an attack if there is deviation from expected behavior. Different from their work, our scheme works in a totally distributed manner and requires no special gateway.

4.2.9 Summary

In this section, we employed rate limiting to mitigate flood attacks in opportunistic mobile networks, and proposed a scheme which exploits *claim-carry-and-check* to probabilistically detect the violation of rate limit in mobile environments. Our scheme uses efficient constructions and sampling techniques to keep the computation, communication and storage cost low. Also, we analyzed the lower bound and upper bound of detection probability. Extensive trace-driven simulations showed that our scheme is effective to detect flood attacks and it achieves such effectiveness in an efficient way. Our scheme works in a distributed manner, not relying on any online central authority or infrastructure, which well fits opportunistic mobile networks. Besides, it can tolerate a small number of attackers to collude.

4.3 Mitigating Routing Misbehavior

4.3.1 Introduction

In opportunistic mobile networks, a node may misbehave by dropping packets even when it has sufficient buffers. Routing misbehavior can be caused by selfish nodes that are unwilling to spend resources such as power and buffer on forwarding packets of others, or caused by malicious nodes that drop packets to launch attacks.

Routing misbehavior will significantly reduce the packet delivery ratio and waste the resources of the mobile nodes that have carried and forwarded the dropped packets. To demonstrate this, we simulate the effects of routing misbehavior in two popular routing algorithms SimBet [35] and Delegation [38] based on the Reality trace [108]. SimBet is a *forwarding-based* algorithm where a packet only has one replica. Delegation is a *replication-based* algorithm where a packet may have multiple replicas. As shown in Figure 4.28, when 30% of the nodes with higher connectivity are misbehaving, SimBet only delivers 3% of the packets whereas Delegation only delivers 40%. Moreover, 95% of the transmissions in SimBet and 80% in Delegation are wasted since the packets are finally dropped by misbehaving nodes. Although Burgess *et al.* [129] studied the effects of packet dropping on packet delivery ratio, they did not consider the wasted transmission (bandwidth) caused by dropping. Therefore, it is extremely important to detect packet dropping and mitigate routing misbehavior in opportunistic mobile networks.

Routing misbehavior has been widely studied in mobile ad hoc networks [45, 46, 47, 48, 49]. These works use neighborhood monitoring [45, 46, 47] or acknowledgement (ACK) [48, 49] to detect packet dropping, and avoid the misbehaving nodes in path selection. However, they do not consider the intermittent connectivity in opportunistic mobile networks and cannot be directly applied to such networks.

In this section, we address routing misbehavior in opportunistic mobile networks by answering two questions: how to detect packet dropping and how to limit the traffic flowing to the misbehaving nodes. We first propose a scheme which detects packet dropping in a distributed manner. In this scheme, a node is required to keep previous signed contact records such as the buffered packets and the packets sent or received, and report them to the next contact node which can detect if the node has dropped packets based on the reported records. Misbehaving nodes may falsify some records to avoid being detected, but this will violate some consistency rules. To detect such inconsistency, a small part of each contact record is disseminated to some selected nodes which can collect appropriate contact records and detect the misbehaving nodes with certain probability. Then we propose a scheme to mitigate routing misbehavior by limiting the number of packets forwarded to the misbehaving nodes.

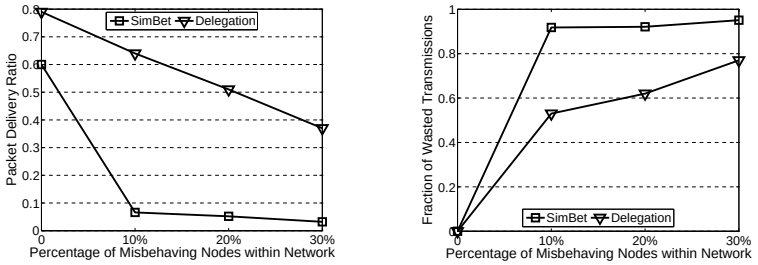

(a) (b)

Figure 4.28. The effects of routing misbehavior when SimBet and Delegation are used as the routing algorithms.

4.3.2 Preliminaries

4.3.2.1 Network and Routing Model

Similar to many other works (*e.g.*, [34]), we assume each node has two separate buffers. One has unlimited space and is used to store its own packets; the other one has limited space and is used to store packets received from other nodes.

We assume the network is loosely synchronized; i.e., any two nodes should be in the same time slot at any time. Since the inter-contact time is usually at the scale of minutes or hours, the time slot can be at the scale of one minute. Thus, such loose time synchronization is not hard to achieve.

4.3.2.2 Security Model

There are two types of nodes: *misbehaving node* and *normal node*. A misbehaving node drops the received packets even if it has available buffers[4], but it does not drop its own packets. It may also drop the control messages of our detection scheme. We assume a small number of misbehaving nodes may collude to avoid being detected, and they may synchronize their actions via out-band communication channels. A normal node may drop packets when its buffer overflows, but it follows our protocol.

In some applications, each packet has a certain lifetime, and then expired packets should be dropped no matter there is buffer space or not. Such dropping can be identified if the expiration time of the packet is signed by the source. Such dropping

[4]In the rest of this section, when we mention "buffer" we mean the buffer that is used to store the packets received from other nodes.

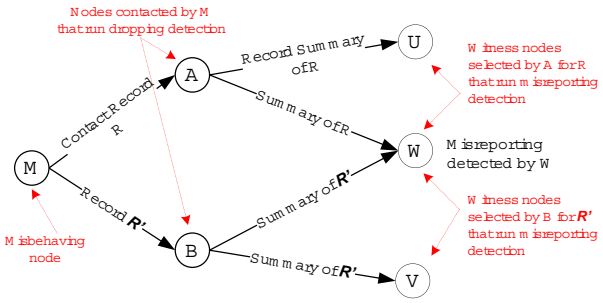

(a) Packet Dropping Detection. Misbehaving node M reports two forged contact records R and R' which are inconsistent.

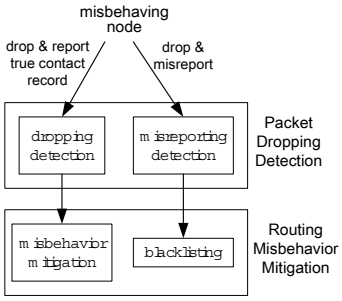

(b) Misbehavior Mitigation

Figure 4.29. An overview of our approach.

is not a misbehavior, and will not be considered in the following presentations.

We assume a public-key authentication service is available. For example, Hierarchical Identity-Based Cryptography [132] has been shown to be practical in opportunistic mobile networks [133]. In identity-based authentication, only the offline trusted Private Key Generator can generate a public/private key pair, so a misbehaving node itself cannot forge node identifiers (*e.g.*, to launch Sybil attacks). Generally speaking, a node's private key is only known by itself; however, colluding nodes may know each other's private key.

4.3.2.3 Overview of Our Approach

Our approach consists of a packet dropping detection scheme and a routing misbehavior mitigation scheme. Fig. 4.29(a) illustrates our basic approach for misbehavior detection. The misbehaving node (M in Fig. 4.29(a)) is required to generate a *contact record* during each contact and report its previous contact records to

the contacted node (A and B in Fig. 4.29(a)). Based on the reported contact records, the contacted node detects if the misbehaving node has dropped packets. The misbehaving node may misreport (i.e., report forged contact records) to hide its misbehavior, but forged records cause inconsistencies which make misreporting detectable. To detect misreporting, the contacted node also randomly selects a certain number of *witness nodes* for the reported records and sends a summary of each reported record to them when it contacts them. The witness node (W in Fig. 4.29(a)) that collects two inconsistent contact records can detect the misreporting node.

Fig. 4.29(b) illustrates our approach for routing misbehavior mitigation. It reduces the data traffic that flows into misbehaving nodes in two ways: 1) If a misbehaving node misreports, it will be blacklisted (after the misreporting is detected) and will not receive any packet from other nodes; 2) if it reports its contact records honestly, its dropping behavior can be monitored by its contacted nodes, and it will receive much less packets from them.

4.3.2.4 Terms and Notations

We use N, N_i, N_j, *etc.* to denote a node, and use M or M' to denote a misbehaving node. We use $SIG\{*\}$ to denote a node's signature over the content in the bracket. $H(*)$ denotes a cryptographically strong hash function (*e.g.*, SHA-1), and "|" denotes the concatenation operation.

4.3.3 Packet Dropping Detection: A Basic Scheme

This section presents our basic packet dropping detection scheme. We first introduce the basic idea and then describe how to detect packet dropping and how to detect misreporting. Collusions will not be considered in this section, and will be addressed in Chapter 4.3.4.

4.3.3.1 Basic Idea

When two nodes contact, they generate a *contact record* which shows when this contact happens, which packets are in their buffers before data exchange, and what packets they send or receive during the data exchange. The record also includes

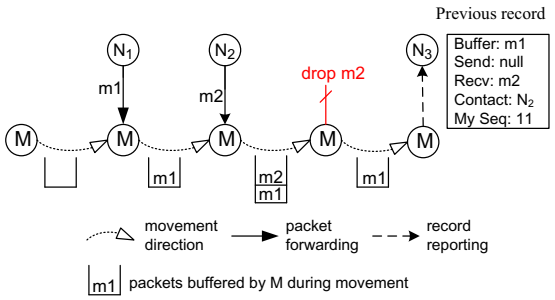

(a) Dropping Detection

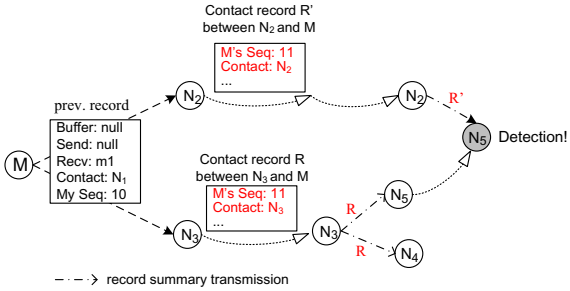

(b) Misreporting Detection

Figure 4.30. Examples of packet dropping detection and misreporting detection. In (b), M reports the same contact record to N_2 and N_3 as its "previous" record, and then it has to assign the same sequence number to the contact with N_2 and N_3, which violates consistency rules.

the unique sequence number that each of them assigns for this contact. The record is signed by both nodes for integrity protection.

A node is required to carry the record of its previous contact, and report the record to its next contacted node, which will detect if it has dropped packets since the previous contact. We illustrate this with an example shown in Fig. 4.30(a). M buffers packet $m1$ before the contact with node N_2 and it receives $m2$ from N_2 in the contact. Such information is included in the contact record that M reports to its next contacted node N_3. From the record N_3 can deduce that M should still buffer $m1$ and $m2$ at the current time. If M has dropped $m2$ after the contact with N_2, N_3 will detect the dropping when it exchanges the buffer state with M.

A misbehaving node may report a false record to hide the dropping from being detected. However, misreporting will result in inconsistent contact records generated by the misbehaving node. To detect misreporting, for each contact record that a normal node generates with (or receives from) other nodes, the normal node

selects w witness nodes and transmits the record summary to them. The summary only includes a part of the record necessary for detecting the inconsistency caused by misreporting. With some probability, the summaries of two inconsistent contact records will reach a common witness node which will detect the misreporting node.

We use the example in Fig. 4.30(b) to show how misreporting causes inconsistency and how it can be detected. After dropping $m2$, M does not report the contact record with N_2 to N_3, but it dishonestly reports the contact record with N_1 as the "previous" record to N_3 as if it did not contact N_2. Based on this record N_3 cannot detect the dropping of $m2$. Since this record is reported to both N_2 and N_3, M has to assign the same sequence number to the contact with N_2 and N_3, which is one plus the sequence number it assigned to the reported "previous" record. Since the same sequence number should not be assigned to two different contacts, the two records that M generates with N_2 and N_3 are inconsistent. Suppose both N_2 and N_3 have selected N_5 as the witness node for their contact record. When N_5 receives the summaries of the two inconsistent records from $N2$ and $N3$, it will detect the misreporting of M.

4.3.3.2 Contact Record and Record Summary

Suppose a contact happens between node N_i and N_j at time t. Without loss of generality, suppose $i < j$. Let BV_i and BV_j denote the vector of packets buffered by N_i and N_j before this contact, respectively. Let RV_i and RV_j denote the identifiers of the packets received by N_i and N_j during this contact, respectively. Then the record of this contact that N_i will store and report is as follows:

$$\begin{aligned} \mathcal{R} &= N_i, sn_i, N_j, sn_j, t, BV_i, RV_i, RV_j, sig_i^1, sig_j^1, sig_i^2, sig_j^2 \\ sig_{i,j}^1 &= SIG_{i,j}\{H(N_i|sn_i|N_j|sn_j|t|BV_i)\} \\ sig_{i,j}^2 &= SIG_{i,j}\{H(N_i|sn_i|N_j|sn_j|t|H(RV_i)|H(RV_j))\} \end{aligned} \tag{4.20}$$

sn_i and sn_j are the sequence numbers assigned by N_i and N_j for this contact, respectively. A node assigns sequence number 1 to its first contact, and increases the number by one after each contact. The sequence number is large enough (*e.g.* 32 bits) so that a node will not use the same number twice. The summary of this

record is:

$$\mathcal{S} = N_i, sn_i, N_j, sn_j, t, H(RV_i), H(RV_j), sig_i^2, sig_j^2 \tag{4.21}$$

The size of record summary is constant, no matter how many packets are buffered before or exchanged during the contact. Note that the record of this contact that N_j will store and report is similar to that by N_i except that BV_i is replaced with BV_j.

If the two nodes contact each other several times without contacting any other node, the transactions in the second and later contacts can be seen as an extension of the transaction of the first contact. Then, only one record is generated in the first contact, and its RV and the appropriate signature components are updated in later contacts.

4.3.3.3 Packet Dropping Detection

In a contact, each of the two contacting nodes reports its previous contact record (see Eq. 4.20) to the other node. In this contact the two nodes also exchange their current vector of buffered packets (as a step of contact record generation). In this way, one node knows the two sets of packets the other node buffers at the beginning of the previous contact and the beginning of the current contact, which are denoted by $\mathbb{S}_{bgn}$ and $\mathbb{S}_{end}$, respectively. It also knows the two sets of packets the other node sends and receives in the previous contact, which are denoted by $\mathbb{S}_{snd}$ and $\mathbb{S}_{rcv}$, respectively. If forwarding-based routing is used, the other node has dropped packets iff:

$$\exists\, m \in \mathbb{S}_{bgn} \cup \mathbb{S}_{rcv}, \quad m \notin \mathbb{S}_{end} \;\; and \;\; m \notin \mathbb{S}_{snd} \tag{4.22}$$

If replication-based routing is used, the other node has dropped packets iff:

$$\exists\, m \in \mathbb{S}_{bgn} \cup \mathbb{S}_{rcv}, \quad m \notin \mathbb{S}_{end} \tag{4.23}$$

A misbehaving node may drop a packet but keep the packet ID, pretending that it still buffers the packet. However, the next contacted node may be a better relay for the dropped packet according to the routing protocol, which can be determined when the two exchange the destination (included in packet ID) of the buffered

packets. In this case, the misbehaving node should forward the packet to the next contacted node, but it cannot since it has dropped the packet. Thus, the next contacted node can easily detect this misbehavior and will not forward packets to this misbehaving node.

4.3.3.4 Misreporting Detection

Suppose a misbehaving node M has dropped some packets. To hide the dropping from being detected by the next contacted node, M will not report the true record of the previous contact. However, when there is no collusion, M cannot modify the true record since it is signed by the previous contacted node. Also, M cannot forge a contact record because it does not know the private key of any other node. Thus, the only misreporting it can perform is to replay an old record generated before the previous contact as illustrated in Fig. 4.30(b). This misreporting is referred to as *replay-record*. Note that other types of misreporting are possible when collusions exist, and we will address them in Chapter 4.3.4.

Consistency rules There exist two simple rules which are obeyed by normal nodes but violated by misreporting nodes:

- Rule 1: Use a unique sequence number in each contact.
- Rule 2: For two records signed by the same node, the record with a smaller contact time also has a smaller sequence number.

With replay-record, the misreporting node violates Rule 1 and/or Rule 2. In the example shown in Fig. 4.30(b), M replays the record that it has reported to N_2 when it contacts N_3, and it has to assign the same sequence number (i.e., 11) for the contacts with N_2 and N_3, which means Rule 1 is violated. If M replays an earlier record, the sequence number it assigns for the contact with N_3 will be smaller than the number it assigns for the contact with N_2, which means Rule 2 is violated. For a special case where the misbehaving node does not report any previous record pretending that it has not had any contact, every time it does so, it has to claim that the current contact is its first contact and assign 1 as its sequence number. Then, Rule 1 is violated.

Detection To detect the inconsistency caused by misreporting, for each contact record generated and received in a contact, a node selects w random nodes as the

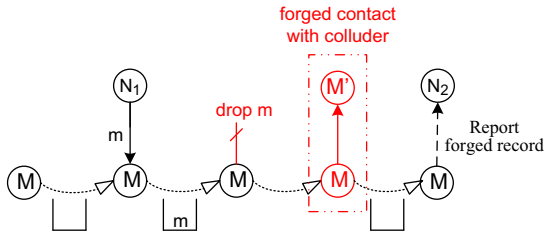

Figure 4.31. Two colluding nodes M and M' try to hide the dropping of packet m by forging a contact (via the out-band channel) and reporting the forged contact record. The forged record may show that M has not received m, M has forwarded m to M', *etc.*

witness nodes of this record, and transmits the summary of this record to them when it contacts them. It selects the witness nodes from the nodes that it has directly contacted. Here, the nodes contacted a long time ago are not used since they may have left the network.

In this manner, each node can collect some record summaries for which it is a witness. When it receives a new summary, it checks the summary against the already collected summaries signed by the same node to see if the signer has violated any of the two consistency rules. If a violation is detected, it further verifies the signatures included in the inconsistent summaries. If the signature verification succeeds, the signer is detected as misreporting.

Alarm After detection, the witness node floods an alarm (via Epidemic routing [134]) to all other nodes. The alarm includes the two inconsistent summaries. When a node receives this alarm it verifies the inconsistency between the included summaries and the signature of the summaries. If the verification succeeds, this node adds the appropriate misreporting node into a blacklist and will not send any packets to it. If the verification fails, the alarm is discarded and will not be further propagated. A misreporting node will be kept in the blacklist for a certain time before being deleted.

4.3.4 Dealing with Collusions

This section extends the basic scheme presented in Chapter 4.3.3 to address the collusions among misbehaving nodes.

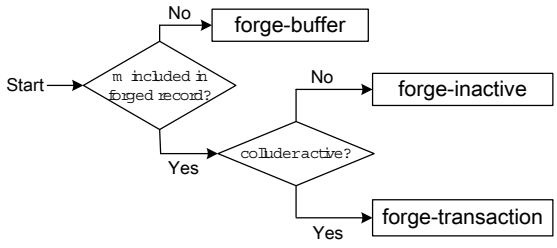

Figure 4.32. A decision-tree based exploration of misreporting

4.3.4.1 Misreporting with Collusion

Suppose a misbehaving node M drops a packet. If M reports the true record of its previous contact to the next contacted (normal) node, the dropping can be detected. To hide the dropping, M can forge a contact with its colluder M' after dropping the packet, and report the falsified contact record to the next contacted node, as illustrated in Fig. 4.31.

The two colluding nodes can hide the dropping in several ways. We use a decision tree to describe the possible collusions, as shown in Fig. 4.32. The following explanations are based on the the example shown in Fig. 4.31.

M and M' first need to decide if the forged record lists the dropped packet m as being buffered by M. If not, M will tell N_2 that it did not receive m, and N_2 cannot detect the dropping of m. This misreporting behavior is referred to as *forge-buffer*.

If the forged record lists m as being buffered by M, then to hide the dropping, the forged record should also show that M has forwarded m to M' in a forged contact. M is safe to report this record to N_2 without being detected, but if M' reports this record to its next contacted (normal) node, M' will be detected as having dropped m. Thus, M' cannot report such a record.

There are two choices for M' to avoid being detected. 1) M' does not report any record to non-colluding nodes in the future. Then, it has to keep inactive, e.g., turning off its wireless transmitter. This misreporting behavior is referred to as *forge-inactive*. 2) M' keeps active and it reports a record of the forged contact to its next contacted node, but the record reported by M' is different from the one reported by M. This means that M and M' generate two different records for the same forged contact. This misreporting behavior is referred to as *forge-transaction*.

In forge-transaction, two different records are generated for the same forged contact. Thus, forge-transaction violates Rule 1 and can be detected by the basic scheme presented in Chapter 4.3.3. In the following, we address other collusions.

4.3.4.2 Forge-Buffer

Forge-buffer can hide packet dropping because the normal nodes contacted by the misbehaving node and its colluder cannot see a long-enough contact history of them. To address this problem, the basic scheme is extended such that each node is required to report more than one previous record in its contact. The number of records the node needs to report is determined by its current *report window*.

Let r ($r \geq 2$) denote the number of colluding nodes. The report window of a node includes the minimum number of its most recent contacts so that it includes at least r different nodes. As shown in Fig. 4.33 ($r = 2$), when contacting N_2, M's report window includes the contact with N_0 and the contact with N_1 since these two contacts are with two different nodes. However, when contacting N_4, M's report window includes the contact with N_2 and the two contacts with N_3. Due to the opportunistic nature of contacts, the average size of the report window is usually close to r. For the Reality trace [108], the average window size is 2.34 when $r = 2$.

During a contact, the two contacting nodes exchange records of the contacts in their report window. In this way, a node knows more history information about the packets that the contacting node buffers, sends and receives. Then it can detect if the other node has dropped packets during the report window similar to that in the basic scheme (see Chapter 4.3.3.3). Since the contacts in a report window happen successively, a node does not need to report the vector of its buffered packets in the intermediate contacts of the window, which can reduce the communication cost.

In forge-buffer, since the misreporting node is required to report the recent records with at least r distinct nodes but it only has $r - 1$ colluders, the record of its previous real contact has to be reported. Then it is trivial for the contacted node to detect the packet dropping, and forge-buffer fails.

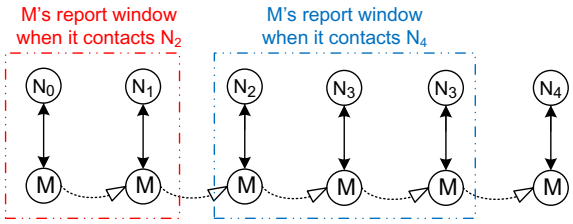

Figure 4.33. Examples of report window when $r = 2$. A node is required to report the records of the contacts in its current report window to the next contacted node.

4.3.4.3 Forge-Inactive

To address forge-inactive, a forwarding rule is added which requires that packets can only be forwarded to an *active node*, which is defined as the node that contacts at least r different nodes within the recent time interval T_{active}[5].

To support the forwarding rule, each node maintains an *activeness table* which includes the active nodes it knows from local knowledge. Each table entry has three elements, the identifier of an active node, the most recent time this active node has proved to be active, and the activeness proof. The activeness proof contains part of the active node's most recent r contact records with r different nodes. An entry expires when T_{active} has passed since the time given by the second element. Then the entry is deleted and the active node is tagged as inactive.

The activeness of a node can be easily proved by the recent contact records it reports to other nodes. During a contact one node is supposed to be able to obtain the contacted node's most recent contact records with r nodes. Based on these records, it updates its activeness table entry for the contacted node. If it has some packets to the contacted node, it forwards them only when the contacted node is active. Even if the contacted node is inactive, the two nodes still generate a record for this contact although the packet is not forwarded. This will help newly joined nodes quickly accumulate contact records and quickly become a packet forwarder.

The two nodes also check if anyone has broken the rule and forwarded packets to inactive nodes. Suppose from the reported contact records N_i knows that N_j has forwarded packets to node N_k. If N_k is not active from the local knowledge of N_i, then N_j should show N_i the activeness proof of N_k. If N_j cannot provide a

[5]The packets destined to a node which can only contact $r-1$ other nodes can still be delivered to it.

valid proof, N_i knows that N_j has invalidly forwarded packets to an inactive node, and it adds N_j into the blacklist.

In forge-inactive, M' becomes inactive after the forged contact. Although M can still "forward" packets to M' within the next T_{active}, it cannot continue to do so after T_{active} due to the forwarding rule. Then forge-inactive becomes useless to M.

The forwarding rule has a side effect: packets will not be forwarded to the nodes which are not able to contact more than $r-1$ other nodes. Since these nodes' forwarding capability cannot be exploited, packet delivery ratio may be reduced. However, when r is small, these nodes have limited forwarding capability and probably there are not too many of them. Thus, the side effect on packet delivery ratio should be marginal.

4.3.4.4 Record and Summary Deletion

A node deletes the record that it generates in a contact after the contact has been purged out of its report window, probably after a few contacts. It deletes the records received from the contacted node right after this contact, since these received records are only used to check if the contacted node has dropped packets recently.

The witness node should keep its collected record summaries for a long enough time to detect misreporting. For simplicity, our scheme uses a time-to-live parameter T_{delete}, which denotes the time for the collected summaries to be stored before being deleted.

In forge-inactive, the colluder M' may become active again after being inactive for some time, and then perform forge-transaction. If the inactive time is longer than T_{delete}, this misreporting may not be detected, since the record reported by M which is inconsistent with the record reported by M' may have been deleted by the witness nodes. Considering this problem, a witness node can keep the most recent r record summaries generated by each inactive node even if these summaries have expired. The witness nodes that receive the summary of the record reported by M will keep the summary and (with certain probability) detect the misreporting when M' becomes active again.

4.3.4.5 Discussion

After M tells the next contacted node that it has forwarded the dropped packet m to the colluder M', M' may tell its own next contacted node that it has forwarded m to M or another colluder M''. This is equivalent to the case that M' has dropped m and it wants to hide the dropping with the help of M or M''. Such fake forwarding can continue among the colluding nodes.

When only two nodes collude ($r = 2$), this phenomenon can be easily detected with report window. Since the forged contacts between the two colluding nodes are within their report window, their next contacted node can detect that m is forwarded back-and-forth between the two colluding nodes.

However, report window may not work when three or more nodes collude because a report window may not include all the colluding nodes in the chain of fake forwarding. A more generic solution is needed. Since the number of colluders is limited and small, the chain of fake forwarding cannot extend forever and it will loop back. In the above example, suppose there are only three colluders. Then M'' will have to claim that it has forwarded m back to M or M'. This means that at least one colluding node in the chain will "receive" m twice or more. However, in most routing protocols a normal node will not receive the same packet more than once. Therefore, repeated receiving of the same packet can be used to detect such fake forwarding. From the reported contact records, nodes can monitor each other on the packets they have received, and raise an alarm when repeated receiving of the same packet is detected.

4.3.5 Analysis of Misreporting Detection

In our scheme, a misreporting node can be detected when a witness node receives two inconsistent summaries generated by this misreporting node. Due to the opportunistic nature of contacts, the detection is also opportunistic. In this section, we analyze the probability of detection and the detection delay. We also analyze the cost of the detection scheme.

Models and Notations For simplicity, we base our analysis on the mobility models such as Random Waypoint and Random Direction where the contacts between node pairs can be modeled as i.i.d. Poisson processes [135]. Then a node

will encounter any other node in its next contact with the same probability. Poisson contact model has been experimentally validated by [139, 112, 140] to fit well to realistic traces. In the analysis, we assume a node can disseminate a record summary to its selected witness nodes, and the witness nodes store the summary for a long enough time.

Let n denote the number of nodes in the network, and q denote the proportion of misbehaving nodes. Without loss of generality, the following analysis considers forge-transaction in which misreporting node M and its colluder M' generate two inconsistent contact records $\mathcal{R}$ and $\mathcal{R}'$. M reports $\mathcal{R}$ to its next two contacted nodes which constitute a set $\mathbb{S}$, and M' reports $\mathcal{R}'$ to its next two contacted nodes which constitute a set $\mathbb{S}'$.

For convenience, we define function $P_o(x, y)$ as the probability that two randomly and independently selected sets of nodes with size x and y ($x, y < n$) have at least one common node. It is trivial to get $P_o(x, y) = 1 - \binom{n-x}{y} / \binom{n}{y}$.

Detection Probability We first analyze the probability P_d that a single misreporting instance can be detected. If $\mathbb{S}$ overlaps with $\mathbb{S}'$ and the overlapping node is a normal node, the attack can be detected by the overlapping node. This probability is given by $P_o(2, 2) = \frac{4n-6}{n(n-1)}$. Since n is usually large, it is negligible. In the following, we consider the case where $\mathbb{S}$ and $\mathbb{S}'$ do not overlap.

The detection succeeds when: (i) there is at least one normal node in $\mathbb{S}$ and $\mathbb{S}'$; (ii) the normal nodes in $\mathbb{S}$ and those in $\mathbb{S}'$ select one or more common witness nodes for the two records; and (iii) at least one common witness is a normal node. Obviously, the three conditions hold independently. The probability that the first two conditions hold depends on how many nodes in $\mathbb{S}$ and $\mathbb{S}'$ are normal. In the case that both the two nodes in $\mathbb{S}$ ($\mathbb{S}'$) are normal, the probability that they select a common witness for $\mathcal{R}$ ($\mathcal{R}'$) is given by $P_o(w, w)$, which is small since $w \ll n$. For simplicity, in this case we assume their selected witness nodes do not overlap, i.e., they select $2w$ witness nodes for $\mathcal{R}$ ($\mathcal{R}'$). Then the probability that the first two conditions hold is given by:

$$P_o(w, w) \cdot [2q(1-q)]^2 + P_o(w, 2w) \cdot [4q(1-q)(1-q)^2] + P_o(2w, 2w) \cdot (1-q)^4$$

Since the third condition holds with probability not smaller than $1-q$, the detection probability has a lower bound:

$$\begin{aligned} P_d = \; & P_o(w,w) \cdot 4q^2(1-q)^3 \\ & + P_o(w,2w) \cdot 4q(1-q)^4 + P_o(2w,2w) \cdot (1-q)^5 \end{aligned}$$

Numerical results on P_d are shown in Fig. 4.34(a). P_d increases as the number of witness nodes w increases, and it is higher than 0.5 even when w is smaller than the square root of n.

If a high P_d is required, w is not very small. However, in reality, it may not be necessary to detect each misreporting instance (which requires a high P_d). A misbehaving node needs to drop packets many times to make a reasonable impact and misreport many times to hide its misbehavior. A good-enough security can be provided if the misbehaving node can be detected with a high probability after a reasonably small number of misreporting instances. Suppose a misbehaving node launches k misreporting instances independently. Then the node will be detected with probability $P' = 1 - (1 - P_d)^k$, which is much higher than P_d when $k > 1$. Given a certain required probability P' (*e.g.*, 0.95), we can find the minimum w with which the misbehaving node can be detected with probability not less than P' after it misreports for k times. Fig. 4.34(b) shows the minimum w required to detect misbehaving nodes with probability not less than 0.95 when different numbers of misreporting instance k can be tolerated. Basically, w will be significantly reduced if k increases.

Detection Delay Detection delay (T_d) is defined as the elapsed time from when $\mathcal{R}$ and $\mathcal{R}'$ have been reported to the nodes in set $\mathbb{S}$ and $\mathbb{S}'$ respectively, to the time when the misreporting instance is detected by a witness node. Detection delay is meaningful only when misreporting can be detected.

If a misreporting is detected, there is at least one witness node which receives the summary of both $\mathcal{R}$ and $\mathcal{R}'$. When there is only one such witness node, the detection delay is the time needed for the summary of $\mathcal{R}$ and $\mathcal{R}'$ to be transmitted to *this* witness node; when there are multiple witness nodes, detection delay is the time needed for the summary of $\mathcal{R}$ and $\mathcal{R}'$ to be transmitted to *any* of these witness nodes. Since the contact patterns between different node pairs are i.i.d.,

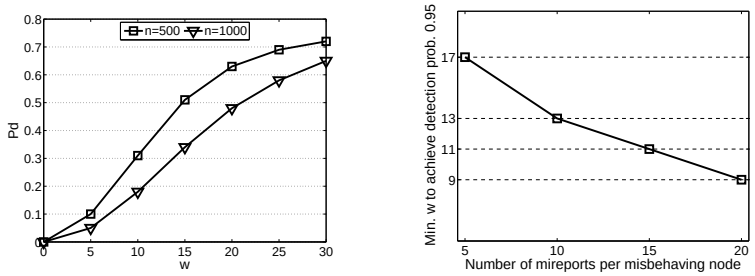

(a) (b)

Figure 4.34. Numerical results on misreporting detection where 20% of nodes are misbehaving (i.e., $q = 0.2$). (a) Detection probability when each misbehaving node misreports once. (b) The minimum w required to detect each misreporting node with probability not less than 0.95 when $n = 1000$.

the expected delay is longer in the former case. Let T_d' denote the detection delay in that case. We derive the expectation of T_d' to obtain an upper bound of the expected T_d.

Let λ denote the Poisson contact rate. Then the cumulative distribution function (CDF) of inter-contact time between any node pair is $F_c(t) = 1 - \exp(-\lambda t)$. Since the witness node receives the summary of $\mathcal{R}$ and $\mathcal{R}'$ independently, the CDF of T_d' is:

$$F_d(t) = (1 - \exp(-\lambda t))^2,$$

and the probability density function (PDF) of T_d' is:

$$f_d(t) = F_d'(t) = 2\lambda(1 - \exp(-\lambda t)) \exp(-\lambda t).$$

Then the expectation of T_d' is:

$$E(T_d') = \int_0^{+\infty} 2\lambda t(1 - \exp(-\lambda t)) \exp(-\lambda t) dt = \frac{3}{2\lambda}$$

Now we have an upper bound for the expected detection delay:

$$E(T_d) \leq \frac{3}{2\lambda}$$

False Positive Our misreporting detection scheme does not have false positive when detecting replay-record and forge-transaction. This is because normal nodes

do not violate any of the consistency rules.

An attacker may spoof another normal node and insert new inconsistent contact records or record summaries on behalf the normal node, so that when the witness receives the inconsistent record summaries it detects the normal node as a misreporting attacker. However, in our scheme both contact record and record summary are protected by the signature of the node that generates them. Since the attacker do not know the private key of any normal node (as our assumption), it cannot forge a valid contact record or record summary.

Cost We analyze the computation cost per contact in terms of signature generations and verifications. In each contact, the two nodes invocate six signature generations and verifications to generate the contact record. The reported records require $8r$ signature verifications in total (assuming one report window contains r contacts). To enforce the forwarding rule each node in the worst case verifies $2r$ signatures (i.e., $4r$ in total). Also, the summary of each contact is disseminated to $4w$ witness nodes. Note that the witness nodes verify the signatures of the summary only when some violation is detected. If there is no misreporting node, there is no signature verification. To sum up, each contact requires 6 signature generations and at most $12r+6$ signature verifications. This cost is low considering that signature verification is usually much faster than signature generation.

For the communication cost, in each contact, the buffer states of the two nodes are exchanged, a few contact records are reported, and a few activeness proofs may be transmitted. Each of the contacting nodes transmits the two reported summaries for at most w times. Since only meta data is transmitted and for very limited time, the communication overhead is low. The storage cost mainly comes from the record summaries. Since each summary only has around 100 bytes (see the setting in Chapter 4.3.7 and Equation 4.21) and will be deleted later, the storage cost is also low.

4.3.6 Routing Misbehavior Mitigation

To mitigate routing misbehavior, we try to reduce the number of packets sent to the misbehaving nodes. If a node is detected to be misreporting, it should be blacklisted and should not receive packets from others. However, if a misbehaving

Algorithm 9 : FP Update (run by N_i when it contacts N_j)

Require: The gauge list GL that N_i maintains form N_j
Require: The r nodes N_x ($1 \leq x \leq r$) contacted by N_j in its report window
Require: *drop*=FALSE, *receive*=FALSE, *forward*=FALSE
Require: $0 < \delta < 1$, $0 \leq \rho < 1$
1: Delete the two oldest elements of GL
2: Insert N_x ($1 \leq x \leq r$) into GL
3: **if** N_x is the most-frequent element of GL but not N_i itself **then**
4: Tag N_x as *special*
5: **else**
6: Tag N_x as *plain*
7: **end if**
8: **if** N_j has dropped packets in the report window **then**
9: *drop*=TRUE
10: **end if**
11: **if** N_j has received packets from a *plain* node (N_x) **then**
12: *receive*=TRUE
13: **end if**
14: **if** N_j has forwarded packets to a *plain* node (N_x) **then**
15: *forward*=TRUE
16: **end if**
17: **if** *drop*==TRUE **then**
18: $\gamma = \gamma \cdot \rho$
19: **else if** *receive*==TRUE **or** *forward*==TRUE **then**
20: $\gamma = \min\{\gamma + \delta, 1\}$
21: **else**
22: $\gamma = \max\{\gamma - \delta, 0\}$
23: **end if**

node does not misreport, we cannot simply blacklist it because it is dropping packets, since a normal node may also drop packets due to buffer overflow. In the following we focus on how to mitigate routing misbehavior without affecting normal nodes too much when misbehaving nodes do not misreport.

Our basic idea is to maintain a metric *Forwarding Probability (FP)* for each node based on if the node has dropped, received and forwarded packets in recent contacts, which can be derived from its reported contact records. The nodes that frequently drop packets but seldom forward packets will have a small FP and will receive few packets from others. Our scheme borrows ideas from congestion control to update FP. More specifically, it combines additive increase, additive decrease and multiplicative decrease to differentiate misbehaving nodes from normal nodes.

4.3.6.1 FP Maintenance

Each node maintains a FP for every other node it has contacted based on the local knowledge obtained from previous contacts, and updates the FP with new contacts. Let γ $(0 \leq \gamma \leq 1)$ denote the FP that node N_i maintains for N_j. When N_i contacts N_j, it obtains the recent contact records of N_j which are used to derive if N_j has dropped, received and forwarded packets in the report window. If N_j has dropped packets, N_i decreases γ by a multiplicative factor ρ $(0 \leq \rho < 1)$. If N_j has not dropped packets, there will be two subcases. If N_j has received packets or forwarded packets out, N_i knows that N_j has contributed its buffer or bandwidth to the network, and it increases γ by an additive amount δ $(0 < \delta < 1)$. If N_j has not received or forwarded any packets, it can either be a misbehaving node or a normal node. For security concerns, N_i conservatively takes N_j as misbehaving, and decreases γ by δ.

A misbehaving node may "forward" packets to or "receive" packets from its colluder via the out-band channel, to deceive its contacted nodes to increase the FP for it. To address this problem, node N_i keeps a *gauge list* for every other node N_j it has contacted, which includes the nodes contacted by N_j that N_i observes in the recent c contacts with N_j. If N_j frequently launches the above collusion behavior, its colluder will appear frequently in the gauge list. When N_i observes that N_j has forwarded (received) packets in the report window, N_i checks if the packets are forwarded to (received from) the top $r-1$ nodes which appear most frequently in the gauge list. If this is true, it is very likely that N_j has "forwarded" packets to ("received" packets from) its colluder, and N_i will not increase the FP for N_j. Here, r is the number of colluders. When r is small, we use $c = 10$.

The initial value of FP is recommended to be set smaller than 1, which means a node from the start does not fully trust other nodes but it gradually builds the trust on them. We set the initial FP as 0.6. Experimentally, we found out that a lower ρ which means a fast decrement, coupled with a low δ which means a slow increment can result in good performances. We use $\rho = 0.1$ and $\delta = 0.1$. The Pseudo-code of FP update is shown in Alg. 9.

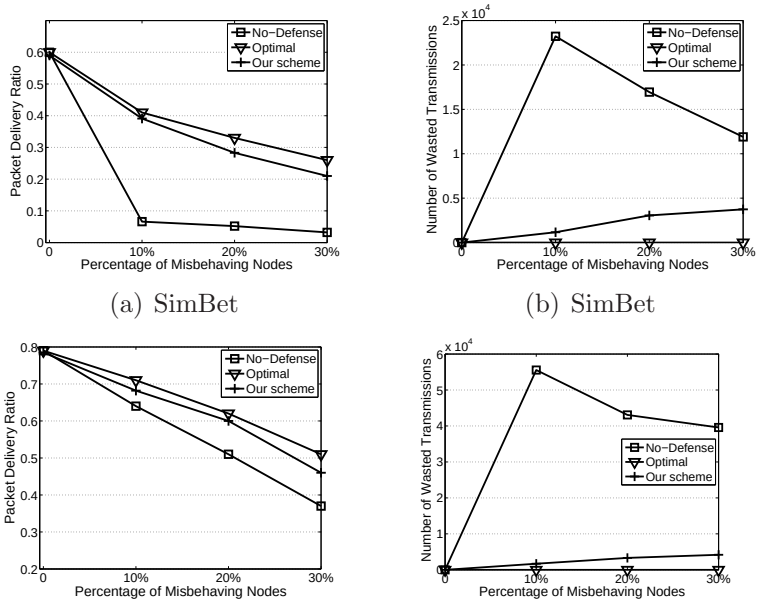

(a) SimBet (b) SimBet

(c) Delegation (d) Delegation

Figure 4.35. Comparison results when misbehaving nodes are selectively deployed to high-connectivity nodes which drop all received packets. The Reality trace is used.

4.3.6.2 Dealing with Packet Dropping

Suppose node N_i has selected a set of packets (according to the routing algorithm) to forward to its contacted node N_j. Let $\mathbb{S}_{opt}$ denote this set of packets. Then N_i forwards them with the following policy:

$$\text{For } m \in \mathbb{S}_{opt}, \quad \text{forward } m \text{ with probability } \gamma$$

Our scheme can effectively mitigate routing misbehavior, since if a node is misbehaving and frequently drops packets, it will be assigned a low FP by its contacted nodes and receive few packets from them. Our scheme has the minimal (or no) effect on the normal nodes that seldom or never drop packets. For the "hot spot" normal nodes that receive many packets from others and frequently drop them due to buffer overflow, our scheme will reduce the amount of packets forwarded to them, and thus relieve the congestion at these nodes.

4.3.7 Performance Evaluations

4.3.7.1 Experiment Setup

We evaluate our solutions both on a synthetic trace generated by the Random Waypoint (RWP) model [135] and on the MIT Reality trace [108] collected from the real world.

In the synthetic trace, 97 nodes move in a 500×500 area with the RWP model. The moving speed is randomly selected from $[1, 1.6]$ to simulate the speed of walking, and the transmission range is 10m to simulate that of Bluetooth. Each simulation lasts 5×10^5 time units.

In the Reality trace, 97 phones are carried by students and staff at MIT over ten months. These phones run Bluetooth device discovery every five minutes and log about 110 thousand contacts with each other. Each logged contact includes the two contact parties, the start-time, and the contact duration. We use these contacts to generate trace-driven simulations.

In our simulations, misbehaving nodes are either *randomly deployed* or *selectively deployed*. In the latter case, they are the high-connectivity nodes which have the most frequent contacts with others. Misbehaving nodes drop all or part of the packets they receive from others. In default, each normal node generates one packet (with size 10KB) every day to a random destination. A misbehaving node does not generate packets as done in [129] and [122]. Each node has buffer size 5MB and bandwidth 2Mbps. Results are averaged over 10 runs with different random seeds.

4.3.7.2 Routing Algorithms

SimBet [35]: a forwarding-based routing algorithm. It calculates a metric using two social measures (similarity and betweenness), and a packet is forwarded to a node if that node has higher metric than the current one.

Delegation [38]: a replication-based routing algorithm, where the receiving node replicates the packet to a neighbor if the neighbor has the highest utility it has seen. We use the contact frequency with the destination as the utility metric.

4.3.7.3 Metrics

- **Packet delivery ratio** The percentage of packets delivered to their destinations out of all generated packets.
- **Number of wasted transmissions** In forwarding-based routing, a transmission is wasted if the transmitted packet is dropped by misbehaving nodes before reaching the destination; in replication-based routing, a transmission is wasted if it directly transmits a packet to a misbehaving node that drops the packet. Here, we only count the wasted packets dropped by routing misbehavior.
- **Detection rate** The percentage of misreporting nodes detected by normal nodes.
- **Detection delay** The time needed for misreporting to be detected.
- **Bytes transmitted per contact** The number of bytes transmitted in a contact for control.
- **Bytes stored per node** The number of bytes stored at a node for control.

4.3.7.4 Experimental Results

We compare our scheme to two solutions: one is called *No-Defense*, which does not deal with routing misbehavior; the other one is the *optimal* scheme, which assumes that all misbehaving nodes are known and no packet will be forwarded to them.

Routing Misbehavior Mitigation We first evaluate the case where misbehaving nodes drop all received packets. Fig. 4.35 shows the comparison results on the Reality trace. Generally speaking, our scheme performs much better than No-Defense. For SimBet where the routing performance is the major concern, our scheme is close to the optimal in terms of packet delivery ratio; for Delegation where the reduction of wasted transmission is the major concern, our scheme is close to the optimal in terms of wasted transmissions.

When SimBet is used as the routing algorithm, as shown in Fig. 4.35(a), the packet delivery ratio of all three schemes decreases as the percentage of misbehaving nodes increases, because fewer nodes can be used for packet forwarding.

However, our scheme still delivers much more packets than No-Defense, since it can effectively limit the number of packets forwarded to misbehaving nodes. For similar reasons, our scheme has a much lower number of wasted transmissions than No-Defense, as shown in Fig. 4.35(b). In No-Defense, the number of wasted transmissions first increases and then decreases as the percentage of misbehaving nodes increases. This is because with more misbehaving nodes, more packets are dropped but the average number of hops traversed by each dropped packet is smaller. As a result, the maximum is reached at some middle point.

When Delegation is used as the routing algorithm, again, our scheme delivers more packets than No-Defense. As shown in Fig. 4.35(c), when 30% of nodes are misbehaving, our scheme delivers 46% of packets which is 24% higher than that of No-Defense. No-Defense performs worse due to the following reason. In Delegation, although replicating a packet to a misbehaving node does not decrease the probability of other replicas carried by normal nodes to reach the destination, it can reduce the probability of the packet to be further replicated. As a result, fewer replicas are created and the overall probability of reaching the destination is reduced. For the number of wasted transmissions as shown Fig. 4.35(d), our scheme performs much better than No-Defense.

Then we evaluate the case where misbehaving nodes only drop part of the received packets. Figure 4.36 shows the comparison results when SimBet is used as the routing algorithm on the Reality trace. When misbehaving nodes only drop part of the received packets, *optimal* does not necessarily perform the best since some packets can be delivered by misbehaving nodes. Thus, *optimal* is not compared here. As shown in Figure 4.36(a), the packet delivery ratio of No-Defense decreases from 59% to 22% as the percentage of received packets that a misbehaving node drops increases from 0% to 100%, because more packets are dropped. The packet delivery ratio of our scheme is much higher than that of No-Defense. For example, when misbehaving nodes drop 60% of the received packets, our scheme delivers 50% of the generated packets, and it outperforms No-Defense by 80%. This shows that our scheme can still effectively limit the number of packets forwarded to misbehaving nodes. For the number of wasted transmissions as shown in Figure 4.36(b), our scheme performs much better than No-Defense.

Misreporting Detection In this group of simulations 10 pairs of misbehaving

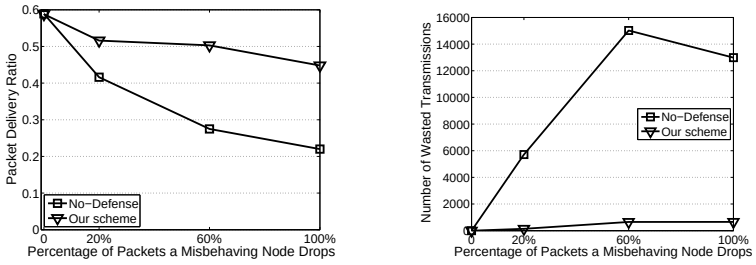

(a) (b)

Figure 4.36. Comparison results when misbehaving nodes are randomly deployed and they only drop part of the received packets. The Reality trace is used, and the fraction of misbehaving nodes is fixed at 30%.

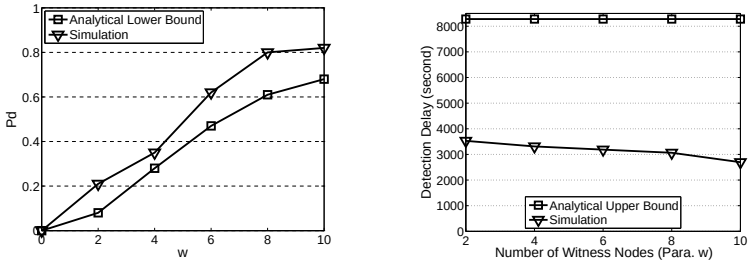

(a) Detection Probability (b) Detection Delay

Figure 4.37. Comparison of analysis and simulation results on the detection probability and detection delay of a single misreporting instance. The synthetic trace is used.

nodes (i.e., 20 in total) launch forge-transaction independently.

First of all, we verify our analysis results on the detection probability and detection delay of a single misreporting instance (i.e., P_d and T_d in Sec. 4.3.5). The synthetic trace is used since it is accordant to the mobility assumption in Sec. 4.3.5. In each run, 200 misreporting events are generated and detected independently. As shown in Fig. 4.37, the detection probability in the simulations is higher than the analytical lower bound, but the difference is small which means the analytical result is a good approximation. The detection delay in the simulations is lower than the analytical upper bound[6].

Then we evaluate the detection rate of our scheme on the Reality trace. As shown in Fig. 4.38(a), the detection rate increases as the number of witness nodes for each record summary increases. When misbehaving nodes are randomly de-

[6]In Random Waypoint model, $\lambda \approx \frac{8\omega r v}{\pi S}$ [135], where $\omega \approx 1.3683$, r is the transmission range of node, v is the moving speed of node (we use the average moving speed 1.3), and S is the size of the simulation area.

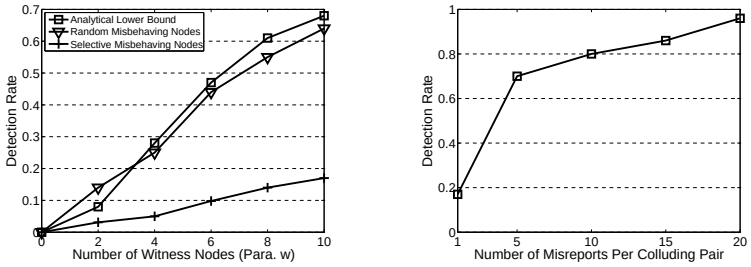

(a) Each collusion pair misreports once

(b) Parameter $w = 10$

Figure 4.38. The detection rate of our scheme in the Reality trace.

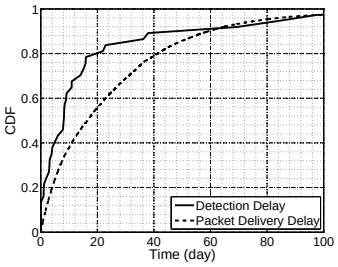

Figure 4.39. The detection delay compared with the packet delivery delay.

ployed, the detection rate is close to the analytical result, which implies that the set of witness nodes randomly selected from a node's local view can be roughly seen as a random subset of the global node set. However, when misbehaving nodes are selectively deployed, the detection rate is much lower since misbehaving nodes contact normal nodes less frequently and a forged record has less chances to be disseminated by a normal node. Despite this, our scheme can still effectively detect the selectively deployed misbehaving nodes when they launch more misreporting instances. As shown in Fig. 4.38(b), when each colluding pair misreports 20 times, 96% of them are detected.

Next we evaluate the detection delay of our scheme on the Reality trace. To better evaluate the delay caused by node mobility, we set T_{delete} as infinity in this group of simulations. Fig. 4.39 shows the CDF of detection delay compared with packet delivery delay when Delegation is used in the Reality trace. It shows that 80% of misreporting instances are detected within 20 days, but it needs 40 days to deliver 80% of the packets. Thus, the detection delay is much shorter than the packet delivery delay.

Cost The size of record and summary is set as follows: node ID, sequence number

Table 4.5. The average communication overhead per contact

w	2	4	6	8	10
Communication (KB)	10.3	10.5	10.8	11.3	11.5
Pkt. Generation Rate (pkt/node/day)	0.5	1	2	4	8
Communication (KB)	6.7	10.5	14.7	20.6	27.5

Table 4.6. The average storage overhead per node

w	2	4	6	8	10
Storage (KB)	47	71	89	108	127
T_{delete} (days)	20	30	40	50	60
Storage (KB)	45	71	92	126	170
Pkt. Generation Rate (pkt/node/day)	0.5	1	2	4	8
Storage (KB)	70	71	72	74	79

and timestamp has 4B each; a hash has 16B; a signature has 40B [141]. In default $w = 4$ and $T_{delete} = 30$ days. Delegation is used and all nodes are normal.

The communication cost of our scheme is given in Table 4.5. We can see that the communication overhead increases with the parameter w, but very slowly. This is because w only affects how many times a record summary is transmitted. Since only one record summary is generated per contact, the transmission of summaries is only a minor source of communication. On the contrast, the major source of communication overhead comes from the reporting of contact records which include the vector of buffered packets. For this reason, when the packet generation rate increases, the communication overhead increases significantly as shown in Table 4.5. However, the overall communication overhead is still low, *e.g.*, less than 30KB when each node generates 10 packets per day.

The storage cost of our scheme is shown in Table 4.6. The storage overhead increases significantly with the parameter w and T_{delete} since record summaries are stored at more nodes and for a longer time. However, the storage overhead only increases slowly with the packet generation rate. This is because the major source of storage overhead is record summaries which are stored for a relatively long time, not contact records which are deleted soon, and the number of generated record summaries only depends on the number of contacts, not on the traffic load. Generally, the storage overhead of our scheme is low, less than 200KB at each node.

4.3.8 Related Work

In mobile ad hoc networks, much work has been done to detect packet dropping and mitigate routing misbehavior. To detect packet dropping, Marti *et al.* [45] proposed watchdog based solutions in which the sending node operates in promiscuous mode and overhears the medium to check if the packet is really sent out by its neighbor. Some follow up works [46, 47] have used this neighborhood monitoring approach to detect packet dropping. However, neighborhood monitoring relies on a connected link between the sender and its neighbor, which most likely will not exist in opportunistic mobile networks. In opportunistic mobile networks, a node may move away right after forwarding the packet to its neighbor, and thus cannot overhear if the neighbor forwards the packet.

Another line of work uses the acknowledgement (ACK) packet [48, 142, 49] sent from the downstream node along the routing path to confirm if the packet has been forwarded by the next hop. Liu *et al.* [48] proposed a 2ACK scheme in which the sending node waits for an ACK from the next hop of its neighbor to confirm that the neighbor has forwarded the data packet. However, this technique is vulnerable to collusions, i.e., the neighbor can forward the packet to a colluder which drops the packet. Although end-to-end ACK schemes [142] are resistent to such colluding attacks, the ACK packets may be lost due to the opportunistic data delivery in opportunistic mobile networks. Moreover, in routing protocols [34, 37, 38] where each packet has multiple replicas, it is difficult for the source to verify which replica is acknowledged since there is no persistent routing path between the source and destination in opportunistic mobile networks.

To mitigate routing misbehavior, existing works [45, 48, 142] in mobile ad hoc networks reduce the traffic flowing to the misbehaving nodes by avoiding them in path selection. However, they cannot be directly applied to opportunistic mobile networks due to the lack of persistent path.

In opportunistic mobile networks, one serious routing misbehavior is the blackhole attack, in which a blackhole node advertises itself as a perfect relay for all destinations, but drops the packets received from others. Li *et al.* [122] proposed an approach that prevents the forgery of routing metrics. However, if the blackhole node indeed has a good routing metric for many destinations, their approach will not work, but our approach still works by limiting the number of packets forwarded

to the blackhole node. Another related attack is the wormhole attack, which has been recently addressed by Ren *et al.* [123].

To address selfish behaviors, Shevade *et al.* proposed a gaming-based approach [39] and Chen *et al.* [40] proposed a credit-based approach which provide incentives for selfish nodes to forward packets. Li *et al.* [42, 41] proposed a social selfishness aware routing algorithm to allow user selfishness and provide better routing performance in an efficient way. Our work is complementary since besides dealing with selfish routing we also consider the misbehavior of malicious nodes whose goal is not to maximize their own benefits but to launch attacks.

Our solution has some similarity with previous work (*e.g.*, [137]) on detecting node clone attacks in sensor networks, since both detect the attacker by identifying some inconsistency. However, our work relies on a different kind of inconsistency, and opportunistic mobile networks do not have the reliable link connection used in existing solutions for node clone attacks.

4.3.9 Summary

In this section, we presented a scheme to detect packet dropping in opportunistic mobile networks. The detection scheme works in a distributed way; i.e., each node detects packet dropping locally based on the collected information. Moreover, the detection scheme can effectively detect misreporting even when some nodes collude. Analytical results on detection probability and detection delay were also presented. Based on our packet dropping detection scheme, we then proposed a scheme to mitigate routing misbehavior in opportunistic mobile networks. The proposed scheme is very generic and it does not rely on any specific routing algorithm. Trace-driven simulations show that our solutions are efficient and can effectively mitigate routing misbehavior.

4.4 Chapter Summary

In this chapter, we explored using opportunistic mobile networks for sensing data delivery when no communication infrastructure is available. Specifically, we addressed three security issues that may degrade the performance of sensing da-

ta delivery, which are social selfishness, flood attacks, and routing misbehavior. To deal with social selfishness, we proposed a routing protocol SSAR which allows users to behave in the socially selfish way. SSAR improves performance by considering both user willingness and contact opportunity when selecting relays. Extensive simulations on the MIT Reality trace and Infocom05 trace showed that SSAR can maintain social selfishness and achieve very good routing performance in an efficient way. To defend against flood attacks, we adopted the approach of rate limiting, and proposed a distributed scheme which exploits *claim-carry-and-check* to probabilistically detect the violation of rate limit in opportunistic mobile networks. Extensive trace-driven simulations showed that this scheme is effective to detect flood attacks and it has very low cost. To mitigate routing misbehavior, we proposed a distributed scheme to detect packet dropping in opportunistic mobile networks, and designed techniques to detect misreporting caused by colluders. Based on the dropping detection scheme, we then devised a scheme which mitigates routing misbehavior by reducing the packets forwarded to misbehaving nodes. Trace-driven simulations show that our solutions are efficient and can effectively mitigate routing misbehavior.

Chapter 5

Conclusions and Future Work

5.1 Conclusions

In this dissertation, we proposed a comprehensive set of techniques to provide security and privacy support for mobile sensing, and ultimately facilitate the proliferation of mobile sensing applications. These techniques are summarized as follows.

In Chapter 2, we addressed the problem of providing privacy-aware incentives for mobile sensing, so as to facilitate large-scale deployment of sensing applications. Specifically, we proposed two credit-based privacy-aware incentive schemes, corresponding to the scenarios with and without a TTP respectively. These schemes reward users with credits for their contributed data, and simultaneously provide anonymity for users. The first scheme relies on a TTP to provide anonymity and prevent abuse attacks. Purely built upon cryptographic hash functions, this scheme has very low computation and storage cost at each mobile node. The second scheme does not rely on any TTP for privacy protection, but employs blind signature, partially blind signatures, and commitment techniques to achieve anonymity and security. This scheme ensures that no third party can break any node's privacy. We implemented these schemes on Nexus S smartphones. Measurements based on the implementation show that these schemes have low computation cost and power consumption. To our best knowledge, they are the first privacy-aware incentive schemes for mobile sensing.

In Chapter 3, we addressed the problem of providing privacy support for aggre-

gation of time-series data in mobile sensing. Specifically, we proposed a protocol to obtain the Sum aggregate of time-series data, which can achieve differential privacy–a strong privacy guarantee. To construct the protocol, we first designed a novel HMAC-based encryption scheme which allows the aggregator to obtain the sum of all users' data but nothing else, and then devised a novel ring-based overlapped grouping technique to efficiently deal with dynamic joins and leaves of users. Compared to prior works, our protocol is the first purely based on computationally efficient symmetric-key cryptography. Thus, it has very low computation cost. Due to the overlapped grouping technique, our protocol also has very low communication overhead for dynamic joins and leaves. Besides, it achieves differential privacy with only O(1) aggregation error. Based on the Sum aggregation protocol, we also proposed two schemes to obtain the Min aggregate of time-series data. One scheme obtains the accurate Min while the other one obtains an approximate Min with provable error guarantee at much lower cost. Evaluations show that our protocol runs orders of magnitude faster than existing work, and only a small number of nodes need to be updated for each join or leave when 20% of nodes are compromised. Due to low computation and communication cost, our protocol can be applied to a wide range of mobile sensing systems with various scales, aggregation loads and resource constraints.

In Chapter 4, we addressed the problem of providing secure networking support for mobile sensing when no communication infrastructure is available. For mobile devices without infrastructure support and for circumstances of unavailable or cost-inefficient infrastructures, we proposed to use opportunistic mobile networks for sensing data delivery, and addressed three security issues (i.e., social selfishness, flood attacks, and routing misbehavior) that may degrade the performance of sensing data delivery. We first addressed social selfishness by proposing a routing protocol SSAR. SSAR allows users to behave in the socially selfish way, but improves performance by considering both user willingness and contact opportunity when selecting relays. Trace-driven simulations showed that SSAR can maintain social selfishness and achieve good routing performance with low cost. We then adopted the approach of rate limiting to defend against flood attacks. To enforce rate limiting in opportunistic mobile networks, we proposed a distributed scheme which can probabilistically detect the violation of rate limit. Evaluations showed

that this scheme can effectively detect flood attacks in an efficient way. Lastly, we designed a distributed scheme to detect packet dropping in opportunistic mobile networks, and provided analytical results on detection probability as well as detection delay. To mitigate the effect of routing misbehavior, we also devised a scheme which reduces the amount of packets forwarded to misbehaving nodes. Evaluations showed that our solutions can effectively mitigate routing misbehavior at low cost.

5.2 Future Directions

Secure and privacy-ware mobile sensing is an emerging area. This dissertation has provided a series of solutions for security and privacy of mobile sensing, but there are still many other issues that deserve in-depth investigation. In the following, we outline several interesting directions that could be further explored.

- **Usable privacy:** As the producer of data, users must decide what data to share. For example, should a user share his location when he is at home, in office, and in a shopping mall? However, making such decisions requires a deep understanding of the interactions between the user's desired level of privacy, the methods for sharing data, and the scope of that sharing. Based on the observation that the potential for privacy leakage can be mitigated by controlling the quality of shared sensing data (e.g., the accuracy of GPS reading and the sampling rate of an accelerometer), one future direction is to investigate the correlation between the quality of sensor data and the degree of privacy leakage. In particular, it is interesting to investigate the correlation under the assumption of strong attackers that have auxiliary information obtained elsewhere (e.g., from the Internet). Challenges include how to model the privacy level achieved by a scheme or protocol. Differential privacy is a good privacy model defined for numeric data, but it is still unknown how to define similar concepts for more general data. Based on the investigation, a further step is to derive context-aware models that enable the data source to automatically control what data to be shared, when to be shared, and how to be shared according to a required privacy level.

- **Trustworthy data collection:** Mobile sensing systems usually run in un-

trusted environments. Some mobile users may manipulate sensing data for economic benefits or malicious disruptions. For the data collector, data credibility is probably the most important requirement. Here, data credibility means that the sensors' data is indeed collected from the claimed device and in the claimed environment. Unfortunately, little work has been done to address data credibility. In mobile sensing, ensuring data credibility is a challenge due to the lack of a trust infrastructure and the use of privacy enhancing technologies. Thus, it deserves further exploration to achieve privacy-aware and trustworthy data collection. Possible directions of investigation include designing anonymous reputation systems which allow the collector to evaluate the credibility of data based on the reputation of the user generating the data, and devising cross-validation techniques which rely on colocated users to validate each other's data.

- **Empirical study:** A lot of mobile sensing systems have been developed (see a recent survey of these systems in [9]). Current mobile sensing systems primarily focus on providing new sensing functions, but not enhancing security and privacy. We are developing a prototype system, which implements the security enhancements presented in this dissertation on Samsung Nexus S smartphones. Plans include distributing these smartphones among students at Penn State University, and evaluating how our security enhancements work in the real world. The project provides unique opportunities to empirically study the interactions among incentive, privacy, user participation, and trustworthy data in the context of mobile sensing.

Bibliography

[1] Bicheno, S. (2012), "Global Smartphone Installed Base Forecast by Operating System for 88 Countries: 2007 to 2017," http://www.strategyanalytics.com/default.aspx?mod=reportabstractviewer&a0=7834.

[2] BodyMedia, "FIT Armband," http://www.bodymedia.com/Support-Help/BodyMedia-FIT-Advantage.

[3] International, R., "MicroPEM," http://www.rti.org/page.cfm?objectid=E19BDB1B-A77F-E4A3-F83126CB83065E76.

[4] Consolvo, S., D. W. McDonald, T. Toscos, M. Y. Chen, J. Froehlich, B. Harrison, P. Klasnja, A. LaMarca, L. LeGrand, R. Libby, I. Smith, and J. A. Landay (2008) "Activity sensing in the wild: a field trial of ubifit garden," in *Proc. CHI*, pp. 1797–1806.

[5] Lane, N. D., M. Mohammod, M. Lin, X. Yang, H. Lu, S. Ali, A. Doryab, E. Berke, T. Choudhury, and A. Campbell (2011) "BeWell: A Smartphone Application to Monitor, Model and Promote Wellbeing," in *Intl. ICST Conf. on Pervasive Computing Technologies for Healthcare*.

[6] Mun, M., S. Reddy, K. Shilton, N. Yau, J. Burke, D. Estrin, M. Hansen, E. Howard, R. West, and P. Boda (2009) "PEIR, the personal environmental impact report, as a platform for participatory sensing systems research," in *Proc. ACM MobiSys*, pp. 55–68.

[7] Thiagarajan, A., L. Ravindranath, K. LaCurts, S. Madden, H. Balakrishnan, S. Toledo, and J. Eriksson (2009) "VTrack: accurate, energy-aware road traffic delay estimation using mobile phones," in *Proc. SenSys*, pp. 85–98.

[8] Lane, N. D., E. Miluzzo, H. Lu, D. Peebles, T. Choudhury, and A. T. Campbell (2010) "A survey of mobile phone sensing," *IEEE Comm. Mag.*, **48**(9), pp. 140–150.

[9] Khan, W. Z., Y. Xiang, M. Y. Aalsalem, and Q. Arshad (2013) "Mobile Phone Sensing Systems: A Survey," *IEEE COMMUNICATIONS SURVEYS & TUTORIALS*, **15**(1), pp. 402–427.

[10] iReport, "http://www.ireport.com/," .

[11] Paulos, E., M. Foth, C. Satchell, Y. Kim, P. Dourish, and J. H. jeong Choi (2008) "Ubiquitous sustainability: Citizen science and activism," in *In UbiComp Workshops*.

[12] "App Games. Swine Flu Tracker Map iPhone Game, 2000." .

[13] Bilandzic, M., M. Banholzer, D. Peev, V. Georgiev, F. Balagtas-Fernandez, and A. De Luca (2008) "Laermometer: a mobile noise mapping application," in *Proceedings of the 5th Nordic conference on Human-computer interaction: building bridges*, NordiCHI '08, pp. 415–418.

[14] Honicky, R., E. Paulos, E. Brewer, and R. White (2008) "N-SMARTS: Networked Suite of Mobile Atmospheric Real-time Sensors," in *In NSDR*.

[15] Ramanathan, N., S. Reddy, J. Burke, and D. Estrin (2007) "Participatory Sensing for Surya," in *In SenSys 2007 Workshop on Sensing on Everyday Mobile Phones in Support of Participatory Research*.

[16] Golle, P. and K. Partridge (2009) "On the Anonymity of Home/Work Location Pairs," in *Proceedings of the 7th International Conference on Pervasive Computing*, Pervasive '09, Springer-Verlag, Berlin, Heidelberg, pp. 390–397.

[17] Hoh, B., M. Gruteser, H. Xiong, and A. Alrabady (2006) "Enhancing Security and Privacy in Traffic-Monitoring Systems," *IEEE Pervasive Computing*, **5**, pp. 38–46.

[18] Krumm, J. (2007) "Inference attacks on location tracks," in *Proceedings of the 5th international conference on Pervasive computing*, PERVASIVE'07, Springer-Verlag, Berlin, Heidelberg, pp. 127–143.

[19] Cornelius, C., A. Kapadia, D. Kotz, D. Peebles, M. Shin, and N. Triandopoulos (2008) "Anonysense: privacy-aware people-centric sensing," in *Proceedings of the 6th international conference on Mobile systems, applications, and services (MobiSys)*, ACM, pp. 211–224.

[20] Cristofaro, E. D. and C. Soriente (2011) "Short paper: PEPSI—privacy-enhanced participatory sensing infrastructure," in *Proc. ACM WiSec*, pp. 23–28.

[21] Christin, D., C. Rosskopf, M. Hollick, L. A. Martucci, and S. S. Kanhere "IncogniSense: An anonymity-preserving reputation framework for participatory sensing applications," in *Proc. IEEE PerCom*.

[22] Yang, D., G. Xue, X. Fang, and J. Tang (2012) "Crowdsourcing to Smartphones: Incentive Mechanism Design for Mobile Phone Sensing," in *Proc. ACM MobiCom*.

[23] Li, Q. and G. Cao (2013) "Providing Privacy-Aware Incentives for Mobile Sensing," in *Proc. IEEE PerCom*.

[24] Hicks, J., N. Ramanathan, D. Kim, M. Monibi, J. Selsky, M. Hansen, and D. Estrin (2010) "AndWellness: an open mobile system for activity and experience sampling," in *Proc. Wireless Health*, pp. 34–43.

[25] Dwork, C. (2006) "Differential Privacy," *Invited talk at ICALP*.

[26] Dwork, C., F. McSherry, K. Nissim, and A. Smith (2006) "Calibrating noise to sensitivity in private data analysis," *TCC*.

[27] Rastogi, V. and S. Nath (2010) "Differentially Private Aggregation of Distributed Time-Series with Transformation and Encryption," *ACM SIGMOD*.

[28] Shi, E., T.-H. H. Chan, E. Rieffel, R. Chow, and D. Song (2011) "Privacy-Preserving Aggregation of Time-Series Data," *Network and Distributed System Security Symposium (NDSS)*.

[29] Chan, T.-H. H., E. Shi, and D. Song (2012) "Privacy-Preserving Stream Aggregation with Fault Tolerance," *Financial Cryptography and Data Security (FC)*.

[30] Jawurek, M. and F. Kerschbaum (2012) "Fault-Tolerant Privacy-Preserving Statistics," in *The 12th Privacy Enhancing Technologies Symposium (PETS)*.

[31] Li, Q. and G. Cao (2013) "Efficient Privacy-Preserving Stream Aggregation in Mobile Sensing with Low Aggregation Error," *Proceedings of the 13th Privacy Enhancing Technologies Symposium (PETS)*.

[32] ——— (2012) "Efficient and Privacy-Preserving Data Aggregation in Mobile Sensing," in *Proc. IEEE ICNP*, pp. 1–10.

[33] Lindgren, A., A. Doria, and O. Schelen (2003) "Probabilistic routing in intermittently connected networks," *ACM SIGMOBILE CCR*, **7**(3), pp. 19–20.

[34] Burgess, J., B. Gallagher, D. Jensen, and B. Levine (2006) "MaxProp: Routing for Vehicle-Based Disruption-Tolerant Networks," *Proc. INFOCOM*.

[35] Daly, E. and M. Haahr (2007) "Social network analysis for routing in disconnected delay-tolerant MANETs," *Proc. MobiHoc*, pp. 32–40.

[36] Balasubramanian, A., B. N. Levine, and A. Venkataramani (2007) "DTN Routing as a Resource Allocation Problem," *Proc. ACM SIGCOMM*.

[37] Hui, P., J. Crowcroft, and E. Yoneki (2008) "Bubble rap: social-based forwarding in delay tolerant networks," *Proc. MobiHoc*, pp. 241–250.

[38] Erramilli, V., A. Chaintreau, M. Crovella, and C. Diot (2008) "Delegation Forwarding," *Proc. MobiHoc*.

[39] Shevade, U., H. Song, L. Qiu, and Y. Zhang (2008) "Incentive-Aware Routing in DTNs," *IEEE ICNP*.

[40] Chen, B. and C. Choon (2010) "MobiCent: A Credit-Based Incentive System for Disruption Tolerant Network," *Proc. IEEE INFOCOM*.

[41] Li, Q., W. Gao, S. Zhu, and G. Cao (2012) "A Routing Protocol for Socially Selfish Delay Tolerant Networks," *Ad Hoc Networks*, **10**(8), pp. 1619–1632.

[42] Li, Q., S. Zhu, and G. Cao (2010) "Routing in Socially Selfish Delay Tolerant Networks," in *Proc. IEEE INFOCOM*, pp. 1–9.

[43] Raghavan, B., K. Vishwanath, S. Ramabhadran, K. Yocum, and A. Snoeren (2007) "Cloud Control with Distributed Rate Limiting," *Proc. ACM SIGCOMM*.

[44] Li, Q., W. Gao, S. Zhu, and G. Cao (2013) "To Lie or to Comply: Defending against Flood Attacks in Disruption Tolerant Networks," *IEEE Transactions on Dependable and Secure Computing*, **10**(3), pp. 168–182.

[45] Marti, S., T. J. Giuli, K. Lai, and M. Baker (2000) "Mitigating routing misbehavior in mobile ad hoc networks," *Proc. IEEE MobiCom*, pp. 255–265.

[46] Yang, H., J. Shu, X. Meng, and S. Lu (2006) "SCAN: self-organized network-layer security in mobile ad hoc networks," *IEEE JSAC*, **24**(2).

[47] Buchegger, S. and J.-Y. L. Boudec (2002) "Performance analysis of the CONFIDANT protocol (cooperation of nodes: Fairness in dynamic ad-hoc networks)," *Proc. MobiHoc*, pp. 226–236.

[48] Liu, K., J. Deng, P. K. Varshney, and K. Balakrishnan (2007) "An Acknowledgment-Based Approach for the Detection of Routing Misbehavior in MANETs," *IEEE Transactions on Mobile Computing*, **6**(5).

[49] Awerbuch, B., D. Holmer, C.-N. Rotaru, and H. Rubens (2002) "An On-Demand Secure Routing Protocol Resilient to Byzantine Failures," *WiSe*.

[50] Li, Q. and G. Cao (2012) "Mitigating Routing Misbehavior in Disruption Tolerant Networks," *IEEE Transactions on Information Forensics and Security*, **7**(2), pp. 664–675.

[51] Chaum, D. (1982) "Blind signatures for untraceable payments," in *Advances in Cryptology: Proceedings of CRYPTO '82*, Plenum.

[52] ——— (1983) "Blind Signature System," in *Advances in Cryptology: Proceedings of CRYPTO '83*, Plenum.

[53] Abe, M. and T. Okamoto (2000) "Provably Secure Partially Blind Signatures," in *Proc CRYPTO*, pp. 271–286.

[54] Merkle, R. (1980) "Protocols for public key cryptosystems," *IEEE S&P*.

[55] Abe, M. and E. Fujisaki (1996) "How to Date Blind Signatures," in *Proc. ASIACRYPT*, pp. 244–251.

[56] Pidcock, S., R. Smits, U. Hengartner, and I. Goldberg (2011) "NotiSense: An Urban Sensing Notification System To Improve Bystander Privacy," in *PhoneSense*.

[57] Shao, M., Y. Yang, S. Zhu, and G. Cao (2008) "Towards Statistically Strong Source Anonymity for Sensor Networks," in *Proc. IEEE INFOCOM*.

[58] Zhu, Z. and G. Cao (2011) "APPLAUS: A Privacy-Preserving Location Proof Updating System for Location-based Services," in *Proc. IEEE INFOCOM*.

[59] Huang, K. L., S. S. Kanhere, and W. Hu (2009) "Towards privacy-sensitive participatory sensing," in *The 5th International Workshop on Sensor Networks and Systems for Pervasive Computing*.

[60] Shao, M., S. Zhu, W. Zhang, and G. Cao (2009) "pDCS: Security and Privacy Support for Data-Centric Sensor Networks," *IEEE Transactions on Mobile Computing*, **8**(8), pp. 1023–1038.

[61] Yang, Y., M. Shao, S. Zhu, B. Urgaonkar, and G. Cao (2008) "Towards Event Source Unobservability with Minimum Network Traffic in Sensor Networks," in *Proc. ACM WiSec*.

[62] De Cristofaro, E. and R. Di Pietro (2012) "Preserving query privacy in urban sensing systems," in *Proc. of the 13th intl. conf. on Distributed Computing and Networking (ICDCN)*, Springer-Verlag, pp. 218–233.

[63] Gilbert, P., L. P. Cox, J. Jung, and D. Wetherall (2010) "Toward trustworthy mobile sensing," in *Proc. ACM HotMobile*, pp. 31–36.

[64] Ganti, R. K., N. Pham, Y.-E. Tsai, and T. F. Abdelzaher (2008) "PoolView: stream privacy for grassroots participatory sensing," in *Proc ACM SenSys*, pp. 281–294.

[65] Shi, J., R. Zhang, Y. Liu, and Y. Zhang (2010) "Prisense: privacy-preserving data aggregation in people-centric urban sensing systems," in *Proc. IEEE INFOCOM*, pp. 758–766.

[66] Ion, M., G. Russello, and B. Crispo (2010) "Supporting publication and subscription confidentiality in pub/sub networks," in *SecureComm*.

[67] Hull, B., V. Bychkovsky, Y. Zhang, K. Chen, M. Goraczko, A. Miu, E. Shih, H. Balakrishnan, and S. Madden (2006) "Cartel: a distributed mobile sensor computing system," in *SenSys*.

[68] Honicky, R., E. A. Brewer, E. Paulos, and R. White (2008) "N-smarts: networked suite of mobile atmospheric real-time sensors," in *NSDR*.

[69] MNDOLI, "MNOSHA Permissible Exposure Limits," Available at http://www.dli.mn.gov/OSHA/PDF/pels.pdf.

[70] Eisenman, S. B., E. Miluzzo, N. D. Lane, R. A. Peterson, G.-S. Ahn, and A. T. Campbell (2007) "The BikeNet mobile sensing system for cyclist experience mapping," in *Proceedings of the 5th international conference on Embedded networked sensor systems (SenSys)*, pp. 87–101.

[71] Apte, M. G., W. J. Fisk, and J. M. Daisey (2000) "Indoor Carbon Dioxide Concentrations and SBS in Office Workers," in *Proceedings of Healthy Buildings*, pp. 133–138.

[72] Bonet, D., E.-J. Goh, and K. Nissim (2005) "Evaluating 2-DNF formulas on ciphertexts," *TCC*.

[73] Gentry, C. (2009) "Fully homomorphic encryption using ideal lattices," in *ACM symposium on Theory of computing (STOC)*, pp. 169–178.

[74] Castelluccia, C., A. C.-F. Chan, E. Mykletun, and G. Tsudik (2009) "Efficient and provably secure aggregation of encrypted data in wireless sensor networks," *ACM Transactions on Sensor Networks (TOSN)*, **5**(3), pp. 20:1–20:36.

[75] Yang, Y., X. Wang, S. Zhu, and G. Cao (2008) "SDAP: A Secure Hop-by-Hop Data Aggregation Protocol for Sensor Networks," *ACM Transactions on Information and System Security (TISSEC)*, **11**(4).

[76] Yang, Z., S. Zhong, and R. N. Wright (2005) "Privacy-Preserving Classification of Customer Data without Loss of Accuracy," in *SIAM SDM*, pp. 21–23.

[77] Goldreich, O. "Secure multi-party computation," *http://www.wisdom.weizmann.ac.il/ oded/PS/prot.ps*.

[78] Fouque, P.-A., G. Poupard, and J. Stern (2000) "Sharing Decryption in the Context of Voting or Lotteries," in *Proceedings of the 4th International Conference on Financial Cryptography*, FC '00, pp. 90–104.

[79] Rieffel, E. G., J. Biehl, W. van Melle, and A. J. Lee (2010) "Secured histories: computing group statistics on encrypted data while preserving individual privacy." *In submission*.

[80] Ács, G. and C. Castelluccia (2011) "I have a DREAM!: differentially private smart metering," in *Proc. IH*, pp. 118–132.

[81] Li, S., H. Zhu, Z. Gao, X. Guan, K. Xing, , and X. S. Shen (2012) "Location Privacy Preservation in Collaborative Spectrum Sensing," in *Proc. IEEE INFOCOM*.

[82] Goetz, M. and S. Nath (2011) *Privacy-Aware Personalization for Mobile Advertising*, *Tech. rep.*, No. MSR-TR-2011-92.

[83] Chen, R., A. Reznichenko, P. Francis, and J. Gehrke (2012) "Towards Statistical Queries over Distributed Private User Data," in *Proc. of NSDI*.

[84] Proserpio, D., S. Goldberg, and F. McSherry (2012) "A workflow for differentially-private graph synthesis," in *Proc. ACM workshop on online social networks (WOSN)*, pp. 13–18.

[85] Sala, A., X. Zhao, C. Wilson, H. Zheng, and B. Y. Zhao (2011) "Sharing graphs using differentially private graph models," in *Proc. ACM IMC*, pp. 81–98.

[86] Castelluccia, C. (2005) "Efficient aggregation of encrypted data in wireless sensor networks," in *In MobiQuitous*, IEEE Computer Society, pp. 109–117.

[87] Bellare, M. (2006) "New proofs for NMAC and HMAC: security without collision-resistance," in *Proceedings of the 26th annual international conference on Advances in Cryptology*, CRYPTO'06, Springer-Verlag, pp. 602–619.

[88] Ghosh, A., T. Roughgarden, and M. Sundararajan (2009) "Universally utility-maximizing privacy mechanisms," in *ACM symposium on Theory of computing (STOC)*, pp. 351–360.

[89] Bernstein, D. J. and T. L. (editors) "eBACS: ECRYPT Benchmarking of Cryptographic Systems," *http://bench.cr.yp.to, accessed 11 Feb 2012.*

[90] Hui, P., A. Chaintreau, J. Scott, R. Gass, J. Crowcroft, and C. Diot (2005) "Pocket Switched Networks and Human Mobility in Conference Environments," *SIGCOMM Workshops.*

[91] Motani, M., V. Srinivasan, and P. Nuggehalli (2005) "PeopleNet: engineering a wireless virtual social network," *Proc. MobiCom*, pp. 243–257.

[92] Grid Computing Center, S. J. T. U. "Shanghai Taxi Trace Data," *http://wirelesslab.sjtu.edu.cn/.*

[93] Fall, K. (2003) "A delay-tolerant network architecture for challenged internets," *Proc. SIGCOMM*, pp. 27–34.

[94] Granovetter, M. (1973) "The Strength of Weak Ties," *The American Journal of Sociology*, **78**(6).

[95] Jaramillo, J. J. and R. Srikant (2007) "DARWIN: Distributed and Adaptive Reputation mechanism for WIreless ad-hoc Networks," *Proc. MobiCom.*

[96] Zhong, S., J. Chen, and Y. R. Yang (2003) "Sprite: A simple, cheat-proof, credit-based system for mobile ad-hoc networks," *Proc. IEEE INFOCOM*, **3**, pp. 1987–1997.

[97] Dunbar, R. (1992) "Neocortex size as a constraint on group size in primates," *Journal of Human Evolution*, **22**, pp. 469–493.

[98] McCarty, C., P. Killworth, H. Bernard, E. Johnsen, and G.Shelley (1992) "Comparing Two Methods for Estimating Network Size," *Human Organization*, **60**, pp. 28–39.

[99] Degirmencioglu, S., K. Urberg, J. Tolson, and P. Richard (1998) "Adolescent Friendship Networks: Continuity and Change Over the School Year," *Merrill-Palmer Quarterly*, **44**, pp. 313–337.

[100] Gilbert, E. and K. Karahalios (2009) "Predicting Tie Strength With Social Media," *Proc. CHI*.

[101] Josang, A. and S. Pope (2005) "Semantic Constraints for Trust Tansitivity," *Proceedings of the Asia-Pacific Conference of Conceptual Modelling (APCCM) (Volume 43 of Conferences in Research and Practice in Information Technology)*.

[102] Mclachlan, G. (1992) *Discriminant Analysis and Statistical Pattern Recognition*, Wiley.

[103] Friedman, J. H., J. L. Bentler, and R. A. Finkel (1977) "An Algorithm for Finding Best Matches in Logrithmic Expected Time," *ACM Transactions on Mathimatical Software*, **3**(3), pp. 209–226.

[104] Gonzalez, T. (1985) "Clustering to minimize the maximum inter-cluster distance," *Theoret. Comput. Sci.*, **38**, pp. 293–306.

[105] Loftsgaarden, D. . and C. P. Quesenberry (1965) "A nonparametric estimate of a multivariate density function," *Ann. Math. Statist.*, **36**.

[106] Dawande, M., J. Kalagnanam, P. Keskinocak, R. Ravi, and F. Salman (2000) "Approximation Algorithms for the Multiple Knapsack Problem with Assignment Restrictions," *Journal of Combinatorial Optimization*, **4**, pp. 171–186.

[107] Chaintreau, A., P. Hui, J. Crowcroft, C. Diot, R. Gass, and J. Scott (2007) "Impact of Human Mobility on Opportunistic Forwarding Algorithms," *IEEE Trans. on Mobile Computing*, pp. 606–620.

[108] Eagle, N. and A. Pentland (2006) "Reality mining: sensing complex social systems," *Personal and Ubiquitous Computing*, **10**(4), pp. 255–268.

[109] community resource for archiving wireless data at Dartmouth, A., "http://crawdad.cs.dartmouth.edu/data.php," .

[110] Mislove, A., M. Marcon, K. P. Gummadi, Druschel, and Bhattacharjee (2007) "Measurement and Analysis of Online Social Networks," *Proc. IMC*.

[111] Boldrini, C., M. Conti, and A. Passarella (2008) "ContentPlace: Social-aware Data Dissemination in Opportunistic Networks," *Proc. M-SWiM*.

[112] Gao, W., Q. Li, B. Zhao, and G. Cao (2009) "Multicasting in Delay Tolerant Networks: A Social Network Perspective," *Proc. ACM MobiHoc*.

[113] Gao, W. and G. Cao (2010) "On Exploiting Transient Contact Patterns for Data Forwarding in Delay Tolerant Networks," *Proc. IEEE ICNP*, pp. 193–202.

[114] ——— (2011) "User-Centric Data Dissemination in Disruption Tolerant Networks," *Proc. IEEE INFOCOM*.

[115] Zhao, J. and G. Cao (2006) "VADD: Vehicle-Assisted Data Delivery in Vehicular Ad Hoc Networks," *Proc. IEEE INFOCOM*.

[116] Zhang, Y., J. Zhao, and G. Cao (2009) "Roadcast: A Popularity Aware Content Sharing Scheme in VANETs," *IEEE International Conference on Distributed Computing Systems (ICDCS)*.

[117] Hui, P., K. Xu, V. O. Li, J. Crowcroft, V. Latora, and P. Lio (2009) "Selfishness, Altruism and Message Spreading in Mobile Social Networks," *Proceeding of First IEEE International Workshop on Network Science For Communication Networks (NetSciCom09)*.

[118] Thompson, N., S. C. Nelson, M. Bakht, T. Abdelzaher, and R. Kravets (2010) "Retiring Replicants: Congestion Control for Intermittently-Connected Networks," *Proc. IEEE INFOCOM*.

[119] Mirkovic, J., S. Dietrich, D. Dittrich, and P. Reiher (2005) "Internet Denial of Service: Attack and Defense Mechanisms," *Prentice Hall*.

[120] Karlof, C. and D. Wagner (2003) "Secure routing in wireless sensor networks: Attacks and countermeasures," *First IEEE International Workshop on Sensor Network Protocols and Applications*.

[121] Gao, W., G. Cao, M. Srivatsa, and A. Iyengar (2012) "Distributed Maintenance of Cache Freshness in Opportunistic Mobile Networks," in *IEEE International Conference on Distributed Computing Systems (ICDCS)*.

[122] Li, F., A. Srinivasan, and J. Wu (2009) "Thwarting Blackhole Attacks in Distruption-Tolerant Networks using Encounter Tickets," *Proc. IEEE INFOCOM*.

[123] Ren, Y., M. C. Chuah, J. Yang, and Y. Chen (2010) "Detecting Wormhole Attacks in Delay Tolerant Networks," *IEEE Wireless Communications Magazine (IEEE WCM)*, **17**(5).

[124] Li, Q. and G. Cao (2011) "Mitigating Routing Misbehavior in Disruption Tolerant Networks," *IEEE Trans. on Information Forensics and Security*.

[125] Zhu, H., X. Lin, R. Lu, X. S. Shen, D. Xing, and Z. Cao (2010) "An opportunistic Batch Bundle Authentication Scheme for Energy Constrained DTNs," *IEEE INFOCOM*.

[126] F-SECURE "F-secure malware information pages: Smsworm:symbos/feak," *http://www.f-secure.com/v-descs/smsworm_symbos_feak.shtml*.

[127] Spyropoulos, T., K. Psounis, and C. S. Raghavendra (2007) "Efficient Routing in Intermittently Connected Mobile Networks: The Multiple-Copy Case," *IEEE/ACM Trans. on Networking (ToN)*, **16**(1), pp. 77–90.

[128] Gao, W. and G. Cao (2010) "On Exploiting Transient Contact Patterns for Data Forwarding in Delay Tolerant Networks," *Proc. IEEE ICNP*.

[129] Burgess, J., G. D. Bissias, M. Corner, and B. N. Levine (2007) "Surviving Attacks on Disruption-Tolerant Networks without Authentication," *Proc. ACM MobiHoc*.

[130] Nelson, S. C., M. Bakht, and R. Kravets (2009) "Encounter-Based Routing in DTNs," *Proc. IEEE INFOCOM*, pp. 846–854.

[131] Spyropoulos, T., K. Psounis, and C. Raghavendra (2005) "Spray and wait: an efficient routing scheme for intermittently connected mobile networks," in *Proceedings of 2005 ACM SIGCOMM workshop on Delay-tolerant networking*, pp. 252–259.

[132] Gentry, C. and A. Silverberg (2002) "Hierarchical ID-Based Cryptography," *Proc. International Conference on the Theory and Application of Cryptography and Information Security*.

[133] Seth, A., D. Kroeker, M. Zaharia, S. Guo, and S. Keshav (2006) "Lowcost Communication for Rural Internet Kiosks Using Mechanical Backhaul," *ACM Proc. of Mobicom*.

[134] Vahdat, A. and D. Becker (2000) "Epidemic routing for partially connected ad hoc networks," *Technical Report CS-200006, Duke University*.

[135] Groenevelt, R. (2006) "Stochastic Models in Mobile Ad Hoc Networks," *Technical report, University of Nice, Sophia Antipolis, INRIA*.

[136] Chaintreau, A., A. Mtibaa, L. Massoulie, and C. Diot (2007) "The diameter of opportunistic mobile networks," *Proc. ACM CoNEXT*.

[137] Parno, B., A. Perrig, and V. Gligor (2005) "Distributed Detection of Node Replication Attacks in Sensor Networks," *Proc. IEEE S&P*.

[138] Natarajan, V., Y. Yang, and S. Zhu (2011) "Resource-Misuse Attack Detection in Delay-Tolerant Networks," *Proceedings of International Performance Computing and Communications Conference (IPCCC)*.

[139] Conan, V., J. Leguay, and T. Friedman (2007) "Characterizing Pairwise Intercontact Patterns in Delay Tolerant Networks," *ACM Autonomics*.

[140] Zhu, H., L. Fu, G. Xue, Y. Zhu, M. Li, and L. Ni (2010) "Recognizing Exponential Inter-Contact Time in VANETs," *IEEE Proc. of INFOCOM*, pp. 101–105.

[141] Cha, J. C. and J. H. Cheon (2003) "An identity-based signature form gap Diffie-Hellman groups," *Proc. of PKC*.

[142] Xue, Y. and K. Nahrstedt (2004) "Providing Fault-Tolerant Ad-Hoc Routing Service in Adversarial Environments," *Wireless Personal Comm.*, **29**(3-4).

Vita

Qinghua Li

Qinghua Li received his B.E. degree from Xi'an Jiaotong University, Xi'an, China, in 2004, and M.S. degree from Tsinghua University, Beijing, China, in 2007. He enrolled in the Ph.D. program in Computer Science and Engineering at The Pennsylvania State University in August 2007. He is a student member of IEEE.

Publications during the Ph.D. study:

- Qinghua Li, Wei Gao, Sencun Zhu, and Guohong Cao, "To Lie Or To Comply: Defending against Flood Attacks in Disruption Tolerant Networks," *IEEE Transactions on Dependable and Secure Computing (TDSC)*, Vol. 10, No. 3, pp. 168-182, 2013.

- Qinghua Li and Guohong Cao, "Efficient Privacy-Preserving Stream Aggregation in Mobile Sensing with Low Aggregation Error," *The 13th Privacy Enhancing Technologies Symposium (PETS)*, 2013.

- Qinghua Li and Guohong Cao, "Providing Privacy-Aware Incentives for Mobile Sensing," *IEEE International Conference on Pervasive Computing and Communications (PerCom)*, 2013.

- Qinghua Li and Guohong Cao, "Efficient and Privacy-Preserving Data Aggregation in Mobile Sensing," *IEEE International Conference on Network Protocols (ICNP)*, 2012.

- Qinghua Li and Guohong Cao, "Mitigating Routing Misbehavior in Disruption Tolerant Networks," *IEEE Transactions on Information Forensics and Security (TIFS)*, Vol. 7, No. 2, pp. 664-675, 2012.

- Qinghua Li, Wei Gao, Sencun Zhu, and Guohong Cao, "A Routing Protocol for Socially Selfish Delay Tolerant Networks," *Ad Hoc Networks*, Vol. 10, No. 8, pp. 1619-1632, 2012.

- Qinghua Li, Sencun Zhu, and Guohong Cao, "Routing in Socially Selfish Delay Tolerant Networks," *IEEE Conference on Computer Communications (INFOCOM)*, 2010.